

THE UNIVERSITY OF MICHIGAN
INDUSTRY PROGRAM OF THE COLLEGE OF ENGINEERING

A STUDY OF COLUMN SEPARATION ACCOMPANYING
TRANSIENT FLOW OF LIQUIDS IN PIPES

Robert A. Baltzer

A dissertation submitted in partial fulfillment
of the requirements for the degree of
Doctor of Philosophy in the
University of Michigan
Department of Civil Engineering
1967

February, 1967

IP-768

JMPL0186

ACKNOWLEDGMENTS

The writer is indebted to Professor Victor L. Streeter, graduate committee co-chairman and thesis advisor, for his suggestion of this topic and for his inspiration, incisive guidance, and patience; to Professor Ernest F. Brater, committee co-chairman, for his timely counsel, encouragement, and unfailing support; and to Professors Lawrence C. Maugh, William P. Graebel, and James W. Daily, committee members, for their interest and cooperation throughout the course of the study. Appreciation is also due Professors Arthur G. Hansen and Russell F. Dodge, who have since left The University, for their interest during the early phases of the study.

The writer is appreciative of the sound advice and craftsmanship rendered by Messrs. George L. Geisendorfer and Waldemar G. Buss, who assisted with the construction of the experimental apparatus. A word of gratitude is also extended to many unnamed individuals, including fellow graduate students, who have contributed to this study in various ways.

Without the use of the excellent facilities and the services available at The University of Michigan Computing Center, this study would not have been possible. The writer is particularly grateful to The University for the use of these facilities and for the valuable experience gained thereby.

For assistance with the collection and evaluation of the experimental data and for aid with the preparation of the manuscript, the writer is indebted to his wife, Lisa. Appreciation is also due

the staff of the Industry Program of the College of Engineering for final preparation and publication of the manuscript.

The study was supported in part by a fellowship tendered by The University of Michigan from National Science Foundation Grant No. 340. The writer expresses his appreciation of this financial support.

TABLE OF CONTENTS

	<u>Page</u>
ACKNOWLEDGEMENTS.....	ii
LIST OF TABLES.....	vi
LIST OF FIGURES.....	vii
SYMBOLS.....	xi
CHAPTER	
I INTRODUCTION.....	1
Description of Problem.....	1
Review of Literature.....	3
Scope of Investigation.....	7
II THEORETICAL ANALYSIS.....	11
III ANALYTIC INTERPRETATION AND EVALUATION PROCEDURES.....	20
Equations of Transient Motion -- Pipe Flowing Full.....	22
Equation of Continuity.....	23
Equation of Motion.....	41
Characteristics Equations.....	44
Finite Difference Solution.....	46
Boundary Conditions.....	54
Equations of Transient Motion -- Horizontal Pipe Flowing Partially Full.....	57
Equation of Continuity.....	58
Equation of Motion.....	61
Characteristics Equations.....	64
Finite Difference Solution.....	66
Boundary Conditions.....	71
IV COMPUTER SIMULATION.....	75
Flow System.....	75
Boundary Conditions.....	76
Sequence of Operations.....	83
Digital Computer Program.....	84

TABLE OF CONTENTS (CONT'D)

	<u>Page</u>
CHAPTER	
V EXPERIMENTAL APPARATUS AND LABORATORY INVESTIGATION.....	91
General Description of Pipe System.....	91
Instrumentation.....	97
System Calibration.....	101
Experimental Procedures.....	106
VI COMPARISON AND DISCUSSION OF EXPERIMENTAL AND THEORETICAL RESULTS.....	111
Conditions Investigated.....	111
Comparison of Results.....	114
Pressure Rises.....	114
Column-Separation Voids.....	122
Significance of Findings.....	135
VII CONCLUSIONS.....	145
SELECTED REFERENCES.....	148
APPENDIX	
I MAIN COMPUTER PROGRAM.....	153
II SUBROUTINE PROGRAMS USED WITH MAIN COMPUTER PROGRAM.....	168
III EXPERIMENTAL DATA; RUNS NUMBERS 25 AND 29.....	182
IV COMPUTER SIMULATED RESULTS.....	194

LIST OF TABLES

<u>Table</u>		<u>Page</u>
I	Copper Pipe Properties	95
II	Plastic Pipe Properties	96
III	Summary of Experimental Runs	113

Tables in Appendix III

I	Experimental Run Number 25 Pressure-Rise Data at Gate Valve	183
II	Experimental Run Number 25 Column-Separation Void Data	186
III	Experimental Run Number 34 Pressure-Rise Data at Gate Valve	188
IV	Experimental Run Number 34 Column-Separation Void Data	192

LIST OF FIGURES

<u>Figure</u>		<u>Page</u>
1	Photograph of a Typical Vapor Cavity Accompanying Column Separation	12
2	Schematic Time-Sequence Representation of Column Separation and Pressure Pattern in a Pipe System Undergoing Transient Flow	14
3	Definition Sketch Depicting Transient Conditions in Pipe Segment Flowing Full	24
4	Definition Sketch Depicting Stressed Element Located Within Pipe Wall	28
5	Curves Defining Relationship Between Pipe Constraint Coefficient, c , and the Ratio of Outside to Inside Pipe Radii, b/R , for Various Conditions of Constraint and Different Values of Poisson's Ratio	38
6	Definition Sketch Showing Intersection of $C+$ and $C-$ Characteristics Curves in the $x-t$ Plane	47
7	Definition Sketch Showing a Space-Time Grid Superimposed on the $x-t$ Plane	49
8	Definition Sketch Showing Relationship Between Space-Time Grids and Characteristics Curves at a Pipe Junction	56
9	Definition Sketch Illustrating Element of Free-Surface Flow in a Pipe	60
10	Definition Sketch Illustrating Domain of Dependence Governed by Characteristics Passing Through Grid Points L and R	72
11	Schematic Representation of Laboratory Flow System Used in Experimental Investigation	77
12	Definition Sketch Showing a Parabolic Cylinder Intersecting a Circular Cylinder	81
13	An Abridged Flow Diagram Setting Forth the Sequence of Operations Used to Simulate Transient Pipe Flow and the Accompanying Column Separation	85
14	Detailed Schematic of Laboratory Flow System	93

TABLE OF FIGURES (Cont'd)

<u>Figure</u>		<u>Page</u>
15	View of Constant-Head Weir Box and Loosely Coiled Copper Pipe on Wooden Frame	94
16	View of Coiled Copper Pipe, Plexiglas Pipe, Solenoid-Operated Gate Valve, and Assorted Instrumentation	98
17	Top View of Plexiglas Pipe and Solenoid-Operated Gate Valve	98
18	Close-Up View of Principal Test Section Showing Depth Gages and Pressure Transducer Mounted in Plexiglas Pipe	100
19	Enlarged View of Sample Depth Gage	100
20	Diagram of Circuit Designed for Use with a Miniature Wave Gage	102
21	Close-Up View of Dual-Channel Oscillograph Units, Camera-Equipped Oscilloscope, and Bridge Amplifier Unit	103
22	Flow-Resistance Relationships for the Copper and Plexiglas Pipes	104
23	Transient Pressures, Photographically Recorded from the Oscilloscope Cathode-Ray Tube During Laboratory Run Number 19, are Typical of the Experimental Pressures Observed at the Gate Valve	108
24	The Time-Dependent, Oscillograph Data Trace Shown at Top is Typical of the Free-Surface Flow Depths Observed at Gage Number 1 During Periods of Column Separation in the Pipe	109
25	Comparison of the Computer-Simulated, Transient Pressures with the Experimentally-Determined Pressures Observed at the Gate Valve During Laboratory Runs Numbers 25 and 34	115
26	Detailed Comparison of the Computer-Simulated Initial Pressure Rise with the Corresponding Experimentally-Determined Initial Pressure Rises for Laboratory Runs Numbers 25 and 34	117

LIST OF FIGURES (Cont'd)

<u>Figure</u>		<u>Page</u>
27	Detailed Comparison of the Computer-Simulated Second Pressure Rise with the Corresponding Experimentally-Determined Second Pressure Rises for Laboratory Runs Numbers 25 and 34	118
28	Transient Pressures Observed at Gate Valve During Laboratory Run Number 25	119
29	Transient Pressures Observed at Gate Valve During Laboratory Run Number 34	119
30	An Isometric Representation of the Computer-Simulated Transient Pressures at the Gate Valve and Concurrent Free-Surface Profiles at Selected Distances from the Gate Valve as Determined from Theoretical Considerations	123
31	An Isometric Representation of the Experimentally-Determined Transient Pressures at the Gate Valve and Concurrent Free-Surface Profiles at Selected Distances from the Gate Valve as Observed During Laboratory Run Number 25	124
32	An Isometric Representation of the Experimentally-Determined Transient Pressures at the Gage Valve and Concurrent Free-Surface Profiles at Selected Distances from the Gate Valve Due to Column Separation During Laboratory Run Number 34	125
33	Comparison of the Computer-Simulated and Experimentally-Determined, Time-Dependent, Free-Surface Profiles at Selected Gages During Periods of Column Separation in the Pipe	126
34	Computer-Simulated Sequence of Water-Surface Profiles for the Initial Period of Column Separation in the Pipe	127
35	Computer-Simulated Sequence of Water-Surface Profiles for the Second Period of Column Separation in the Pipe	128
36	Advancing Column-Separation Void Photographed During Run Number 19	130

LIST OF FIGURES (Cont'd)

<u>Figure</u>		<u>Page</u>
37	Advancing Column-Separation Void.....	130
38	Column-Separation Void in a State of Suspended Motion Just Prior to Retreat and Collapse Against Valve	131
39	Diagram Relating Static Pressure to Bubble Size	139

SYMBOLS

<u>Symbols</u>	<u>Units</u>	<u>Descriptive Identification</u>
A	ft. ²	Cross sectional area, pipe flowing full
A	ft. ²	Cross segmental area, pipe flowing partially full
a	ft./sec.	Celerity of transient pressure pulse, pipe flowing full
a		Subscript denoting ambient condition
b	ft.	Outside pipe radius
C+, C-		Characteristics curves
C ₁ , C ₂ , C ₃ , c'		Constants of integration
c, c ₁ , c ₂ , c ₃		Coefficients of pipe support and restraint
c		Subscript denoting circumferential direction
D	ft.	Inside pipe diameter
E	lb./ft. ²	Modulus of Elasticity of pipe wall
e, exp		Napierian base
f		Darcy-Weisbach frictional resistance term
f		Function notation
g	ft./sec. ²	Acceleration of gravity
g		Subscript denoting gaseous condition
H	ft.	Piezometric head (P/ρg + z)
H		Coordinate axis
H _f	ft.	Head loss due to resistance to flow
i		Counting integer or indexing subscript
J	ft.lb.	Parameter denoting air mass in bubble
K	lb./ft. ²	Bulk modulus of elasticity of liquid
k		Counting integer or indexing subscript; usually refers to pipe segment

SYMBOLS (Cont'd)

<u>Symbols</u>	<u>Units</u>	<u>Descriptive Identification</u>
L		Left grid point on x,t plane; frequently used as subscript
L		Length of an undefined pipe segment
M		Middle grid point on x,t plane; frequently used as subscript
m	sec. ⁻¹	Linear multiplier coefficient $\pm \sqrt{A/gT}$; pipe flowing partially full
m		Subscript denoting x-position
n	sec. ⁻¹	Linear multiplier coefficient $\pm g/a$; pipe flowing full
P		Grid point and intersection point of characteristics curves on x,t plane; frequently used as subscript
P _w	ft.	Wetted perimeter; pipe flowing partially full
p	lb./ft. ²	Internal pipe pressure
p	lb./ft. ²	Internal bubble pressure
p		Subscript, denotes x-length of parabolic void
q	lb./ft. ²	External pressure on pipe
R		Right grid point on x,t plane; frequently used as subscript
R	ft.	Inside pipe radius
R	ft.lb./lb./Deg.	Gas constant for air
R _H	ft.	Hydraulic radius; pipe flowing partially full
r	ft.	Radial distance
r	ft.	Cavitation nucleus radius
r		Subscript denoting radial direction
T	ft.	Free surface width; pipe flowing partially full

SYMBOLS (Cont'd)

<u>Symbols</u>	<u>Units</u>	<u>Descriptive Identification</u>
T		Coordinate axis
t	sec.	Time
t		Subscript denoting travel time
u	ft./sec.	Mean velocity; pipe flowing partially full
Ψ	ft. ³	Volume
v	ft./sec.	Mean velocity; pipe flowing full
v		Subscript denoting vapor condition
X		Coordinate axis
x	ft.	Distance measured in longitudinal space direction
Z		Coordinate axis
z	ft.	Depth of flow; pipe flowing partially full
α		Intersection point of C+ and t-grid on x,t plane; frequently used as a subscript
Γ	ft./sec. ²	Equation of motion; pipe flowing full
Γ	ft./sec.	Equation of continuity; pipe flowing full
Γ	ft./sec.	Equation of continuity; pipe flowing partially full
Γ	ft./sec.	Equation of motion; pipe flowing partially full
ϵ		Intersection point of C- and t-grid on x,t plane; frequently used as a subscript
η	ft./ft.	Strain
θ		Radial angle subtended by pipe wall element
θ		A decimal parameter
θ		Gradient angle of pipe ($x_x = -\sin\theta$)
Λ	ft./sec.	Linear sum of Γ_3 and Γ_4

SYMBOLS (Cont'd)

μ		Poisson's ratio
ξ	ft.	Radial increment of displacement
ρ	slugs/ft. ³	Liquid density
σ	lb./ft. ²	Stress
σ	lb./ft.	Surface tension
τ	lb./ft. ²	Boundary shear stress at pipe wall
Φ		Coefficient correcting K for changing pressure
φ		ψ/r
X		Coefficient for change in pipe size
Ψ		Coefficient for change in pipe size
ψ		$\sigma_r r$
Ω	ft./sec. ²	Linear sum of Γ_1 and Γ_2
R		Reynolds number

CHAPTER I

INTRODUCTION

Engineering treatment of the phenomenon of the liquid column separation frequently accompanying transient pipe flow has lacked rational interpretation in terms of the governing fluid dynamics. This study of column-separation attempts to provide better insight into the mechanics and dynamics of the phenomenon while establishing a more rational physical basis for its interpretation and analysis.

Description of Problem

Consider the liquid pressure at a point in a pipeline which is flowing full. Should this point pressure decrease, regardless of cause, to the vapor pressure of the flowing liquid, a vapor cavity will form. This vapor cavity is sometimes referred to as a vapor column. The phenomenon of vapor cavity formation is commonly referred to as a "column separation," meaning separation or interruption of the liquid column. It often occurs following rapid closure of a valve in a pipeline which is flowing full. Nevertheless, column separation may also occur under other circumstances, for instance, following propagation of a transient wave of low pressure into an elevated portion of a pipeline flowing full. Such a low-pressure wave, for example, could be caused by a sudden pump failure in a liquid transmission or distribution system. The severe damage which the high pressures associated with collapse of the vapor column can inflict upon the pipe system causes column separation to be a problem of significant engineering concern.

Certain features associated with column separation have been the cause of speculation in the past. The physical laws, for example, governing the shape and movement of the vapor column have not been adequately described. Moreover, the nature of the collapse of such a vapor column is even less well defined. Definition of these physical laws together with a broader understanding of vapor column collapse would be of appreciable aid in providing enlightened engineering design and trouble-free operation of both large and small, closed-conduit, hydraulic systems.

The problem of column separation is clearly an integral part of the much broader problem of transient liquid flow in both open and closed conduits; that is, flow in which the velocities and pressures vary with location and with time. In pipes the phenomenon of transient flow of liquids is commonly referred to by the imprecise, lay term, "water hammer." However, column separation has a unique and distinctive feature which sets it apart from the ordinary water-hammer type phenomenon. In the portion of pipe momentarily occupied by the vapor cavity, any flow of liquid occurring beneath the cavity appears to be free-surface flow, in other words, flow in which gravity would be the principal governing factor. Thus, transient flow conditions occur throughout a system composed of both closed-conduit flow (pipe flowing full) and open-channel flow (pipe flowing partially full). However, in that phase of the problem involving transient, open-channel flow, the pressure variations which occur with time and location are manifested by fluctuations of free surface head (depth of liquid) above a datum.

The motivation for the present study was the belief that pertinent information regarding the various undetermined aspects of column

separation could be qualitatively defined and quantitatively determined through the development of an experimentally-verified, mathematical model simulating transient, liquid, pipe flow with column separation.

Review of Literature

Study of transient flow in both open and closed conduits is not a new area for research in fluid dynamics in any sense of the word. To be sure, water hammer occurring in pipe flow was a topic of interest to many of the noted hydraulicians of the early and middle 19th century. However, rational physical interpretation and true understanding of this closed conduit phenomenon did not evolve until 1898 when Joukowsky⁽²⁹⁾ published his treatise on the subject. His work, an outgrowth of the experimental studies and mathematical analysis which he conducted while supervising design of the then new Moscow waterworks, provided many of the basic concepts and relationships essential to comprehension and further study of closed conduit, transient flow. Some four years later Allievi⁽¹⁾ expanded and greatly extended Joukowsky's analytic work. However, Allievi did not publish his rather extensive mathematical and graphical treatment of water hammer until 1913. Nevertheless, this work became the truly definitive study from which much of the modern day interpretative analysis of closed conduit, transient flow can be traced.

Meanwhile, during the decades after the mid 19th century, the fraternity of French hydraulicians, among them Saint-Venant, Dupuit, Bresse, and Boussinesq, were concerning themselves with the analysis of open-channel hydraulics. In 1871 Saint-Venant⁽⁴⁵⁾ presented a paper to the French Academy of Sciences which contained a form of the equation of motion for unsteady flow in open channels. Six years later in 1877 the Academy

published Boussinesq's outstanding essay on hydraulics,⁽⁷⁾ the third section of which presents an analysis of wave stability and wave propagation celerity in open channels. Taken together, these contributions provided the foundation necessary for the present day study of transient flow in open conduits.

Although the rudimentary dynamics of transient flow in both open channels and closed conduits had been more or less correctly appraised and partially formulated by the early years of the 20th century, techniques for the analysis of the phenomena still remained to be developed and applied. Drawing extensively upon Allieve's graphical methods, Bergeron⁽⁶⁾ and others expanded and applied these techniques in order to approximate solutions for various problems involving electrical, mechanical, as well as fluid transients. It is entirely anachronistic, however, to discover that in 1860, the German mathematician Riemann^(41,48,49,60) had already developed and used the then unnamed method of characteristics to achieve an explicit solution of a second order partial differential equation depicting sound-wave propagation in steady, two-dimensional air flow. An interlude of nearly 30 years passed before Massau discovered Riemann's work and transformed his solution into a graphical technique in 1889. Later, in 1900, after extending the graphical technique to apply to first order partial differential equations as well, Massau⁽³⁶⁾ published a fully-documented study of his application of the method of characteristics. It is of particular interest to note that his presentation included examples specifically treating transient, open-channel flow. Yet, despite Massau's important contribution, the potential value of the method of characteristics as a powerful tool for the explicit solution of problems concerning both open and closed conduit transient flows, remained largely unrecognized.

In fact, the basic physical and mathematical similarity of the two flow situations--the transient, pressure-wave phenomenon in pipes on the one hand and the transient, gravity-wave phenomenon in open channels on the other--was only vaguely appreciated.

Meanwhile, Thomas,⁽⁵⁸⁾ in a particularly noteworthy paper, attacked the open-channel, flood-routing problem as truly a problem in transient flow. Starting with the fundamental partial differential equations for unsteady flow, he outlined a tentative procedure for their numerical solution. Stoker, treating the same problem, outlined an implicit procedure⁽⁵⁶⁾ based upon an iterative solution of the partial difference equations. Drönkers⁽¹⁵⁾ and Schönfeld,⁽⁴⁷⁾ studying the closely related problem of tide-induced, transient flow in estuaries, outlined a solution technique employing power series as well as one based upon characteristics. Chow⁽¹⁰⁾ presented a graphical solution based upon the method of characteristics as first developed by Lin.

However, all of the above-mentioned solution techniques for handling problems in both open and closed conduit transient flow suffer from one common and very serious drawback; namely, an overwhelming amount of very tedious, exacting, and extremely time-consuming computation. This formidable drawback has been all but eliminated within the past decade by the introduction and rapid development of the high speed digital computer and sophisticated computer programming languages. It is now economically practicable as well as technically feasible to solve a great variety of transient flow problems by digital computer techniques as evidenced by the recent technical literature.^(4,5,21,30,53,54,55)

During the first half of the 20th century Allievi's analysis of water hammer was refined and the graphical techniques which he and Bergeron had devised were tediously applied to a variety of practical, closed-conduit, transient-flow problems.^(2,28,37,39,42,52) It was the treatment of certain of these practical problems which began to focus attention upon the specific phenomenon of liquid column separation and the associated free-surface flow taking place beneath the resulting vapor cavity.^(31,43) A search of the literature, however, evidences little actual investigation of the mechanics of column separation in transient flow systems. Recent publications by Li^(32,33) and by Walsh⁽³⁴⁾ are notable exceptions. In 1962 Li presented a theoretical treatment of column separation in a pipe of rectangular cross section with frictionless flow. Although several different separation conditions were considered, cavity behavior was treated as an isolated phenomenon rather than a phenomenon integrally dependent upon the transient flow conditions prevailing throughout the entire conduit system. No experimental verification of the analysis was presented in the paper. The chief result of this study appeared to be that the form of the separation void has little bearing on the magnitude of the resulting pressure decay. Heath⁽⁸⁾ also studied column separation accompanying the rapid closure of a valve located at the end of a long pipe. However, flow in the pipe was assumed to be frictionless and an equivalent friction loss was inserted in the graphical analysis.

In a subsequent paper Li and Walsh reported their investigation of the maximum pressure resulting from the collapse of the vapor cavity. Escande⁽¹⁸⁾ treats column separation occurring in a penstock subject to instantaneous valve closure by using graphical means. However, neither

the growth nor the collapse of the vapor cavity, nor the dynamics of the flow beneath the cavity is adequately treated in the investigations mentioned above. What is perhaps more significant is that the cavity resulting from the liquid column separation was not interpreted as a manifestation of free-surface, open-channel, transient flow occurring adjunctly and simultaneously with closed conduit transient flow in the same pipe system.

In recent years considerable interest has developed concerning the dynamic conditions and liquid properties prevailing at the inception of cavitation. As a result of their investigation of the roles of air diffusion and liquid tensile stresses upon incipient cavitation, Parkin and Kermeen⁽³⁸⁾ have shown that air diffusion in flowing water is responsible for the growth of microscopic bubbles on the solid boundaries in a region where the pressure is slightly greater than vapor pressure. Moreover, the microscopic air bubbles serve as nuclei for the explosive growth of vapor cavities as the pressure decreases, according to Ripken and Killen.⁽⁴⁴⁾ Other apparent properties of incipient cavitation are presented by Stepanoff and Kawaguchi⁽⁵⁰⁾ and by Hooper.⁽²⁷⁾

Scope of Investigation

This study of column separation may be divided into two major phases. The first phase treats the theoretical analysis and analytical interpretation of the problem of transient liquid flow with column separation; the second phase concerns the accompanying experimental investigations.

A theoretical interpretation of the problem of column separation is presented in Chapter II. The fundamental, quasilinear, partial differential equations representing one-dimensional, transient, liquid motion

in pipes as well as in open channels are derived and reviewed in Chapter III. The friction losses encountered in both types of flow are included in the respective sets of equations. Techniques for evaluating these sets of equations, based upon numerical interpretations of the method of characteristics for first-order, hyperbolic, partial differential equations, are also developed and presented in Chapter III.

The two sets of partial differential equations together with the respective evaluation techniques provide the basic building blocks used to formulate the mathematical model simulating transient liquid flow with column separation. Chapter IV is devoted to formulation of this model in terms of an operational program for high-speed digital computer. The functions and operating sequence of the model are presented in a flow chart. The digital computer program together with all major subroutines and supporting programs are presented in Appendices I and II, respectively.

The flow system employed in the second or experimental phase of the study was specifically designed to facilitate the laboratory measurement of column separation. A rapid-closing, solenoid-operated, gate valve was employed in order to produce column separation and to fix its initial occurrence within the system to a face of the gate in the solenoid-operated valve. Although column separation could certainly have been induced at the downstream face of the valve gate, the incipient formation of the vapor cavity would tend to take place while the gate was still in the process of closing. Moreover, flow separation on the downstream face of the gate could seriously disturb the liquid flow pattern. Clearly, these conditions could lead to distortion of the ultimate shape of the vapor cavity. In order to avoid this possibility, a flow system was selected

consisting of a long pipe leading from a constant-level, low-head reservoir to an elevated position. The solenoid gate-valve was situated at the end of an elevated, horizontal section of pipe. A short return pipe connected the valve to a sump. Flow was maintained by syphon action such that column separation would occur without cavity distortion at the upstream face of the gate of the solenoid-operated valve following abrupt valve closure. The separation phenomenon was achieved once the initial wave of high pressure produced at the moment of valve closure had propagated from the valve to reservoir, and the counterpart, low-pressure wave had propagated back to the valve. Water was used as the liquid throughout the laboratory investigation. Column separation was confined to the elevated section of horizontally-mounted pipe. A detailed discussion of the experimental apparatus, of the instrumentation used in measuring column separation, and of the measurements themselves is presented in Chapter V.

In order to acquire specific information about column separation from the mathematical model, it must be activated and numerically evaluated by the digital computer for the particular set of bounding parameters delineating the experimental flow system being investigated in the laboratory. Chapter VI presents a comparison of the analytic and experimental results obtained for various laboratory conditions. A discussion of the findings and some concluding remarks are also contained in Chapter VI. Chapter VII briefly summarizes the principal conclusions derived from the study.

All apparatus used in the experimental phase of the study was assembled and all experimental work conducted in the G. G. Brown Fluids Engineering Laboratory at The University of Michigan. The digital computer

program and associated subroutines were written in MAD, the Michigan Algorithm Decoder language,⁽³⁾ and executed on an IBM 7090/1410 digital computing system at The University of Michigan Computing Center.

CHAPTER II
THEORETICAL ANALYSIS

Contrary to what one might deduce from literal interpretation of the term "column separation," complete physical interruption of liquid flow in a horizontal pipe does not take place for the magnitudes of transient pressures and velocities ordinarily encountered in horizontal closed conduit fluid systems. In fact, once nascent development of a vapor cavity has occurred at a point in the pipe, the cavity expands and propagates in the direction of flow as an elongated "bubble." A typical example of a vapor cavity resulting from column separation in water flow in a horizontal pipe is shown in Figure 1. While the vapor cavity occupies the upper volume segment within the pipe, liquid continues to flow with a free surface in the lower volume segment.

With identification and recognition of the typical physical circumstances commonly encountered with column separation, two key questions immediately come to mind. These questions are the following:

- (a) Once a vapor cavity has formed and the liquid has pulled away from the uppermost, inner surface of the pipe, is not the flow which is occurring beneath the cavity simply free-surface, gravity flow?
- (b) If time is measured from the moment of column separation, must not the volume of the vapor cavity at any subsequent instant be equivalent to the accumulated volume of liquid discharged through the pipe just ahead of the cavity?

Deductive reasoning and rational analytic interpretation of the column separation phenomenon seem to indicate that the answer to both of these questions is unquestionably affirmative.

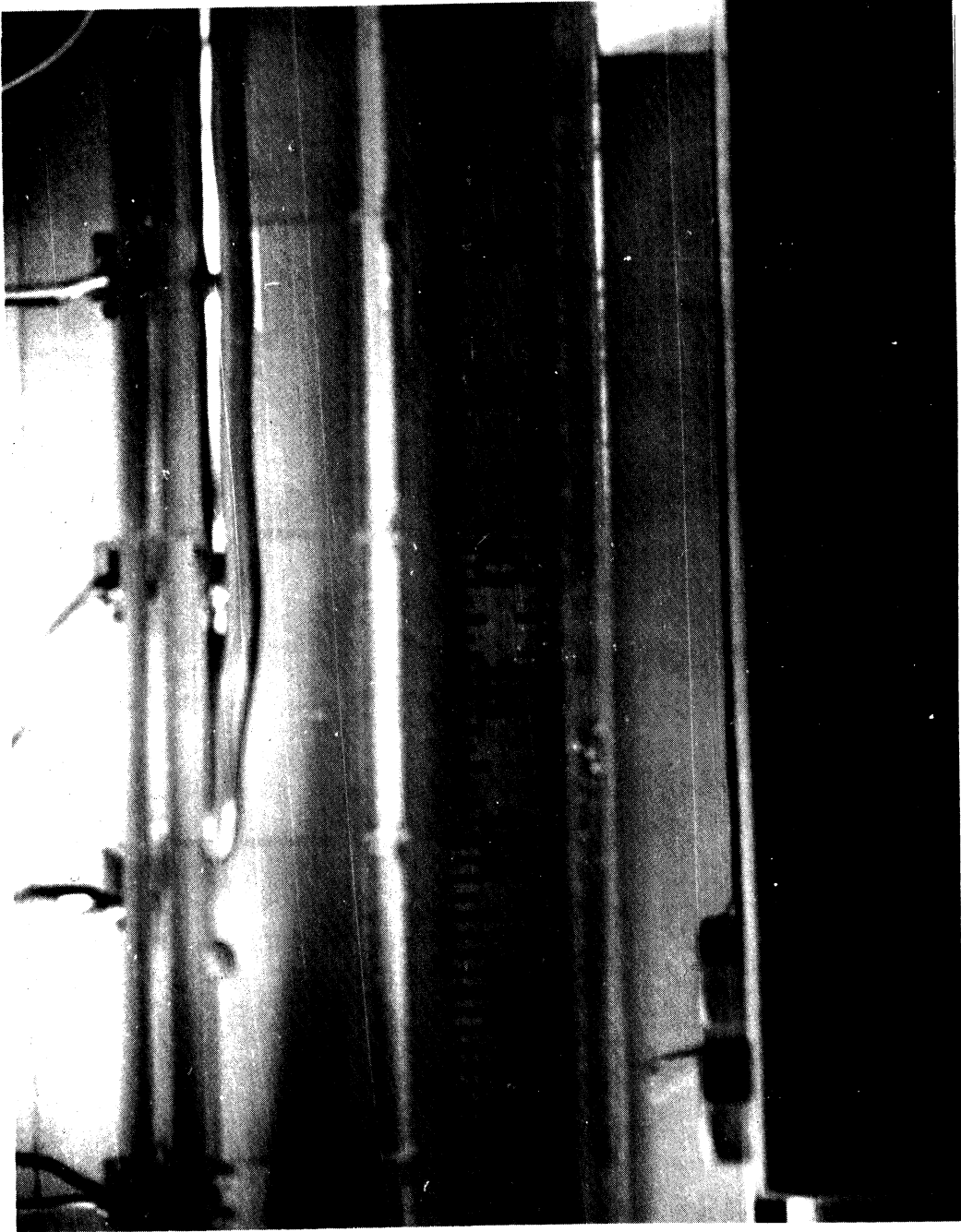


Figure 1. Photograph of a Typical Vapor Cavity Accompanying Column Separation.

Although a surface tension mechanism must appreciably influence the actual separation of the liquid from the inner surface of the pipe wall, the effects of this mechanism can only be very local and temporal at best. Once separation has occurred and a free liquid surface exists, the remaining forces--namely, gravity and fluid friction forces--must be the principal forces acting upon the flow. Of course, the flowing liquid continues to have momentum. Therefore, one may hypothesize that the flow occurring beneath the vapor cavity is simply unsteady, open-channel flow in a circular conduit. More specifically, the free-surface, gravity flow produced by column separation is hypothesized to be analogous to a negative surge wave in an open channel of circular section.

Meanwhile, pipe flow ahead of the vapor cavity is assumed to continue as full-pipe flow. One may further hypothesize that transient conditions continue to govern the flow in this portion of the pipe system. However, the magnitude of the pressure fluctuations must rapidly diminish as a result of the change in the boundary conditions introduced by the vapor cavity. In fact, liquid motion in the portion of the pipe which continues to flow full must approximate surge flow.

By way of illustration consider a reservoir and a quick-closing gate valve connected by a long, horizontal pipe. Let the reservoir be exposed to atmospheric pressure as shown in Figure 2. The mean velocity of flow in the pipe system is v while the pressure is $p = \gamma(h_0 - h_f)$ in which γ is the specific weight of the liquid, h_0 is the head of liquid in the reservoir, and h_f the head loss created by fluid friction in the pipe. If the gate valve at point C is abruptly closed at time t_0 , transient flow conditions are created in the pipe. A positive (high pressure) wave

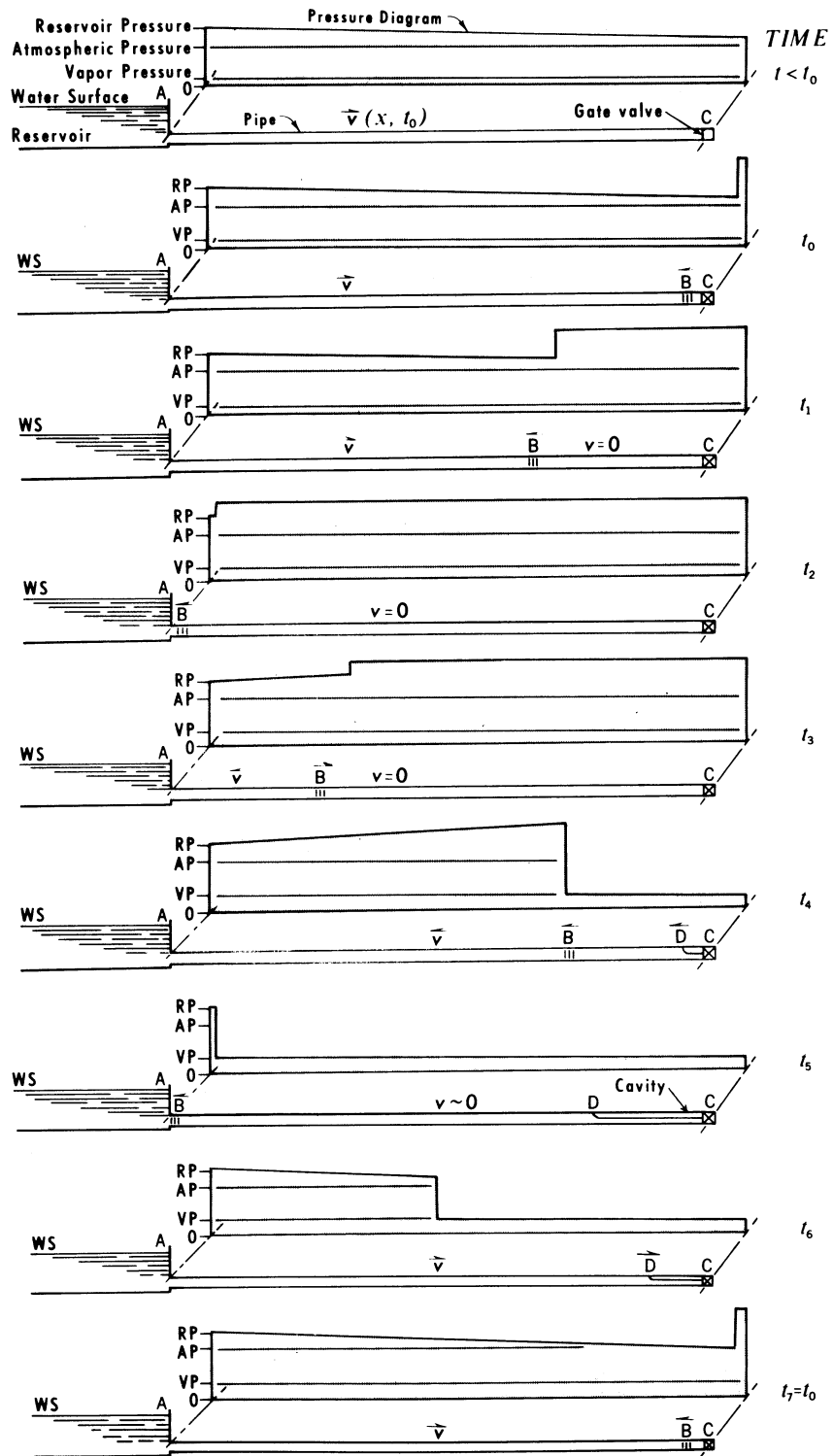


Figure 2. Schematic Time-Sequence Representation of Column Separation and Pressure Pattern in a Pipe System Undergoing Transient Flow.

caused by the rapid deceleration of the liquid propagates from point C toward the reservoir at point A as indicated by the wave front at B . At time t_1 flow from the reservoir continues with undiminished velocity toward B . However, between B and C the velocity is reduced to nearly zero; the pressure, which greatly exceeds p , compresses the liquid and tends to expand and, in some instances, elongate the pipe segment. When the positive pressure wave reaches A at time t_2 , the pressure is abruptly reduced to the sustaining pressure of the reservoir. The compressed liquid in the pipe begins to expand and starts flowing toward A . The pressure between A and B returns to p as the pressure-drop, delimited by the wave front B propagates toward C at time t_3 . However, when the pressure drop reaches C , the entire column of liquid, AC , is moving toward A with velocity v . Because the gate at point C remains closed, the water column abruptly decelerates and the pressure decreases below p . A negative (low pressure) wave tends to develop, but because the pressure becomes less than the vapor pressure of the liquid, a vapor cavity is assumed to occur at the uppermost point on the valve gate at C and column separation takes place at time t_4 . The cavity expands until at time t_5 the transient velocity in the segment of pipe flowing full, that is, segment AD , becomes zero. Meanwhile, unsteady, free surface flow has been occurring beneath the cavity in the pipe segment DC . However, the differential pressure between the reservoir and the vapor cavity causes the liquid column, AD , to flow toward C as indicated at time t_6 , thereby initiating the imminent collapse of the vapor cavity. At time t_7 the vapor cavity collapses and conditions in the system are again equivalent to those which occurred at t_0 . The

phenomenon will continue to repeat itself, although diminished in magnitude by the energy losses caused by fluid friction, until the pressure fails to drop below vapor pressure and column separation fails to occur.

The above description of the sequence of physical events--though admittedly somewhat oversimplified and idealized--provides a basic familiarity with the transient-flow, column-separation phenomena as encountered in the experimental system.

A more penetrating and detailed analysis of these phenomena leads one to hypothesize circumstances which could bring about the genesis, growth, and collapse of the vapor cavity anticipated at time t_4 in the above system. Because the causative drop in pressure first takes place at the gate valve, it is reasonable to assume that cavitation will originate at the point of lowest pressure on the upstream face of the valve gate. The actual point of origin is probably at the topmost intersection of the vertical valve gate with the upstream port in the valve itself. As the pressure rapidly drops below atmospheric pressure and approaches the vapor pressure of the water, one or more undissolved microscopic air cavities--air nuclei--attached to the uppermost edge of the gate or to particulate matter in the flow begin to expand. Molecules of free gaseous air coming out of solution in the immediate vicinity of the point of lowest pressure enter the bubble and help to increase its size. Mutual coalescence takes place between adjacent bubbles and the larger resultant bubbles continue to expand until one is of sufficient magnitude that the difference between its internal pressure and the decreasing external pressure is enough to offset the surface-tension pressure which is inversely proportional to its size. Once this threshold size is reached,

the bubble will expand explosively as a water-vapor-filled cavity. Calculations show that the threshold bubble diameter must exceed approximately 8×10^{-4} inches (20 microns) in order for vapor cavity expansion to occur at pressures normally encountered in practical situations. It is quite probable that for a fleeting moment the water undergoes tensile stress (as demonstrated⁽³⁸⁾ in recent water tunnel experiments) until the nascent bubble can sustain explosive cavitation after which the pressure reverts to the vapor pressure of the liquid water. The complete hypothesized sequence of events, starting with the rapid drop in pressure and concluding with the onset of the explosive growth of the vapor cavity, occurs, of course, in a very brief time span--probably a few milliseconds in duration at most.

During the same time interval in which cavitation is initiated, the horizontal column of water (denoted by AC, Figure 2) starts to undergo deceleration of its flow upstream, toward the reservoir. This deceleration, of which the pressure drop responsible for inception of cavitation is but a manifestation, first occurs in the water adjacent to the gate valve. Although the considerable momentum of the water moving as a column tends to cause it to separate from the vertical face of the gate, the change in momentum caused by the deceleration of the flow is ordinarily insufficient to completely overcome gravitational effects. As a result the tendency for column separation at the gate is satisfied by the explosive growth of the nascent air bubble into a water-vapor cavity occupying the topmost segment of the pipe. Gravity causes some of the decelerating flow to remain in the bottom segment of the pipe and in contact

with the gate. The upstream flow in the pipe continues to decelerate as the front of the pressure wave, B, delimiting the drop to vapor pressure propagates toward the reservoir. Meanwhile the vapor cavity, advancing (D) behind this wave front and seemingly tearing the water from the topmost inner surface of the pipe wall, expands to occupy a volume equivalent to the volume vacated by the receding full-pipe flow. Surface tension may have some nominal effect upon the shape of the advancing edge of the cavity.

Ultimately, the forces created by the frictional resistance to flow and by the differential pressure between the reservoir and the vapor cavity bring water column AD to a momentary rest. At the same time the free-surface, transient flow taking place beneath the cavity (DC) gradually diminishes to a minimum. The vapor cavity will achieve its maximum expansion at the moment of rest. But because the differential pressure force continues to act, the water in column AD now reverses direction and begins to flow downstream toward the gate valve. Conditions are now right for collapse of the vapor cavity. As column AD accelerates in the downstream direction, one hypothesizes that the interface between the vapor cavity and the water column becomes a surging, free-surface front. Although surface tension is believed to be a factor of nominal overall effect, it is assumed to aid reattachment of this free surface to the pipe wall. Moreover, the total volume of the cavity decreases at the same rate at which full-pipe flow is occurring at D. At the instant of total collapse of the water-vapor cavity, the abrupt deceleration of the water column by the closed gate valve once again produces high pressures at time t_7 . The minute volume of gaseous air which initiated

cavity formation is readily forced back into solution, and, except for the loss of energy expended to overcome flow friction, conditions in the system at time t_7 are analogous to those at time t_0 .

Now that the theoretical concepts of transient pipe flow with column separation have been hypothesized and explicitly set forth, the analytic conditions believed to describe and govern these phenomena can be ascribed. This is done in the following chapter.

CHAPTER III

ANALYTIC INTERPRETATION AND EVALUATION PROCESS

Derivations of the basic differential equations describing transient liquid motion, first in a pipe flowing full and then in a horizontal pipe flowing partially full, are given in this chapter. Flow is simulated mathematically according to conventional one-dimensional analysis in which the longitudinal space-dimension and time are the independent variables governing analysis.

Several underlying assumptions are needed to provide a foundation and a starting point from which to undertake theoretical analysis of column separation in transient pipe flow. These assumptions concern the physical properties of the liquid, the physical properties of the pipe material, and the kinematics of the flow:

- (a) The fluid used in the flow system is elastic and of homogeneous density when in its liquid state.
- (b) The minute fluctuations of the liquid vapor pressure, resulting from the latent heat of vaporization and occurring at the instant of vapor-cavity formation or collapse, are insignificant by comparison with the difference between atmospheric pressure and vapor pressure.⁽³³⁾ Therefore, these pressure fluctuations may be, and in fact, are disregarded.
- (c) The pipe is constructed of a sectionally homogeneous, isotropic, elastic solid in which the stresses never exceed the yield point of the material.

- (d) The velocity and the pressure in the pipe when flowing full are considered to be uniformly distributed over any cross section transverse to the pipe, with the result that the flow may be treated as one-dimensional, closed-conduit flow.
- (e) The velocity in the pipe when flowing partially full is considered to be uniformly distributed over any transverse cross segment of flow. Moreover, vertical accelerations of the water surface are considered to be insignificant, implying that hydrostatic pressure prevails, and thereby permitting the flow to be treated as one-dimensional, open-channel flow.
- (f) The frictional resistance encountered with transient flow, whether it be in a closed conduit or in an open channel, is assumed to be proportional to some power of the mean velocity in a cross section (or segment) transverse to the flow. The extent to which frictional resistance may be dependent upon the transient character of the flow is believed nominal^(14,46) and is disregarded.
- (g) Surface tension forces in the regions where the free water surface intersects the solid, pipe-wall boundary are assumed to be of insignificant overall effect and are disregarded. This assumption is somewhat less valid for pipes of small diameter.

In deriving each of the sets of partial differential equations according to the assumptions set forth above, elements of water are considered which are bounded by two fixed planes normal to the longitudinal

axis of flow. Discharge and velocity are assumed to be positive when water is flowing in the positive x direction. A pipe having finite wall thickness is considered in the derivation of the equations describing transient liquid motion in the pipe flowing full. The laws of conservation of mass and conservation of momentum govern the derivation of the equation of continuity and the equation of dynamic equilibrium, respectively, for both regimes of flow.

Once the sets of partial differential equations describing transient liquid motion have been derived, they are recognized to be of the hyperbolic type and are then transformed into sets of total differential equations which are valid along their respective "characteristics" curves. These sets--one set for the pipe flowing full and another for the pipe flowing partially full--are then expressed as sets of finite difference equations readily amenable to solution by high-speed, digital computer. The actual finite difference technique used in developing the computer solution is an adaptation of the specific time interval procedure advanced by Hartree and others. (11,12,19,20,21,25,26,35) Initial values obtained from steady flow conditions, together with expressions for the various boundary conditions encountered at the valve, at junctions between pipes, and at the reservoir make an explicit solution possible.

Equations of Transient Motion--Pipe Flowing Full

Transient motion in a pipe flowing full is a function of two independent variables. These variables are the space and time coordinates, x and t , respectively. Let x be the axial location measured along the pipe from some arbitrarily fixed reference point. Two quasi-linear partial differential equations are written to represent the transient

velocities and pressures in the pipe. Once derived these relationships are transformed into a set of four total differential equations which are the so-called "characteristic" equations. The characteristic equations are subsequently written as finite difference equations after which numerical methods are introduced and a solution technique developed to permit their evaluation by high-speed, electronic digital computer. The appropriate boundary conditions which govern the solution are examined and set forth.

Equation of Continuity

The equation of continuity states that the net mass inflow per unit time into a pipe segment is equal to the time rate of mass increase taking place within the segment. This statement is premised upon the concept of the conservation of mass. A typical control segment of a pipe that is flowing full is shown in Figure 3.

If v is the average velocity and ρ the density of the liquid flowing into the segment (Figure 3) then the mass influx per unit time is ρAv , where A is the cross-sectional area at (1). At cross section (2) the efflux of mass from the segment is given by

$$\rho Av + \frac{\partial(\rho Av)}{\partial x} dx .$$

The net mass inflow into the segment is

$$\rho Av - [\rho Av + \frac{\partial(\rho Av)}{\partial x} dx]$$

or

$$- \frac{\partial(\rho Av)}{\partial x} dx . \quad (1)$$

The total mass in the segment is $\rho A dx$. Therefore, the time rate of mass increase occurring within the segment is

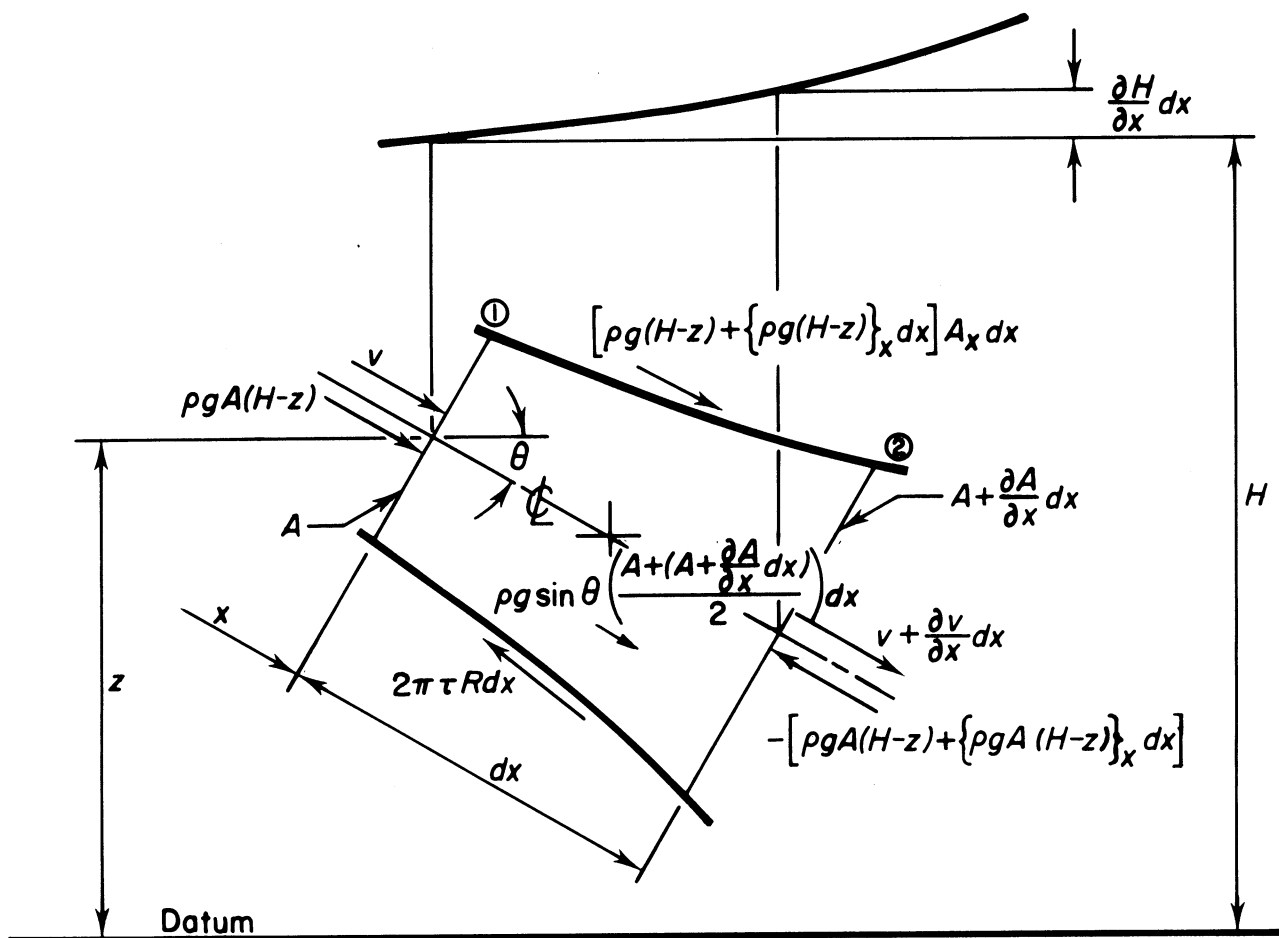


Figure 3. Definition Sketch Showing Transient Conditions in Pipe Segment Flowing Full.

$$\frac{\partial(\rho A dx)}{\partial t} . \quad (2)$$

Equating the expressions given by Equation (1) and (2) according to the definition above, one has

$$- \frac{\partial(\rho A v)}{\partial x} dx = \frac{\partial(\rho A dx)}{\partial t} \quad (3)$$

Normally, x is independent of t and, therefore, $\frac{\partial(dx)}{\partial t}$ is zero.

However, if the pipe is supported in such a manner that the pipe segment is subject to axial strain, η_x , then $\frac{\partial(dx)}{\partial t} = \frac{d\eta_x}{dt} dx$. In this expression η represents the strain; the subscript x , the direction. Consequently, expansion of Equation (3), subsequently divided by the mass of the fluid element, $\rho A dx$, results in the expression

$$v_x + v \frac{A_x}{A} + v \frac{\rho_x}{\rho} + \frac{A_t}{A} + \frac{\rho_t}{\rho} + \frac{d\eta_x}{dt} = 0 \quad (4)$$

or by rearranging

$$\frac{1}{\rho} (v\rho_x + \rho_t) + \frac{1}{A} (vA_x + A_t) + v_x + \frac{d\eta_x}{dt} = 0 . \quad (5)$$

Here the subscripts x and t denote partial differentiation with the respective variable. However, since

$$\frac{d\rho}{dt} = \frac{\partial\rho}{\partial x} \frac{dx}{dt} + \frac{\partial\rho}{\partial t}$$

or simply

$$\frac{d\rho}{dt} = v\rho_x + \rho_t ,$$

and, similarly, because

$$\frac{dA}{dt} = vA_x + A_t ,$$

Equation (5) may be written

$$\frac{1}{\rho} \frac{d\rho}{dt} + \frac{1}{A} \frac{dA}{dt} + v_x + \frac{d\eta_x}{dt} = 0 . \quad (6)$$

The essential task, now, is to represent the liquid density and the pipe cross-sectional area changes with respect to time as functions of the velocity of the flow and the pressure. First, by recalling that the bulk modulus of elasticity for liquids denoted by K is defined as

$$K = - \frac{dp}{d\bar{v}/\bar{v}} = \frac{dp}{d\rho/\rho} , \quad (7)$$

where p is the pressure and \bar{v} is the volume, one can rewrite Equation (7) as

$$\frac{d\rho}{\rho} = \frac{dp}{K} . \quad (8)$$

Subsequent differentiation with respect to time gives

$$\frac{1}{\rho} \frac{d\rho}{dt} = \frac{1}{K} \frac{dp}{dt} . \quad (9)$$

In order to treat the change in the cross-sectional area of the pipe, consider the circumferential strain to be given by η_c . Therefore, the increase in the cross-sectional area with time is given by

$$\frac{dA}{dt} = \frac{d\eta_c}{dt} (2\pi R)R = \frac{d\eta_c}{dt} 2\pi R^2 = 2A \frac{d\eta_c}{dt}$$

or

$$\frac{1}{A} \frac{dA}{dt} = 2 \frac{d\eta_c}{dt} . \quad (10)$$

Thus, Equation (6) becomes

$$\frac{1}{K} \frac{dp}{dt} + 2 \frac{d\eta_c}{dt} + v_x + \frac{d\eta_x}{dt} = 0 . \quad (11)$$

The magnitudes of the various terms in the continuity equation clearly depend upon the radial or the circumferential strain. But the circumferential strain depends upon the physical characteristics of the pipe itself, as well as upon the restraint to deformation imposed by the particular manner in which it is supported. In order to evaluate the terms $d\eta_c/dt$ and $d\eta_x/dt$, a general expression must be developed in which the physical characteristics of the pipe and its support conditions are treated as parameters.

The relationship between stress and strain is commonly given by $\text{Stress}/E = \text{Strain}$, where E is the modulus of elasticity of the pipe wall material. Moreover, stresses in any one direction create strains in the two other normal directions according to Poisson's ratio, μ . Thus, the following relationships can be written to express the radial, circumferential, and axial pipe strains in terms of their appropriate stresses:

$$\eta_r = \frac{1}{E} [\sigma_r - \mu(\sigma_c + \sigma_x)] \quad (12)$$

$$\eta_c = \frac{1}{E} [\sigma_c - \mu(\sigma_r + \sigma_x)] \quad (13)$$

$$\eta_x = \frac{1}{E} [\sigma_x - \mu(\sigma_r + \sigma_c)] \quad (14)$$

The term, σ , denotes stress; the subscripts r , c , and x denote the principal directions. These relationships provide the connecting link which will subsequently allow Equation (11) to be rewritten in terms of velocities and pressures. (9,40,59)

Consider the stressed element located within the pipe wall shown in Figure 4. The element, which is denoted by $abcdefgh$, has the length, the curved-width, and the thickness dimensions, d_x , $rd\theta$, and dr ,

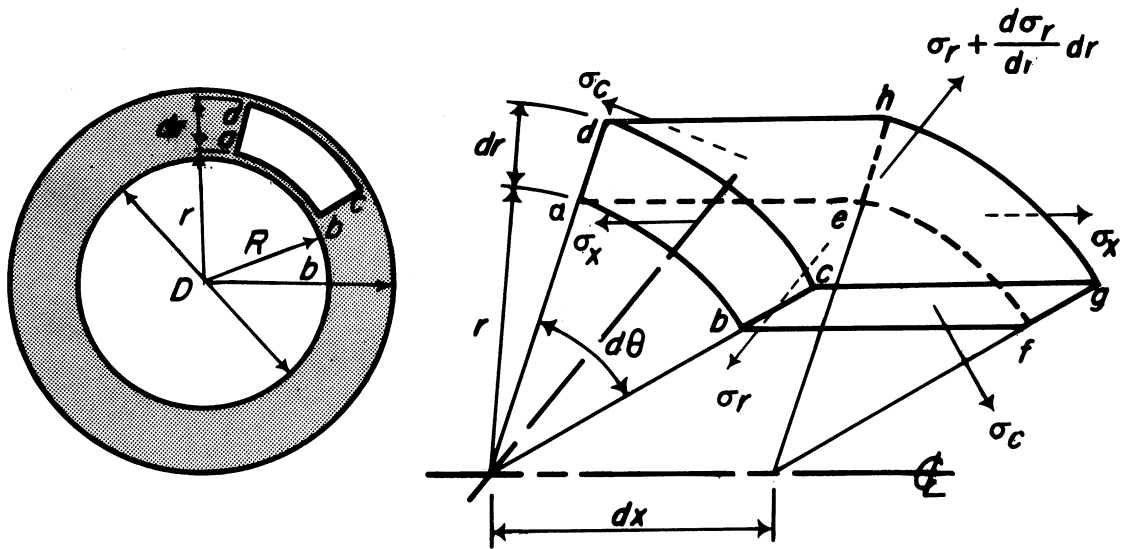


Figure 4. Definition Sketch Depicting Stressed Element Located Within Pipe Wall. Transverse Cross-Section is Shown on the Left and Three Dimensional Enlargement is Shown on the Right.

respectively. In Figure 4, $d\theta$ is the radial angle subtended by the element, r is the radial distance to the element measured from the axis of the pipe, R is the inside pipe radius, and b is the outside pipe radius.

When considering the open-ended element shown in Figure 4, one must be mindful of two basic conditions which are assumed valid:

- (a) The axial strain created by the radial stress is constant.
- (b) Displacement perpendicular to the axis is radial and dependent only upon the radius.

The unstrained radial distance to the particle is r . Let its strained radial distance be given by $r + \xi$ where ξ is the total increment of displacement in the radial direction. Thus, the radial strain is

$$\eta_r = \frac{d\xi}{dr},$$

while the circumferential strain is

$$\eta_c = \frac{\xi}{r}.$$

The axial strain is a constant,

$$\eta_x = \text{constant}.$$

The summation of forces acting upon the element $abcdefgh$, in which the outward direction of the radial bisector in Figure 4 is taken to be positive, is

$$\sigma_r r d\theta + \sigma_c dr \frac{d\theta}{2} + \sigma_c dr \frac{d\theta}{2} - \left(\sigma_r + \frac{d\sigma_r}{dr} dr\right)(r+dr)d\theta = 0$$

or

$$\sigma_r r d\theta + \sigma_c dr d\theta - \sigma_r r d\theta - \sigma_r dr d\theta - \frac{rd\sigma_r}{dr} dr d\theta - \frac{d\sigma_r}{dr} (dr)^2 d\theta = 0$$

or, after combining like terms, eliminating higher order terms, and dividing by $dr d\theta$

$$\sigma_c - \sigma_r - r \frac{d\sigma_r}{dr} = 0 .$$

Reduced to simplest terms

$$\sigma_c = \frac{d(r\sigma_r)}{dr} . \quad (15)$$

Equations (12-14) can be rewritten as follows:

$$\sigma_r - \mu(\sigma_c + \sigma_x) = \eta_r E = E \frac{d\xi}{dr} \quad (16)$$

$$\sigma_c - \mu(\sigma_r + \sigma_x) = \eta_c E = E \frac{\xi}{r} \quad (17)$$

$$\sigma_x - \mu(\sigma_r + \sigma_c) = \eta_x E = \text{constant} . \quad (18)$$

However, by rewriting Equation (17) as

$$r\{\sigma_c - \mu(\sigma_r + \sigma_x)\} = E\xi$$

and then differentiating with respect to r ,

$$\{\sigma_c - \mu(\sigma_r + \sigma_x)\} + \frac{d}{dr} \{\sigma_c - \mu(\sigma_r + \sigma_x)\} = E \frac{d\xi}{dr} , \quad (19)$$

one can eliminate $E \frac{d\xi}{dr}$ from Equation (16) and (19). This is now done.

Let $\psi = \sigma_r r$ in Equation (16) and (19):

$$\begin{aligned} \frac{\psi}{r} - \mu \left(\frac{d\psi}{dr} + \sigma_x \right) &= \frac{d}{dr} \left(r \frac{d\psi}{dr} - \mu r \sigma_x - \mu \psi \right) \\ \frac{\psi}{r} - \mu \frac{d\psi}{dr} - \mu \sigma_x &= r \frac{d^2\psi}{dr^2} + \frac{d\psi}{dr} - \mu r \frac{d\sigma_x}{dr} - \mu \sigma_x - \mu \frac{d\psi}{dr} \end{aligned}$$

$$r \frac{d^2\psi}{dr^2} + \frac{d\psi}{dr} - \frac{\psi}{r} = \mu r \frac{d\sigma_x}{dr} . \quad (20)$$

Differentiation of Equation (18) with respect to r produces

$$\frac{d\sigma_x}{dr} - \mu \frac{d(\sigma_r + \sigma_c)}{dr} = 0$$

or, written in terms of ψ ,

$$\frac{d\sigma_x}{dr} = \mu \left(\frac{1}{r} \frac{d\psi}{dr} - \frac{\psi}{r^2} + \frac{d^2\psi}{dr^2} \right) \quad (21)$$

Therefore, using Equation (21) one may write

$$\mu r \frac{d\sigma_x}{dr} = \mu^2 \left(\frac{d\psi}{dr} - \frac{\psi}{r} + r \frac{d^2\psi}{dr^2} \right) ,$$

which when substituted into Equation (20) produces the homogeneous linear differential equation

$$\left(\frac{d^2\psi}{dr^2} + \frac{1}{r} \frac{d\psi}{dr} - \frac{\psi}{r^2} \right) (1-\mu^2)r = 0 \quad (22)$$

By letting $\psi = r\phi$ for which $\psi' = r\phi' + \phi$ and $\psi'' = r\phi'' + 2\phi'$, Equation (22) may be solved in the following manner:

$$r\phi'' + 2\phi' + \phi' + \frac{\phi}{r} - \frac{\phi}{r} = 0$$

$$\phi'' + \frac{3}{r} \phi' = 0 .$$

The integration factor for this equation is $\exp\left[\int \frac{3}{r} dr\right] = \exp(3 \ln r) = e^{\ln r^3} = r^3$, thus

$$r^3\phi'' + 3r^2\phi' = 0 \quad (23)$$

for which the exact differential is $r^3\phi'$. In order for Equation (23) to be valid $r^3\phi'$ must equal a constant. Thus,

$$\varphi' = \frac{C_1}{r^3}$$

and

$$\varphi = \int \varphi' dr = -\frac{C_1}{2r^2} + C_3 = \frac{C_2}{r^2} + C_3 .$$

But because $\varphi = \frac{\psi}{r}$, it is possible to write

$$\psi = \frac{C_2}{r} + rC_3$$

and since $\sigma_r = \frac{\psi}{r}$,

$$\sigma_r = C_3 + \frac{C_2}{r^2}, \quad (24)$$

and from Equation (15)

$$\sigma_c = \frac{d(r\sigma_r)}{dr} = C_3 - \frac{C_2}{r^2}. \quad (25)$$

Once the constants C_3 and C_2 are evaluated, the circumferential and radial stress terms will become known.

Let $\sigma_r = -p$ when the internal pipe pressure is p and the inner radius is R . By the same token let $\sigma_r = -q$ when the pressure acting upon the pipe externally is q and the outer pipe radius is b . Then one can write

$$p - q = \frac{C_2}{b^2} - \frac{C_2}{R^2} = C_2 \left(\frac{R^2 - b^2}{R^2 b^2} \right)$$

or

$$C_2 = \frac{(p-q)R^2 b^2}{R^2 - b^2}. \quad (26)$$

Consequently, evaluation of C_3 is readily accomplished using Equation (24).

$$-p = C_3 + \frac{(p-q)R^2b^2}{(R^2-b^2)R^2}$$

or

$$C_3 = - \left(\frac{pR^2 - pb^2 + pb^2 - qb^2}{R^2 - b^2} \right) = \frac{qb^2 - pR^2}{R^2 - b^2} \quad (27)$$

Thus, the radial and circumferential stress relationships may be written

$$\sigma_r = \frac{1}{b^2 - R^2} \left[pR^2 - qb^2 + \frac{R^2b^2}{r^2} (q-p) \right] \quad (28)$$

$$\sigma_c = \frac{1}{b^2 - R^2} \left[pR^2 - qb^2 - \frac{R^2b^2}{r^2} (q-p) \right] \quad (29)$$

Note, also, that the combined stress term,

$$\sigma_r + \sigma_c = 2 \frac{(pR^2 - qb^2)}{b^2 - R^2},$$

is independent of both the circumferential and the axial positions; thus, σ_x is truly a constant at any cross section as originally postulated.

Clearly, there are several methods by which a section of pipe may be supported. But it should be just as apparent that the tolerable, pressure-induced strains are governed in large measure by the support conditions. Using Equation (12) and (14), one can write the relationship given in Equation (11) in terms of the appropriate stress conditions:

$$\frac{1}{K} \frac{dp}{dt} + \frac{2}{E} \left[\frac{d\sigma_c}{dt} - \mu \left(\frac{d\sigma_r}{dt} + \frac{d\sigma_x}{dt} \right) \right] + v_x + \frac{1}{E} \left[\frac{d\sigma_x}{dt} - \mu \left(\frac{d\sigma_r}{dt} + \frac{d\sigma_c}{dt} \right) \right] = 0 \quad (30)$$

Let the external pipe pressure, q , be considered zero. Equation (30) may then be evaluated for the three commonly encountered conditions of pipe support described below:

Condition I. Assume a section of pipe anchored at one end, but otherwise free to deform both radially and axially with respect

to this fixed location. In order to determine the deformation which occurs within the pipe let $r = R$. Then, from Equations (29) and (28), respectively, it is apparent that

$$\sigma_c = \frac{pR^2}{b^2-R^2} \left[1 + \frac{b^2}{R^2} \right] \quad (31)$$

while

$$\sigma_r = \frac{pR^2}{b^2-R^2} \left[1 - \frac{b^2}{R^2} \right]. \quad (32)$$

The axial stress, which is determined by dividing the end pressure force by the cross sectional pipe area, is given by

$$\sigma_x = \frac{p\pi R^2}{\pi(b^2-R^2)} = \frac{pR^2}{(b^2-R^2)}. \quad (33)$$

Therefore, Equation (30) can be written

$$\begin{aligned} \frac{1}{K} \frac{dp}{dt} + \frac{2}{E} \left[\frac{dp}{dt} \left(\frac{R^2}{b^2-R^2} \right) \left(1 + \frac{b^2}{R^2} \right) - \mu \frac{dp}{dt} \left(\frac{R^2}{b^2-R^2} \right) \left(1 - \frac{b^2}{R^2} + 1 \right) \right] \\ + v_x + \frac{1}{E} \left[\frac{dp}{dt} \left(\frac{R^2}{b^2-R^2} \right) - \mu \frac{dp}{dt} \left(\frac{R^2}{b^2-R^2} \right) \left(1 - \frac{b^2}{R^2} + 1 + \frac{b^2}{R^2} \right) \right] = 0 \end{aligned}$$

or

$$\frac{dp}{dt} \left[\frac{1}{K} + \frac{1}{E} \left(\frac{R^2}{b^2-R^2} \right) \left\{ 3 + \frac{2b^2}{R^2} - \mu \left(6 - \frac{2b^2}{R^2} \right) \right\} \right] + v_x = 0$$

or simply

$$\frac{dp}{dt} \left[\frac{1}{K} + \frac{1}{E} \left(\frac{R}{b-R} \right) c_1 \right] + v_x = 0 \quad (34)$$

$$\text{where } c_1 = \frac{2R}{b+R} (1.5 - 3\mu + \frac{b^2}{R^2} (1+\mu)). \quad (35)$$

Note that differentiation of R and b with respect to time t results in insignificant terms which are not included above.

Condition II. Assume a section of pipe anchored throughout its length such that axial strains cannot occur, but otherwise free to undergo radial deformation. In order to determine the internal deformation within the pipe let $r = R$. Then, Equations (29) and (28) give

$$\sigma_c = \frac{pR^2}{b^2 - R^2} \left[1 + \frac{b^2}{R^2} \right] \quad (36)$$

and

$$\sigma_r = \frac{pR^2}{b^2 - R^2} \left[1 - \frac{b^2}{R^2} \right] \quad (37)$$

Because no strain is permitted in the axial direction, the axial stress must be

$$\sigma_x = 2\mu p \frac{R^2}{b^2 - R^2} \quad (38)$$

according to Poisson's ratio. In this instance Equation (30) becomes

$$\frac{1}{K} \frac{dp}{dt} + \frac{2}{E} \left[\frac{dp}{dt} \left(\frac{R^2}{b^2 - R^2} \right) \left(1 + \frac{b^2}{R^2} \right) - \mu \frac{dp}{dt} \left(\frac{R^2}{b^2 - R^2} \right) \left(1 - \frac{b^2}{R^2} + 2\mu \right) \right] + v_x = 0$$

or

$$\frac{dp}{dt} \left[\frac{1}{K} + \frac{2}{E} \left(\frac{R^2}{b^2 - R^2} \right) \left(1 + \frac{b^2}{R^2} - \mu + \mu \frac{b^2}{R^2} - 2\mu^2 \right) \right] + v_x = 0$$

or simply

$$\frac{dp}{dt} \left[\frac{1}{K} + \frac{1}{E} \left(\frac{R}{b-R} \right) c_2 \right] + v_x = 0 \quad (39)$$

where $c_2 = \frac{2R}{b+R} \left(1 - \mu - 2\mu^2 + \frac{b^2}{R^2} (1+\mu) \right)$. (40)

Condition III. Assume a section of pipe with numerous expansion joints or their equivalent, such that radial deformation may occur without the occurrence of axial stresses or strains. Let $r = R$ in order that the inner deformation may be found. Then, Equations(29) and (28) give

$$\sigma_c = \frac{pR^2}{b^2-R^2} \left[1 + \frac{b^2}{R^2} \right] \quad (41)$$

and

$$\sigma_r = \frac{pR^2}{b^2-R^2} \left[1 - \frac{b^2}{R^2} \right] \quad (42)$$

From the conditions stated

$$\sigma_x = 0 \quad (43)$$

and Equation (30) becomes

$$\frac{1}{K} \frac{dp}{dt} + \frac{2}{E} \left[\frac{dp}{dt} \left(\frac{R^2}{b^2-R^2} \right) \left(1 + \frac{b^2}{R^2} \right) - \mu \frac{dp}{dt} \left(\frac{R^2}{b^2-R^2} \right) \left(1 - \frac{b^2}{R^2} \right) \right] + v_x = 0 \quad (44)$$

or

$$\frac{dp}{dt} \left[\frac{1}{K} + \frac{2}{E} \left(\frac{R^2}{b^2-R^2} \right) \left(1 + \frac{b^2}{R^2} - \mu + \mu \frac{b^2}{R^2} \right) \right] + v_x = 0$$

or simply

$$\frac{dp}{dt} \left[\frac{1}{K} + \frac{1}{E} \left(\frac{R}{b-R} \right) c_3 \right] + v_x = 0 \quad (45)$$

where

$$c_3 = \frac{2R}{b+R} \left(1 - \mu + \frac{b^2}{R^2} (1+\mu) \right) . \quad (46)$$

Thus, to summarize, the continuity equation may be written

$$\frac{dp}{dt} \left[\frac{1}{K} + \frac{c}{E} \frac{R}{(b-R)} \right] + v_x = 0 \quad (47)$$

for which the parameter, c , in the three particular mounting conditions investigated above is given by the following:

$$c_1 = \frac{2R}{b+R} \left[1.5 - 3\mu + \frac{b^2}{R^2} (1+\mu) \right] \quad (35)$$

$$c_2 = \frac{2R}{b+R} \left[1 - \mu - 2\mu^2 + \frac{b^2}{R^2} (1+\mu) \right] \quad (40)$$

$$c_3 = \frac{2R}{b+R} \left[1 - \mu + \frac{b^2}{R^2} (1+\mu) \right] . \quad (46)$$

Halliwell,⁽²⁴⁾ following a different procedure, derived the same results at approximately the same time. For the limiting condition when $b \rightarrow R$ and the pipe wall becomes thin, the three parameters reduce to simply the following:

$$c_1 = 2 \left[\frac{5}{4} - \mu \right] \quad (48)$$

$$c_2 = 2 \left[1 - \mu^2 \right] \quad (49)$$

$$c_3 = 2 . \quad (50)$$

The variation of the coefficient, c , is shown as a function of the ratio of the outside to inside pipe radii for various commonly encountered values of Poisson's ratio in Figure 5. Each of the three conditions of support is considered.

By referring back to Figure 3 it is apparent that the pressure acting at cross section (1) is given in terms of the static head

$$p = \rho g(H-z)$$

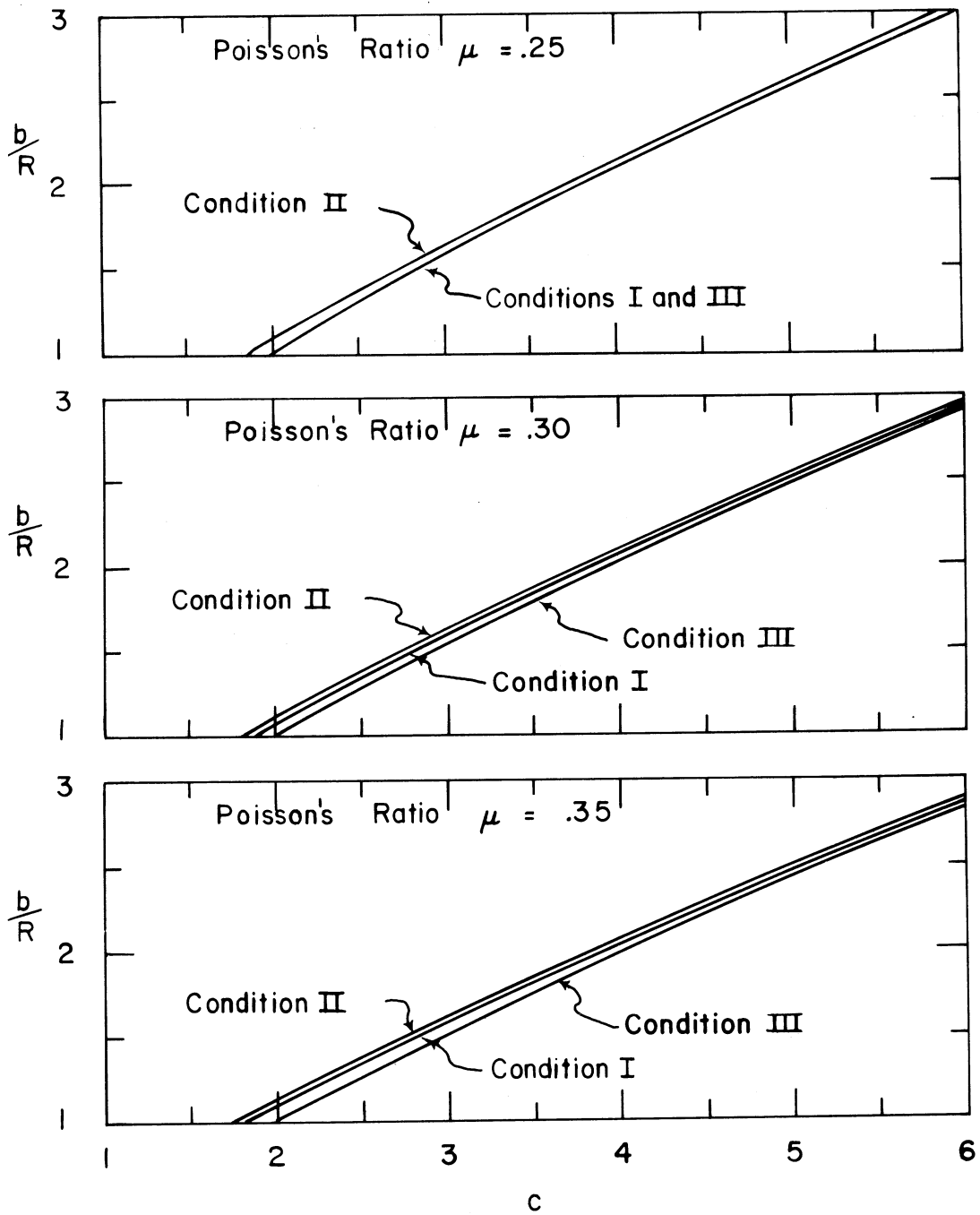


Figure 5. Curves Defining Relationship Between Pipe Constraint Coefficient, c , and the Ratio of Outside to Inside Pipe Radii, b/R , for Various Conditions of Constraint and Different Values of Poisson's Ratio.

Since
$$\frac{dp}{dt} = \frac{\partial p}{\partial x} \frac{dx}{dt} + \frac{\partial p}{\partial t} = \frac{\partial p}{\partial x} v + \frac{\partial p}{\partial t} \quad (51)$$

it is possible to determine $\frac{\partial p}{\partial x}$ and $\frac{\partial p}{\partial t}$, as follows:

$$\frac{\partial p}{\partial x} = \rho g(H_x - z_x) + g(H-z)\rho_x \quad (52)$$

$$\frac{\partial p}{\partial t} = \rho g(H_t - 0) + g(H-z)\rho_t \quad (53)$$

However, $\frac{\partial z}{\partial x} = -\sin\theta$; Equation (52) thus becomes

$$\frac{\partial p}{\partial x} = \rho g(H_x + \sin\theta) + g(H-z)\rho_x \quad (54)$$

Integration of Equation (8) results in

$$p = K \ln \rho + c'$$

Subsequent partial differentiation of p with respect to x and t gives

$$p_x = K \frac{\rho_x}{\rho}$$

and

$$p_t = K \frac{\rho_t}{\rho}$$

Thus, one may write

$$\frac{1}{K} p_x = \frac{\rho_x}{\rho} = \frac{\rho g}{K} (H_x + \sin\theta) + \frac{g}{K} (H-z)\rho_x$$

and

$$\frac{1}{K} p_t = \frac{\rho_t}{\rho} = \frac{\rho g}{K} (H_t) + \frac{g}{K} (H-z)\rho_t$$

or, after gathering like terms

$$\rho_x = \rho^2 g (H_x + \sin\theta) \left(\frac{1}{K - \rho g (H-z)} \right) \quad (55)$$

and

$$\rho_t = \rho^2 g H_t \left(\frac{1}{K - \rho g (H-z)} \right) \quad (56)$$

Equations(55) and (56) may be substituted into Equations(53) and (54) and after gathering like terms;

$$\frac{\partial p}{\partial t} = \rho g H_t \left[1 + \rho g \frac{(H-z)}{(K - \rho g (H-z))} \right]$$

and

$$\frac{\partial p}{\partial x} = \rho g (H_x + \sin\theta) \left[1 + \rho g \frac{(H-z)}{(K - \rho g (H-z))} \right]$$

Thus, using the above expressions for $\frac{\partial p}{\partial x}$ and $\frac{\partial p}{\partial t}$, one may rewrite Equation (51) as

$$\frac{dp}{dt} = \rho g \left[(H_x + \sin\theta)v + H_t \right] \left[1 + \rho g \frac{(H-z)}{(K - \rho g (H-z))} \right]. \quad (57)$$

Consequently, the continuity equation, Equation (47), may be written

$$\rho g \left[(H_x + \sin\theta)v + H_t \right] \left[\frac{1}{K} + \frac{C}{E} \frac{R}{(b-R)} \right] \left[1 + \rho g \frac{(H-z)}{K - \rho g (H-z)} \right] + v_x = 0$$

or simply

$$H_t + v(H_x + \sin\theta) = - \frac{a^2}{g} v_x \Phi \quad (58)$$

where

$$a = \sqrt{\frac{1}{\rho \left(\frac{1}{K} + \frac{C}{E} \left(\frac{R}{b-R} \right) \right)}} \quad (59)$$

and

$$\Phi = \left[\frac{1}{1 + \frac{\rho g (H-z)}{K - \rho g (H-z)}} \right] \quad (60)$$

The term a is an expression for the celerity of the pressure pulse through the pipe system when flowing full; the term Φ compensates for the change in the bulk modulus of elasticity with increasing pressure. For water the term Φ remains approximately unity for moderate pressures. For the range of pressure heads encountered in this study the magnitude of Φ will be assumed to be unity.

Equation of Motion

According to Newton's second law of motion, the net flux of momentum from the control segment and the time rate of change of momentum within the segment must be instantaneously equivalent to the resultant of the external forces acting on the segment.

Consider again the control segment of a circular pipe flowing full shown in Figure 3. Recall that the area at cross section (1) is A and the area at cross section (2) is $A + \frac{\partial A}{\partial x} dx$. The gradient of the pipe is downward (negative gradient) at an angle θ . Flow occurs in the positive x -direction.

The mass of the element is given by

$$\rho \left(A + \frac{1}{2} \frac{\partial A}{\partial x} dx \right) dx .$$

The acceleration in the positive x -direction is given by the total derivative of the velocity with respect to time

$$\frac{dv}{dt} = \frac{\partial v}{\partial x} \frac{dx}{dt} + \frac{\partial v}{\partial t} = v \frac{\partial v}{\partial x} + \frac{\partial v}{\partial t} .$$

The product of the mass and the acceleration is

$$\rho A v \frac{\partial v}{\partial x} dx + \rho A \frac{\partial v}{\partial t} dx + \frac{1}{2} \rho v \frac{\partial A}{\partial x} \frac{\partial v}{\partial x} (dx)^2 + \frac{1}{2} \rho \frac{\partial A}{\partial x} \frac{\partial v}{\partial t} (dx)^2$$

or, after eliminating higher order terms, simply

$$\rho Av_v dx + \rho Av_t dx \quad (61)$$

The pressure force acting upon the cross section at (1) is

$$\rho g A(H-z) . \quad (62)$$

At cross section (2) the pressure force is

$$-\left[\rho g A(H-z) + (\rho g A(H-z))_x dx \right] . \quad (63)$$

An additional pressure force acting upon the expanding cross section of the pipe between (1) and (2) is

$$\left[\rho g(H-z) + (\rho g(H-z))_x dx \right] A_x dx . \quad (64)$$

Fluid resistance to motion is interpreted as a boundary shear force and denoted by

$$-\tau 2\pi R dx , \quad (65)$$

where τ is the fluid shear stress at the pipe wall. The body force due to gravity is

$$\rho g \sin \theta \left[\frac{A + (A + \frac{\partial A}{\partial x} dx)}{2} \right] dx \quad (66)$$

The summation of Equations (62) through (66) is the resultant of the forces acting upon the control segment in the x -direction:

$$\begin{aligned} & \rho g A(H-z) - \rho g A(H-z) - \rho g A(H)_x dx - \rho g A \sin \theta dx \\ & - \rho g(H-z) A_x dx + \rho g(H-z) A_x dx + \rho g(H_x + \sin \theta) A_x (dx)^2 \\ & - \tau 2\pi R dx + \rho g \sin \theta A dx + \rho g \frac{\sin \theta}{2} \frac{\partial A}{\partial x} (dx)^2 \end{aligned}$$

or upon the elimination of higher order terms

$$- \rho g A H_x dx - 2\tau \pi R dx \quad (67)$$

The equation of motion may now be written by equating Equations(61) and (67),

$$- \rho g A H_x dx - 2\tau \pi R dx = \rho A v v_x dx + \rho A v_t dx \quad (68)$$

Now then, for dynamic equilibrium of the flow in the pipe, the stress-created shear force at the pipe wall must equal the so-called frictional head loss per unit length, L , that is

$$\tau 2\pi R = \frac{\Delta p}{\Delta L} \pi R^2 = \rho g \frac{\Delta H_f}{\Delta L} \pi R^2$$

where H_f is the friction loss in terms of head loss. The Darcy-Weisbach expression for head loss per unit length resulting from friction is

$$\frac{\Delta H_f}{\Delta L} = \frac{f}{2R} \frac{v|v|}{2g}$$

Consequently, the shear stress is

$$\tau = \rho f \frac{v|v|}{8}$$

Therefore, substituting Equation (69) into Equation (68) and dividing by $\rho g A dx$ results in the relationship

$$H_x + \frac{fv|v|}{2gD} - \frac{1}{g} (v v_x + v_t) = 0 \quad (70)$$

The absolute value sign is introduced into the frictional term so that it has the proper sign depending on the direction of flow.

Characteristics Equations

The partial differential expressions, Equations(58) and (70), derived in the previous section and representing transient liquid motion in a pipe flowing full, may now be rewritten as

$$\Gamma_1 = v_t + v v_x + gH_x + \frac{fv|v|}{2D} = 0 \quad (71)$$

$$\Gamma_2 = \frac{a^2}{g} v_x + H_t + vH_x + v\sin\theta = 0 . \quad (72)$$

These two equations form a set of simultaneous, quasi-linear, hyperbolic, partial differential equations of the first order in two independent and two dependent variables. Again the subscripts x and t indicate partial differentiation with respect to these independent variables.

The expressions Γ_1 and Γ_2 may be combined linearly such that

$$\Omega = \Gamma_1 + n\Gamma_2 \quad (73)$$

or

$$\begin{aligned} \Omega = v_t + \left(v + \frac{na^2}{g} \right) v_x + nH_t + (g+nv)H_x \\ + \frac{f}{2D} v|v| + nv\sin\theta = 0 \end{aligned} \quad (74)$$

Now, if $v = v(x,t)$ and $H = H(x,t)$ are solutions of Equations(71) and (72), then

$$dv = \frac{\partial v}{\partial x} dx + \frac{\partial v}{\partial t} dt \quad \text{and} \quad dH = \frac{\partial H}{\partial x} dx + \frac{\partial H}{\partial t} dt$$

or

$$\frac{dv}{dt} = v_t + v_x \frac{dx}{dt} \quad \text{and} \quad \frac{dH}{dt} = H_t + H_x \frac{dx}{dt} . \quad (75)$$

From inspection of Equation 74 it is readily apparent that it may be re-written

$$\Omega = \frac{dv}{dt} + n \frac{dH}{dt} + \frac{f}{2D} v|v| + nv \sin \theta = 0 \quad (76)$$

provided

$$\frac{dx}{dt} = v + \frac{na^2}{g} = \frac{g+nv}{n} \quad (77)$$

or in other words provided

$$\frac{dv}{dt} = v_t + \left(v + \frac{na^2}{g} \right) v_x$$

and

$$\frac{dH}{dt} = H_t + \left(\frac{g}{n} + v \right) H_x .$$

From Equation (77) one finds

$$n^2 a^2 = g^2$$

or

$$n = \pm \frac{g}{a} \quad (78)$$

By substituting Equation (78) into Equations (76) and (77), one has the pair of relations

$$C_+ \left\{ \begin{array}{l} \Omega dt = dv + \frac{g}{a} dH + \frac{f}{2D} v|v| dt + \frac{g}{a} v \sin \theta dt = 0 \end{array} \right. \quad (79)$$

$$\left\{ \begin{array}{l} \frac{dt}{dx} = \frac{1}{v+a} \end{array} \right. \quad (80)$$

and

$$C_- \left\{ \begin{array}{l} \Omega dt = dv - \frac{g}{a} dH + \frac{f}{2D} v|v| dt - \frac{g}{a} v \sin \theta dt = 0 \end{array} \right. \quad (81)$$

$$\left\{ \begin{array}{l} \frac{dt}{dx} = \frac{1}{v-a} \end{array} \right. \quad (82)$$

To summarize what has been accomplished, Equations(79) and (81) are two separate total differential equations for which solutions for v and H may be determined along the families of characteristics curves occurring in the $x-t$ plane. These curves are defined by the total differential expressions given by Equations(80) and (82), respectively. In other words, the characteristics curves represent the paths along which infinitesimally small velocity and pressurehead differences propagate. Equations (79) and (80) are applicable along a positively directed characteristics curve, while Equations(81) and (82) are applicable along the negatively-directed characteristics.

Finite Difference Solution

Equations (79-82) may now be solved by means of a finite difference technique. If the step size of the increments used in the solution is small, one can solve by a first order approximation for which

$$\int_{x_0}^{x_1} f(x)dx \approx f(x_0)(x_1-x_0) ;$$

otherwise, a second order approximation technique requiring iteration should be considered. A first order technique is used throughout this development.

Consider the fact that for a set of two hyperbolic differential equations the characteristics curves at a point have real and distinct directions; therefore, the curves must intersect at the point. Let P_i be a point on the $x-t$ plane as shown in Figure 6. Two characteristics curves from the families of positively and negatively directed characteristics curves are shown passing through P_i .

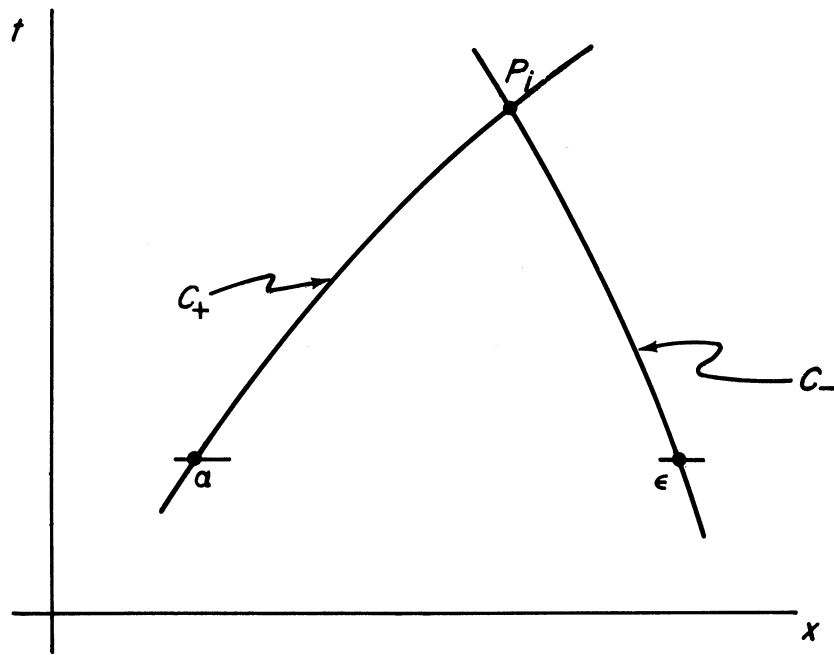


Figure 6. Definition Sketch Showing Intersection of C_+ and C_- Characteristics Curves in the $x-t$ Plane.

The objective of this solution technique is to provide a means for obtaining values of velocity and head (pressure) at selected locations throughout the x-t plane. Figure 7 shows a portion of a rectangular grid in the x-t plane. The two pairs of characteristic equations, Equations (79-82), representing transient motion in a pipe flowing full may be written in the following manner:

$$\left. \begin{aligned} dt - \frac{dx}{v+a} &= 0 \\ dv + \frac{g}{a} dH + \left(\frac{f}{2D} v|v| + \frac{g}{a} v \sin\theta \right) dt &= 0 \end{aligned} \right\} C_+$$

$$\left. \begin{aligned} dt - \frac{dx}{v-a} &= 0 \\ dv - \frac{g}{a} dH + \left(\frac{f}{2D} v|v| - \frac{g}{a} v \sin\theta \right) dt &= 0 \end{aligned} \right\} C_-$$

When written in incremental form these equations become

$$(t_P - t_\alpha) - \frac{1}{(v+a)_\alpha} (x_P - x_\alpha) = 0 \quad (83)$$

$$(v_P - v_\alpha) + (H_P - H_\alpha) \frac{g}{a_\alpha} + \left(\frac{f}{2D} v|v| + \frac{g}{a} v \sin\theta \right)_\alpha (t_P - t_\alpha) = 0 \quad (84)$$

$$(t_P - t_\epsilon) - \frac{1}{(v-a)_\epsilon} (x_P - x_\epsilon) = 0 \quad (85)$$

$$(v_P - v_\epsilon) - (H_P - H_\epsilon) \frac{g}{a_\epsilon} + \left(\frac{f}{2D} v|v| - \frac{g}{a} v \sin\theta \right)_\epsilon (t_P - t_\epsilon) = 0 \quad (86)$$

where the subscripts P, α , and ϵ refer to locations on the x-t plane in Figure 7. The grid in this figure has specified incremental distance and time intervals, Δx and Δt . The points P_0 and P_n are boundary points. Note that time $t_L = t_\alpha = t_M = t_\epsilon = t_R$; also, note that distance $x_P = x_M$.

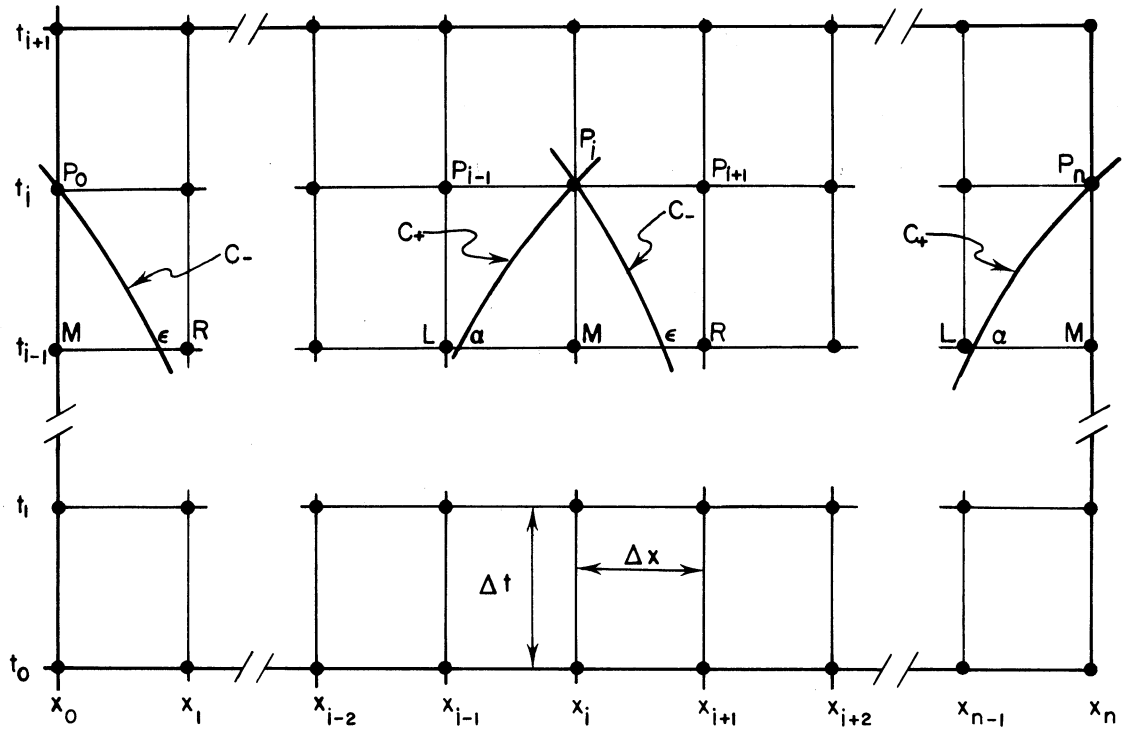


Figure 7. Definition Sketch Showing a Space-Time Grid Superimposed on the $x-t$ Plane. Positive and Negative Characteristics Curves are Shown Passing Through Grid Intersection Points, P_0 , P_i , and P_n .

Clearly, the exact location of P_i which is at a grid point is known with respect to x and t . However, the locations of α and ϵ although known with respect to t , are unknown with respect to x and need to be so determined. The values of v and H at the points α and ϵ need to be determined in order to determine v_p and H_p . It is assumed that v and H are known at specific point $(L, M, R, \text{ etc.})$ along the x -axis at the preceding times t_{i-1} , t_{i-2} , etc., either by having been initially given or previously calculated.

Linear interpolation is used to determine v and H at α and ϵ , thus

$$\frac{v_\alpha - v_L}{x_\alpha - x_L} = \frac{v_M - v_L}{x_M - x_L} = \frac{v_M - v_L}{\Delta x} \quad (87)$$

and

$$\frac{v_R - v_\epsilon}{x_R - x_\epsilon} = \frac{v_R - v_M}{x_R - x_M} = \frac{v_R - v_M}{\Delta x} \quad (88)$$

In order to determine v_α , v_ϵ , H_α , and H_ϵ one must note, first of all, that the two characteristic equations, namely, Equations (83) and (85), can be written

$$x_M - x_\alpha = (v+a)_\alpha \Delta t \quad (89)$$

and

$$x_\epsilon - x_M = -(v-a)_\epsilon \Delta t \quad (90)$$

These equations describe C_+ and C_- , respectively, at α and ϵ . Equations (87) and (88) may be respectively rewritten as

$$\left(\frac{v_{\alpha} - v_L}{v_M - v_L} \right) \Delta x = x_{\alpha} - x_L \quad (91)$$

and

$$\left(\frac{v_R - v_{\epsilon}}{v_R - v_M} \right) \Delta x = x_R - x_{\epsilon} \quad (92)$$

Inspection of Figure 7 clearly reveals

$$x_{\alpha} - x_L = \Delta x - (x_M - x_{\alpha})$$

or, following substitution of Equation (89),

$$x_{\alpha} - x_L = \Delta x - (v+a)_{\alpha} \Delta t$$

into which substitution of Equation (91) yields

$$\left(\frac{v_{\alpha} - v_L}{v_M - v_L} \right) \Delta x = \Delta x - (v+a)_{\alpha} \Delta t$$

$$v_{\alpha} = v_L + (v_M - v_L) \left[1 - (v+a)_{\alpha} \frac{\Delta t}{\Delta x} \right],$$

or by approximation

$$v_{\alpha} = v_L + (v_M - v_L) \left[1 - (v+a)_M \frac{\Delta t}{\Delta x} \right]. \quad (93)$$

Figure 7 also reveals that

$$x_R - x_{\epsilon} = \Delta x - (x_{\epsilon} - x_M)$$

or, by substituting Equation (90),

$$x_R - x_{\epsilon} = \Delta x + (v-a)_{\epsilon} \Delta t,$$

into which substitution of Equation (92) yields

$$v_{\epsilon} = v_R + (v_M - v_R) \left[1 + (v-a)_M \frac{\Delta t}{\Delta x} \right]. \quad (94)$$

The linear interpolation expressions used to determine H_α and H_ϵ are

$$\frac{H_\alpha - H_L}{x_\alpha - x_L} = \frac{H_M - H_L}{x_M - x_L} = \frac{H_M - H_L}{\Delta x}$$

and

$$\frac{H_R - H_\epsilon}{x_R - x_\epsilon} = \frac{H_R - H_M}{x_R - x_M} = \frac{H_R - H_M}{\Delta x}$$

The same general procedure used to determine v_α and v_ϵ is followed to determine H_α and H_ϵ , with the result that

$$H_\alpha = H_L + (H_M - H_L) \left[1 - (v+a)_M \frac{\Delta t}{\Delta x} \right] \quad (95)$$

and

$$H_\epsilon = H_R + (H_M - H_R) \left[1 + (v-a)_M \frac{\Delta t}{\Delta x} \right] \quad (96)$$

In summary, Equations (93)-(96), which define v_α , v_ϵ , H_α , and H_ϵ may be simply written

$$v_\alpha = v_M - (v_M - v_L)(v+a)_M \frac{\Delta t}{\Delta x} \quad (97)$$

$$H_\alpha = H_M - (H_M - H_L)(v+a)_M \frac{\Delta t}{\Delta x} \quad (98)$$

$$v_\epsilon = v_M + (v_M - v_R)(v-a)_M \frac{\Delta t}{\Delta x} \quad (99)$$

$$H_\epsilon = H_M + (H_M - H_R)(v-a)_M \frac{\Delta t}{\Delta x} \quad (100)$$

Note that $(v+a)_\alpha \approx (v+a)_M$ and $(v-a)_\epsilon \approx (v-a)_M$ are assumed to be entirely valid approximations provided the grid of points is closely spaced. Using the four equations for v_α , H_α , v_ϵ , and H_ϵ , one can rewrite Equations (84) and (86) in preparation for determining v_p and H_p :

$$(v_P - v_\alpha) + (H_P - H_\alpha) \left(\frac{g}{a} \right)_M + \left(\frac{f}{2D} v_\alpha |v_\alpha| \right) \Delta t + \left(\frac{g}{a} \right)_M v_\alpha \sin \theta \Delta t = 0 \quad (101)$$

$$(v_P - v_\epsilon) - (H_P - H_\epsilon) \left(\frac{g}{a} \right)_M + \left(\frac{f}{2D} v_\epsilon |v_\epsilon| \right) \Delta t - \left(\frac{g}{a} \right)_M v_\epsilon \sin \theta \Delta t = 0 \quad (102)$$

To solve for v_P and H_P , Equations (101) and (102) are first added,

$$2v_P - (v_\alpha + v_\epsilon) - (H_\alpha - H_\epsilon) \left(\frac{g}{a} \right)_M + \left(\frac{f}{2D} \right)_M (v_\alpha |v_\alpha| + v_\epsilon |v_\epsilon|) \Delta t + \left(\frac{g}{a} \right)_M (v_\alpha - v_\epsilon) \sin \theta \Delta t = 0$$

$$v_P = \frac{1}{2}(v_\alpha + v_\epsilon) + \frac{1}{2}(H_\alpha - H_\epsilon) \left(\frac{g}{a} \right)_M - \left(\frac{f}{4D} \right)_M (v_\alpha |v_\alpha| + v_\epsilon |v_\epsilon|) \Delta t - \frac{1}{2} \left(\frac{g}{a} \right)_M (v_\alpha - v_\epsilon) \sin \theta \Delta t \quad (103)$$

and then subtracted,

$$\begin{aligned} -v_\alpha + v_\epsilon + 2H_P \left(\frac{g}{a} \right)_M - (H_\alpha + H_\epsilon) \left(\frac{g}{a} \right)_M \\ + \left(\frac{f}{2D} \right)_M (v_\alpha |v_\alpha| - v_\epsilon |v_\epsilon|) \Delta t + \left(\frac{g}{a} \right)_M (v_\alpha + v_\epsilon) \sin \theta \Delta t = 0 \end{aligned}$$

$$H_P = \frac{1}{2}(v_\alpha - v_\epsilon) \left(\frac{a}{g} \right)_M + \frac{1}{2}(H_\alpha + H_\epsilon) - \left(\frac{f}{4D} \right)_M \left(\frac{a}{g} \right)_M (v_\alpha |v_\alpha| - v_\epsilon |v_\epsilon|) \Delta t - \frac{1}{2}(v_\alpha + v_\epsilon) \sin \theta \Delta t \quad (104)$$

Thus, using Equations (103) and (104) it is now possible to determine the velocity and pressure head, v_P and H_P , at each interior point on the $x-t$ grid. The evaluation process advances with time throughout the bounded x -region.

It should be noted that the size of the increments Δx and Δt cannot be selected independently of each other. On the contrary, their size is integrally dependent. Since the finite difference solution scheme which has been outlined above converges to the exact characteristics solution as Δx approaches zero, one can conclude the following: (a) the values of v and H at any point P within the region of existence of the solution are determined solely by the initial values prescribed along

the segment of the x-axis subtended by the two characteristics passing through P, and (b) the two characteristics through P are themselves determined solely by the initial values on the segment. The segment of the x-axis determined by α and ϵ is, thus, the domain of dependence of the point P as shown in Figure 6. Therefore, when Δx is arbitrarily selected, Δt is automatically limited to an interval no larger in magnitude than that given by the relationship

$$\Delta t \leq \frac{\Delta x}{|v_{\pm a}|} .$$

In other words, the point P must lie within the region bounded by the intersecting characteristics curves through L and R and the subtended segment of the x-axis.

Boundary Conditions

The finite difference solution technique used with the characteristic equations must now be extended to include the various boundary conditions which are to be encountered.

Consider the situation at the right edge of Figure 7 in which only the positively directed characteristic curve C_+ is shown. One condition at point P_n is assumed to be given. This given condition may be either v_p or H_p . In order to calculate the unknown condition, it is necessary to first calculate v_α and H_α . The given boundary condition can then be used to determine the remaining unknown condition. Equations (97) and (98) are used to determine H_α and v_α . If v_p is the known boundary condition at point P_n , Equation (101) can be rearranged to give H_{P_n} ,

$$H_P = H_\alpha - (v_P - v_\alpha) \left(\frac{a}{g} \right)_M - \left\{ \frac{f}{2D} v_\alpha |v_\alpha| + \left(\frac{g}{a} \right)_M v_\alpha \sin \theta \right\} \left(\frac{a}{g} \right)_M \Delta t . \quad (105)$$

On the other hand, if H_P is given, this same equation may be rearranged to provide v_P at point n ,

$$v_P = v_\alpha - (H_P - H_\alpha) \left(\frac{g}{a} \right)_M - \left\{ \frac{f}{2D} v_\alpha |v_\alpha| + \left(\frac{g}{a} \right)_M v_\alpha \sin \theta \right\} \Delta t . \quad (106)$$

At the left end of the $x-t$ grid shown in Figure 7, the C_- characteristics govern the unknown boundary value. Again one begins by calculating v_ϵ and H_ϵ from Equations (99) and (100). When v_P is the known boundary value at point P_1 , Equation (102) can be rearranged to provide H_P at P_1 ,

$$H_P = H_\epsilon + (v_P - v_\epsilon) \left(\frac{a}{g} \right)_M + \left\{ \frac{f}{2D} v_\epsilon |v_\epsilon| - \left(\frac{g}{a} \right)_M v_\epsilon \sin \theta \right\} \left(\frac{a}{g} \right)_M \Delta t \quad (107)$$

and when v_P is the given boundary value at P_1 , Equation (102) is similarly rearranged to give

$$v_P = v_\epsilon + (H_P - H_\epsilon) \left(\frac{g}{a} \right)_M - \left\{ \frac{f}{2D} v_\epsilon |v_\epsilon| - \left(\frac{g}{a} \right)_M v_\epsilon \sin \theta \right\} \Delta t \quad (108)$$

Now then, Equations (105-108) provide the boundary values appropriate for use in conjunction with the general Equations (103) and (104).

Attention must be given to the boundary conditions occurring at the junction between two pipes of different sizes and different materials. A typical portion of the $x-t$ grid at such a junction is shown in Figure 8. In addition to the four boundary equations, Equations (105-108), already developed above, two other relationships prevail. These relationships are (1) the continuity-of-mass relationship, $v_I D_I^2 = v_{II} D_{II}^2$, and (2) the energy-equilibrium relationship, $H_I = H_{II}$. Minor losses at the

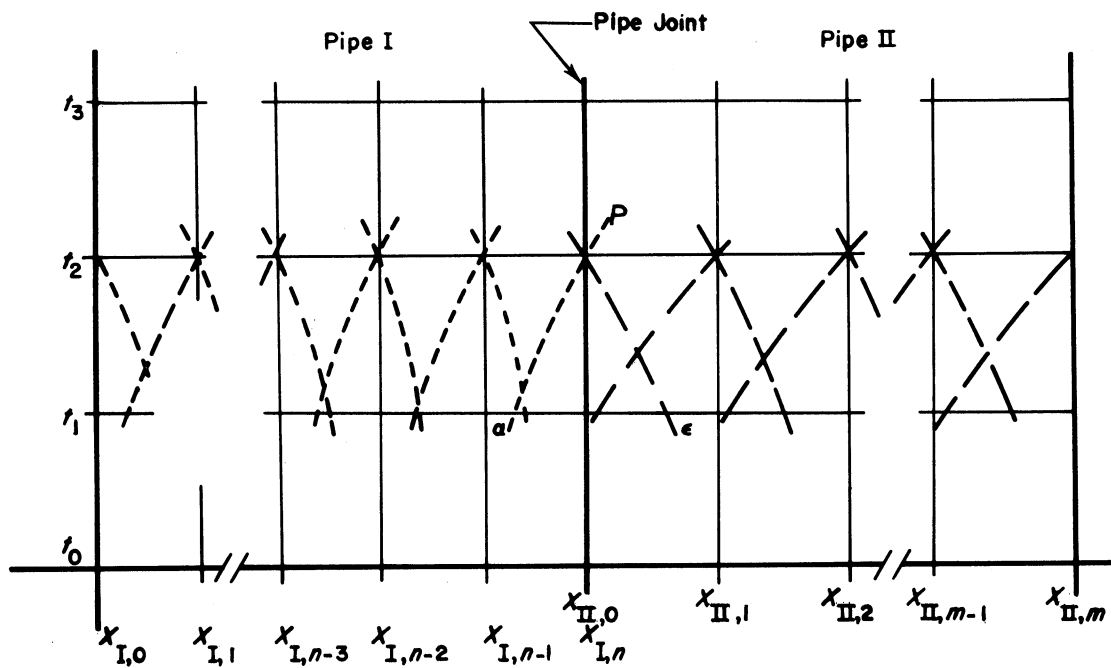


Figure 8. Definition Sketch Showing Relationship Between Space-Time Grids and Characteristics Curves at a Pipe Junction.

junction are ignored. Using the boundary equations one can derive an expression in v_{PI} and H_{PI} by adding Equations(105) and (106),

$$v_{PI} + H_{PI} \left(\frac{g}{a} \right)_{M_I} = v_{\alpha} + H_{\alpha} \left(\frac{g}{a} \right)_{M_I} - \left(\frac{f}{2D} v_{\alpha} |v_{\alpha}| \right)_{M_I} \Delta t - v_{\alpha} \sin \theta \left(\frac{g}{a} \right)_{M_I} \Delta t = \Psi \quad (109)$$

Similarly, Equations(107) and (108) may be subtracted and combined to give

$$v_{PII} - H_{PII} \left(\frac{g}{a} \right)_{M_{II}} = v_{\epsilon} - H_{\epsilon} \left(\frac{g}{a} \right)_{M_{II}} - \left(\frac{f}{2D} v_{\epsilon} |v_{\epsilon}| \right)_{M_{II}} \Delta t + v_{\epsilon} \sin \theta \left(\frac{g}{a} \right)_{M_{II}} \Delta t = X \quad (110)$$

Now, substituting $v_{PI} = v_{PII} \left(\frac{D_{II}}{D_I} \right)^2$ and $H_{PI} = H_{PII}$ into Equation (109),

$$\Psi = v_{PII} \left(\frac{D_{II}}{D_I} \right)^2 + H_{PII} \left(\frac{g}{a} \right)_{M_I},$$

and rewriting Equation (110),

$$X = v_{PII} - H_{PII} \left(\frac{g}{a} \right)_{M_{II}} ;$$

one can eliminate v_{PII}

$$H_{PII} \left[\left(\frac{g}{a} \right)_{M_I} \left(\frac{D_I}{D_{II}} \right)^2 + \left(\frac{g}{a} \right)_{M_{II}} \right] = \Psi \left(\frac{D_I}{D_{II}} \right)^2 - X$$

or

$$H_{PI} = H_{PII} = \frac{\Psi \left(\frac{D_I}{D_{II}} \right)^2 - X}{\left[\left(\frac{g}{a} \right)_{M_I} \left(\frac{D_I}{D_{II}} \right)^2 + \left(\frac{g}{a} \right)_{M_{II}} \right]} \quad (111)$$

Equations of Transient Motion--
Horizontal Pipe Flowing Partially Full

Transient liquid motion in a horizontal pipe flowing partially full, that is to say, flowing with a free surface, is comparable in many ways to the previously discussed transient liquid motion in a pipe flowing

full. Analytic treatment of the free surface flow as presented below will more clearly identify the similarities as well as the principal differences between the two types of transient motion.

Transient flow in a horizontal pipe having a free liquid surface is a function of two independent variables. These variables are the space and time variables, x and t , respectively; and are exactly comparable to the independent variables used previously with a pipe that is flowing full. Relative position in space is denoted by x as measured axially along the pipe. The gate valve is arbitrarily designated the point of zero reference. For pipe flow with a free surface the two dependent variables are the mean velocity of the free surface flow, u , and the depth of flow, z . In order to represent the variable velocities and depths, two quasi-linear, partial differential equations are developed and then transformed into four total differential equations--the characteristics equations of transient, open-channel flow. After being rewritten as finite difference equations in a manner comparable to the one used with the equations for the pipe flowing full, numerical methods are again introduced to enable evaluation by high-speed, digital computer. The governing boundary conditions are examined and interpreted analytically. The section concludes with a brief comparison of the similar analytic properties of transient, free-surface, pipe flow and transient liquid motion in a pipe flowing full.

Equation of Continuity

The net inflow of mass into a segment of free surface flow must equal the rate of mass increase taking place within the segment per unit

time. This statement sets forth the conservation of mass concept upon which the equation of continuity is based. Figure 9 shows an element of free-surface flow in a pipe. The element is bounded on the left and right by cross sections (2) and (1), respectively. For u equal to the mean velocity and A equal to the cross segmental area at cross section (1), the mass influx through this segment is ρAu . At cross section (2), flow leaves the element; therefore, the efflux of mass is given by

$$-[\rho Au + (\rho Au)_x dx] .$$

The net increase of mass in the control element per unit of time is

$$\rho Au - \left[\rho Au + \frac{\partial(\rho Au)}{\partial x} dx \right]$$

or

$$-\rho (Au)_x dx \quad (112)$$

The rate of mass increase occurring in the control segment per unit time is

$$\left[\frac{1}{2} (A + (A + \frac{\partial A}{\partial x} dx)) \rho dx \right]_t$$

or

$$\frac{\rho}{2} [(A_t + A_t + \frac{\partial^2 A}{\partial x \partial t}) dx]$$

or finally

$$\rho A_t dx \quad (113)$$

after higher order terms are eliminated.

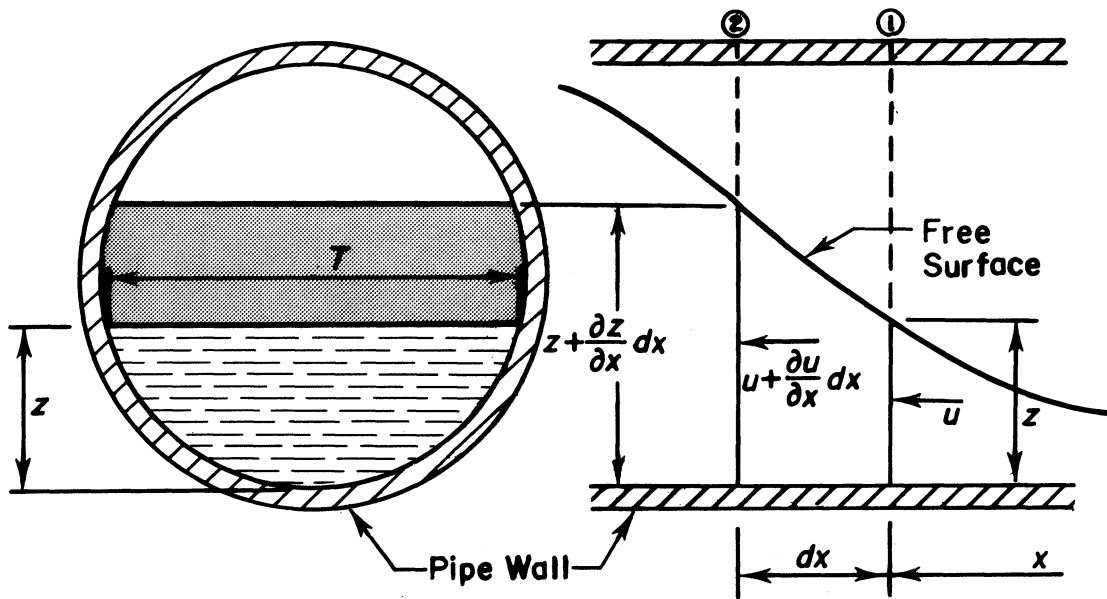


Figure 9. Definition Sketch Illustrating Element of Free-Surface Flow in a Pipe. Transverse Cross-Segment is Shown On the Left and Longitudinal Flow Profile is Shown On the Right.

The continuity equation may now be set forth by equating expressions (112) and (113) above:

$$-\rho(Au)_x dx = \rho(A_t) dx$$

or

$$\rho u A_x + \rho A u_x + \rho A_t = 0 . \quad (114)$$

Note that the small pressure changes associated with the changes in depth accompanying open-channel flow have no significant effect upon liquid density. Therefore, ρ is independent of both x and t .

The cross segmental area is a function of the flow depth, in other words, $A = A(z)$, and thus, $dA = T dz$ where T is the surface width $2\sqrt{zD-z^2}$ and D is the inside pipe diameter. Moreover,

$$A_x = \frac{\partial A}{\partial z} \frac{\partial z}{\partial x} = T \frac{\partial z}{\partial x} = T_{zx} , \quad (115)$$

and by the same token

$$A_t = T_{zt} . \quad (116)$$

Equation (114) may now be written as

$$uz_x + \frac{A}{T} u_x + z_t = 0 , \quad (117)$$

which is the form of the continuity equation used in subsequent parts of the analysis.

Equation of Motion

The net flux of momentum from the control element and the time rate of change of momentum within the element must be instantaneously equivalent to the resultant of the external forces acting on the element.

The flux of momentum through cross section (1) in Figure 9 is actually an influx of momentum into the control element, namely $-\rho(Au^2)$. At section (2) the efflux of momentum is $+\rho(Au^2) + \rho \frac{\partial(Au^2)}{\partial x} dx$. Therefore, the net flux of momentum from the control element is

$$+ \rho \frac{\partial(Au^2)}{\partial x} dx . \quad (118)$$

The time rate of increase of momentum within the control element is

$$\left[\rho \left\{ A + \left(A + \frac{\partial A}{\partial x} dx \right) \right\} \frac{1}{2} \left\{ u + \left(u + \frac{\partial u}{\partial x} dx \right) \right\} \frac{1}{2} dx \right]_t$$

or simply

$$\rho(Au)_t dx \quad (119)$$

after all higher order terms have been eliminated.

The net hydrostatic pressure force, as is clearly illustrated in Figure 9, is

$$-\rho g \left(A + \frac{\partial A}{\partial x} dx \right) \left(\frac{\partial z}{\partial x} dx \right) .$$

Once again higher order terms are eliminated to give

$$-\rho g A z_x dx . \quad (120)$$

The flow resistance force may be attributed to the shear stresses developed at the pipe wall. It is given by

$$-\tau P_w dx , \quad (121)$$

where P_w is the wetted perimeter and τ the boundary shear stress.

By equating the terms depicting a change in momentum to the force terms, one obtains the expression

$$+ \rho(Au^2)_x dx + \rho(Au)_t dx = - \rho g A z_x dx - \tau P_w dx$$

or

$$2\rho Au u_x dx + \rho u^2 A_x dx + \rho Au_t dx + \rho u A_t dx + \rho g A z_x dx + \tau P_w dx = 0 .$$

Division by $\rho A dx$ reduces this expression to simply

$$2uu_x + u^2 \frac{A_x}{A} + u_t + u \frac{A_t}{A} + gz_x + \frac{\tau}{\rho R_H} = 0 . \quad (122)$$

The variable R_H represents the hydraulic radius. Because the shear stress can be defined as

$$\tau = \rho f \frac{u|u|}{8} , \quad (69)$$

where f is again the pipe friction factor noted previously, the flow resistance term may be written

$$\tau P_w dx = f \frac{\rho u |u| P_w dx}{8} ,$$

after which, division by $\rho A dx$ leaves

$$\frac{\tau}{\rho R_H} = \frac{f u |u|}{8 R_H} . \quad (123)$$

Equation 122 can now be rearranged to include this expression,

$$gz_x + u^2 \frac{T}{A} z_x + u \frac{T}{A} z_t + 2uu_x + u_t + \frac{f u |u|}{8 R_H} = 0 . \quad (124)$$

Write the continuity equation (Equation (117)) with each term multiplied by $u \frac{T}{A}$:

$$u^2 \frac{T}{A} z_x + u \frac{T}{A} z_t + uu_x = 0 . \quad (125)$$

Subtraction of Equation (125) from Equation (124) reduces the momentum equation to the form

$$gz_x + uu_x + u_t + \frac{fu|u|}{8R_H} = 0 \quad (126)$$

which is used in the subsequent parts of this analysis.

Characteristics Equations

The set of simultaneous, quasi-linear, hyperbolic, partial differential equations which describes transient liquid movement in a pipe flowing partially full, is rewritten below

$$\Gamma_3 = uz_x + z_t + \frac{A}{T} u_x = 0 \quad (127)$$

$$\Gamma_4 = gz_x + uu_x + u_t + \frac{fu|u|}{8R_H} = 0 \quad (128)$$

Linear combination of the expressions Γ_3 and Γ_4 produces

$$\Lambda = \Gamma_3 + m\Gamma_4 \quad (129)$$

or

$$\Lambda = mu_t + \left(\frac{A}{T} + mu \right) u_x + z_t + (u+mg)z_x + \frac{mfu|u|}{8R_H} \quad (130)$$

The dependent variables u and z are functions of the space and time variables x and t by assumption. As a result, if u and z are, in fact, solutions of Equations (127) and (128), then

$$du = \frac{\partial u}{\partial x} dx + \frac{\partial u}{\partial t} dt$$

or

$$\frac{du}{dt} = \frac{\partial u}{\partial x} \frac{dx}{dt} + \frac{\partial u}{\partial t} ,$$

and

$$dz = \frac{\partial z}{\partial x} dx + \frac{\partial z}{\partial t} dt$$

or

$$\frac{dz}{dt} = \frac{\partial z}{\partial x} \frac{dx}{dt} + \frac{\partial z}{\partial t} .$$

Therefore, Equation (130) can be written

$$\Lambda = m \frac{du}{dt} + \frac{dz}{dt} + m \frac{f}{8R_H} u|u| = 0 \quad (131)$$

provided

$$\frac{dx}{dt} = \frac{\frac{A}{\Gamma} + mu}{m} = \frac{m(u+mg)}{m} . \quad (132)$$

Equation (132) is valid if

$$\frac{du}{dt} = u_t + \frac{A}{m\Gamma} + u u_x \quad (133)$$

and

$$\frac{dz}{dt} = z_t + (u+mg) z_x . \quad (134)$$

If Equation (132) is now solved for m , one finds that

$$m = \pm \sqrt{\frac{A}{g\Gamma}} \quad (135)$$

By substituting Equation (135) into Equations(131) and (132), two pairs of linear relations are determined, namely,

$$C_+ \begin{cases} 0 = \sqrt{\frac{A}{gT}} du + dz + \sqrt{\frac{A}{gT}} \frac{f}{8R_H} u|u|dt = \Lambda dt & (136) \\ \frac{dt}{dx} = \frac{1}{u + \sqrt{\frac{Ag}{T}}} & (137) \end{cases}$$

and

$$C_- \begin{cases} 0 = -\sqrt{\frac{A}{gT}} du + dz - \sqrt{\frac{A}{gT}} \frac{f}{8R_H} u|u|dt = \Lambda dt & (138) \\ \frac{dt}{dx} = \frac{1}{u - \sqrt{\frac{Ag}{T}}} & (139) \end{cases}$$

which are total differential equations. These four equations are the characteristics equations governing the transient velocities and depths in a horizontal circular conduit flowing partially full.

In retrospect, Equation (136) simply states that there is a constant, velocity-depth relationship for a point whose motion in the x, t -plane is characterized by Equation (137). Likewise, a similar relationship exists between Equation (138) and (139). In other words, Equations (137) and (139) define the families of solution curves along which Equations(136) and (138) are valid.

Finite Difference Solution

The technique devised for finite difference solution of the characteristics equations depicting free-surface flow in a pipe is analogous to the technique described previously for solution of the characteristics equations representing liquid motion in a pipe flowing full. The size of

the stepping increment used in the solution is made small enough to insure that first order approximation is adequate.

The fact that any point on the x,t -plane is an intersection for a specific positive curve and a specific negative curve belonging to the respective families of characteristics curves associated with partial differential equations of the hyperbolic type is the basis for the solution technique. Figure 6 shows the intersection of a positive characteristics curve with a negative characteristics curve at P_i . Given the necessary initial and boundary conditions, it is the purpose of the solution technique to permit evaluation of mean velocity, u , and depth, z , at point P_i . In more general terms it must permit evaluation of u and z at any network of selected grid points on the x,t -plane, such as the rectangular grid illustrated in Figure 7.

Characteristics Equations, Equations (136)-(139), may be rewritten as follows:

$$C_+ \begin{cases} dt - \frac{dx}{u + \sqrt{\frac{gA}{T}}} = 0 \\ dz + \sqrt{\frac{A}{gT}} du + \sqrt{\frac{A}{gT}} \frac{f}{8R_H} u|u|dt = 0 \end{cases} \quad (140)$$

$$C_- \begin{cases} dt - \frac{dx}{u - \sqrt{\frac{gA}{T}}} = 0 \\ dz - \sqrt{\frac{A}{gT}} du - \sqrt{\frac{A}{gT}} \frac{f}{8R_H} u|u|dt = 0 \end{cases} \quad (141)$$

If written in finite difference form these expressions become

$$(t_P - t_\alpha) - (x_P - x_\alpha) / (u + \sqrt{\frac{Ag}{T}})_\alpha = 0 \quad (142)$$

$$(z_P - z_\alpha) + \sqrt{\frac{A}{gT}} (u_P - u_\alpha) + \left(\sqrt{\frac{A}{gT}} \alpha \left(\frac{f}{8R_H} u |u| \right) \right)_\alpha (t_P - t_\alpha) = 0 \quad (143)$$

$$(t_P - t_\epsilon) - (x_P - x_\epsilon) / (u - \sqrt{\frac{Ag}{T}})_\epsilon = 0 \quad (144)$$

$$(z_P - z_\epsilon) - \sqrt{\frac{A}{gT}} (u_P - u_\epsilon) - \left(\sqrt{\frac{A}{gT}} \epsilon \left(\frac{f}{8R_H} u |u| \right) \right)_\epsilon (t_P - t_\epsilon) = 0 \quad (145)$$

where the subscripts P, α , and ϵ refer to locations on the x,t-plane in Figure 7.

Values of u and z are assumed known, i.e., given initially or computed previously at all the grid points along the x-axis at prior to time t_{i-1} . Although the points on the grid are separated by specified space and time intervals, the locations of α and ϵ while known with respect to time are unknown with respect to x. These locations must be determined. If the solution is to advance with respect to time so that u_P and z_P can be determined at time t_i , the appropriate values of u and z at α and ϵ must be found first. This may be done using linear interpolation:

$$\frac{u_\alpha - u_L}{x_\alpha - x_L} = \frac{u_M - u_L}{x_M - x_L} = \frac{u_M - u_L}{\Delta x} \quad (146)$$

$$\frac{u_R - u_\epsilon}{x_R - x_\epsilon} = \frac{u_R - u_M}{x_R - x_M} = \frac{u_R - u_M}{\Delta x} \quad (147)$$

Now, by recognizing that $x_P = x_M$, and $t_M = t_\alpha = t_\epsilon$, Equations (142) and (144) can be written

$$x_M - x_\alpha = \left(u + \sqrt{\frac{Ag}{T}} \right)_\alpha (t_P - t_\alpha) = \left(u + \sqrt{\frac{Ag}{T}} \right)_\alpha \Delta t \quad (148)$$

and

$$x_\epsilon - x_M = - \left(u - \sqrt{\frac{Ag}{T}} \right)_\epsilon (t_P - t_\epsilon) = - \left(u - \sqrt{\frac{Ag}{T}} \right)_\epsilon \Delta t, \quad (149)$$

which represent the increment slopes of C+ and C- at α and ϵ , respectively. Equations (146) and (147) may be rewritten:

$$\left(\frac{u_{\alpha} - u_L}{u_M - u_L} \right) \Delta x = x_{\alpha} - x_L = \Delta x - (x_M - x_{\alpha}) \quad (150)$$

$$\left(\frac{u_R - u_{\epsilon}}{u_R - u_M} \right) \Delta x = x_R - x_{\epsilon} = \Delta x - (x_{\epsilon} - x_M) \quad (151)$$

Substitution of Equation (148) into Equation (150) and Equation (149) into Equation (151) gives Equations (152) and (153), respectively:

$$u_{\alpha} - u_L = (u_M - u_L) \left[1 - \left(u + \sqrt{\frac{Ag}{T}} \right)_{\alpha} \frac{\Delta t}{\Delta x} \right] \quad (152)$$

$$u_R - u_{\epsilon} = (u_R - u_M) \left[1 + \left(u - \sqrt{\frac{Ag}{T}} \right)_{\epsilon} \frac{\Delta t}{\Delta x} \right] \quad (153)$$

By using linear interpolation to determine z_{α} and z_{ϵ} , and then by reasoning in an analogous manner, the equations of depth complementing Equations (152) and (153) are found:

$$z_{\alpha} - z_L = (z_M - z_L) \left[1 - \left(u + \sqrt{\frac{Ag}{T}} \right)_{\alpha} \frac{\Delta t}{\Delta x} \right] \quad (154)$$

$$z_R - z_{\epsilon} = (z_R - z_M) \left[1 + \left(u - \sqrt{\frac{Ag}{T}} \right)_{\epsilon} \frac{\Delta t}{\Delta x} \right] \quad (155)$$

Hence, the desired values of u and z at α and ϵ become known:

$$u_{\alpha} = u_M + (u_L - u_M) \left(u + \sqrt{\frac{Ag}{T}} \right)_M \frac{\Delta t}{\Delta x} \quad (156)$$

$$z_{\alpha} = z_M + (z_L - z_M) \left(u + \sqrt{\frac{Ag}{T}} \right)_M \frac{\Delta t}{\Delta x} \quad (157)$$

$$u_{\epsilon} = u_M + (u_M - u_R) \left(u - \sqrt{\frac{Ag}{T}} \right)_M \frac{\Delta t}{\Delta x} \quad (158)$$

$$z_{\epsilon} = z_M + (z_M - z_R) \left(u - \sqrt{\frac{Ag}{T}} \right)_M \frac{\Delta t}{\Delta x} \quad (159)$$

Note that it is assumed that $\left(u + \sqrt{\frac{Ag}{T}}\right)_\alpha \approx \left(u + \sqrt{\frac{Ag}{T}}\right)_M$ and $\left(u - \sqrt{\frac{Ag}{T}}\right)_\epsilon \approx \left(u - \sqrt{\frac{Ag}{T}}\right)_M$, which is quite reasonable for a closely spaced rectangular grid.

Mean velocity and depth at point P_i can now be computed.

Equations (143) and (145) are rewritten

$$(z_P - z_\alpha) + \left(\sqrt{\frac{A}{gT}}\right)_M (u_P - u_\alpha) + \left(\sqrt{\frac{A}{gT}}\right)_M \left(\frac{f}{8R_H} u |u|\right)_\alpha \Delta t = 0 \quad (160)$$

$$(z_P - z_\epsilon) - \left(\sqrt{\frac{A}{gT}}\right)_M (u_P - u_\epsilon) - \left(\sqrt{\frac{A}{gT}}\right)_M \left(\frac{f}{8R_H} u |u|\right)_\epsilon \Delta t = 0, \quad (161)$$

then added to find z_P ,

$$2z_P = (z_\alpha + z_\epsilon) + (u_\alpha - u_\epsilon) \left(\sqrt{\frac{A}{gT}}\right)_M - \left(\frac{f}{8R_H}\right)_M (u_\alpha |u_\alpha| - u_\epsilon |u_\epsilon|) \left(\sqrt{\frac{A}{gT}}\right)_M \Delta t$$

$$z_P = \frac{1}{2} (z_\alpha + z_\epsilon) + \frac{1}{2} (u_\alpha - u_\epsilon) \left(\sqrt{\frac{A}{gT}}\right)_M - \left(\frac{f}{16R_H}\right)_M (u_\alpha |u_\alpha| - u_\epsilon |u_\epsilon|) \left(\sqrt{\frac{A}{gT}}\right)_M \Delta t \quad (162)$$

and subtracted to find u_P

$$2u_P = u_\alpha + u_\epsilon + (z_\alpha - z_\epsilon) \left(\sqrt{\frac{gT}{A}}\right)_M - \left(\frac{f}{8R_H}\right) (u_\alpha |u_\alpha| + u_\epsilon |u_\epsilon|) \Delta t$$

$$u_P = \frac{1}{2} (u_\alpha + u_\epsilon) + \frac{1}{2} (z_\alpha - z_\epsilon) \left(\sqrt{\frac{gT}{A}}\right)_M - \left(\frac{f}{16R_H}\right) (u_\alpha |u_\alpha| + u_\epsilon |u_\epsilon|) \Delta t. \quad (163)$$

Clearly, it is now possible to determine the velocity and depth of the free surface flow at any interior point on the x -axis not only at time t_i but at all times after t_i simply by repetitively using Equations (156)-(159) together with Equations (162) and (163).

As previously pointed out while developing the finite difference solution for the pipe flowing full, the size of the increments Δx and Δt are interdependent. The same is true of the Δx and Δt increments

of free-surface pipe flow. With reference to Figure 6, the segment of the x-axis bounded on the left at α and on the right by ϵ is the domain of dependence of the point P_i . Thus, whenever Δx is arbitrarily selected, Δt is limited to an increment of magnitude no larger than

$$\Delta t \leq \frac{\Delta x}{(|u| + \sqrt{\frac{Ag}{T}})} .$$

Another way of expressing this is to specify that any point P at which u_P and z_P are to be computed must lie within the domain of dependence bounded by the characteristics curves, C^+ and C^- , passing through L and R, respectively. Figure 10 graphically illustrates the significance of this requirement.

Boundary Conditions

At the right edge of Figure 7 where $x = x_n$ only one characteristics curve, C^+ , is shown. This curve passes through the boundary point P_n . One value, either u_P or z_P is assumed to be given at this point. By first calculating u_α and z_α from Equations (156) and (157), the given boundary value can then be used to determine the unknown value. Suppose that u_P is the known value. Then Equation (160) can be rewritten to give z_P ,

$$z_P = z_\alpha - (u_P - u_\alpha) \left(\sqrt{\frac{A}{gT}} \right)_M - \left(\frac{f}{8R_H} u|u| \right)_\alpha \left(\sqrt{\frac{A}{gT}} \right)_M \Delta t . \quad (164)$$

If z_P is the known boundary condition, then Equation (160) can be rewritten

$$u_P = u_\alpha - (z_P - z_\alpha) \left(\sqrt{\frac{gT}{A}} \right)_M - \left(\frac{f}{8R_H} u|u| \right)_\alpha \Delta t . \quad (165)$$

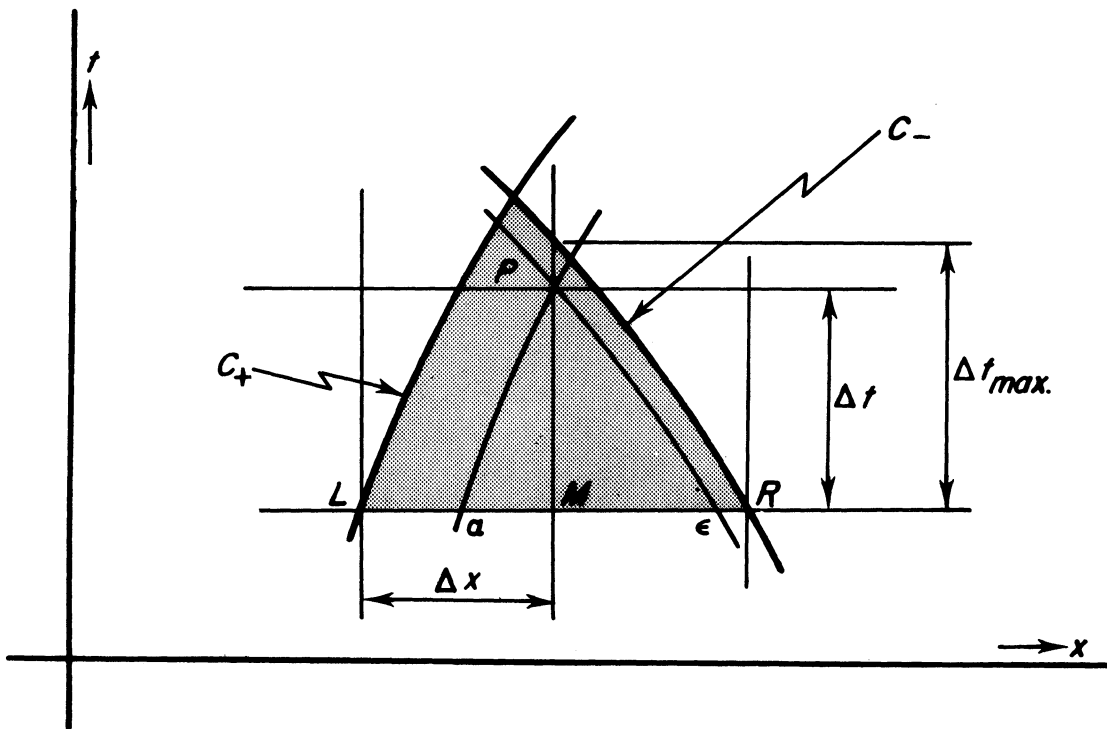


Figure 10. Definition Sketch Illustrating Domain of Dependence Governed by Characteristics Passing Through Grid Points L and R . Point P Must Lie Within Region Bounded by Line Segment LR and Characteristics Curves C+ and C- .

At the left edge of Figure 7 where only one characteristics curve, C-, passes through P₀ the analogous boundary condition equations can be found using Equations (158) and (159) with Equation (161), first for u_p known and then for z_p known:

$$z_p = z_e + (u_p - u_e) \left(\sqrt{\frac{A}{gT}} \right)_M + \left(\frac{f}{8R_H} u |u| \right)_e \left(\sqrt{\frac{A}{gT}} \right)_M \Delta t \quad (166)$$

$$u_p = u_e + (z_p - z_e) \left(\sqrt{\frac{gT}{A}} \right)_M - \left(\frac{f}{8R_H} u |u| \right)_e \Delta t . \quad (167)$$

Before concluding this chapter, it is certainly worth noting the very pronounced similarity between the equations of transient motion for the pipe flowing full and the equations of transient motion for a horizontal pipe with free surface flow. The latter is analogous to unsteady, open-channel flow. By comparing Equation (72) with Equation (127) and Equation (71) with Equation (128), one becomes clearly aware of this similarity. The similarity is further evidenced by comparing the respective sets of characteristics equations, namely, Equations (79)-(82) and Equations (136)-(139).

Note that in the closed pipe the celerity of the internal pressure wave is

$$\sqrt{\frac{1}{\rho \left(\frac{1}{K} + \frac{C}{E} \left(\frac{R}{b-R} \right) \right)}}$$

On the other hand in a pipe undergoing flow with a free surface, the celerity of the infinitesimal surface wave--a pressure wave in the external sense--is given by the expression $\sqrt{\frac{Ag}{T}}$. In each instance the celerity is affected by the particular properties of the liquid. It is also affected by the particular liquid-solid and/or liquid-gas interface conditions.

When the pipe is flowing full the celerity is a function of the pipe constraint and elasticity as well as the liquid properties, whereas, when the pipe is flowing partially full the celerity is a function of the shape-geometry of the flow and of the liquid properties. Nevertheless, both expressions are dimensionally similar.

When one recognizes that transient flow conditions in a pipe flowing full on the one hand and in a pipe flowing with a free surface on the other hand are basically very similar hydrodynamic phenomena, then the similarity of the respective analytic treatments and mathematical results is not surprising. However, recognition of the hydrodynamic similarity has been delayed perhaps, by the traditional division of hydrodynamics into "pipe-flow" problems and "open-channel" problems.

CHAPTER IV
COMPUTER SIMULATION

Column separation precipitated by transient flow in a pipe was interpreted theoretically in Chapter II. Its two principal regimes of liquid motion were the subjects of analysis which included the development of numerical processes for their evaluation in Chapter III. In this chapter the theoretical concepts of transient-flow, column separation phenomenon, and the mathematical treatment of its two regimes of liquid motion are used to formulate a working mathematical model for simulating the phenomenon by digital computer. The specific boundary criteria applicable to the model are discussed in detail. The sequence of operations followed in the model is described and presented by means of a flow chart. The structure of the computer program is discussed briefly. The chapter concludes with several general remarks about the operational characteristics of the simulation model.

Flow System

The flow system envisioned for computer simulation of the transient flow, column-separation phenomenon is physically similar to the example system considered in Chapter II (See Figure 2). A constant-head reservoir and a quick-closing gate valve are assumed to be connected by a long length of pipe. The reservoir is open to atmospheric pressure. The gate valve is capable of instantaneous closure. Its elevation, however, is variable with respect to that of the reservoir. The long length of pipe connecting the reservoir to the valve is composed of two (or more) pipe segments, each of which may be of unique diameter,

wall-thickness, length, composition, and may have different friction-loss properties as well as support fixity. The pipe segment connected to the gate valve is the one in which column separation is anticipated. This segment remains horizontal at all times; the other segments are free to assume any inclined position. Because axial distance along the pipe system is measured from the valve, this segment is denoted as segment No. 1. Figure 11 shows a schematic drawing of the flow system.

Initially, the gate valve is assumed to be fully open, thereby permitting steady flow throughout the system. At some time prior to the reference or starting time, t_0 , the velocities and pressure heads on the x,t -plane at the particular points, $x_{k,i}$, are determined from steady-state conditions. These quantities are the initial conditions used to begin simulation of the transient-flow, column-separation phenomenon in the computer model. The notation, k , is an integer subscript denoting the particular pipe segment.

Boundary Conditions

The purpose of this discussion is to identify and set forth the controlling boundary conditions which delimit a unique, well-defined solution of the mathematical model. Without an explicitly stated set of boundary conditions, accurate computer simulation of the transient-flow, column-separation phenomenon observed in a prototype system would be impossible.

Prior to closure of the gate valve two boundary conditions govern steady-state flow in the system: pressure head at the entrance to the pipe and the velocity of flow through the gate valve. Since the constant head reservoir is unable to sustain a pressure other than its

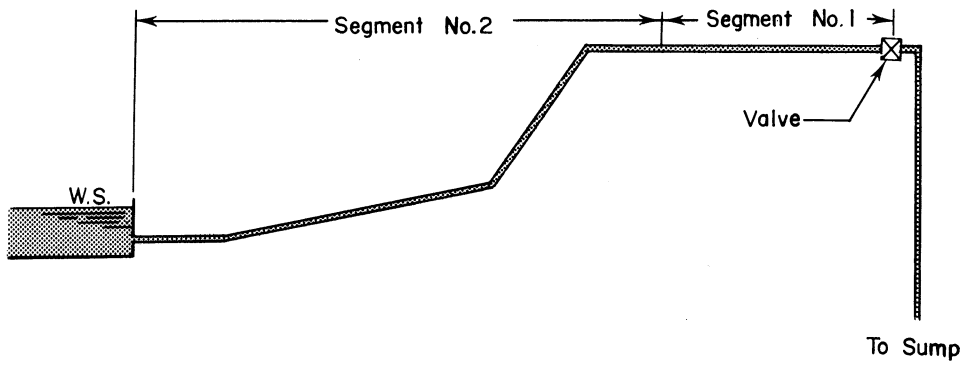


Figure 11. Schematic Representation of Laboratory Flow System Used in Experimental Investigation.

own static pressure head, $H_{k,n}$ is known and constant throughout time. The velocity through the gate valve is equivalent to simply the discharge divided by the area of the cross section at the valve; therefore, $v_{1,0}$ is known, also. $H_{k,n}$ and $v_{1,0}$ are "given" boundary conditions which are used with Equations (105) and (108) in the numerical evaluation process to determine $v_{k,n}$ and $H_{1,0}$.

Transient-flow conditions are initiated by closure of the gate valve. This occurs at time t_0 . Therefore, $v_{1,0}$ is set to zero at time t_0 and remains zero until column separation takes place. However, the pressure head, $H_{k,n}$, at the reservoir remains unchanged and continues to be the second boundary condition needed to define this phase of the flow.

When the pressure head ($H_{1,0}$) at the gate valve falls to the vapor pressure of the water, column separation takes place. At the instant of column separation, new boundary conditions must be defined for the pipe flowing full and another set of boundary conditions introduced to describe conditions governing the free-surface flow in the pipe.

For the pipe flowing full the pressure head at the reservoir, $H_{k,n}$, remains unchanged. However, the boundary condition which formerly governed the condition of flow at the gate valve is now located at the moving interface separating the full flow regime from the free-surface flow regime within the pipe. This boundary condition is $H_{1,0}$ set equal to the water-vapor pressure head where the subscript zero now refers temporarily to the position of the interface. Thus, $H_{k,n}$ and $H_{1,0}$ are used with Equations (108) and (106) to determine $v_{k,n}$ and $v_{1,0}$ at the boundaries of the full-flow system.

One of the conditions governing the free-surface flow occurring in pipe segment No. 1 is the boundary condition at the gate valve. Because the gate valve is closed there can be no flow (with a free-surface or otherwise) through the valve; thus, the boundary condition is simply that the velocity u_0 equal zero. However, a second boundary condition, which suitably pertains to the condition of flow at the interface between the two regimes of liquid motion is not so easily reconciled. A condition is needed prescribing either the velocity of flow or the depth of water at the leading edge of the free surface interface. But because the forefront of the cavity is itself moving with time, this task is formidable.

Repeated laboratory observations of column separation revealed that the leading edge of the cavity appeared to separate from the top-most, inner surface of the pipe wall in a manner which remained basically unchanged regardless of the prior velocity of flow. In fact, the foremost edge of the cavity appeared to maintain a profile of more-or-less constant parabolic shape (See Figure 1). Although the mechanism of liquid separation from the pipe wall is not investigated in this study, local surface tension is thought to be the principal factor governing its behavior. The mechanism of liquid separation from the pipe wall, while fundamentally a three-dimensional flow process, can be adequately treated as a one-dimensional flow process provided the pipe diameter is not too small. Thus, if the foremost tip of the advancing vapor cavity is assumed to actually have a parabolic profile, a means is at hand by which the boundary condition, z_m , can be prescribed.

In the simulation model the shape of the advancing tip of the vapor cavity is assumed to be analytically represented by the similarly shaped void subtended by a parabolic cylinder which intersects at right angles with a circular cylinder, i.e., the pipe, as shown in Figure 12. The equation of the parabola on the x, z -plane is

$$(z - 2R(1-\theta))^2 = 4x_p(-\theta R) ,$$

wherein the focal distance, cb , is θR ; the latus rectum, ad , is $4\theta R$; and the vertex, located on the Z axis, is offset from the X axis by the distance $2R(1-\theta)$. The horizontal length of the subtended void as measured from the vertex of the parabolic cylinder is the variable, x_p , while θ is a preselected decimal parameter. The depth, z , at any point on the surface of intersection depicting the free-surface profile at the forefront of the cavity is given by

$$z = 2R(1-\theta) \mp \sqrt{4\theta R x_p} . \quad (168)$$

The hypothesis advanced in Chapter II asserts that the volume rate-of-growth of the vapor cavity is equivalent to the full-flow discharge that occurs in the pipe immediately ahead of the cavity. Thus, since $v_{1,0}$ can be found by computation and since the pipe diameter is known, the equivalent volume rate-of-growth of the cavity can be determined.

The subtended parabolic void representing the forefront of the cavity takes form at the gate valve, that is, at x_0 . It expands in volume and length with time. As soon as its volume is sufficient to insure an overall length greater than Δx , thus causing it to extend

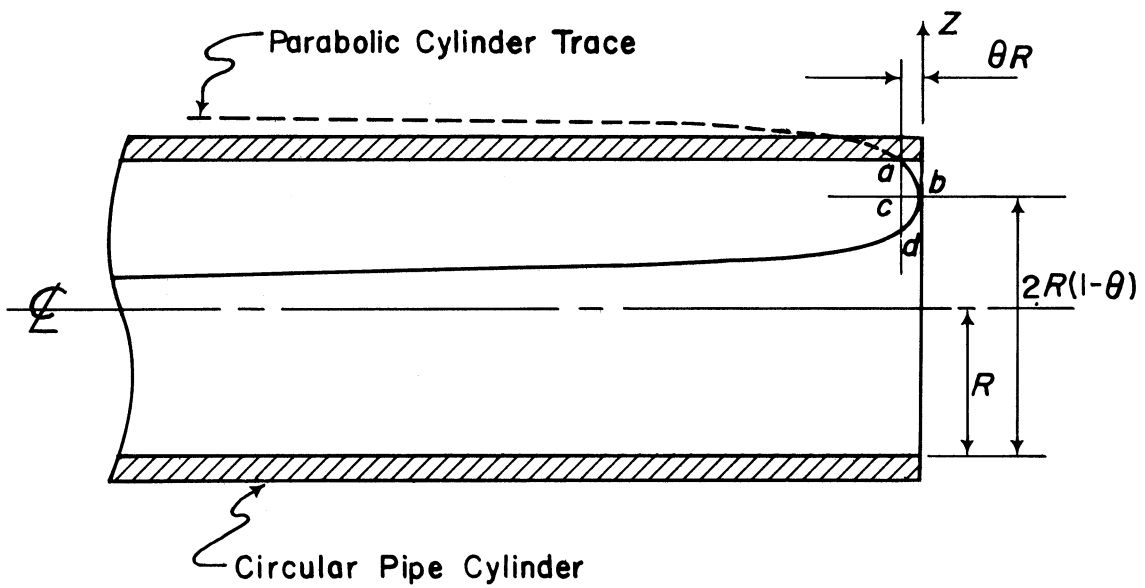


Figure 12. Definition Sketch Showing a Parabolic Cylinder Intersecting a Circular Cylinder. The Shape of the Common Volume Resulting from this Intersection is Considered Representative of the Shape of the Void Typically Encountered at the Leading Edge of the Vapor Cavity.

beyond x_1 , the value of z_0 and z_1 can be determined from Equation (168). As previously stated u_0 equals zero. The velocity u_1 is arbitrarily set equal to $v_{1,0}$, which although an approximation must be very nearly correct. Thus, the initial velocity and depth of the embryonic, free-surface flow at x_0 and x_1 are now known at some time t_i on the x,t -plane. These values serve as "given conditions" with which the characteristics evaluation process can be initiated to compute the changing values of velocity and depth at subsequent intervals in time.

Meanwhile, of course, the actual vapor cavity is continuing to lengthen and increase in total volume. At x_0 the boundary condition $u_0 = 0$ remains unchanged. Although the characteristics evaluation process can be used to simulate the free-surface depths and flow velocities, the boundary depth, z_m , farthest from the gate valve (in other words, the depth at the grid point nearest the cavity tip) must be determined. This boundary depth is computed recursively with time by means of the parabolic-void approximation. However, it is worth noting that this approximation affects only the tip-most portion of the simulated vapor cavity, chiefly that portion of the cavity extending beyond the farthest, free-surface grid point on the x axis. The parabolic void approximation is used to approximate the depth during both the growth and collapse phase of the cavity simulation process. Thus, with the exception of some slight distortion which perhaps may be introduced by the boundary condition imposed at the forefront of the vapor cavity, a well-defined technique for mathematically simulating the column separation accompanying transient flow in pipes is available.

Sequence of Operations

The model employed to mathematically simulate the phenomenon of transient flow in a pipe and the accompanying phenomenon of liquid column separation consists of a multitude of individual operations performed in a specifically prescribed, logical sequence. The operations may be grouped into general categories which are related to particular functions. These functional categories are listed sequentially:

- (a) Introduction, predefinition, and initialization of specific parameters, constants, and control factors used in the simulation model.
- (b) Establishment of the theoretical flow system including initialization of the pre-transient regimen for the pipe system (pipe flowing full).
- (c) Delineation of the boundary conditions and operating controls determining the transient flow phenomenon in the pipe system.
- (d) Successive calculation of the transient velocities and depths throughout the system with respect to time while the pipe is flowing full. The method of characteristics is used to carry out these calculations. Special means are employed to apply the method when the increment Δx equals the overall length of a pipe segment.
- (e) Determination of the occurrence of column separation by means of test conditions. Certain control parameters are set up in order to integrate an additional sequence of operations to be followed during periods of separation.

- (f) Predefinition of functions and computation of initial values and boundary conditions governing free-surface flow.
- (g) Computation of transient free-surface velocities and depths associated with the growth and collapse of the vapor cavity. The computations are carried out by the method of characteristics for free-surface flow concurrently with the calculation for the pipe flowing full.
- (h) Reinitialization of both major and minor control parameters and boundary conditions following collapse of the vapor cavity.

An abbreviated schematic flow diagram depicting the sequence of operations followed in the simulation process is presented in Figure 13. Much of the mathematical detail has been eliminated from the diagram in order to emphasize the logic of the simulation process.

Digital Computer Program

The digital computer program used to transmit the statement of the model simulating the transient-flow, column-separation phenomenon to the computing machine follows the skeletal structure outlined in the flow diagram. The actual computer program is composed of a main program and several subprograms, which when integrated make up the whole program. The main program performs the functions outlined in the flow diagram. Consequently, it is structured similarly. Eleven subprograms or sub-routines were written to perform various operations required by the main program. These subroutines are called upon as needed. In addition, six internal subroutines are defined and embedded in the main program.

Consider the fact that in the particular prototype flow system being simulated, the elapsed time, starting with the moment transient flow is initiated, continuing through the ensuing formation of the first vapor cavity, and concluding with its collapse, is approximately two or three seconds. If the digital computer could simulate this portion of the phenomenon in less than actual time, it would be performing in so-called "fast time." If it required exactly the same number of seconds it would be performing the simulation in "real time." If the computer required longer than the actual time to complete the simulation run, it would be performing in "slow time." Because the ratio of the actual time to that required to simulate the separation phenomenon was approximately 1 to 240, the digital computer simulated column separation in slow time.

The computer program (the main program and special subroutines) is written in the Michigan Algorithm Decoder language commonly known as MAD. This language is an enriched Algol base compiler language which has been designed for implementation on IBM 7090 series computing systems having 32K words of main memory. Certain of the operational characteristics of the program experienced for the particular system configuration investigated are tabulated below:

(a) Required locations in main memory

Main program--8,139 words

Special subroutines--1,639 words

Complete program--17,390 words

(b) Total compilation time of complete program--127 seconds

Complete listings of the main program and of the subroutines are given in Appendices I and II, respectively.

CHAPTER V

EXPERIMENTAL APPARATUS AND LABORATORY INVESTIGATION

Experimental investigation of the column separation phenomenon comprises the second major phase of this study. It serves to complement the theoretical analysis which culminated in the technique for computer simulation of column separation discussed in Chapter IV. Experimental investigation was carried out in a specially constructed pipe system located in the G. G. Brown Fluids Engineering Laboratory on the North Campus at The University of Michigan. This chapter describes the pipe system and the special instrumentation and apparatus used in the laboratory investigation. It also treats the determination of the resistance-to-flow characteristics of the pipe system as well as the calibration of the instrumentation used to measure transient pressure and depth-of-flow. The chapter concludes with a summary of the procedures followed in conducting the experimental measurements.

General Description of Pipe System

The laboratory flow system was comprised of four principal elements: a constant-head weir box; approximately 439 feet of heavy-duty, one-inch inside diameter copper pipe; approximately 8.5 feet of one-inch inside diameter plexiglas (cast acrylic resin) pipe; and a solenoid-operated, quick-closing gate valve. The weir box was connected to the gate valve by means of the copper pipe and the plexiglas pipe. The plexiglas pipe served as the test section in which the anticipated column separation could be observed. It was therefore connected directly to the

gate valve. Water was supplied to the weir box from the laboratory supply and returned to a sump by means of a copper pipe and a heavy duty hose. Siphon action was used to maintain flow through the system. A detailed sketch of the flow system is presented in Figure 14.

The constant-head, weir box was designed to minimize the fluctuations in head caused by changes in the discharge in the pipe system. Two sharp-crested, horizontal, overflow weirs were provided such that if a maximum flow velocity of 3 ft./sec. in the system were suddenly reduced to zero, the maximum increase in head in the box would be less than .011 ft. A manifold was used to introduce water into the weir box with minimum turbulence.

The copper pipe was composed of six segments carefully joined together to form a continuous conduit. A short segment only 1.25 feet in length and integrally attached to the constant-head weir box, serves as the inlet. The next four segments, each approximately 100 feet in length, were joined by soldered sleeve connections. To conserve space these segments were loosely coiled in a helix 5 feet in diameter and supported by a finger-like wooden frame mounted vertically upon a mobile hexagonal platform. The pipe was not constrained by the frame, therefore the coils could freely adjust to imposed strains. Figure 15 shows the constant-head weir box and the coiled pipe on the supporting frame. The final segment of copper pipe extended approximately 37.5 feet from the top of the coil to its junction with the plexiglas pipe. The properties of the various segments of copper pipe used in the system are listed in the table below:

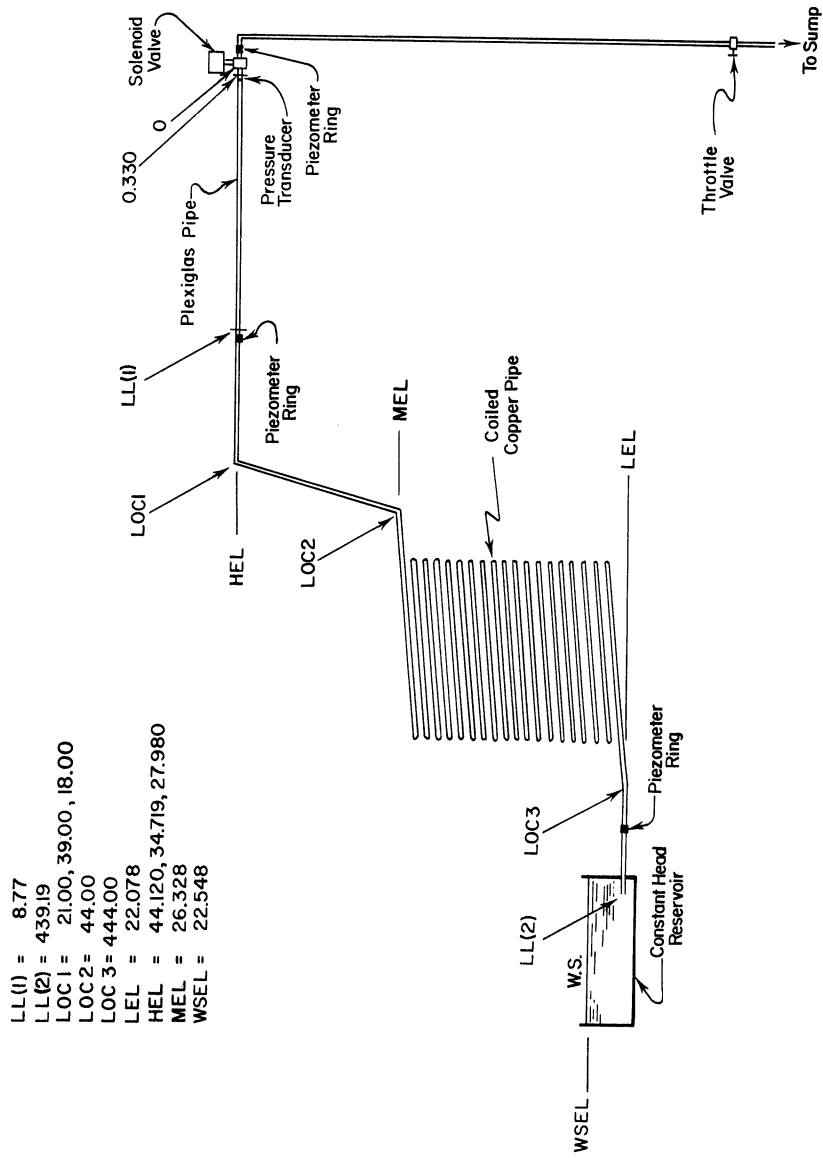


Figure 14. Detailed Schematic of Laboratory Flow System.

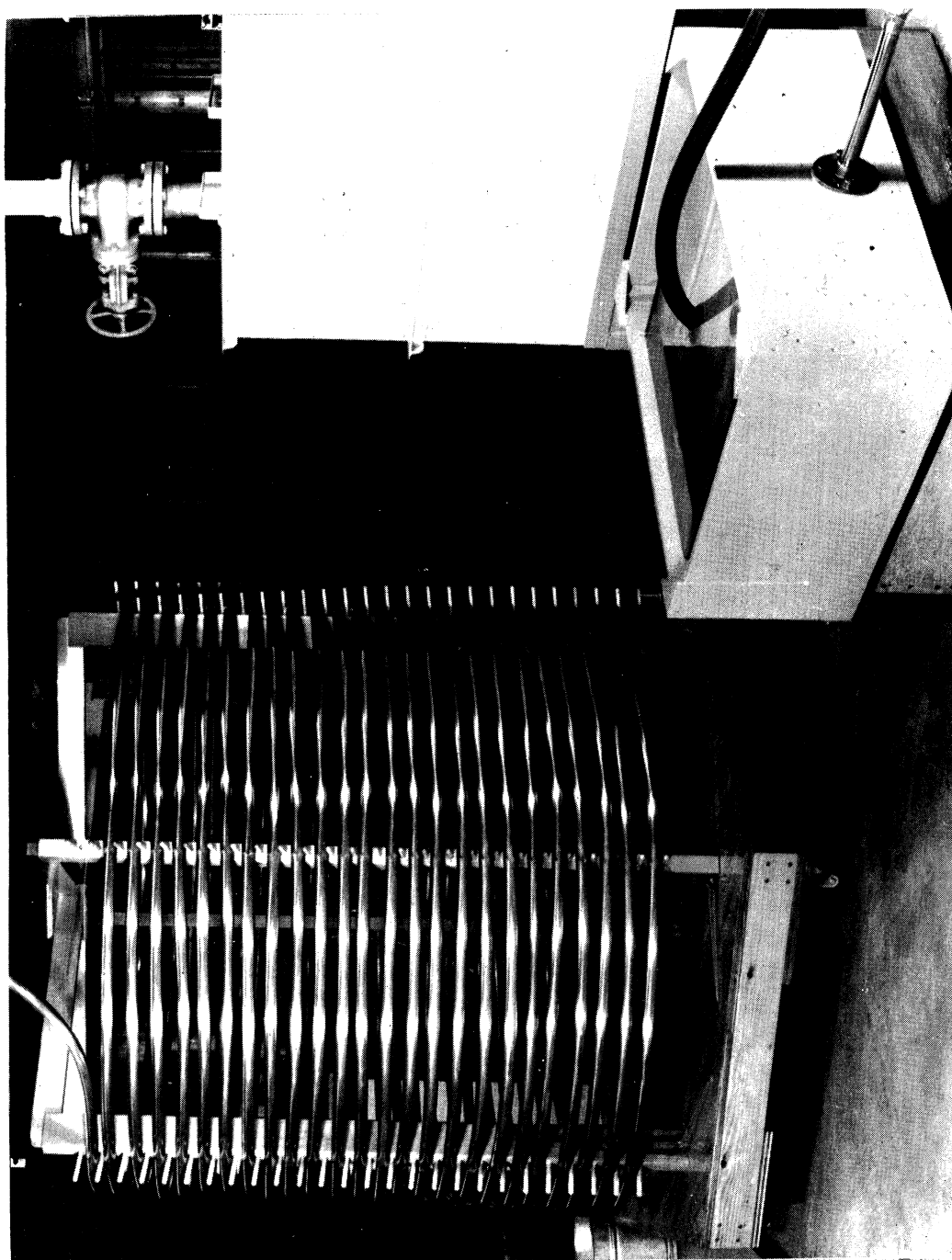


Figure 15. View of Constant-Head Weir Box and Loosely Coiled Copper Pipe on Wooden Frame.

TABLE I
COPPER PIPE PROPERTIES

Segment	Length ft.	Inside Diameter ft.	Wall Thickness ft.	Density lb./ft. ³	Modulus of Elasticity lb. ft. ² x 10 ¹⁰
Inlet	1.25	.0824	.00532	546	.2448
1	100.00	.0836	.00529	558	.2448
2	100.16	.0831	.00535	558	.2448
3	100.19	.0832	.00529	558	.2448
4	100.13	.0816	.00540	558	.2448
Connector	37.46	.0828	.00528	558	.2448
Total or Average Values	439.19	.0829	.00532	558	.2448

Because the properties of the copper pipe segments were similar with respect to each other, they were treated as one continuous pipe having average characteristics.

The plexiglas pipe was constructed of two short lengths of pipe cemented together to form a continuous tube 8.44 feet in length. Plexiglas flanges were machined and fitted to the ends of the pipe, thereby permitting connection to a similar bronze flange attached to the copper pipe on the one hand, and to another bronze flange attached to the gate valve on the other hand. O-rings inserted between the flanges in machined chamfers provided leak-proof connections. A steel frame was used to hold the pipe firmly in position. Although the pipe could still accommodate radial strains, the frame curtailed axial strains. The cast plastic pipe was assumed to be isotropic. Its properties are listed in the table following:

TABLE II
PLASTIC PIPE PROPERTIES

Length ft.	Inside Diameter ft.	Wall Thickness ft.	Density lb./ft. ³	Modulus of Elasticity lb./ft. ² x 10 ⁸
8.77	.0828	.0211	73.63	.5112*

*Methyl Methacrylate (acrylic resin) at 26°C.

The steel frame used to secure the plexiglas pipe also served as a mounting for the quick-closing, solenoid-actuated gate valve. Because this frame was designed to permit rotational adjustments about a horizontal axis, the valve was positioned so that the axis of rotation passed through the center of the gate opening. However, all investigations undertaken in this study were conducted with the plastic pipe in the horizontal position.

The solenoid-actuated valve was normally in the open position. When actuated by the solenoid the sliding gate was pushed downward until the circular passage in the gate was no longer aligned with the inlet and outlet ports. The time-of-closure was found to vary from less than 20 milliseconds to nearly 60 milliseconds, depending upon the phase position of the AC voltage at the moment the solenoid coil was energized. Clearly, the instantaneous valve closure assumed in the theoretical phase of the study was not achieved in the laboratory. However, because the round-trip travel time of the main pressure wave was in fact equivalent to instantaneous valve closure.

Because the flow system was operated under syphon conditions, the drain hole at the bottom of the valve chamber was submerged in a reservoir of water.

Figures 16 and 17 show the plexiglas pipe, the solenoid-operated gate valve, and the steel supporting frame from two different vantage points. Figure 18 provides a close-up view of the principal test section in the plexiglas pipe, the solenoid-actuated gate valve, and the supporting frame and mounting bracket.

A one-inch inside diameter copper pipe was used to return the flow from the valve to a lower elevation. A heavy-duty, one-inch inside diameter rubber hose connected to this pipe returned the flow to the laboratory sump, thereby completing the flow system.

Instrumentation

Three sets of piezometer rings were attached to the copper pipe system. The first ring was located just beyond the entrance to the pipe system at the weir box; the second was placed immediately ahead of the junction between the copper and the plastic pipes; and the third ring was positioned just beyond the gate valve. A removable, fourth plexiglas piezometer ring (shown hanging from the dual manometer stand in Figure 16) was available for insertion at the junction between the plexiglas pipe and the gate valve. When connected to the appropriate manometers these piezometer rings were used to determine the friction loss characteristics of the flow system.

A Dynisco unbonded strain-gage type transducer was used to determine the transient pressures at the gate valve. This transducer, which was mounted nearly flush with the inside wall of the pipe and

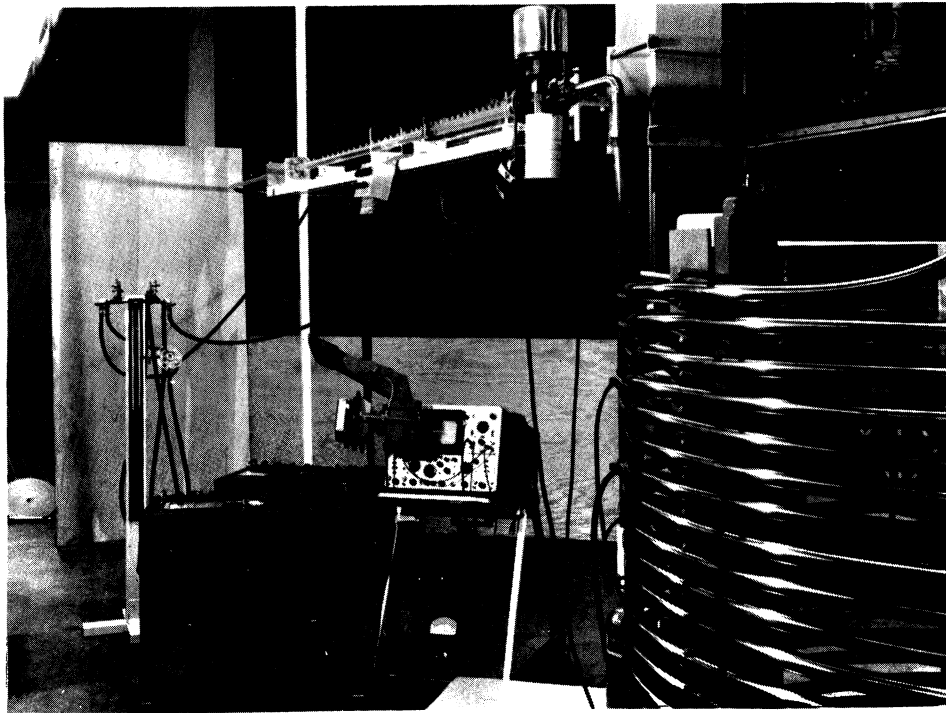


Figure 16. View of Coiled Copper Pipe, Plexiglas Pipe, Solenoid-Operated Gate Valve, and Assorted Instrumentation. Plexiglas Pipe and Gate Valve are Mounted on Steel Frame Clamped to Structural Column.

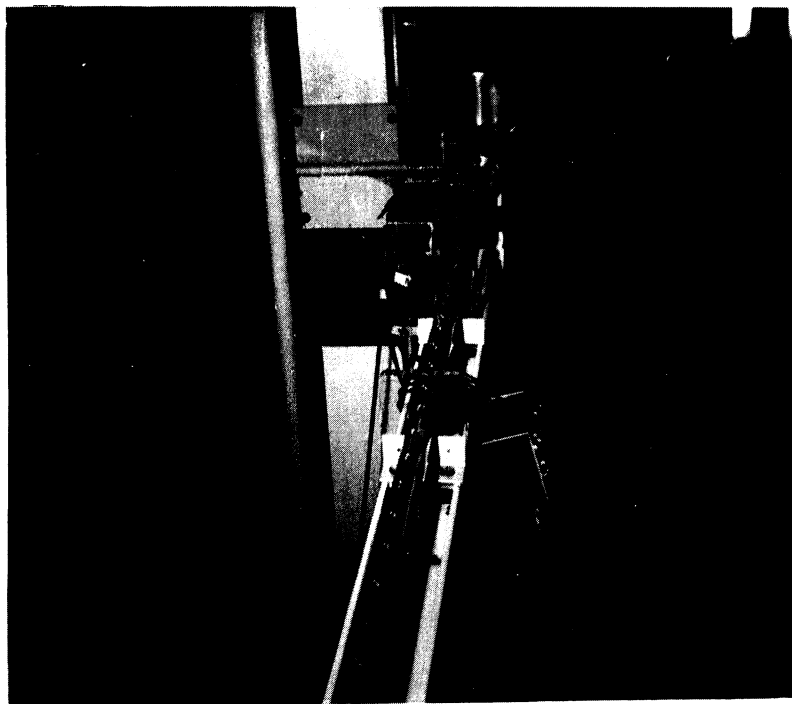


Figure 17. Top View of Plexiglas Pipe and Solenoid Operated Gate Valve.

normal to the longitudinal axis, was temperature compensated throughout its full 0-300 psia pressure sensing range. Its range of frequency response was 0-12,000 cps. The transducer is partially visible on the back side of the pipe in the center of Figure 18. An Ellis BAM-1 bridge amplifier was used not only to supply the input voltage needed to activate the four arms of the Wheatstone bridge circuit in the transducer, but also to amplify the response signal. The output of the amplifier was displayed on a Tektronics Model 565 dual beam oscilloscope equipped with a polaroid camera.

In order to determine the magnitude and shape of the vapor cavities a series of miniature wave gages were very tediously installed throughout the length of the plexiglas pipe. Each gage, consisting of .002-inch diameter nickel-chrome resistance wire threaded in a "W"-like pattern through the walls of the pipe and cemented in place with epoxy resin, could serve as a single leg in a variable conductance Wheatstone bridge circuit. The gages were vertically oriented in a plane normal to the axis of flow. The first gage, located as close to the gate valve as possible, was .342 foot from the near face of the gate while the second gage was .500 foot from the face. The next 17 gages were spaced at 2-inch intervals, the following 16 gages at 3-inch intervals, and the remaining gages at 6-inch intervals. A total of 37 gages were installed in the plexiglas pipe. Figure 19 shows a sample miniature wave gage typical of the gages installed in the plexiglas pipe. Several of the actual gages are visible in Figures 16-18.

Two Sanborn Twin-Viso oscillographs equipped with A.C. amplifiers (2400 cps) were used to activate the gages, amplify the responses, and record the resulting signals. Four identical bridge circuits were provided

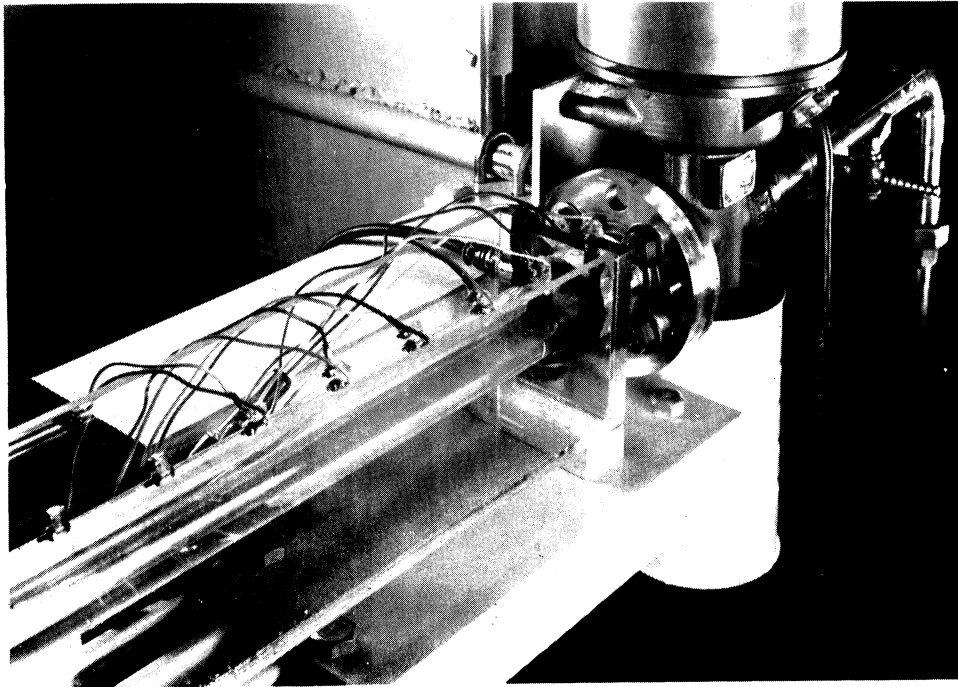


Figure 18. Close-Up View of Principal Test Section Depth Gages and Pressure Transducer Mounted in Plexiglas Pipe.



Figure 19. Enlarged View of Sample Depth Gage.

in order that any four gages could be monitored simultaneously. A schematic diagram of the bridge circuit is shown in Figure 20. The two Sanborn units were interconnected and their circuits slightly modified in other ways to eliminate beat frequencies and minimize cross-signal feedback. Figure 21 provides a closeup view of the two oscillograph units, the camera-equipped oscilloscope, and the bridge amplifier unit used in the study.

System Calibration

The unique frictional resistance characteristics of the laboratory flow system were investigated for the full range of anticipated rates of discharge. The head losses in both the plexiglas pipe (pipe segment 1) and the copper pipe (pipe segment 2), were determined for 55 different rates of discharge. Two differential manometers were used to measure the head losses, while weigh-tank observations were used to determine the flow velocities. These data, together with the appropriate kinematic viscosity data, were used to obtain the steady-state, frictional flow-resistance term f , and the associated Reynolds number. Figure 22 is a graphical representation of the typical flow resistance relationships obtained by plotting the respective data versus the associated Reynolds numbers. While the relationships shown in Figure 22 admittedly represent steady state flow resistance characteristics, the flow resistance relationships for transient flow conditions are assumed to be equivalent.

Before undertaking the investigation of the column separation accompanying transient flow in the experimental laboratory apparatus, both the pressure-sensing instrumentation and the wave or depth-sensing

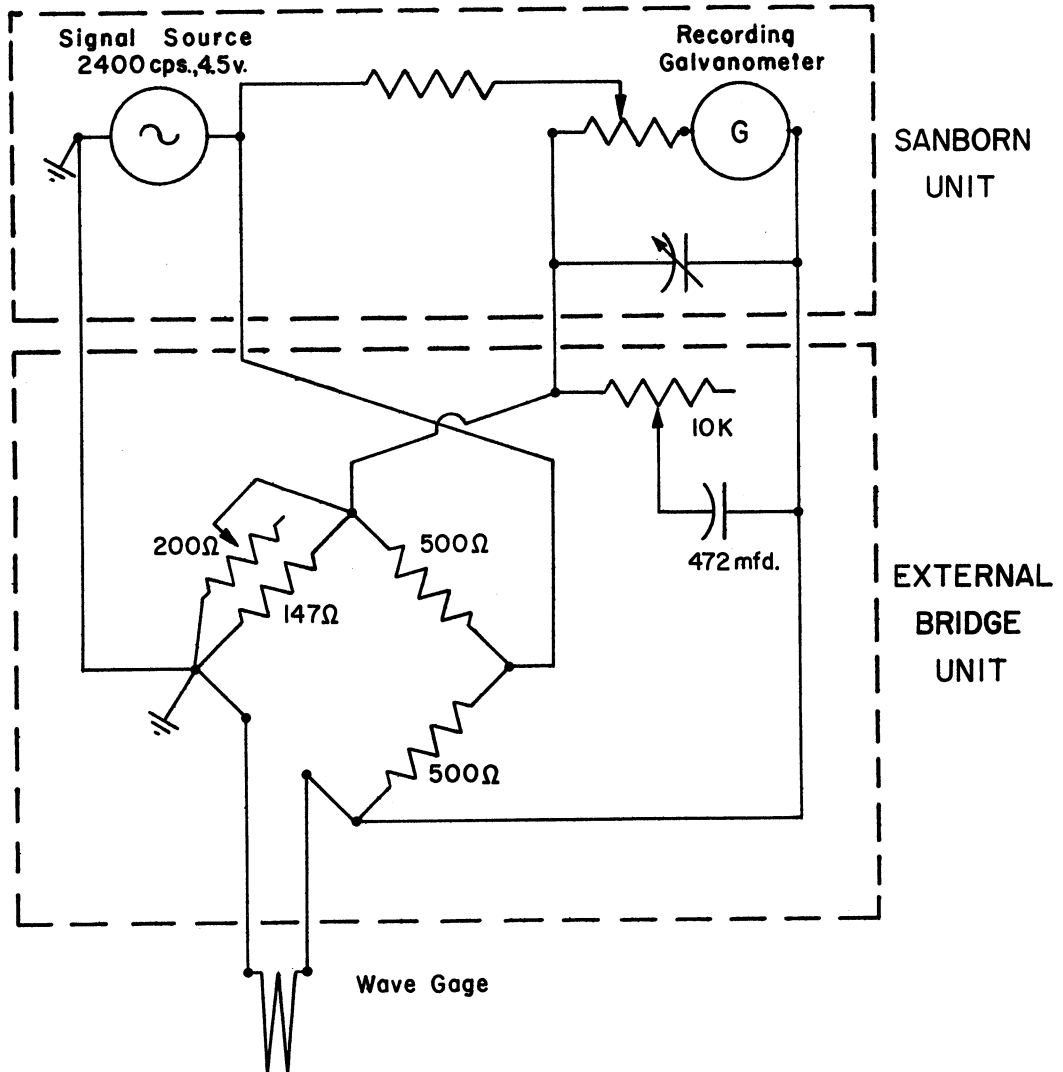


Figure 20. Diagram of Circuit Designed for Use with a Miniature Wave Gage.

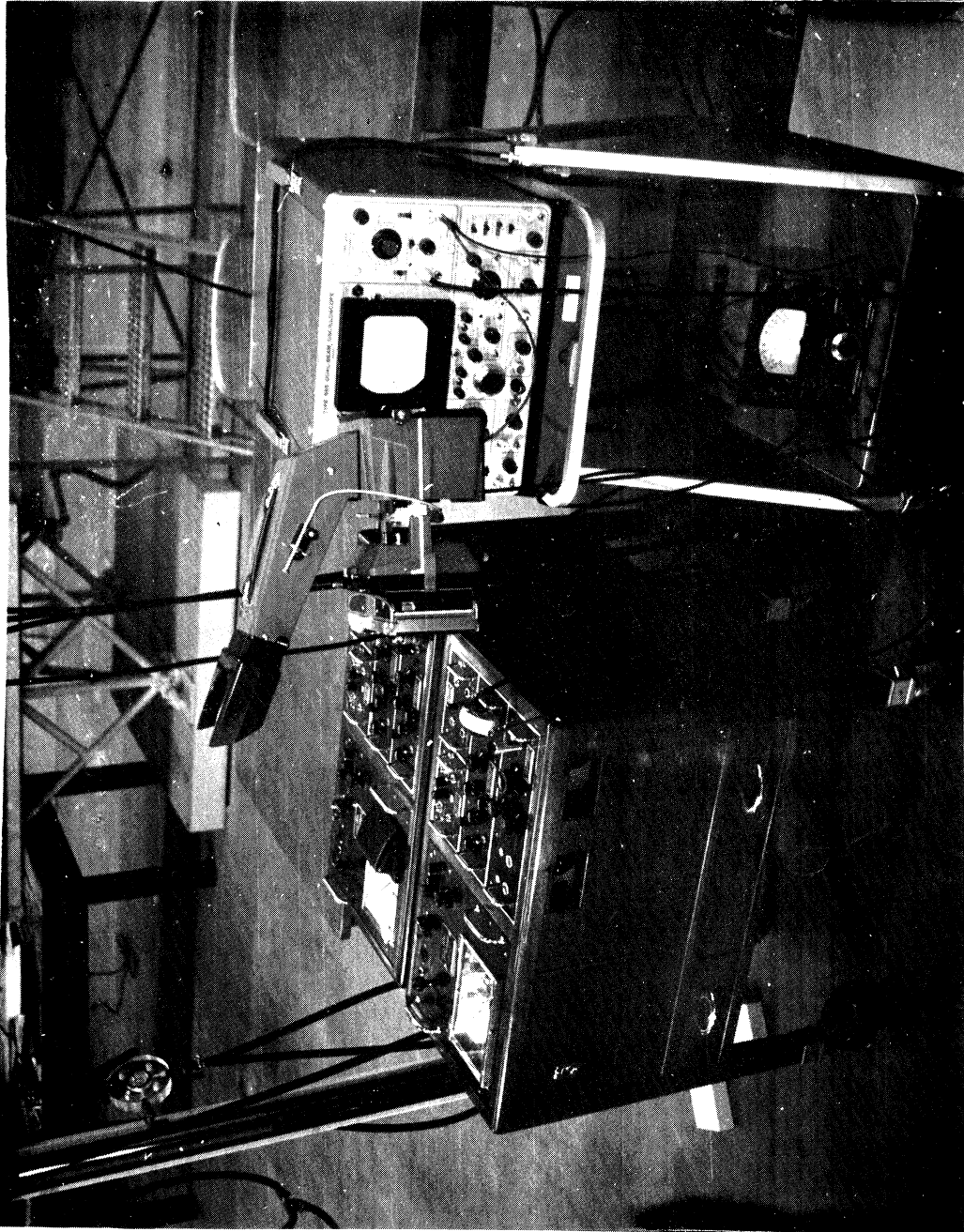


Figure 21. Close-Up View of Dual-Channel Oscillograph Units, Camera Equipped Oscilloscope, and Bridge Amplifier Unit.

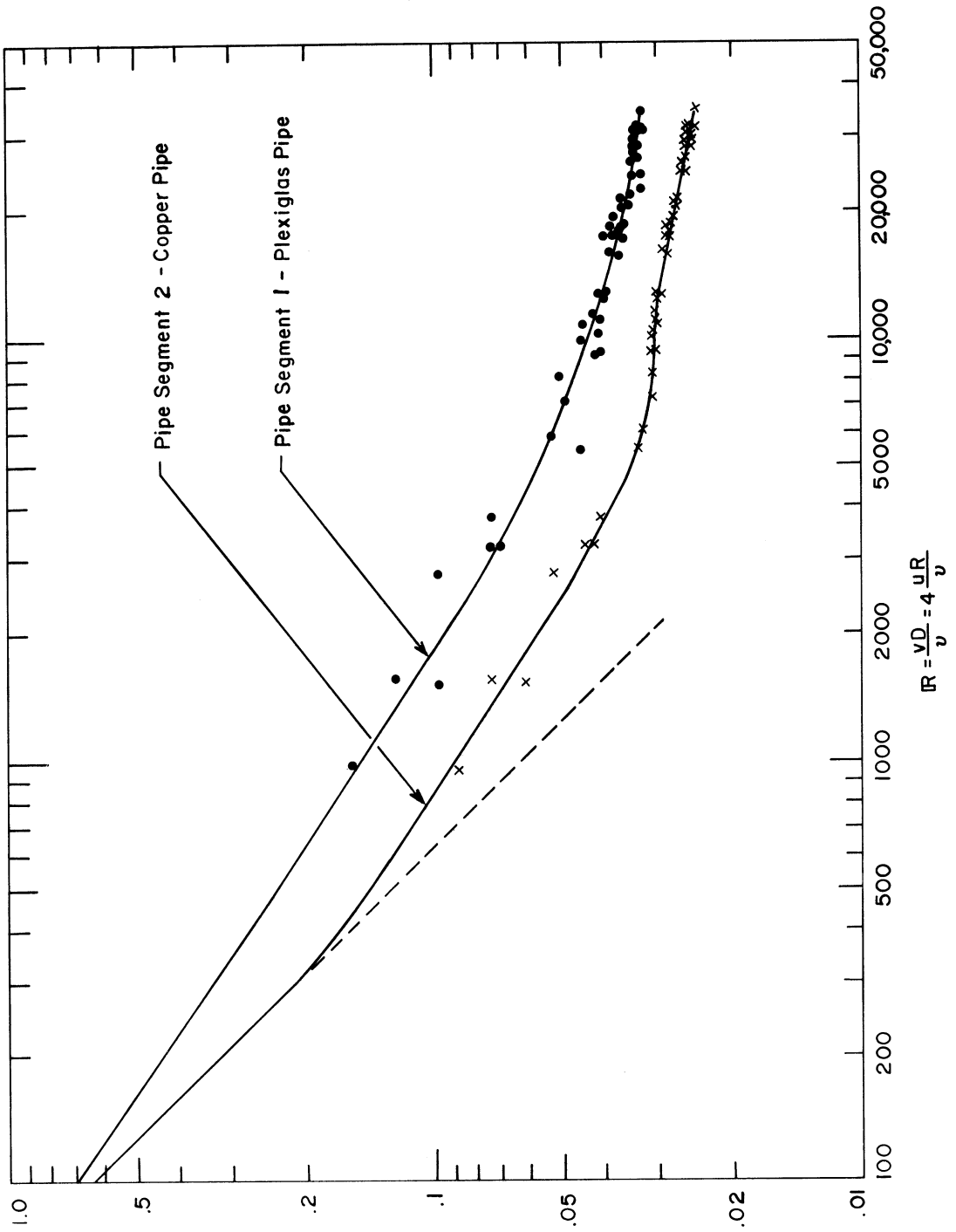


Figure 22. Flow-Resistance Relationships for the Copper and Plexiglas Pipes.

instrumentation had to be thoroughly checked, adjusted, and fully calibrated. In fact, these operations had to be repeated frequently in order to insure that all equipment was functioning properly and that the observed readings were indeed meaningful and accurate.

The pressure transducer was carefully checked for accuracy of full-scale reading using a dead-weight gage tester. Then the proper scaling was established on the Ellis bridge amplifier and on the oscilloscope to give the proper beam deflections on the dual beam cathode ray tube. The dead weight gage tester was used to determine the desired scaling.

Maintenance and calibration of the depth sensing gages proved to be a tedious, complex, and often difficult task. Although these gages were all of similar design, each one had unique calibration characteristics which had to be taken into account. Calibration of these gages consisted of establishing (or reestablishing) the zero flow or dry pipe adjustment of the appropriate oscillograph channels. Next the full-flow reading was used to adjust the various oscillograph channels for proper scaling with a particular gage. Another reading had to be taken to compensate for the pressure condition in the pipe. This reading was subsequently used as an adjustment applied to the recorded values during appropriate periods in time.

The time required to adjust, calibrate, and stabilize the operation of the wave gages ranged from one or two hours to as much as a day or longer. Fortunately, once proper operation was achieved only minor adjustments were required between successive column separation experiments in a sequence of investigations.

Experimental Procedures

Actual column-separation experiments could be undertaken only after all electronic equipment had operated sufficiently long to insure its stability and after all instrument calibration had been successfully accomplished. The first step in an experiment was to prime the pipe system and thereby establish syphon flow. The priming operation was done by temporarily attaching a hose to the inlet of the system in the weir box. Water drawn under pressure from the laboratory constant head tank was used for priming and for flushing out entrapped air. All piezometers were bled to eliminate air which may have become trapped in the piezometer rings. Flow in the system was regulated by means of a throttle valve in the sump return pipe. The steady-state discharge was determined by using a stop watch and a scale to time and weigh, respectively, several sampled quantities of water passing through the system. Water temperature readings and mercury barometer readings were recorded at frequent intervals throughout an experimental period.

To initiate transient flow and the subsequent column separation, the recording oscillographs were started and the shutter of the polaroid camera attached to the oscilloscope was opened immediately prior to the instant the solenoid valve was switched shut. When the valve closed, the self-triggering, beam-sweep circuits in the dual-beam oscilloscope caused the trace of the pressure wave sensed by the transducer at the gate valve to be recorded on film. The upper beam was used to record the individual pressure peaks superimposed, one upon the other, using an expanded time scale. The lower beam recorded the entire sequence of pressure peaks separated by periods of column separation during a 5-second sweep interval. The trace of transient pressures observed at the gate valve and

shown in Figure 23 for laboratory run No. 19 is typical of the data obtained from the pressure transducer. In this figure a major division in the vertical direction is equivalent to 55 psia. A major division in the horizontal direction on the upper scale is equivalent to .05 second; on the lower scale, .5 second.

Meanwhile, the oscillographs recorded the depth of flow at selected points within the travel range of the cavitation void. Figure 24 shows a typical set of data obtained simultaneously on one of the twin-channel, strip-chart oscillographs during laboratory run No. 33. The upper trace represents the depth of flow observed at miniature wave-gage No. 1; the lower trace, the transient pressures at the gate valve. The trace of the transient pressure was frequently recorded on one of the four oscillograph channels to assure the simultaneity of time base for all recording media. One-second tick marks are visible along the lower edge of the chart in Figure 23; the major chart divisions are 5mm., the minor divisions are 1 mm. so that the chart speed was 100 mm. per second. Simultaneous strip-chart traces representing the depth of flow at two other wave gages were recorded on the second, twin-channel oscillograph.

On certain laboratory runs photographs of the cavitation void were taken.

Once column separation had ceased and the transient pressure wave had diminished due to friction, the solenoid valve was opened and the recorded data was removed from the recording instruments and marked for subsequent identification. The system could then be reinitialized

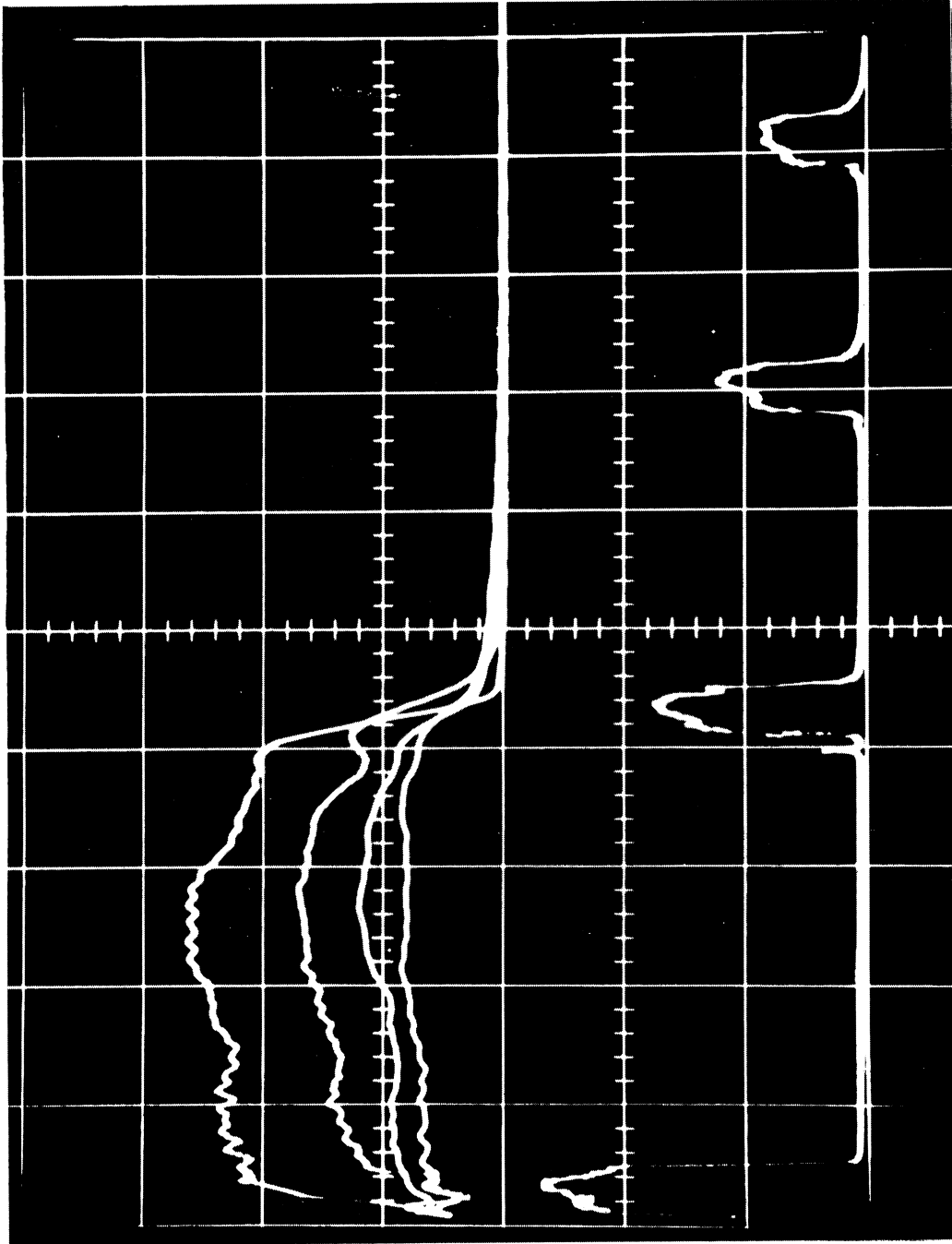


Figure 23. Transient Pressures, Photographically Recorded from the Oscilloscope Cathod-Ray Tube During Laboratory Run Number 19, are Typical of the Experimental Pressures Observed at the Gate Valve.

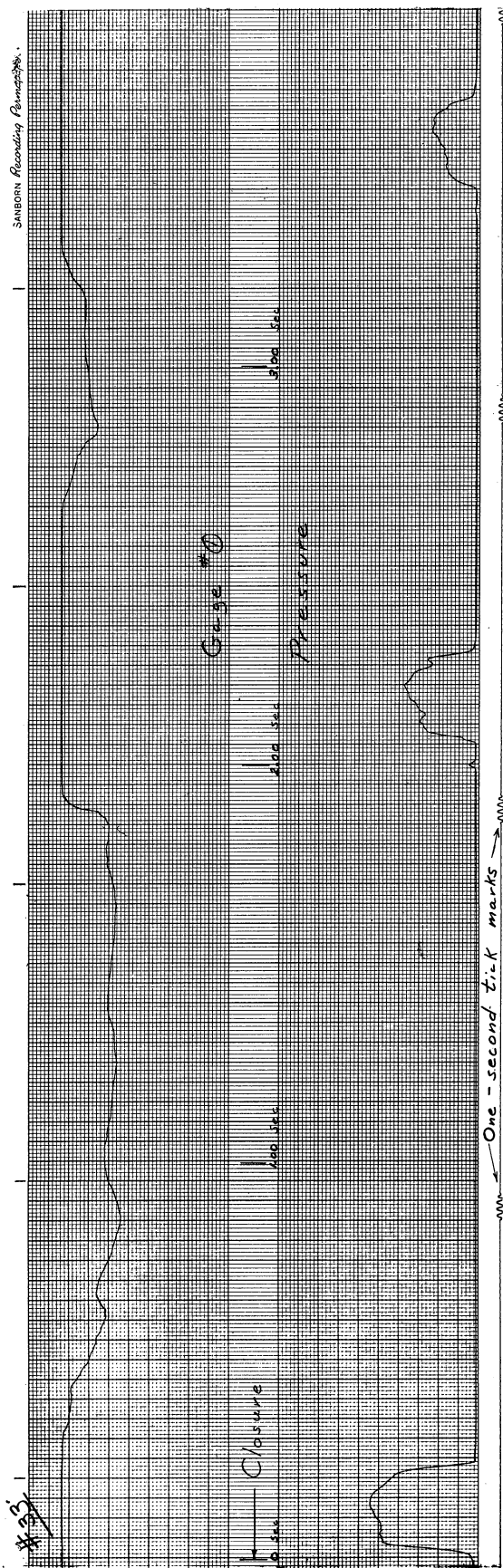


Figure 24. The Time-Dependent, Oscillograph Data Trace Shown at Top is Typical of the Free-Surface Flow Depths Observed at Gage Number 1 During Periods of Column Separation in the Pipe. The Data Trace Shown at Bottom Represents the Simultaneously Observed Transient Pressure at the Nearby Gate Valve. Traces Were Recorded During Laboratory Run Number 33. Depth-of-Flow Data Traces, Not Shown But Similar to the Top Trace, Were Simultaneously Recorded for Two Other Gages on a Second Oscillograph.

and made ready for the next experimental run. It was found essential to recheck all instrument calibrations before starting each new laboratory experimental run.

The experimental results are presented in the next chapter and compared with the theoretical results obtained from computer simulation for the same physical conditions.

CHAPTER VI

COMPARISON AND DISCUSSION OF EXPERIMENTAL AND THEORETICAL RESULTS

The study of column separation accompanying the transient flow of liquids in pipes culminates in this chapter with comparisons of the laboratory-observed, experimental results and the computer-simulated, theoretical results derived from the mathematical model. The ability to throttle the syphon-flow velocity and to vary the elevation of the solenoid-operated valve throughout a range of approximately 26 feet, as well as intrinsic fluctuations in the atmospheric pressure and in the water temperature offered a limitless combination of experimental conditions for laboratory investigation. However, practical constraints on the time which could be profitably expended analyzing laboratory data and economic sanctions on the use of computer time, limited this study to the investigation of only a few selected conditions. These conditions are briefly presented in the first section. A detailed comparison of the experimental and theoretical results obtained for one particular set of investigated conditions is presented in the subsequent section. Analysis and discussion of the similarities and dissimilarities between the theoretical and experimental pressure rises are followed by a similar appraisal of the theoretical and experimental column-separation voids. The significance of these findings is discussed in the final section.

Conditions Investigated

Experimental data were gathered for three distinct sets of laboratory conditions. These conditions differed, one from another, because of differences in the elevation of the solenoid-operated gate valve, differences in the initial steady-state rate of flow, or because of both.

However, minor changes in atmospheric pressure and in water temperature, along with slight fluctuations in the initial rate of flow resulted in subset conditions within two of the principal sets of conditions. Table III is a summary of the 34 data runs considered in the experimental phase of the study. The grouping of the various data runs according to laboratory conditions is tabulated below:

(a) Group I: Runs No. 1-10

Valve Elevation (HEL) = 27.980 feet

Location (Loc 1) = 39.00 feet

Initial Steady-state Discharge (Q) \cong -0.0107 cubic feet
per second

(b) Group II: Runs No. 11-25, 31-34

Valve Elevation (HEL) = 34.719 feet

Location (Loc 1) = 18.00 feet

Initial Steady-State Discharge (Q) \cong -0.0107 cubic feet
per second

(c) Group III: Runs No. 26-30

Valve Elevation (HEL) = 37.719 feet

Location (Loc 1) = 18.00 feet

Initial Steady-State Discharge (Q) \cong -0.0078 cubic feet
per second

These same parameters, together with other parameters describing the nonvariable experimental conditions, were used as input data to the computer program. Computer simulations were then carried out for the three laboratory conditions.

TABLE III
SUMMARY OF EXPERIMENTAL RUNS

Run No.	Date 1964	Configuration		Water Temp. Deg. F	Atmos. Pressure ft	Rho ρ slugs/ft ³	Nu ft ² /sec 10 ⁻⁵	Q ft ³ /sec	Oscilloscope Data	Oscillograph Data		Photo	Max. Extent feet	Rise Time	
		HEEL ft	LOCI ft							Gage	Gage			2nd sec	3rd sec
1	3-3	27.980	39.00	72°	32.683	1.936	1.033	-.01077	Yes	1	2	No	-	1.81	3.12
2	3-3	27.980	39.00	72°	32.683	1.936	1.033	-.01077	Yes	1	2	No	1.06	1.79	3.08
3	3-3	27.980	39.00	72°	32.682	1.936	1.033	-.01077	Yes	1	2	No	1.03	1.76	3.04
4	3-3	27.980	39.00	72°	32.681	1.936	1.033	-.01077	Yes	1	2	No	1.01	1.76	3.03
5	3-3	27.980	39.00	72°	32.680	1.936	1.033	-.01077	Yes	1	2	No	.96	1.72	2.88
6	3-3	27.980	39.00	72°	32.680	1.936	1.033	-.01077	Yes	1	2	No	.92	1.68	2.83
7	3-4	27.980	39.00	75°	32.528	1.935	.995	-.01058	Yes	1	2	No	.99	1.76	2.99
8	3-4	27.980	39.00	75°	32.528	1.935	.995	-.01058	Yes	1	2	No	-	1.69	2.97
9	3-4	27.980	39.00	75°	32.528	1.935	.995	-.01058	Yes	1	2	No	.96	1.69	2.83
10	3-4	27.980	39.00	75°	32.528	1.935	.995	-.01058	Yes	1	2	No	.90	1.68	2.78
11	3-7	34.719	18.00	75°	33.116	1.935	.995	-.01073	Yes	1	4	Yes	1.16	1.98	3.34
12	3-7	34.719	18.00	75°	33.116	1.935	.995	-.01073	Yes	1	4	No	1.14	2.00	3.41
13	3-7	34.719	18.00	75°	33.126	1.935	.995	-.01073	Yes	1	4	No	1.11	1.95	3.22
14	3-7	34.719	18.00	75°	33.134	1.935	.995	-.01073	Yes	1	4	Yes	1.09	1.91	3.20
15	3-7	34.719	18.00	75°	33.152	1.935	.995	-.01073	Yes	1	4	No	1.08	1.91	3.18
16	3-7	34.719	18.00	75°	33.170	1.935	.995	-.01073	Yes	1	3	No	1.18	1.96	3.27
17	3-7	34.719	18.00	75°	33.188	1.935	.995	-.01073	Yes	1	3	Yes	1.22	1.92	3.18
18	3-7	34.719	18.00	75°	33.206	1.935	.995	-.01073	Yes	1	2	No	1.23	1.91	3.17
19	3-7	34.719	18.00	75°	33.224	1.935	.995	-.01073	Yes	1	2	Yes	1.26	2.07	3.45
20	3-7	34.719	18.00	75°	33.239	1.935	.995	-.01073	Yes	1	2	No	1.13	1.90	3.12
21	3-7	34.719	18.00	75°	33.258	1.935	.995	-.01073	Yes	1	2	No	-	1.87	3.06
22	3-10	34.719	18.00	72°	32.421	1.936	1.033	-.01054	No	1	2	No	1.13	2.04	3.37
23	3-10	34.719	18.00	72°	32.421	1.936	1.033	-.01054	Yes	1	2	No	1.25	2.05	3.40
24	3-10	34.719	18.00	72°	32.421	1.936	1.033	-.01054	Yes	1	2	No	1.25	2.05	3.40
25	3-10	34.719	18.00	72°	32.421	1.936	1.033	-.01054	Yes	1	2	No	1.19	2.11	3.32
26	3-10	34.719	18.00	72°	32.421	1.936	1.033	-.00777	Yes	1	2	No	-	1.64	2.75
27	3-10	34.719	18.00	72°	32.421	1.936	1.033	-.00777	Yes	1	2	Yes	-	1.63	2.75
28	3-10	34.719	18.00	72°	32.421	1.936	1.033	-.00777	Yes	1	2	No	.82	1.63	2.73
29	3-10	34.719	18.00	72°	32.421	1.936	1.033	-.00777	Yes	1	2	No	.88	1.66	2.79
30	3-10	34.719	18.00	72°	32.421	1.936	1.033	-.00777	Yes	1	2	No	.78	1.62	2.72
31	3-10	34.719	18.00	72°	32.421	1.936	1.033	-.01054	Yes	1	5	No	1.28	2.05	3.43
32	3-10	34.719	18.00	72°	32.421	1.936	1.033	-.01054	Yes	1	5	No	1.24	2.03	3.42
33	3-10	34.719	18.00	72°	32.421	1.936	1.033	-.01054	Yes	1	5	Yes	1.22	2.05	3.42
34	3-10	34.719	18.00	72°	32.421	1.936	1.033	-.01054	Yes	1	5	Yes	1.18	1.88	2.99

Comparison of Results

In the theoretical analysis presented in Chapter II, the assumption was made that the pipe flow ahead of the void created by column separation would continue to be full-pipe flow. That this assumption is, in fact, not valid became apparent rather early in the experimental phase of the study. While the free-surface, vapor-filled, column-separation void formed as anticipated, small gaseous cavities--bubbles--were observed to occur ahead of the void and throughout the remaining length of the plexiglas pipe. Moreover, with continued propagation of the low-pressure wave toward the constant head reservoir, similar bubbles were heard to occur throughout most of the length of the copper pipe. With the imminent collapse of the column-separation void and with the subsequent creation of a new high-pressure wave propagating toward the reservoir, the cavitation bubbles were observed to diminish, first, and then, to disappear completely (or almost completely), respectively.

The occurrence of vapor-cavity bubbles ahead of the void has a significant bearing on all aspects of the transient-flow, column-separation phenomena. This significance will become fully evident in the comparisons and detailed discussion which follow.

Two experimental runs, Numbers 25 and 34, were selected from the laboratory data in Group II for detailed comparison with the corresponding computer-simulated results. These runs were considered to be entirely representative of the other experimental runs comprising Group II.

Pressure Rises

Figure 25 presents a time comparison of the transient, absolute pressures occurring at the gate valve as derived from the mathematical

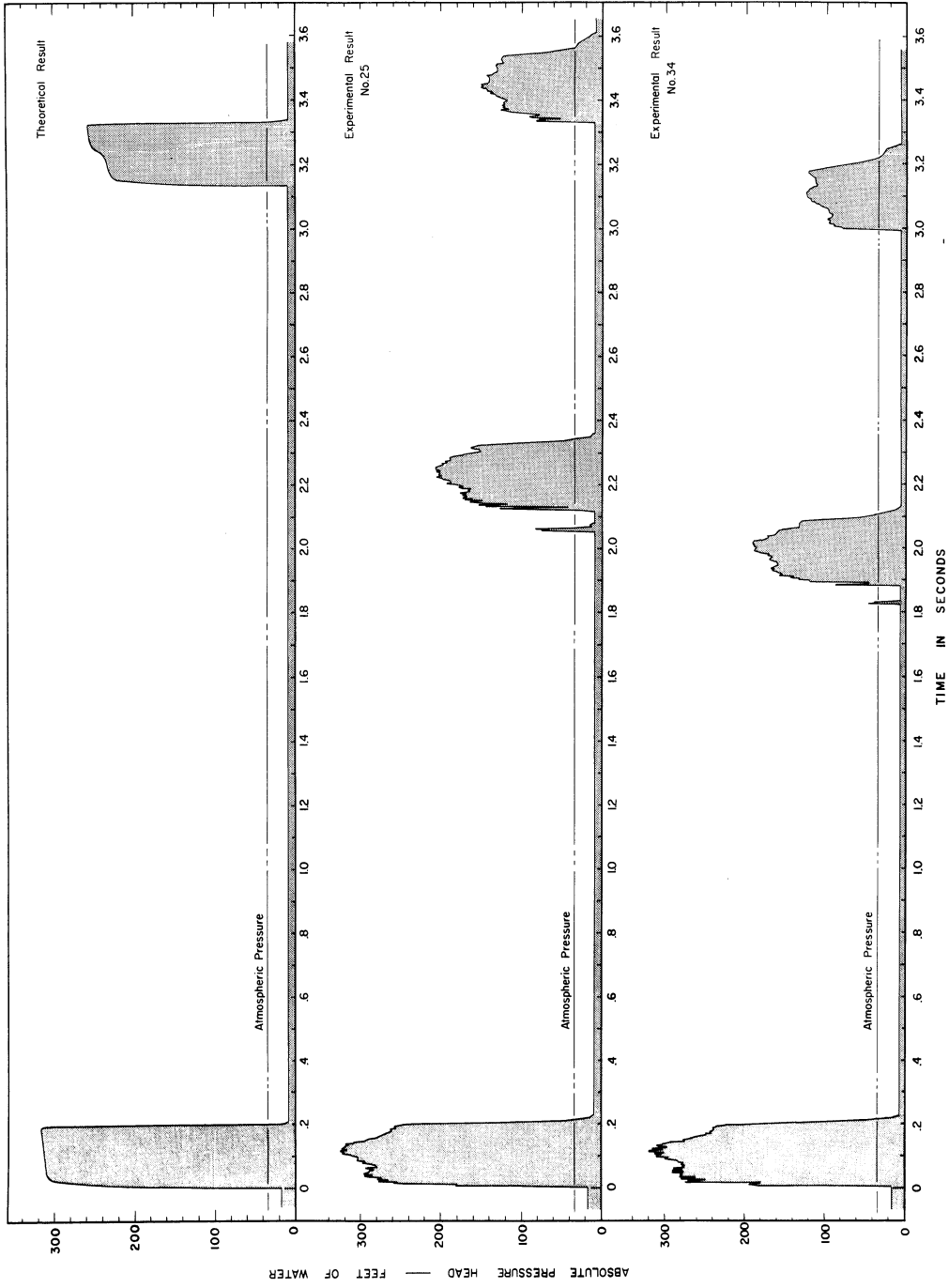


Figure 25. Comparison of the Computer-Simulated, Transient Pressures with the Experimentally Determined Pressures Observed at the Gate Valve During Laboratory Runs Numbers 25 and 34.

model and from laboratory measurements (experimental runs Numbers 25 and 34). Time is measured from the instant the gate valve was closed. For each of the three examples shown, column separation occurs at the valve during the time intervals between the successive pressure rises. Figures 26 and 27 provide detailed overlay comparisons of the computer-simulated and experimentally-determined initial pressure rises and second pressure rises, respectively. Figures 28 and 29 are reproductions of the respective oscilloscope photographs on which the absolute pressure-head data for runs Numbers 25 and 34 were recorded. The numerical data used to plot the experimental results of Figures 25, 26, and 27 are tabulated in Appendix III; many of the data used in plotting the theoretical results are contained in Appendix IV.

Comparative study of Figures 25-27 discloses several factors of note. Principal among these factors are the following:

- (a) In broad terms the overall appearances of the three pressure diagrams shown in Figure 25 are similar; abrupt pressure rises separate intervals of subatmospheric pressure during which time column separation occurs.
- (b) Despite some minor pressure fluctuations and local pressure differences evident in the experimental results, the three initial pressure rises closely resemble each other in time of occurrence, as well as in shape, duration, and magnitude of the pressure rise.
- (c) The experimental second pressure rises, while manifesting the same minor pressure fluctuations and local pressure differences noted in the initial experimental rises, compare favorably in shape and duration with the corresponding

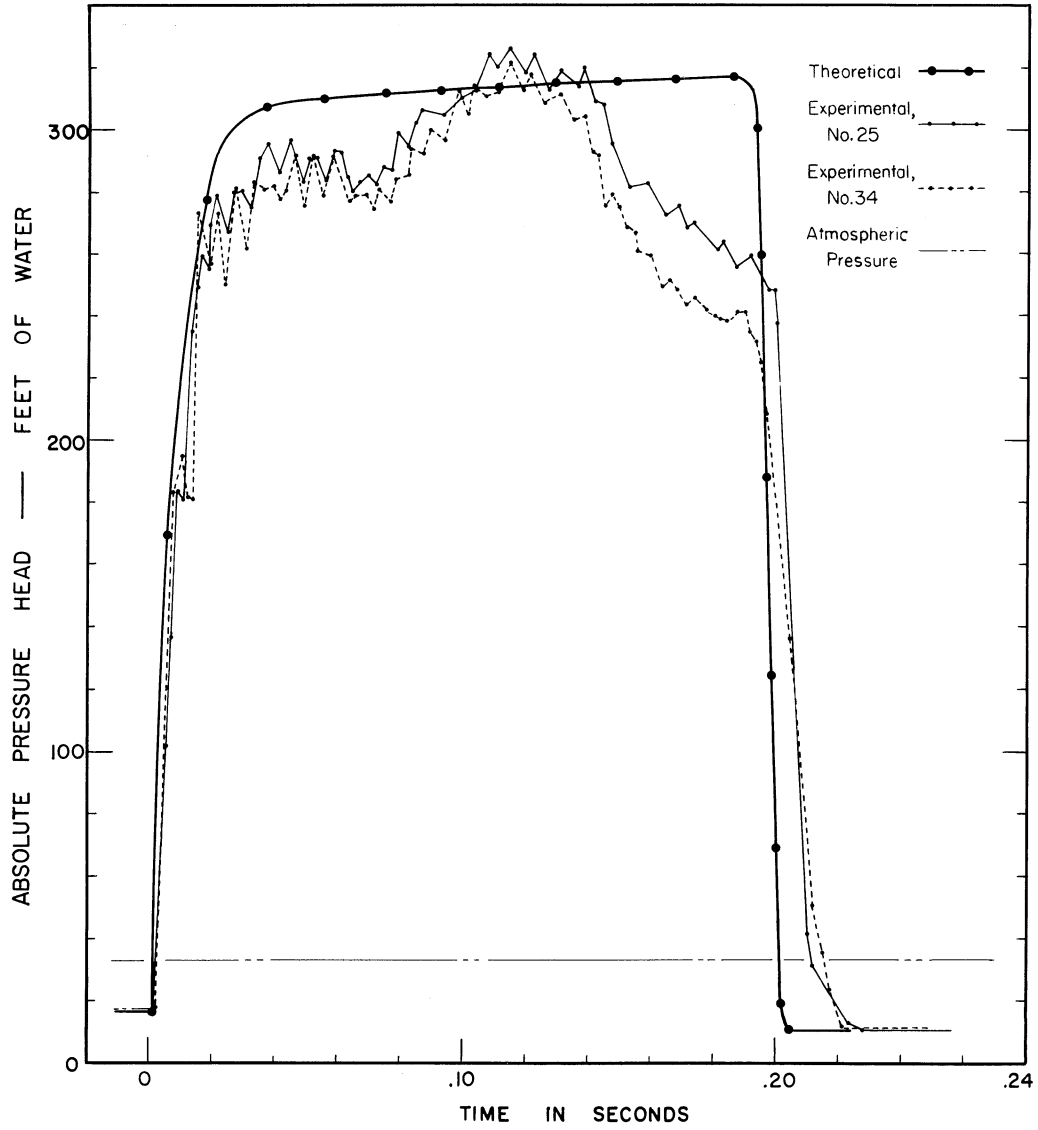


Figure 26. Detailed Comparison of the Computer-Simulated Initial Pressure Rise with the Corresponding Experimentally-Determined Initial Pressure Rises for Laboratory Runs Numbers 25 and 34.

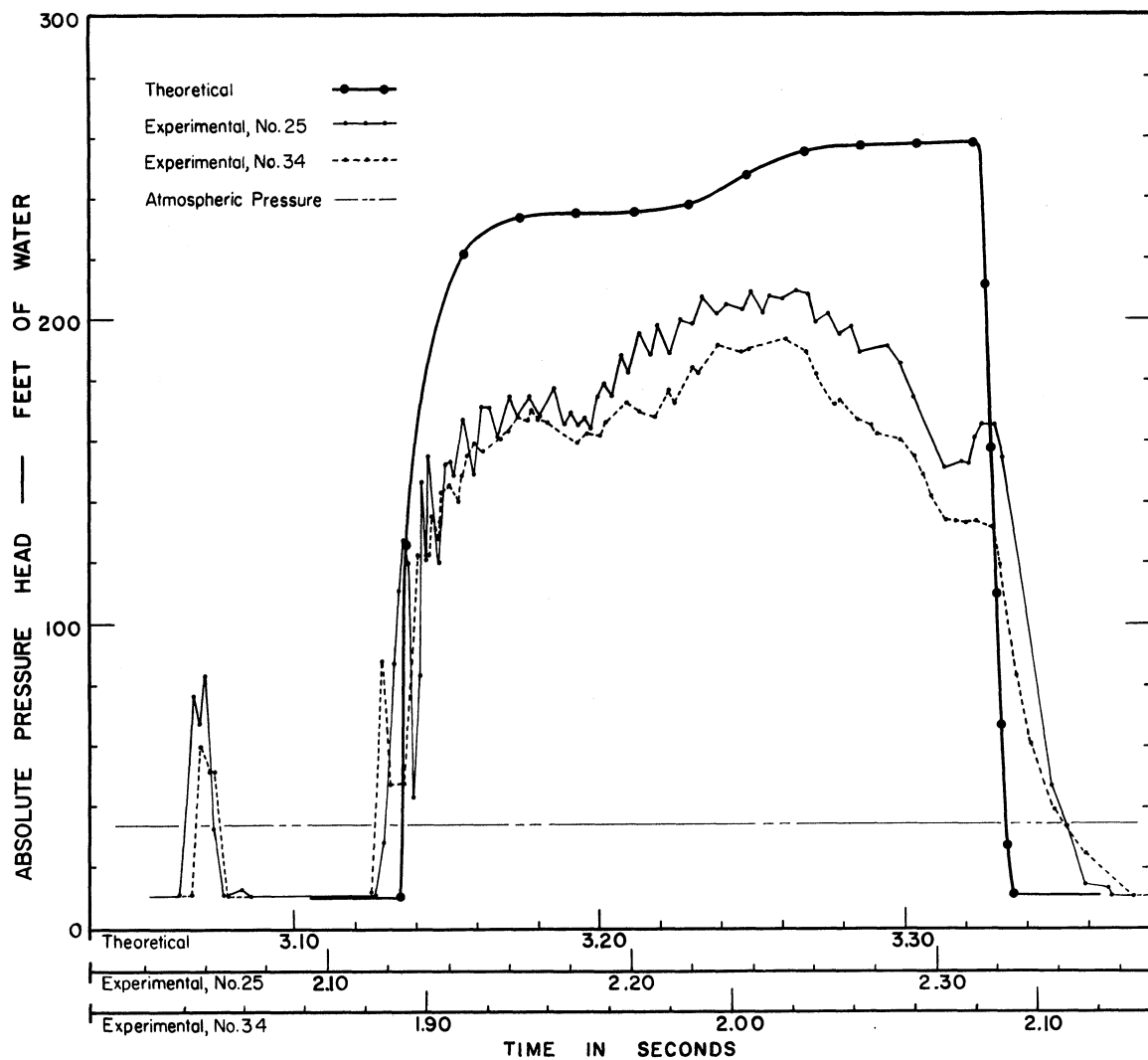


Figure 27. Detailed Comparison of the Computer-Simulated Second Pressure Rise with the Corresponding Experimentally-Determined Second Pressure Rises for Laboratory Runs Numbers 25 and 34.

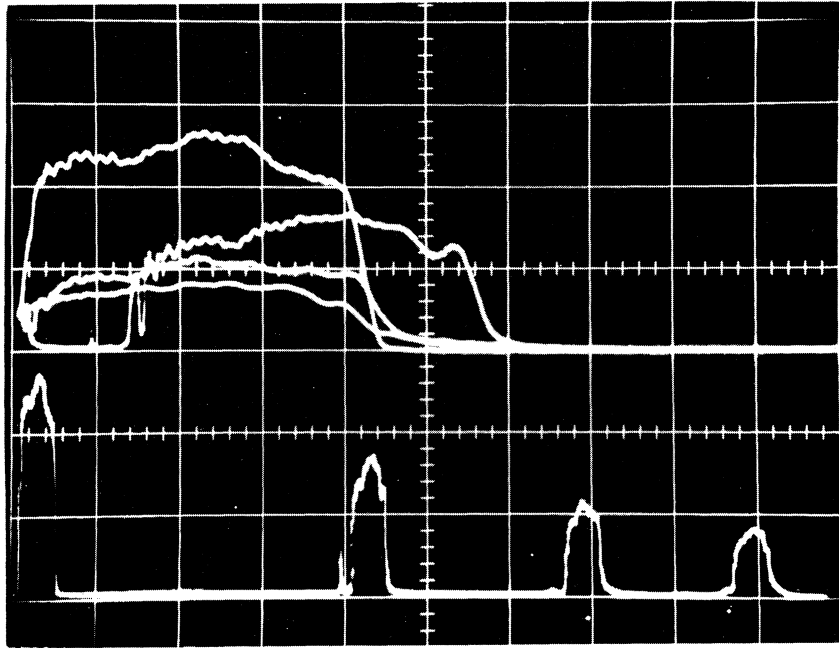


Figure 28. Transient Pressures Observed at Gate Valve During Laboratory Run Number 25.

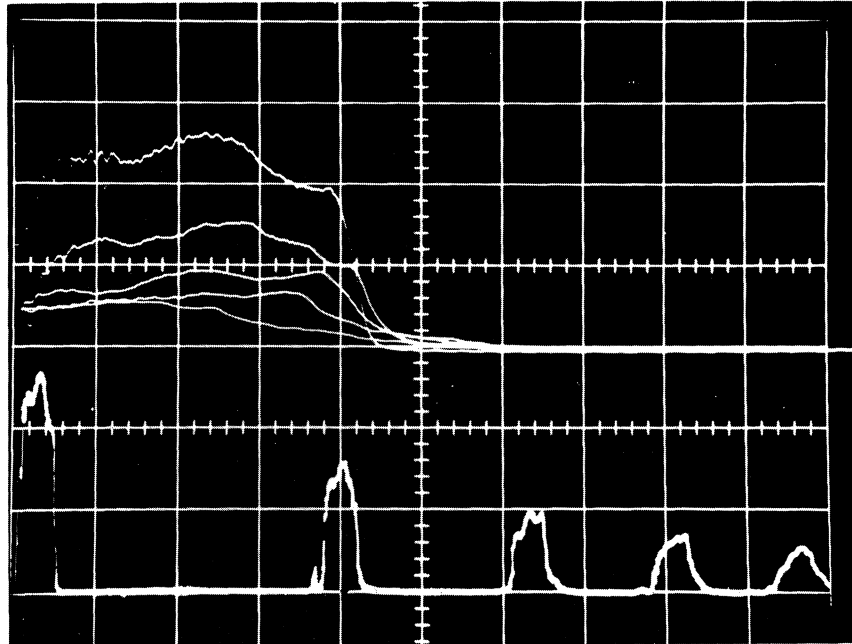


Figure 29. Transient Pressures Observed at Gate Valve During Laboratory Run Number 34.

theoretical pressure rise. However, the magnitudes of the experimental pressure rises are appreciably less than is the magnitude of the theoretically-determined rise.

- (d) The recurrence intervals between successive, experimental pressure rises are of appreciably less duration (35-40 percent less) than are the corresponding intervals determined theoretically. (The third theoretical pressure rise, although not shown in Figure 25, was determined to occur beginning at approximately 5.09 seconds after valve closure.)
- (e) Appreciable differences occur between the experimental data of laboratory runs Numbers 25 and 34 with regard to the magnitudes of the pressure rises and the duration of the recurrence intervals. Yet, both runs were made ostensibly under the same laboratory conditions.
- (f) Minor pressure fluctuations appear superimposed on all of the experimental pressure rises. These fluctuations have an apparent duration ranging from 0.0068 to 0.0072 seconds.
- (g) Although the duration of both the experimentally and theoretically determined initial pressure rises is very close to 0.2 seconds, a slight tendency toward increased duration appears to develop in the second and subsequent experimental rises. This tendency appears to accompany the deterioration in the abruptness with which the pressure rises collapse.

Among the factors listed above two very significant findings are apparent. One is the considerably shorter duration of the experimental, pressure-rise recurrence interval as compared with the duration of the

theoretically-predicted interval. The second is the more rapid rate at which the magnitudes of the second and all successive pressure rises diminish, again as compared with the theoretical findings. Without even comparing the experimentally and theoretically-determined column-separation voids, it is apparent that the duration of these voids must also be considerably shorter than anticipated from theory. It is probable that the extent of their travel will prove to be similarly reduced.

Taken together the two complementary findings are strong evidence suggesting that during periods of column separation the rate of energy dissipation which occurs in the flow ahead of the void is much higher than anticipated. The obvious question is, "why?" There are several conditions which lead one to believe that a higher energy-dissipation rate could be a direct outgrowth of the "bubble" or "plug" flows taking place in the pipe ahead of the column-separation void. However, a thorough discussion of these circumstances is deferred to a subsequent section.

The laboratory flow system was designed to minimize sources of potential disturbance to pressure wave propagation. The intent, of course, was to assure a clean, uncluttered wave form. It was for this reason that syphon flow was preferred over flow induced by a turbine pump located at the outlet of the system. Nevertheless, not all disturbance-producing elements could be eliminated. Using an expression for the round-trip time-of-travel of a pressure wave in fully confined flow, namely, the expression $t_t = 2 L_t/a_1$, one finds that the distance, L_t , from the transducer to a disturbance having a propagation and return interval, t_t , of 0.0066 to 0.0072 seconds ranges from 8.1 to 8.9 feet. The term a_1 represents the celerity of propagation of a pressure disturbance in the

plexiglas pipe. This places the source of the disturbance at or just beyond the junction between the copper and plexiglas pipes. The superimposed, minor, pressure fluctuations appearing on the experimental pressure-rise data are believed to be caused by pressure reflections from the small annular chamber of the piezometer ring attached to the copper pipe and situated 0.3 foot from the pipe junction (8.7 feet from the pressure transducer).

Column-Separation Voids

Figure 30 presents a modified isometric diagram showing the absolute pressures at the gate valve, as well as the column-separation void profiles at five successive distances measured from the valve, all with respect to time. The data on this diagram were derived entirely from the mathematical model by digital computer simulation. Figures 31 and 32 are the companion diagrams presenting the corresponding experimentally-derived data from laboratory runs Number 25 and Number 34, respectively. In each of the diagrams the depth of flow, z , in the pipe is measured on the vertical plane passing through the axis of pipe and normal to the bottom inner pipe surface. Figure 33 presents a more detailed comparison of the superimposed depth profiles for both the experimentally-determined and theoretically-determined voids with respect to time.

In Figures 30-33, the column-separation voids are compared on the basis of profiles in the $z - t$ plane at a particular location, x . The voids can also be studied as phenomena occurring in the $x - z$ plane at a selected time t . Figures 34 and 35 present time-sequence

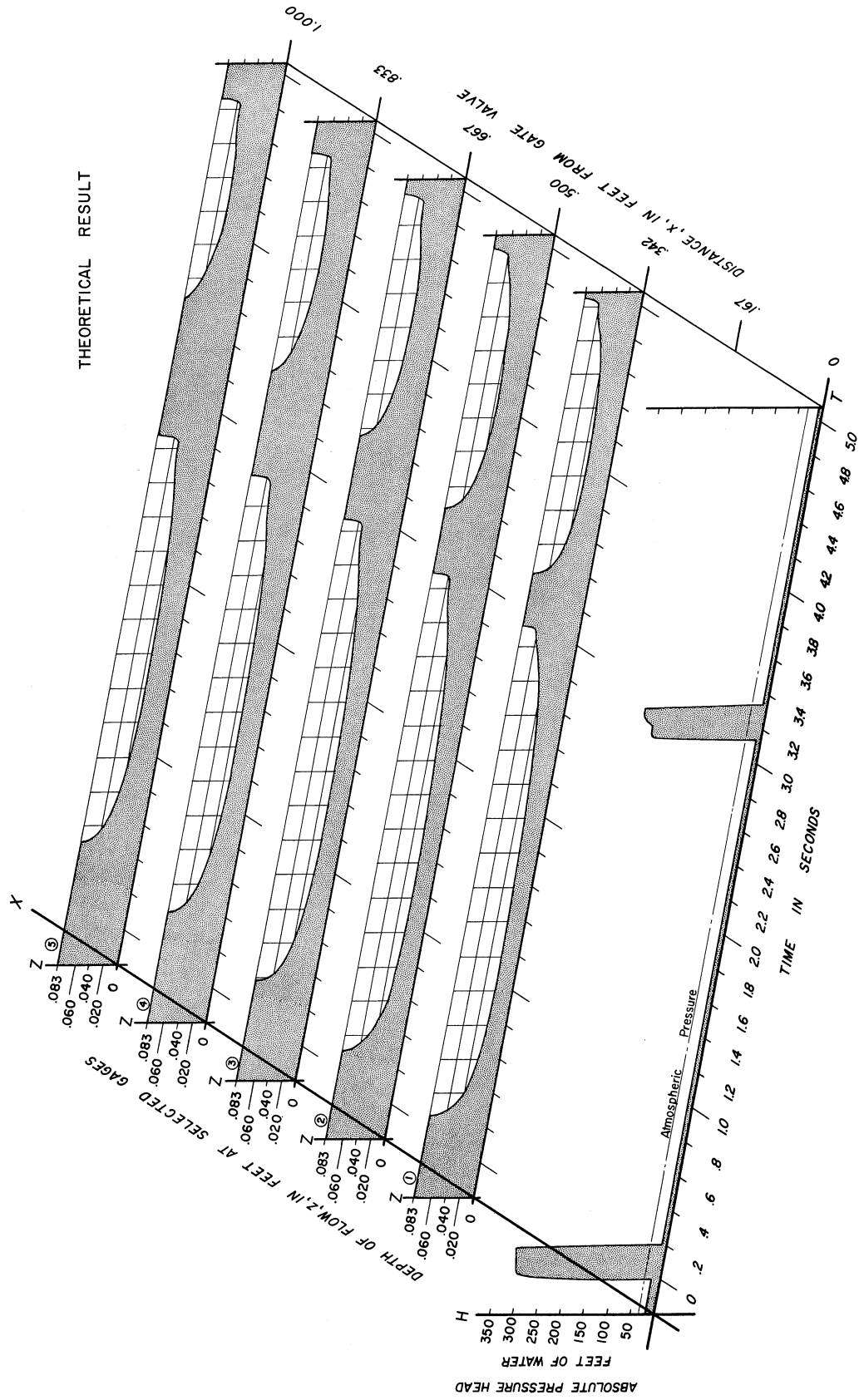
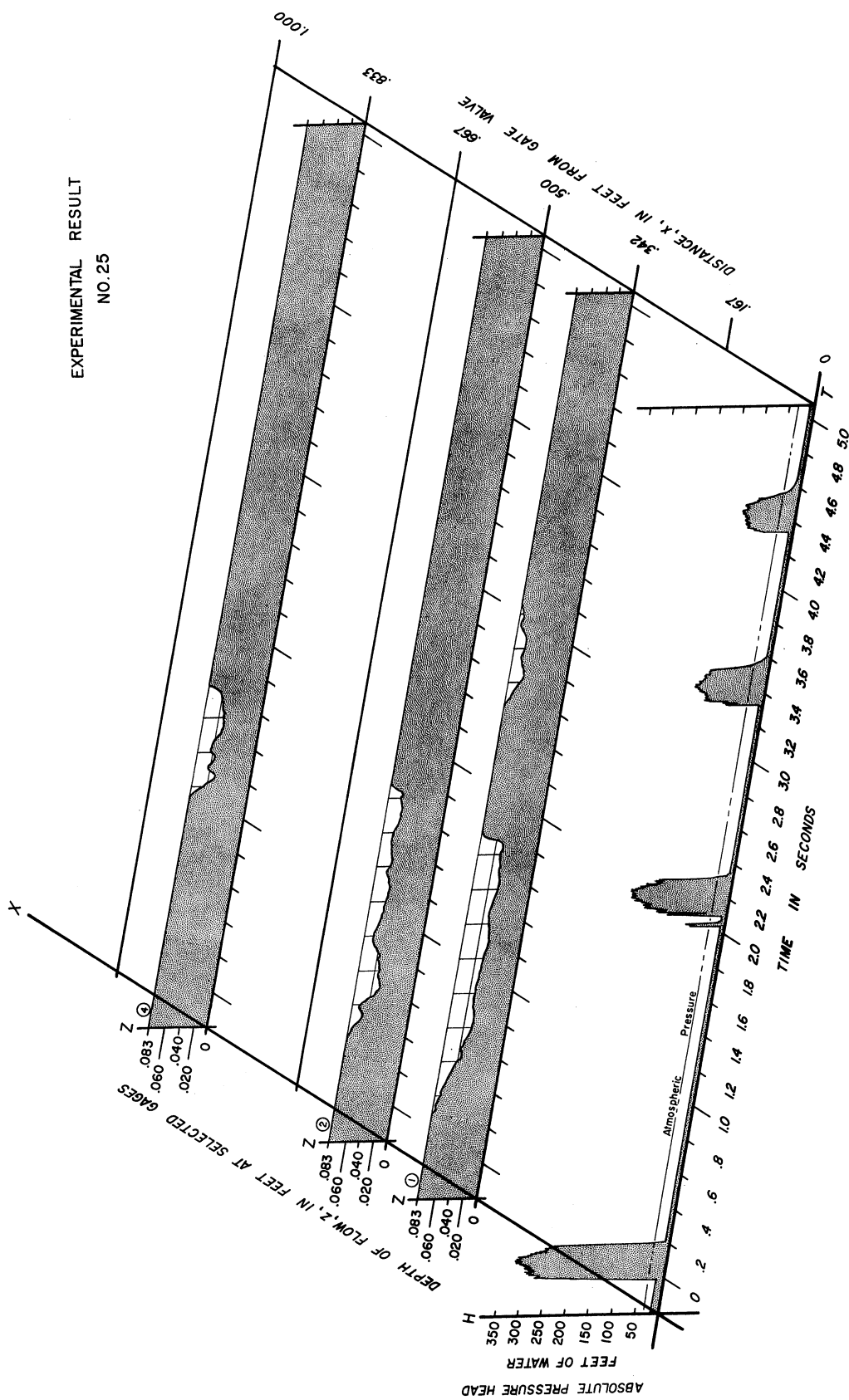


Figure 30. An Isometric Representation of the Computer-Simulated Transient Pressures at the Gate Valve and Concurrent Free-Surface Profiles at Selected Distances from the Gate Valve as Determined from Theoretical Considerations.



EXPERIMENTAL RESULT
NO. 25

Figure 31. An Isometric Representation of the Experimentally-Determined Transient Pressures at the Gate Valve and Concurrent Free-Surface Profiles at Selected Distances from the Gate Valve as Observed During Laboratory Run Number 25.

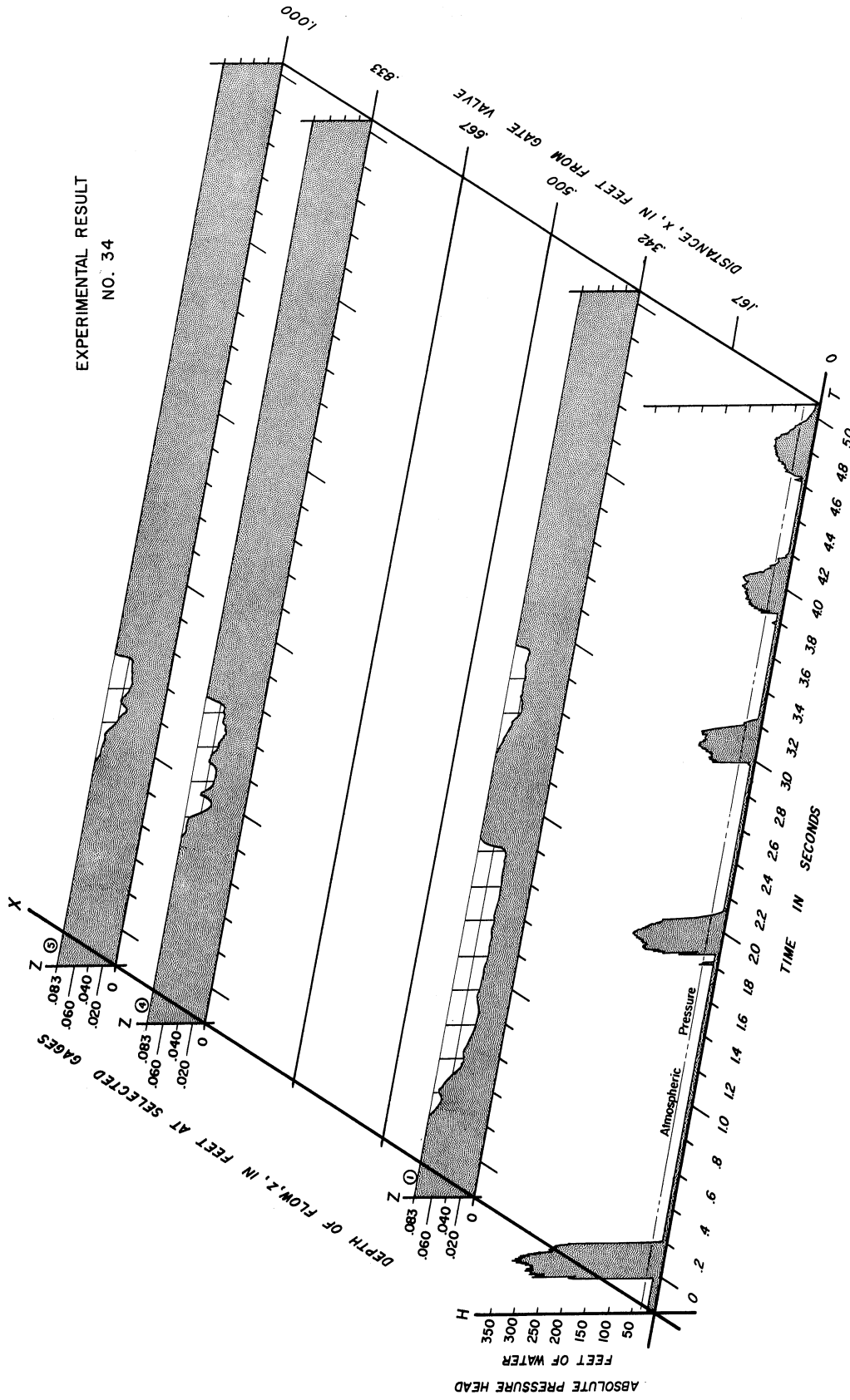


Figure 32. An Isometric Representation of the Experimentally-Determined Transient Pressures at the Gate Valve and Concurrent Free-Surface Profiles at Selected Distances from the Gate Valve Due to Column Separation During Laboratory Run Number 34.

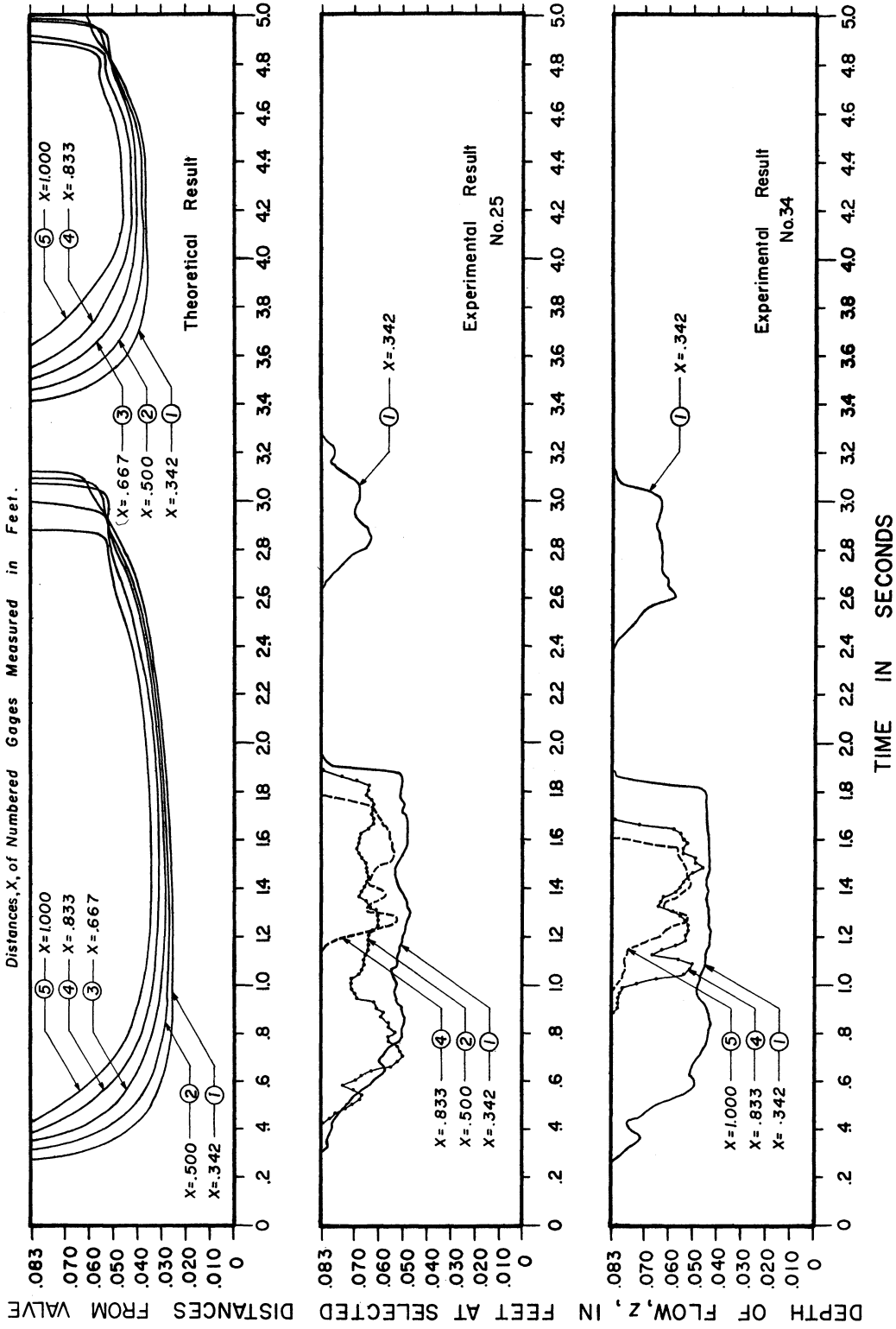


Figure 33. Comparison of the Computer-Simulated and Experimentally-Determined, Time-Dependent, Free-Surface Profiles at Selected Gages During Periods of Column Separation in the Pipe.

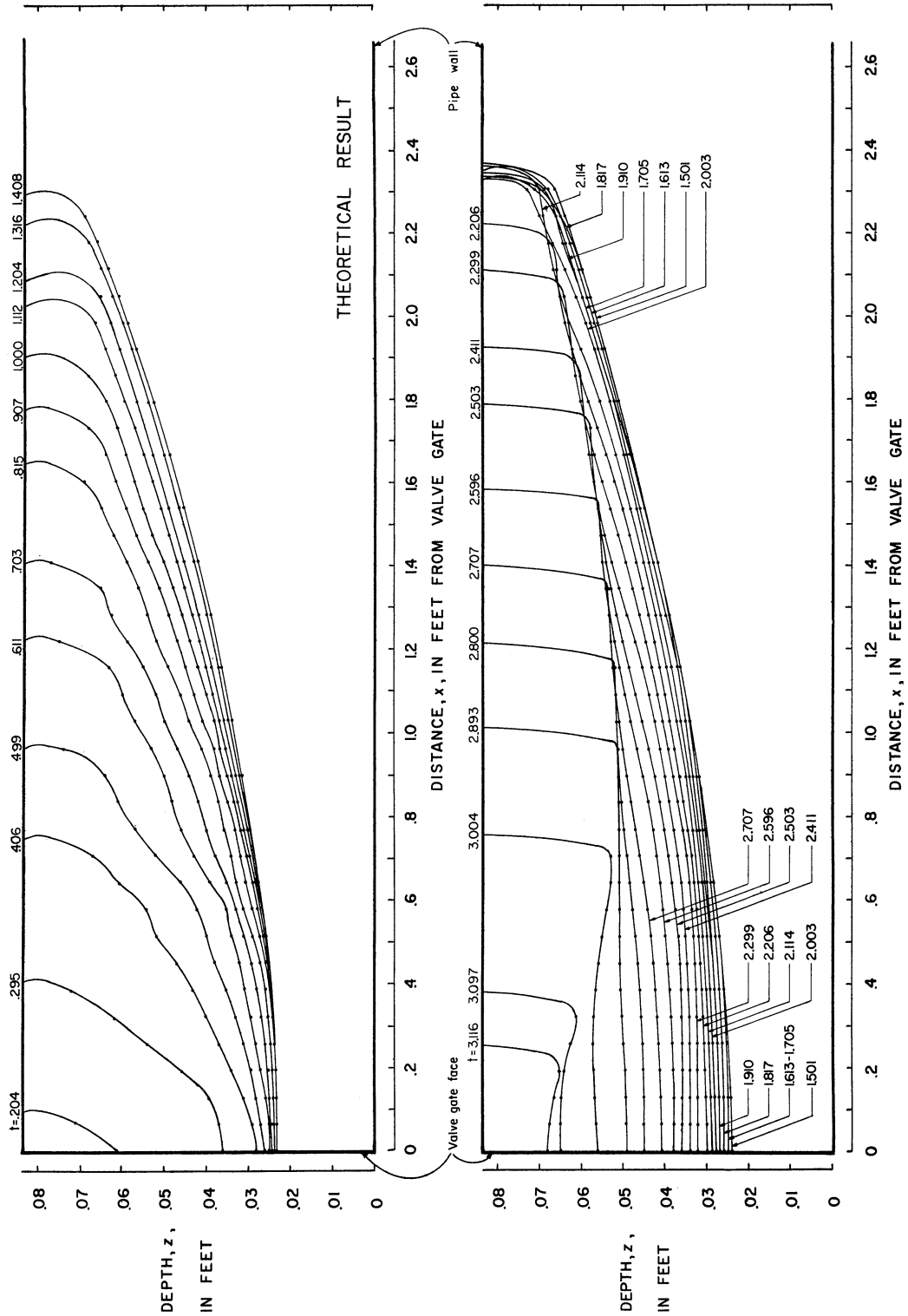


Figure 34. Computer-Simulated Sequence of Water-Surface Profiles for the Initial Period of Column Separation in the Pipe. Individual Profiles are Identified According to the Time of Their Occurrence, t, in Seconds After Closure of the Gate Valve.

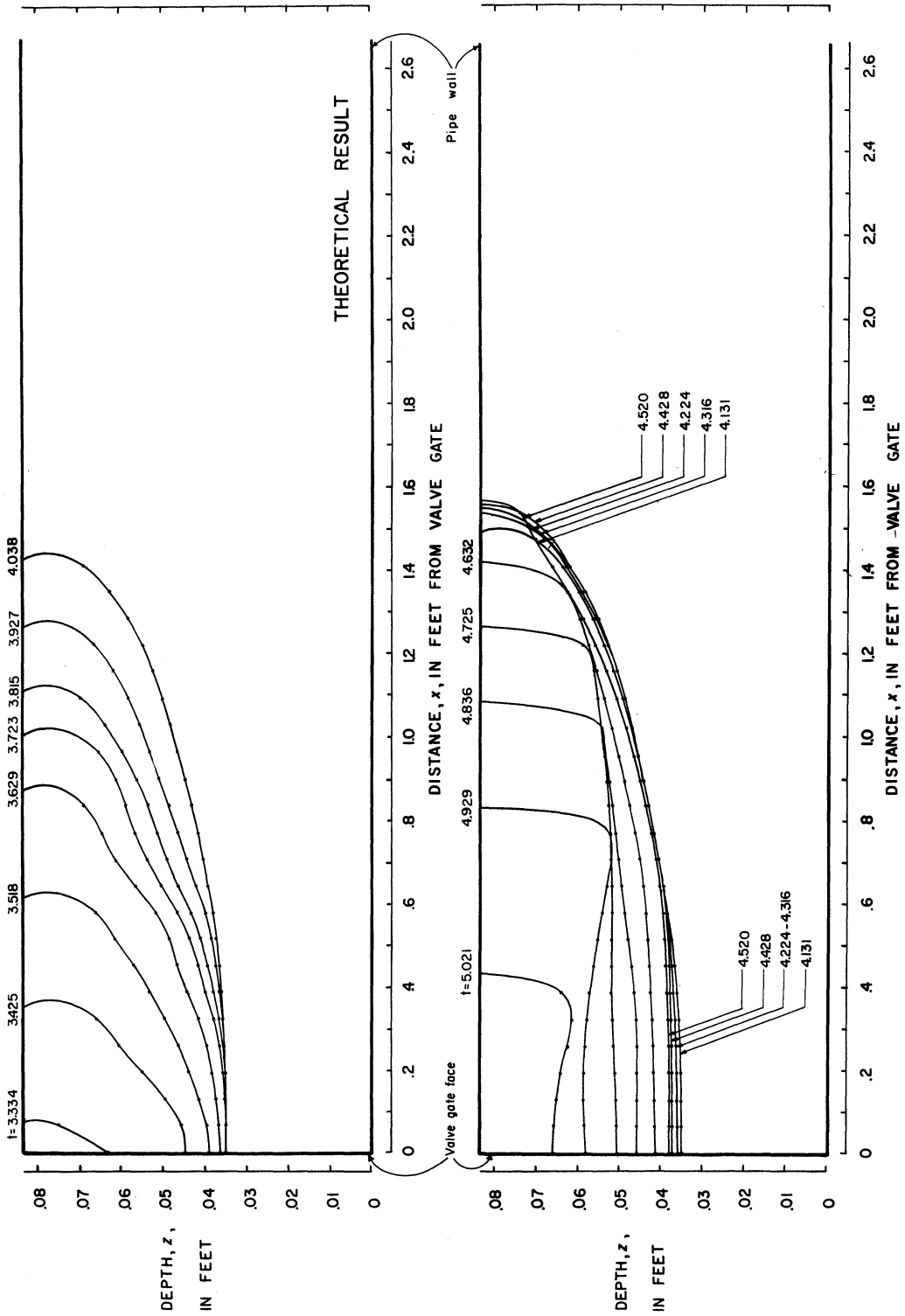


Figure 35. Computer-Simulated Sequence of Water-Surface Profiles for the Second Period of Column Separation in the Pipe. Individual Profiles are Identified According to the Time of Their Occurrence, t , in Seconds After Closure of the Gate Valve.

families of profiles derived from the mathematical model by computer simulation. Figure 34 presents the time-sequence of the water-surface profiles for the initial period of column separation; Figure 35, the water-surface profiles for the second period of column separation. Note that in both figures dissimilar horizontal and vertical scales were used. In each figure the growth sequence of the theoretical void is depicted in the top diagram while its collapse sequence is traced in the bottom diagram. Unfortunately, there were insufficient experimental data with which to plot the companion experimental curves. However, Figures 36, 37, and 38, as well as Figure 1, are typical photographs of the column-separation voids observed in the laboratory. Each of the partial profiles shown in these figures may be thought of as one profile out of a family of profiles similar to the theoretically-determined profiles of Figure 34. Because the photographs shown in Figures 36, 37, and 38 were taken at close range using a camera with a very shallow depth of field and because the inverted tape measure was positioned behind the plexiglas pipe, the apparent distances of points in the void from the gate valve are somewhat distorted and have only approximate significance.

Most of the data used in Figures 30-35 are tabulated in Appendixes III and IV.

The principal factors noted from comparing the theoretically-derived and experimentally-determined column-separation voids are cited below:

- (a) The similarities which exist between the corresponding computer-simulated and experimentally-determined void profiles shown in Figures 30-34 are limited largely to similarities in the gross sense of the term. The shapes of the initial

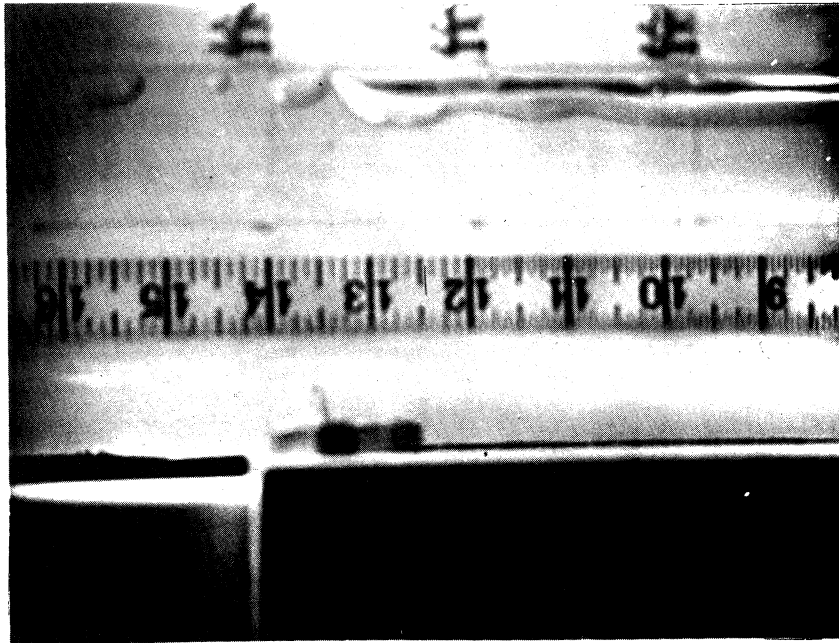


Figure 36. Advancing Column-Separation Void Photographed During Run Number 19. Inverted Scale Gives the Approximate Distance to the Inner Face of the Gate Valve in Inches.

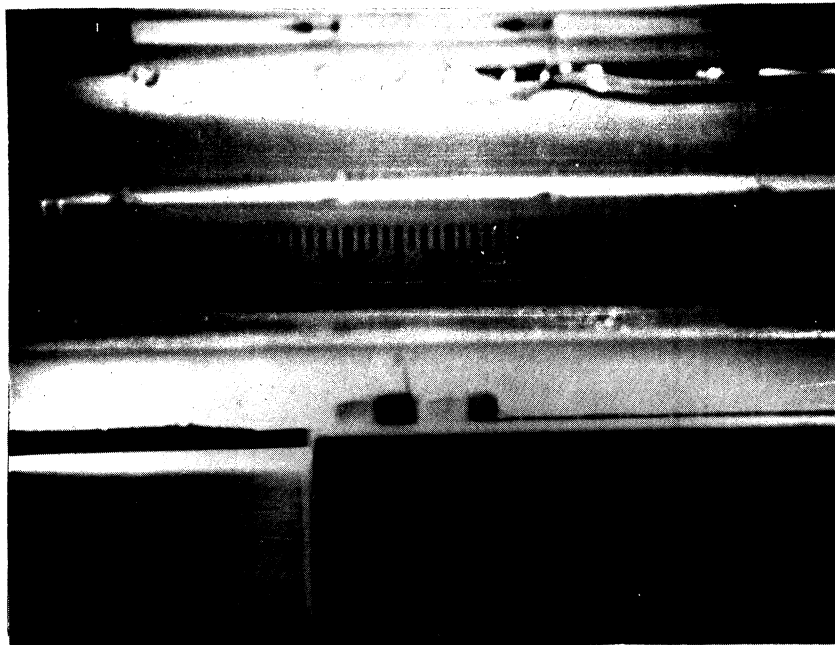


Figure 37. Advancing Column-Separation Void. Notice the Cavitation Bubbles Ahead of the Void and the Ripple Behind the Void.



Figure 38. Column-Separation Void in a State of Suspended Motion
Just Prior to Retreat and Collapse Against Valve.

experimentally-determined void profiles, especially the profiles recorded at wave gage Number 1, have an identifiable resemblance to the corresponding profiles determined from theory despite topical differences and differences in duration.

- (b) The shortened duration of the experimentally-determined voids is coincident with the reduced experimental recurrence interval noted in the previous section. As anticipated the extent of travel of the experimental column-separation void is much reduced -- approximately 50 percent reduced during the initial column-separation cycle -- from that which is predicted by the mathematical model. The experimental maximum extent of travel for each of the initial column-separation voids comprising Group II data is given in Table III.
- (c) The depth of free-surface flow observed in all laboratory runs, but specifically as shown for runs Numbers 25 and 34, is much greater than that derived from theory. This factor, together with the reduced extent of travel, dictates that the transient volumes of the experimentally-determined voids are very much smaller than the predicted volumes.
- (d) The differences between the experimental void profiles recorded at the various wave gages during laboratory runs are even more pronounced than the differences noted for the comparisons of the experimental pressure-rise data.

For example, the two experimental $z - t$ profiles recorded at gage Number 1 have a fair resemblance to each other. Both voids form and collapse at approximately the same times respectively. Yet the associated profiles at gage Number 4 are certainly less comparable.

- (e) The leading front of the experimentally-determined void is less bulbous than the front computed for the simulated void. Moreover, the front of the laboratory-produced void is usually followed by one or more surface ripples not predicted by the mathematical model (see Figures 1, 36-38).
- (f) Small ripples appear on the free-surface of the experimental flow throughout the void. These ripples are not manifest on the theoretically-determined free surface profile.
- (g) On the basis of comparisons with the theoretical conditions, the second experimental column-separation void has, proportionally speaking, an even smaller extent of travel than does the first experimental void.

The single most significant finding evident from the list of factors above is that the experimental void is of less physical magnitude and of less duration than is predicted by the simulation model. The shorter extent-of-travel, the greater depth of free-surface flow which conversely results in a void of shallower depth, the shorter recurrence interval, as well as the proportionally diminished extent-of-travel during the second void cycle, all lend additional support to the belief that during column separation, the rate of energy dissipation occurring in the flow ahead of the void is much higher than anticipated.

The small differences in the appearance of the leading edge of the theoretically and experimentally-determined void profiles are not unexpected. The boundary condition used with the simulation model to represent separation of flow from the pipe wall at the leading edge of the void is premised on a one-dimensional concept of the flow process. Moreover, the effects of surface tension are not considered. Thus, differences -- even greater differences than those observed -- were anticipated. Moreover, as the separation front of an advancing void moved in the pipe, a thin film of water was observed to flow around and laterally down the inner surface of the pipe and rejoin the free-surface just in back of the void front. This flow, entering the free-surface at either side of the pipe, is believed to be the cause of the rather pronounced ripple trailing the separation front of an advancing column-separation void (see Figures 36 and 37).

The factor(s) causing the other small ripples appearing on the experimental void profiles is unknown. One can speculate, however, that these ripples may have been produced by some slight pressure fluctuations occurring ahead of the separation front or by some slight anomaly in the pipe system.

Comparisons of the simulated results and the experimental results were not carried out in as great detail for the laboratory conditions of Groups II and III. However, the same general results were observed. The experimental results obtained in the laboratory had three common characteristics:

- (a) Although the first pressure rise compared favorably in magnitude, form, and duration with the simulated pressure rise, the second pressure rise was of lesser magnitude than its simulated counterpart.
- (b) The duration of the first experimental void was considerably shorter than the duration determined from the mathematical model.
- (c) The extent-of-travel of the first experimental void was considerably shorter than predicted by simulation.

Significance of Findings

The significance of the theoretical and experimental findings cannot be interpreted properly without considering the apparent effects that cavitation and the resulting bubble flow have upon the column separation phenomena. Thus, it is of value at this point to describe in some detail the flow conditions observed in the laboratory during separation and to briefly review the role of gas nuclei and gaseous diffusion in incipient cavitation.

The formation of bubble cavities ahead of the main void was observed regularly during periods of column separation for all of the laboratory conditions investigated. The bubble cavities were observed to develop generally near the pipe wall in the topmost quadrant of the plexiglas pipe and in the portion of the flow-wake immediately behind the individual wires of the wave gages. Bubble cavities were never observed to form in the flow in the lower half of the pipe. Formation occurred very rapidly; so rapidly, in fact, that it was difficult to perceive that it occurred progressively along the pipe with time. The

ultimate size of these bubble cavities varied from nearly spherical bubbles having an approximate diameter of less than .01 foot to larger, elongated bubbles exceeding 0.3 foot in length (see Figures 1, 36, 37, 38). No variation in bubble distribution throughout the length of the plexiglas pipe could be visually detected during any given occurrence. However, the number and ultimate size of the bubble cavities did vary appreciably from one experimental run to another, even under ostensibly unchanged flow conditions. Sometimes many larger bubbles developed; at other times the bubble cavities would be predominantly smaller and more numerous.

It is noteworthy that the smaller bubble cavities appeared to move more or less with the flow whereas the larger ones moved rather sluggishly and tended to "roll" along if they moved at all. Yet, with collapse of the first column-separation void the bubble cavities collapsed and disappeared or at least diminished to a subvisual level. The bubble cavities reappeared during the second and subsequent column separation voids. However, after the collapse of the third or fourth column separation void, the largest bubble cavities did not always disappear completely. Occasionally, a few very small bubbles could be observed remaining in the flow.

It has been fairly well established that under ordinary engineering conditions the inception of cavitation in water results from the growth of submacroscopic nuclei containing liquid vapor and undissolved (free) air. (13,16,38,44) These nuclei may be present in the water, or they may be attached to the boundary surfaces or to particulate matter

in water. For a small spherical bubble in static equilibrium in water, one may write the equation

$$p_g + p_v - p_a = 2 \frac{\sigma}{r} \quad (169)$$

where p_a is the local ambient pressure, p_v is the liquid vapor pressure, p_g is the gas partial pressure, σ is the surface tension, and r is the bubble radius. The pressure, p_g , of a known weight of a perfect gas at constant temperature is

$$p_g = \frac{wRT}{V}$$

where w is the weight of the gas, T is its absolute temperature, V is its volume, and R is the gas constant (53.35 ft. lb./lb./Deg.Rankin). Thus, this expression can be written

$$p_g = \frac{3wRT}{4\pi r^3} = \frac{J}{r^3}$$

where $J = 3wRT/4\pi$ is a parameter indicative of the weight of the gas in a bubble at a particular temperature. Equation (169) becomes

$$p_a - p_v = \frac{J}{r^3} - \frac{2\sigma}{r} \quad (170)$$

The minimum pressure at which this equilibrium relationship is valid is found by differentiating with respect to r :

$$\frac{d(p_a - p_v)}{dr} = \frac{-3J}{r^2} + 2\sigma = 0 .$$

Therefore, the critical pressure, r^* , is

$$r^* = \left(\frac{3J}{2\sigma} \right)^{1/2} .$$

Consequently, the minimum pressure, $(p_a - p_v)_{\min} = p^*$, is

$$p^* = (p_a - p_v)_{\min} = \frac{J}{(3J/2\sigma)^{3/2}} - \frac{2\sigma}{(3J/2\sigma)^{1/2}}$$

or simply

$$p^* = (p_a - p_v)_{\min} = \frac{-4\sigma}{3r^*} \quad (171)$$

for which the critical pressure is below the vapor pressure. If the ambient pressure is decreased even slightly, the bubble (water-vapor-air nucleus) becomes unstable and grows without bound. At greater than critical pressures the bubble is stable and assumes an equilibrium radius according to Equation (170). Figure 39 shows the static relationship between the pressure head and the bubble radius for various masses of gas as given by the parameter J . From this figure it is clear that in order for small diameter bubble nuclei to expand, the pressure must be less than the vapor pressure. Moreover, Strasberg⁽⁵¹⁾ shows that bubbles having a diameter of less than 20 microns (6.6×10^{-5} foot) require negative absolute pressure for cavitation inception.

These simple bubble-nuclei equilibrium arguments are only generally relevant to the observed cavitation phenomenon, since the dynamic effects of an expanding, moving bubble are ignored. Moreover, the arguments assume constant temperature and constant air mass. Nevertheless, these arguments do provide a basis from which to appraise the laboratory findings.

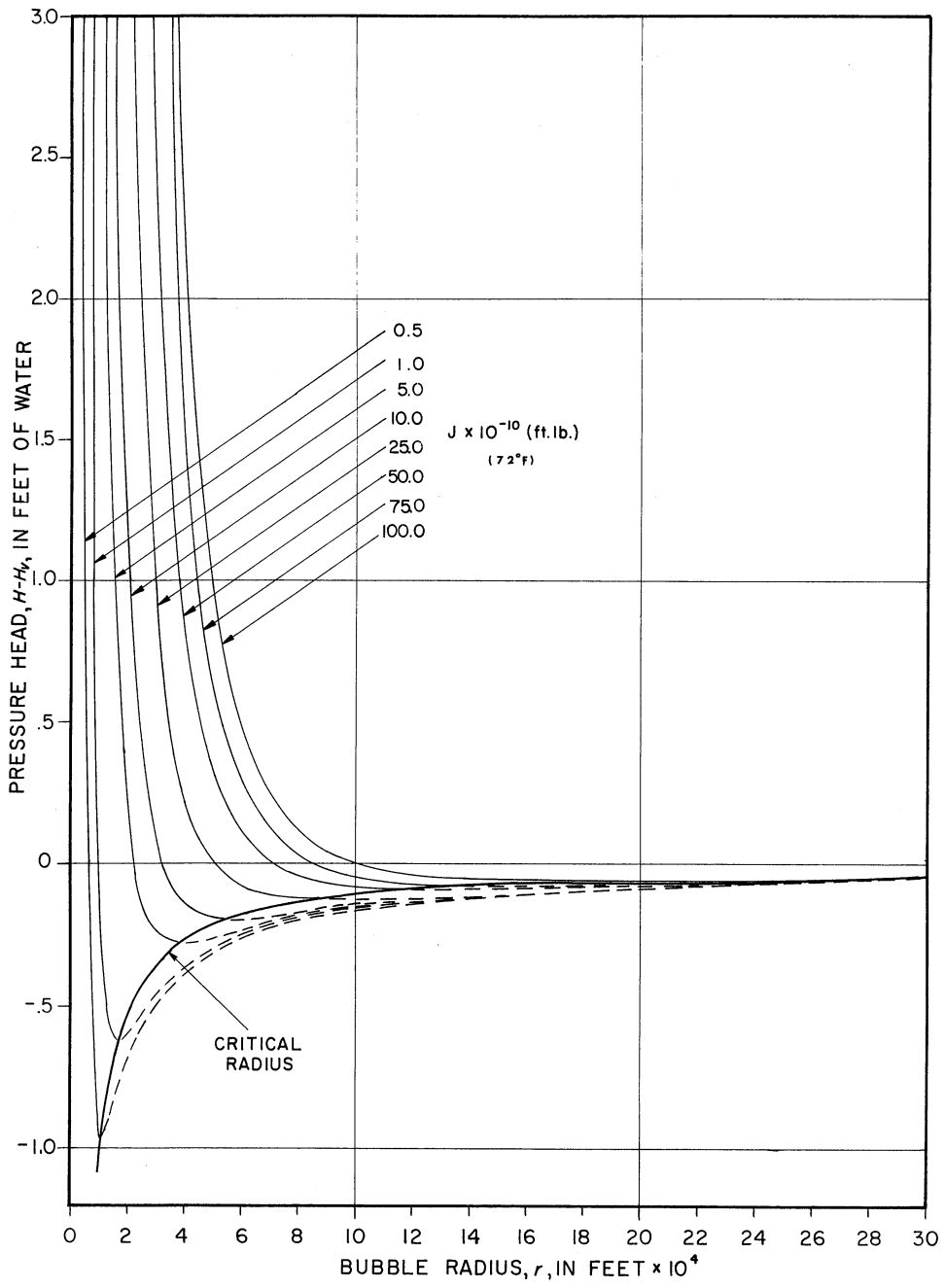


Figure 39. Diagram Relating Static Pressure to Bubble Size.

The water used in the experimental phase of the study was obtained from the main recirculated supply available in the laboratory. It was found to be nearly saturated with air under atmospheric conditions. The fact that the water must have been in a supersaturated state at the point in the laboratory flow system at which column separation occurred might lead one to presume that the cavitation may have been gaseous cavitation. However, Parkin and Kermeen⁽³⁸⁾ determined that even with convective diffusion aiding gaseous cavity growth, the time required for such growth is measured in hundreds of milliseconds, whereas, the time required for true vaporous cavitation is of the order of a few microseconds. Moreover, as noted by Strasberg⁽⁵¹⁾ true vaporous cavitation is virtually independent of the dissolved air content of the water, except insofar as the dissolved air may influence the size and growth of subcritical nuclei. Vaporous cavitation with its explosive bubble growth requires the pressure to fall below the liquid vapor pressure, if only for an instant. Gaseous cavitation, on the other hand, can occur at a pressure above the vapor pressure provided this pressure is maintained long enough to sustain the comparatively slow diffusion process. Thus, three factors indicate that the main column separation void, as well as the cavitation occurring ahead of it are, in fact, of vaporous origin: (a) the almost instantaneous explosive character of bubble-cavity formation, (b) the insufficient time for gaseous cavitation, and (c) the complete (or nearly complete) disappearance of both the separation-void and bubble cavities with the sudden reoccurrence of high pressures.

Recent studies by Ripken and Killen⁽⁴⁴⁾ offer a possible explanation for the appearance of the vaporous bubble cavities near the top, inner surface of the pipe and in the wakes behind the wires of the

wave gages. Their research revealed that vorticity and boundary-layer turbulence promote the diffusive growth of the entrained air-water-vapor nuclei, thereby promoting vaporous cavitation in these regions at the onset of subcritical pressures.

From the laboratory observations and information pertaining to cavitation phenomena presented above, it appears that the mechanism of column separation and the accompanying bubble cavitation occurring ahead of the separation void may be described as follows: The initial high pressures in the pipe are relieved by flow of water toward the reservoir. When the motion of flow extends to the interface between the water column and the closed gate valve, tensile stresses tend to form in the water adjacent to the gate and the local pressure abruptly decreases below ambient pipe pressure. Minute quantities of dissolved air leave solution in free, molecular form and coalesce with the already present submacroscopic air-water-vapor nuclei. Pressures at the gate valve continue to decrease and to propagate from the valve toward the reservoir as a low-pressure wave. The rate of propagation is of the order of 2.5 to 4.5×10^3 feet per second. Concurrently, a submacroscopic nucleus in the vicinity of the topmost region of the water-column, gate-valve interface is subjected to less than the critical equilibrium condition and expands explosively. The result is formation of a column-separation void. The void continues to expand and propagate from the gate valve toward the reservoir, but with a celerity of only a few feet per second. Other nuclei situated between the propagating, low-pressure, wave and the much more slowly advancing separation void encounter less than critical conditions and expand explosively, also. These, then, are the bubble cavities observed to occur ahead of the void.

Contrary to the assumption of Chapter II that flow ahead of the separation void would be full-pipe flow, the bubble cavities produce a highly transient, metastable, two-phase flow characterized by intricate flow geometry and by ever-changing boundary conditions. The outlook for a rational interpretation of the energy dissipation rate under such conditions is dismal at best. However, the rate of energy dissipation that occurs under somewhat similar flow conditions is known to be greater than for comparable single-phase, steady-state, full-pipe flow.⁽⁵⁷⁾ This is so, first of all, because of the complex character of the two-phase flow pattern and, second, because of the energy losses associated with cavitation itself.⁽³³⁾ Nevertheless, the treatment of energy dissipation in two-phase flow, either by rational or empirical means, is beyond the scope of this study.

In order to test the notion that a higher rate of energy dissipation would shorten the duration of the theoretically-determined column separation intervals and would thereby bring the computer-simulated results into closer agreement with the experimental findings, the friction-loss coefficient in the simulation model was arbitrarily adjusted. The computer program was temporarily modified so that whenever the absolute pressure head at any point in the pipe fell below 12 feet of water during periods of column separation, the friction coefficient at that point was increased by a factor of 3. The simulated results obtained with this arbitrary modification did indeed verify the notion; the duration of the first column separation interval was decreased, the distance of travel of the separation void was reduced, and the magnitude of the second pressure rise was brought more nearly into agreement with the laboratory finding. The simulation was not carried beyond the second pressure rise.

From a qualitative point of view, the better agreement between the theoretical and experimental results tends to support the arguments for increased energy dissipation. Quantitatively speaking, however, the arbitrary increase in the friction coefficient is of no significance because the column separation phenomenon is dependent upon the following related factors:

- (a) The nucleation characteristics of the water -- specifically the size spectrum and quantity of submacroscopic nuclei.
- (b) The vorticity and turbulence-generating characteristics of the particular pipe.
- (c) The diameter of the pipe and the velocity of the flow in the pipe.
- (d) The magnitude and occurrence characteristics of the negative pressure initiating column separation.

Although iteration methods could be used to determine the friction coefficients which would bring the theoretical findings into very close agreement with each of the experimental results, such coefficients would be highly empirical and would have very little transfer value to other flow conditions. Thus, the significance of this discussion may be summarized as follows: The theoretical representation of the column separation phenomena depicted by the computer model is a limiting condition. During actual column separation under typical transient flow conditions, the separation void(s) that form will be of shorter duration and lesser extent, and the pressure rises after the initial rise will be of lesser magnitude than predicted by the mathematical model. The actual column

separation phenomena will tend to approach the theoretically predicted conditions derived from the model only when a deficiency of air, water-vapor nuclei in the water inhibits the full development of two-phase flow ahead of the void.

CHAPTER VII

CONCLUSIONS

The primary objective of the study was to provide better insight into the fluid dynamics of liquid column separation. The approach used was to develop a rational, generally applicable, mathematical model with which to numerically simulate transient flow, including liquid column separation, and thereby duplicate the essence of the phenomena without actually attaining reality. The findings derived from simulation were then systematically compared with the corresponding findings obtained from concurrent experimental investigations conducted in the laboratory. The conclusions drawn from the study are:

- (a) The two sets of partial differential equations, describing the transient pressure waves in a pipe flowing full on the one hand, and transient, free-surface, gravity-type waves in the partially-full pipe on the other hand, are both of the nonlinear, hyperbolic type and directly amenable to solution by the method of characteristics. The appropriate effects of fluid friction upon each type of transient flow are readily included in the solution.
- (b) By means of the appropriate boundary conditions and by considering other controlling physical parameters, a sensitive, articulate, and highly sophisticated mathematical model representing the transient-flow, column-separation phenomena can be created.

- (c) Experimental laboratory studies of transient flow with column separation reveal that vaporous cavitation occurs throughout much of the length of the pipe under conditions of supposedly full-pipe flow ahead of the void. As a direct result of this cavitation, flow is temporarily transformed into highly transient, metastable, two-phase flow.
- (d) Comparison of computer-simulated and experimentally-determined transient flows accompanied by column separation reveals that the mathematical model does indeed reproduce the characteristics of the phenomena, e.g. the time sequence of pressure rises at the closed valve separated by column separation voids. The magnitude, duration, and form of the first simulated pressure rise compared very favorable with its experimentally-derived equivalent. However, after the first experimental pressure rise the subsequent rises are observed to diminish in magnitude more rapidly with time than their simulated counterparts. Moreover, the duration and extent-of-travel of the successive experimental voids are also considerably less than predicted from the mathematical model.
- (e) An overall similarity in shape is apparent between the experimental voids and their model-derived counterparts. However, free-surface ripples and other small perturbations are evident on the free surface of the experimental voids that do not appear on the rather idealistically smooth free surface of the simulated voids.

- (f) The higher rate of energy dissipation associated with the two-phase flow produced by cavitation ahead of the void is responsible for the shortened duration and extent of the experimental voids and for the diminished magnitude of the experimental pressure rises subsequent to the first rise. Whereas the model assumes viscous energy dissipation governed by the velocity of the full-pipe flow, the two-phase, cavitation-producing flow is accompanied by thermodynamic as well as more vigorous viscous energy dissipation.
- (g) Computer-simulated transient flows determined from the mathematical model represent a limit or maximum condition which will be approached only when cavitation ahead of the void is nominal. Hence, the model has direct engineering application in the determination of design criteria.

Future study of transient-flow accompanied by column-separation should be directed toward incorporating the thermodynamic aspects of liquid column separation into the mathematical model. Vaporization, heat conduction, and condensation are factors of greater significance as a result of the occurrence of cavitation ahead of the separation void.

Further experimental investigation is desirable using larger diameters of pipe and higher velocities. It is recommended that for any future experimental study stroboscopic photography be used to determine the form of the separation voids rather than the wave gages used in this study. Such a procedure would remove the possible influence of the wave gages on the formation of cavitation, provide more data on the void, and eliminate troublesome instrumentation requiring repeated calibration.

SELECTED REFERENCES

1. Allievi, Lorenzo, Theory of Waterhammer. (translated from Italian to English by Eugene E. Halmos for the ASCE, 1925), Rome, Italy, printed by Richardo Garoni, 1913.
2. Apelt, C. J., "Investigations of Waterhammer", Journal, The Institute of Engineers, Australia, Vol. 28, No. 3, Sidney, Australia, (1956), 75-81.
3. Arden, B., Galler, B., and Graham, R., MAD -- Michigan Algorithm Decoder, University of Michigan, Ann Arbor, Michigan, November 1963, 120 p.
4. Baltzer, R. A., and Shen, John, Flows of Homogeneous Density in Tidal Reaches. U.S. Geological Survey open file report, Washington, D. C., September 1961, 110 p.
5. Baltzer, R. A., and Shen, John, Computation of Flows in Tidal Reaches by Finite-Difference Technique, Proceedings, The First National Coastal and Shallow Water Research Conference, Tallahassee, October 1961, p. 258-264.
6. Bergeron, Louis, Water Hammer in Hydraulics and Wave Surges in Electricity. New York: John Wiley and Sons, 1961.
7. Boussinesq, Joseph, Essai sur la theorie des eaux courantes, Institut de France, Academie des Sciences, Memoires par divers savants, Vol. 23, Paris, 1877.
8. Carstens, M. R., and Hagler, T. W., Jr., Water Hammer Resulting from Cavitating Pumps, Proceedings, American Society of Civil Engineers, Ann Arbor, Michigan, Vol. 89, No. HY6, (1964), pp. 161-184.
9. Case, J. C., The Strength of Materials. 3rd Ed., London, England: Edward Arnold and Co., 1939, p. 437-442.
10. Chow, Ven Te, Open-Channel Hydraulics. New York: McGraw-Hill Book Co., Inc., 1959, p. 525-585.
11. Courant, Richard, and Friedrichs, K. O., Supersonic Flow and Shock Waves. New York: Interscience Publishers, Inc., 1948, p. 37-92.
12. Courant, Richard, and Hilbert, David, Methods of Mathematical Physics, Vol. II, New York: Interscience Publishers, Inc., p. 407-490.

13. Daily, J. W., and Johnson, V. E., Turbulence and Boundary-Layer Effects on Cavitation Inception from Gas Nuclei. First International Symposium on Cavitation in Hydrodynamics, Report No. 4, National Physics Laboratory, Teddington, England, 1955, 13 p.
14. Daily, J. W., and Jordaan, J. M., Effects of Unsteadiness on Resistance and Energy Dissipation. Hydrodynamics Laboratory, Massachusetts Institute of Technology, Technical Report No. 22, Cambridge, Massachusetts, 1956, 48 p.
15. Dronkers, J. J., "Methoden van Getijberekening (Methods of Tidal Calculation)", De Ingenieur, Bouw en Waterbouwkunde, Vol. 49, (1947), p. 121-137.
16. Eisenberg, Phillip, and Tulin, M. P., Cavitation: Handbook of Fluid Dynamics. Section 12, edited by V. L. Streeter, New York: McGraw-Hill Book Co., Inc., 1961, p. 1-46.
17. Ellis, A. T., Slater, M. E., and Fournery, M. E., Some New Approaches to the Study of Cavitation, Proceedings, IAHR - Symposium on Cavitation and Hydraulic Machinery, Sendai, Japan, (1963), p. 59-70.
18. Escande, M. L., Arret Instantane du Debit d'une Conduit forcee avec Cavitations, Proceedings, IAHR - Symposium on Cavitation and Hydraulic Machinery, Sendai, Japan, (1963), p. 113-124.
19. Fox, L., Numerical Solution of Ordinary and Partial Differential Equations. London, England: Addison-Wesley Publishing Co., Inc., 1962, p. 205-366.
20. Garabedian, P. R., Partial Differential Equations. New York: John Wiley and Sons, Inc., 1964, p. 458-518.
21. Gray, C. A. M., "The Analysis of the Dissipation of Energy in Water Hammer", Australian Journal of Applied Science, Sidney, Australia, Vol. 5, No. 2, (1954), p. 125-131.
22. Greenspan, Martin, and Tschiegg, C. E., "Effect of Dissolved Air on the Speed of Sound in Water", Journal of the Acoustical Society of America, Vol. 27 (1956), p. 501.
23. Greenspan, Martin, and Tschiegg, C. E., "Speed of Sound in Water by a Direct Method", Journal of Research of the National Bureau of Standards, Vol. 59, No. 4, Washington, D. C., (1957), p. 249-254.
24. Halliwell, A. R., Velocity of Water Hammer Waves in an Elastic Pipe, Proceedings, American Society of Civil Engineers, Ann Arbor, Michigan, Vol. 89, No. HY4, 1963, p. 1-21.

25. Hartree, D. R., Some Practical Methods of Using Characteristics in the Calculation of Non-Steady Compressible Flows, Atomic Energy Commission, Report LA-HU-1, Los Alamos, 1952.
26. Hartree, D. R., Numerical Analysis. New York: Oxford University Press, Inc., 2nd Edition, 1958.
27. Hooper, L. J., Experimental Investigation of Initiation of Cavitation Behind an Accelerated Circular Disk, Proceedings, IAHR - Symposium on Cavitation and Hydraulic Machinery, Sendai, Japan, 1963, p. 125-141.
28. Jaeger, Charles, Engineering Fluid Mechanics. (English edition), New York: St. Martin's Press, Inc., 1957, p. 359-381.
29. Joukowsky, N. E., Waterhammer (translated by D. Simin from the Memoires of the Imperial Academy of St. Petersburg, Russia), New York, American Water Works Association, Vol. 24, (1898), p. 341-424.
30. Lai, Chintu, A Study of Waterhammer Including Effect of Hydraulic Losses. Ph.D. Thesis, University of Michigan, Ann Arbor, Michigan, 1961, 96 p.
31. Le Conte, J. N., "Experiments and Calculations on the Resurge Phase of Water Hammer", Transactions, American Society of Mechanical Engineers, New York, Vol. 59, 1937, p. 691-694.
32. Li, Wen-Hsiung, Mechanics of Pipe-Flow Following Column Separation, Proceedings, American Society of Civil Engineers, Ann Arbor, Michigan, Vol. 88, No. EM4, 1962, p. 97-118.
33. Li, Wen-Hsiung, Thermal Effect on Growth and Collapse of Cavities, Proceedings, IAHR - Symposium on Cavitation and Hydraulic Machinery, Sendai, Japan, 1963, p. 1-16.
34. Li, Wen-Hsiung, and Walsh, J. P., Pressure Generated by Cavitation in a Pipe, Proceedings, American Society of Civil Engineers, Ann Arbor, Michigan, Vol. 90, No. EM6, 1964, p. 113-133.
35. Lister, Mary, "The Numerical Solution of Hyperbolic Partial Differential Equations by the Method of Characteristics". (Chapter 15 of Mathematical Methods for Digital Computers. edited by Ralston, A., and Wilf, H. S.), New York: John Wiley and Sons, Inc., 1960, p. 165-179.
36. Massau, Junius, Graphical Integration of Partial Differential Equations with Special Applications to Unsteady Flow in Open Channels (a translation by Henri J. Putman of Portions of Memoire sur l'Integration Graphique des Equations aux Derivees Partielles) Rocky Mountain Hydraulics Laboratory, Allenspark, Colorado, 1900, 129 p.

37. O'Brien, M. P., and Hickox, G. H., Applied Fluid Mechanics. New York: McGraw-Hill Book Co., 1937, p. 242-255.
38. Parkin, B. R., and Kermeen, R. W., The Roles of Convective Air Diffusion and Liquid Tensile Stresses During Cavitation Inception, Proceedings, IAHR - Symposium on Cavitation and Hydraulic Machinery, Sendai, Japan, 1963, p. 17-35.
39. Parmakian, John, Waterhammer Analysis. New York: Prentice-Hall, Inc., 1955, 145 p.
40. Prescott, John, Applied Elasticity. London: Longmans, Green and Co., 1924, p. 326-332.
41. Reddick, H. W., and Miller, F. H., Advanced Mathematics for Engineers. New York: John Wiley and Sons, Inc., 1957, p. 110, 114, 139-143.
42. Rich, G. R., Hydraulic Transients. 2nd Ed., New York: Dover Publications, Inc., 1963, p. 1-73, 166-187.
43. Richard, R. T., "Water-Column Separation in Pump Discharge Lines", Transactions, American Society of Mechanical Engineers, New York, Vol. 78, 1956, p. 1297-1306.
44. Ripken, J. F., and Killen, J. M., Gas Bubbles; Their Occurrence, Measurement, and Influence in Cavitation Testing, Proceedings, IAHR - Symposium on Cavitation and Hydraulic Machinery, Sendai, Japan, 1963, p. 37-57.
45. Saint Venant, J. C. B. de, Theorie du Mouvement non-permanent des eaux, Institute de France, Academie des Sciences Comptes Rendus, Vol. 73, Paris, (July 1871), p. 147-237.
46. Schönfeld, J. C., "Resistance and Inertia of Flow of Liquids in a Tube or Open Canal", Applied Science Research, Section A, Vol. 1, No. 13, Netherlands, (1948), p. 169-197.
47. Schönfeld, J. C., Propagation of Tides and Similar Waves, 's-Gravenhage, Netherlands, Staatsdrukkerji Vitgevenijbedijf, 1951, p. 31-69.
48. Solkolnikoff, I. S., and Redheffer, R. M., Mathematics of Physics and Modern Engineering. New York: McGraw-Hill Co., Inc., 1958, p. 509-521.
49. Sommerfield, Arnold, Partial Differential Equations in Physics. New York: Academic Press, 1949, p. 52-55.
50. Stepanoff, A. J., and Kawaguchi, K., Cavitation Properties of Liquids, Proceedings, IAHR - Symposium on Cavitation and Hydraulic Machinery, Sendai, Japan, 1963, p. 71-85.

51. Strasberg, M., Undissolved Air Cavities as Cavitation Nuclei. First International Symposium on Cavitation in Hydrodynamics, Report No. 6, National Physics Laboratory, Teddington, England, 1955, 19 p.
52. Streeter, V. L., Fluid Mechanics. 3rd. Ed., New York: McGraw-Hill Book Co., Inc., 1962, p. 211-222.
53. Streeter, V. L., and Lai, Chintu, Waterhammer Analysis Including Fluid Friction, Proceedings, American Society of Civil Engineers, Ann Arbor, Michigan, Vol. 88, No. HY3, 1962, p. 79-112.
54. Streeter, V. L., Keitzer, W. F., and Bohr, D. F., Pulsatile Pressure and Flow Through Distensible Vessels, Circulation Research, American Heart Association, Vol. XIII, No. 1, 1963, p. 3-20.
55. Stoker, J. J., Numerical Solution of Flood Prediction and River Regulation Problems, New York University, Institute for Mathematics and Mechanics, NYU-200, 1953, 36 p.
56. Stoker, J. J., Water Waves. New York: Interscience Publishers, Inc., 1957, p. 291-314, 451-509.
57. Tek, M. R., Two-Phase Flow: Handbook of Fluid Dynamics. Section 17, edited by V. L. Streeter, New York: McGraw-Hill Book Co., Inc., 1961, p 1-39.
58. Thomas, H. A., The Hydraulics of Flood Movements in Rivers. Pittsburgh, Carnegie Institute of Technology, 1934, p. 9-45.
59. Timoshenko, S., Strength of Materials. Part II. New York: Van Nostrand Co., Inc., 1930, p. 528-533.
60. Tollmein, W., Theory of Characteristics (translated from German), National Aeronautics and Space Administration, 1942, 28 p.

APPENDIX I

MAIN COMPUTER PROGRAM

A complete syntactical listing of the MAD language computer program for simulation of transient flow accompanied by column separation in the pipe system shown in Figure 14 is presented below. The program, which is designated MAIN, is divided into several subsections, each of which is identified and briefly described by comments regarding its primary function. These subdivisions also correspond to the subdivisions of the flow diagram of Figure 13. All internal subroutines are included in the listings. External subroutines, however, are listed syntactically in Appendix II.

070785 04/06/64 10 27 54.8 PM

\$ COMPIL MAD,PRINT OBJECT,EXECUTE,PUNCH OBJECT,I/O DUMP MAIN 001
\$ FULL DUMP

MAD (12 MAR 1964 VERSION) PROGRAM LISTING

THIS PROGRAM IS A THEORETICAL ANALYSIS OF THE PHENOMENA OF LIQUID COLUMN SEPARATION IN A HORIZONTAL PIPE AS ENCOUNTERED UNDER CONDITIONS OF TRANSIENT FLOW. THE PROGRAM HAS BEEN WRITTEN IN MAD, THE MICHIGAN ALGORITHM DECORDER LANGUAGE AND EXECUTED ON THE IBM 7090 AT THE UNIVERSITY OF MICHIGAN COMPUTING CENTER.

```

* * * * *
INTEGER I,J,K,L,M,N,MN,GAP,MAXLIM,CUTOFF,SHUTOF,PRTLIM,PRTRFQ
0 ,PRTCYC,INCVPT,MFSEB,MFCCL,JJ,JQ,KK,JHK,INC,MK,FACTOR,C,
1 SPRK,IPRK,LPRK,FVA,FVB,PMK,MARK,COUNT
1 STATEMENT LABEL STATEP,STATEC,STATED,STATEE
FORMAT VARIABLE FVA,FVB
DIMENSION VL(210,ADIM),H(210,ADIM),VP(210,ADIM),HP(210,ADIM),
C EL(210),THETA(210,ADIM),ALPHA(200),L(2),B(2),ADG(2),
1 LL(2),MN(2),DELTA(2),DELXI(2),MU(2),A(2),ZETA(2),CP(2),
2 GOA(2),LVEL(2),HLDS(2),U(100),Z(100),UP(100),ELP(210,ADIM),
PROGRAM COMMON R(2),XI,D(2),PAREA,NU,GAP,F(102,DIM),ZP(100),
0 SPRK,IPRK,LPRK,FVA,FVB,STATLD,NYDRK,PENNSY,SUZ(11)
VECTOR VALUES DIM = 2,1,51
VECTOR VALUES ADIM = 2,1,105
CONTINUE
READ FORMAT CARD,RHO,KA,VMAX,GAP,HBAR,NU,Q
READ FORMAT PLAN,HEL,MEL,LEL,WSEL,LOC1,LOC2,LOC3
READ FORMAT PIPE1,E(1),ZETA(1),D(1),B(1),R(1),LL(1),MN(1)
READ FORMAT PIPE2,E(2),ZETA(2),D(2),B(2),R(2),LL(2),MN(2)
READ FORMAT CONTRL,MAXLIM,CUTOFF,INCVPT,SHUTOF,PRTLIM,PRTRFQ
0 ,PRTCYC
READ FORMAT QUANT,INC,HVAPOR,XI,FACTOR,IOTA,ZOV
READ FORMAT FRIC1,F(1,0)...F(1,35)
READ FORMAT FRIC2,F(2,0)...F(2,35)
READ FORMAT CSURG,SUZ(10)...SUZ(10)
CP(1) = 1.-ZETA(1)*((B(1)-R(1))/R(1))
CP(2) = 1.-ZETA(2)*((B(2)-R(2))/R(2))-ZETA(2)*ZETA(2)*((B(2)/R
U (2))
PRINT COMMENT $1
0 GIVEN INFORMATION $
PRINT COMMENT $-GIVEN PHYSICAL DATA AND CONSTANTS $
PRINT FORMAT GIVEN,RHO,KA,VMAX,HBAR,Q
PRINT COMMENT $DIMENSIONAL DATA DESCRIBING ANALYTIC MODEL $
PRINT FORMAT SCHEME,HEL,MEL,LEL,WSEL,LOC1,LOC2,LOC3
PRINT COMMENT $PIPE CHARACTERISTICS AND RELATED DATA $
PRINT FORMAT TUBE1,E(1),ZETA(1),D(1),B(1),R(1),LL(1),MN(1)
PRINT FORMAT TUBE2,E(2),ZETA(2),D(2),B(2),R(2),LL(2),MN(2)
PRINT COMMENT $PROGRAM OPERATION AND CONTROL DATA $
PRINT FORMAT ORDERS,MAXLIM,CUTOFF,INCVPT,SHUTOF,PRTLIM,PRTRFQ
0 ,PRTCYC
PRINT COMMENT $FRICTION VALUES FOR CONSECUTIVE REYNOLDS NUMB
0 ERS FROM 100 TO 35100 IN INCREMENTS OF 1000. $

```

UNITED

PART I - PART ONE OF THIS PROGRAM IS PRIMARILY CONCERNED WITH THE TRANSIENT CONDITIONS IN THE FLOW SYSTEM (OR PORTION THEREOF) WHICH IS ALWAYS FLOWING FULL. SEVERAL STATEMENTS OF INTRODUCTION AND INITIALIZATION FOLLOW.

```

* * * * *
WHENEVER MN(1).E.2
STATEA=MICHGV
STATEK=MUNTAN
OTHERWISE
STATEA=MISSIP
STATEB=MAINE
END OF CONDITIONAL
MOFSEP = MAXLIM
JJ = MAXLIM
MARK=0
VEEE=0.
THROUGH STATES,FOR N=0,1,N.G.35
KEY=0=100.+(N*1000.)
PRINT FORMAT RESFAC,REYN,N,F(1,N),N,F(2,N)
THROUGH ALASKA, FOR J = 1,1,J.G.2
ZM=0(J)
A(J) = SQRT.(1./((RHO*(1./KA)+(D(J)*CP(J))/(E(J)*(B(J)-R(J)
0 )))
DELX(J) = LL(J)/MN(J)
IVEL(J) = Q/(3.14159*R(J).P.2)
HLOS(J) = FFC.(ZM,IVEL(J),J)*DELX(J)*
IVEL(J).P.2/(D(J)*64.32)
DELTT(J) = DELX(J)/(ABS.VMAX*ABS.A(J))
WHENEVER DELTT(1).GE.DELTT(2)
DELT = DELTT(2)
UTHERWISE
DELT = DELTT(1)
END OF CONDITIONAL
THROUGH ALABAM, FOR J = 1,1,J.G.2
ADG(J) = A(J)/32.16
GOA(J) = 32.16/A(J)
MU(J) = DELT/DELX(J)
* * * * *

```

PART I - SEC.A. THIS SECTION OF PROGRAM SETS UP THE THEORETICAL FLOW SYSTEM BEING INVESTIGATED AND DELINEATES THE APPROPRIATE POINT ELEVATIONS AND SLOPES AS WELL AS THE VELOCITIES AND HYDRAULIC-GRADIENT HEADS UNDER STEADY STATE CONDITIONS.

```

* * * * *
PRINT COMMENT $1
0 COMPUTED RESULTS $
PRINT COMMENT $- COMPUTED VALUES OF ABSOLUTE PRESSURE HEAD, V
0 ELOCITY, ELEVATION, AND ANGL OF PIPE INCLINATION AT TIME T =
0. $
1 THROUGH ARIZON, FOR N = MN(1)+MN(2),-1,N.L.0
MARS = (N-MN(1))*DELX(2)+LL(1)
WHENEVER MARS.GE.LOC3
ALPHA(N) = 0.
* * * * *

```

*031
*032
*033
*034
*035
*036
*037
*038
*039
*040
*041
*042
*043
*044
*045
*046
*047
*048
*049
*050
*051
*052
*053
*054
*055
*056
*057
*058
*059
*060

*061
*062
*063
*064
*065
*066

```

*067
*068
*069
*070
*071
*072
*073
*074
*075
*076
*077
*078
*079
*080
*081
*082
*083
*084
*085
*086
*087
*088
*089
*090
*091
*092
*093
*094
*095
*096
*097
*098
*099
*100
*101
*102

C1(N) = LEL
OR WHENEVER MARS-GL-LOC3-DLX(2),AND,MARS-L-LOC3
ALPHA(N) = ARCSIN((MEL-LF1)/(LOC3-LOC2))
EL(N) = LEL+SI*(ALPHA(N))*(LOC3-MARS)
OR WHENEVER MARS-GE-LOC2
ALPHA(N) = ALPHA(N+1)
CL(N) = EL(N+1)+SIN-(ALPHA(N))*DELX(2)
OR WHENEVER MARS-GE-LOC2-DELX(2),AND,MARS-L-LOC2
ALPHA(N) = ARCSIN((MEL-MEL1)/(LOC2-LOC1))
EL(N) = MEL+SIN*(ALPHA(N))*(LOC2-MARS)
OR WHENEVER MARS-GE-LOC1
ALPHA(N) = ALPHA(N+1)
EL(N) = EL(N+1)+SIN*(ALPHA(N))*DELX(2)
OTHERWISE
ALPHA(N) = 0.
CL(N) = HEL
END OF CONDITIONAL
MARS = *SET+HBAR
THROUGH CALIF, FOR I = 0,1,I,G,MN(1)
N = I
ELP(1,I)=EL(N)
H(1,I)=HABS-HLOS(2)*MN(2)-HLOS(1)*(MN(1)-N)
V(1,I) = IVEL(1)
THETA(1,I) = ALPHA(N)
PRINT FORMAT MEMO,I,H(1,I),V(1,I),I,ELP(1,I),I,THETA(1,I)
THROUGH NCARD, FOR I = 0,1,I,G,MN(2)
N = I+MN(1)
ELP(2,I)=EL(N)
H(2,I)=HABS-HLOS(2)*MN(2)*MN(2)-I
V(2,I) = IVEL(2)
THETA(2,I) = ALPHA(N)
PRINT FORMAT RANDUM,I,H(2,I),V(2,I),I,ELP(2,I),I,THETA(2,
0 I)
PRINT COMMENT $I VALUES OF KEY VARIABLES USED THROUGHOUT THE
0 COMPUTATIONS IN PART I.
PRINT RESULTS A(1),A(2),DELX(1),DELX(2),DELT(1),DELT(2),
0 DELT, MU(1),MU(2),CP(1),CP(2),AOG(1),AOG(2),GOA(1),GOA(2)
VP(1,0) = V(1,G)
HP(2,MN(2))=H(2,MN(2))
* * * * *
PART I - SEC.B. THIS SECTION OF THE PROGRAM CONTROLS THE
BOUNDARY CONDITIONS USED TO INITIATE TRANSIENT FLOW IN THE
THEORETICAL SYSTEM AND TO CREATE THE VACUOUS CAVITY
PHENOMENA. IT IS PRIMARILY INTENDED TO CONTROL THE
SEQUENCE OF OPERATIONS WITH RESPECT TO TIME THROUGHOUT THE
DURATION OF THE TRANSIENT PHENOMENON.
* * * * *
THROUGH ARKANS, FOR M=1+MARK,I,M,G,MAXLIM
WHENEVER M.G.-CUTOFF
TRANSFER TO HVIRG
OR WHENEVER M.E.-SHUTOF
VP(1,0)=0.
TOFOFF = M*DELT
PRINT FORMAT UBOE,TOFOFF,M
SHUTOF=0
END OF CONDITIONAL

```

*067
*068
*069
*070
*071
*072
*073
*074
*075
*076
*077
*078
*079
*080
*081
*082
*083
*084
*085
*086
*087
*088
*089
*090
*091
*092
*093
*094
*095
*096
*097
*098
*099
*100
*101
*102

*103
*104
*105
*106
*107
*108
*109
*110
*111

```

* * * * *
PART I - SEC.C. THIS SECTION OF THE PROGRAM COMPUTES THE
VELOCITIES AND THE HEADS THROUGHOUT THE X-T PLANE BY THE
METHOD OF CHARACTERISTICS FOR THE SPECIAL CASE OF THE FULL
LENGTH OF A PIPE BEING EQUIVALENT TO AN INCREMENTAL LENGTH,
THAT IS, EITHER THE LENGTH OF INCREMENT MN(1) = LL(1) OR THE
LENGTH OF INCREMENT MN(2) = LL(2).

```

```

* * * * *
HAWAII
      THROUGH COLORA, FOR J=1,1,J,G,2
      ZW=D(J)
      %WHENEVER MN(J).L.2
      VL=V(J,C)
      HL=H(J,0)
      VR=V(J,1)
      HR=H(J,1)
      VAL=VR*(VL-VR)*(VR+A(J))*MU(J)
      HAL=HR*(HL-HR)*(VR+A(J))*MU(J)
      VEP=VL*(VL-VR)*(VL-A(J))*MU(J)
      HEP=HL*(HL-HR)*(VL-A(J))*MU(J)
      %WHENEVER J.L.2.AND.M.GE.MOFSEP
      VP(J,0)=VEP+(HP(J,0)-HEP)*GOA(J)-FFC.(ZW,VL,J)*
      ((VL*.ABS.VL)/(2.*D(J))*DELTA+VEP*SIN.(THETA
      (J,0))*GOA(J))*DELTA
      PSI=VAL+HAL*(GOA(J))-FFC.(ZW,VR,J)*
      ((VR*.ABS.VR)/(2.*D(J))*DELTA-VAL*SIN.(THETA(J,1))
      *(GOA(J))*DELTA
      UR %WHENEVER J.L.2
      HP(J,0)=HEP+(VP(J,0)-VEP)*(AOG(J))+FFC.(ZW,VL,J)*
      ((VL*.ABS.VL)/(2.*D(J))*DELTA+AOG(J)-
      VEP*SIN.(THETA(J,0))*DELTA
      %WHENEVER (HP(1,0)-ELP(1,0)).L.HVAPOR, TRANSFER TO FL
      GRID
      PSI=VAL+HAL*(GOA(J))-FFC.(ZW,VR,J)*
      ((VR*.ABS.VR)/(2.*D(J))*DELTA-VAL*SIN.(THETA(J,1))
      *(GOA(J))*DELTA
      OR %WHENEVER J.G.1
      CHI=VEP-HCP*(GOA(J))-FFC.(ZW,VL,J)*
      ((VL*.ABS.VL)/(2.*D(J))*DELTA+VEP*SIN.(THETA(J,0))
      *(GOA(J))*DELTA
      HP(J,0)=(1.-/((GOA(J))*((D(J-1)/D(J)).P.2.)+GOA(J)))
      *(PSI*(D(J-1)/D(J)).P.2.)-CHI
      %WHENEVER HP(J,0).L.HVAPOR+ELP(J,0).AND.M.GE.MOFSEP,
      HP(J,0)=HVAPOR+ELP(J,0)
      VP(J,0)=CHI+HP(J,0)*(GOA(J)
      HP(J-1,MN(J-1))=HP(J,0)
      VP(J-1,MN(J-1))=VP(J,0)*((D(J)/D(J-1)).P.2.)
      PSI=0.
      CHI=0.
      VP(J,1)=VAL-(HP(J,1)-HAL)*(GOA(J))
      -FFC.(ZW,VR,J)*((VR*.ABS.VR)/
      (2.*D(J))*DELTA-VAL*SIN.(THETA(J,1))*DELTA*GOA(J)
      END OF CONDITIONAL
      TRANSFER TO COLORA
      END OF CONDITIONAL
* * * * *

```

```

*112
*113
*114
*115
*116
*117
*118
*119
*120
*121
*122
*123
*124
*124
*125
*125
*126
*127
*127
*128
*128
*129
*129
*130
*130
*131
*131
*132
*132
*133
*133
*134
*135
*136
*137
*138
*139
*139
*141
*141
*142

```


PART 1 - SEC.D. THIS SECTION OF THE PROGRAM COMPUTES THE VELOCITIES AND THE HEADS THROUGHOUT THE X-T PLANE BY THE METHOD OF CHARACTERISTICS FOR THE GENERAL CASE, THAT IS, FOR THE LENGTH LL(1) EQUIVALENT TO AN INTEGRAL MULTIPLE, MN(1), OF THE INCREMENTAL LENGTH DELX(1), AND THE LENGTH LL(2) EQUIVALENT TO AN INTEGRAL MULTIPLE, MN(2), OF THE INCREMENTAL LENGTH DELX(2).

* * * * *

```

THROUGH COLDR4, FOR I=0,1,I-G,MN(J)-2
VL=V(J,I)
HL=H(J,I)
VM=V(J,I+1)
HM=H(J,I+1)
VR=V(J,I+2)
HR=H(J,I+2)
    
```

DETERMINATION OF PRESSURE AT BOUNDARY CONDITION X = 0, UR AT JUNCTION BETWEEN PIPES.

```

WHENEVER I.L.1
  VEP=VL+(VL-VM)*(VL-A(J))*MU(J)
  HEP=HL+(HL-HM)*(VL-A(J))*MU(J)
  WHENEVER J.L.2.AND.M.GE.MOFSEP
    VP(J,I)=VEP+(HP(J,I)-HEP)*GOA(J)-FFC.(ZM,VL,J)
    *((VL*.ABS.VL)/(2.*D(J)))*DELTA*VLP*SIN.(
      THETA(J,I))*GOA(J)*DELTA
    OR
      WHENEVER J.L.2
        HP(J,I)=HEP+(VP(J,I)-VEP)*(ADG(J))
        +FFC.(ZM,VL,J)*((VL*.ABS.VL)/
          (2.*D(J)))*DELTA*ADG(J)-VEP*SIN.(THETA(J,I))*DELTA
        WHENEVER (HP(I,0)-ELP(I,0)).L.HVAPOR, TRANSFER TO
          FLORID
        OR
          WHENEVER J.G.1
            CHI=VEP-HEP*GOA(J)-FFC.(ZM,VL,J)
            *((VL*.ABS.VL)/(2.*D(J)))*DELTA*VEP*
            SIN.(THETA(J,I))*GOA(J)*DELTA
            HP(J,I)=(1./((GOA(J)-1)*(D(J)-1)/D(J)).P.2.)*
            GOA(J))*PSI*((D(J)-1)/D(J)).P.2.-CHI)
            WHENEVER HP(J,I).L.HVAPOR+ELP(J,I).AND.K.GE.MOFS
              EP,HP(J,I)=HVAPOR+ELP(J,I)
              VP(J,I)=CHI+HP(J,I)*(GOA(J))
              HP(J-1,MN(J-1))=HP(J,I)
              VP(J-1,MN(J-1))=VP(J,I)*((D(J)/D(J-1)).P.2.-)
              PSI=0.
              CHI=0.
            END OF CONDITIONAL
          END OF CONDITIONAL
        END OF CONDITIONAL
    
```

COMPUTATION OF PRESSURES AND VELOCITIES AT INTERIOR POINTS.

```

VAL=VM+(VL-VM)*(VM+A(J))*MU(J)
HAL=HM+(HL-HM)*(VM+A(J))*MU(J)
VEP=VM+(VM-VR)*(VM-A(J))*MU(J)
HEP=HM+(HM-HR)*(VM-A(J))*MU(J)
VALLY = VAL*.ABS.VAL
VEPPY = VEP*.ABS.VEP
FFCC = FFC.(ZM,VM,J)
    
```

*143
*144
*145
*146
*147
*148
*149

*150
*151
*152
*153
*154
*154
*154
*155
*156
*156
*156
*157
*157
*158
*158
*159
*159
*160
*160
*161
*161
*162
*163
*164
*165
*166
*167
*168

*169
*170
*171
*172
*173
*174
*175

```

*176 V2(J,I+1)=0.5*(VAL+VEP)+0.5*(HAL-HEP)*GOA(J)
*176 -FFC*(VALLY+VEPPY)/(4.*D(J))*DEL T-0.5*SIN.
*176 (THETA(J,I+1))*(VAL-VEP)*GOA(J)*DEL T
*177 HP(J,I+1)=0.5*(VAL-VEP)*AOC(J)+0.5*(HAL+HEP)
*177 -FFC*AOC(J)*(VALLY-VEPPY)/(4.*D(J))*DEL T-0.5*SIN.
*177 (THETA(J,I+1))*(VAL+VEP)*DEL T
*178 *WHENEVER HP(J,I+1).I.HVAPOR*ELP(J,I+1).AND.M.GE.MOFSLP
*178 *HP(J,I+1)=HVAPOR*LLP(J,I+1)

```

DETERMINATION OF PRESSURE AT BOUNDARY CONDITION X =
LL(1) + LL(2), OR AT JUNCTION BETWEEN PIPES.

```

*179 *WHENEVER I.GE.MN(J)-2
*180 VAL=VR+(VM-VR)*(VR+A(J))*MU(J)
*181 HAL=HR+(HM-HR)*(VR+A(J))*HU(J)
*182 *WHENEVER J.L.L.2
*183 P.S.I=VAL+HAL*(GOA(J))-FFC.(ZM,VR,J)
*183 *(IVR*ABS.VR)/(2.*D(J))*DEL T-VAL*
*183 SIN.(THETA(J,I+2))*GOA(J)*DEL T
*184 OR *WHENEVER J.G.1
*185 VP(J,I+2)=VAL-(HP(2,MN(J))-HAL)*GOA(J)
*185 -FFC.(ZM,VR,J)*(IVR*ABS.VR)/
*185 (2.*D(J))*DEL T-VAL*SIN.(THETA(J,I+2))*GOA(J)*
*185 DEL T
*186 *END OF CONDITIONAL
*187 *END OF CONDITIONAL
*188 *CONTINUE
*189 *HOLD = V(2,MN(2))
*190

```

COLORA

MOVE FORWARD DELTA T IN THE I-DIRECTION ON X-T PLANE.

```

*191 THROUGH SCARO, FOR J=1,I,J.G.2
*192 THROUGH SCARO, FOR I=0,1,I.G.MN(J)
*193 V(J,I)=VP(J,I)
*194 H(J,I)=HP(J,I)

```

SCARO

PART I - SEC.E. THIS SECTION OF THE PROGRAM GOVERNS THE
PRINTING OF COMPUTED RESULTS AND PROVIDES CERTAIN SWITCHING
OF OPERATIONS TO PART II.

```

*195 * * * * *
*195 *WHENEVER V(2,MN(2))/HOLDD.L.0.,PRINT FORMAT BASSON,M
*196 *DEL T/2.
*196 *WHENEVER M.E.MOFSEP
*197 *VEEE=VEEE+V(1,0)
*198 *PRINT COMMENT $O THE VELOCITIES AND ABSOLUTE HEADS THR
*198 *UGHTOUT THE REMAINDER $O THE FULL-FLOWING PIPE SYSTEM ARE AS
*199 *LISTED BELOW. $
*199 *TRANSFER TO STATEB
*200 *OR *WHENEVER M.GE.MOFSEP.AND.M.L.JJ
*201 *VEEE=VEEE+V(1,0)
*202 *TRANSFER TO ARKANS
*203 *OR *WHENEVER M.GE.MOFSEP.AND.M.E.JJ
*204 *JJ=M*FACTOR
*205 *VEEE=VEEE+V(1,0)
*206 *TRANSFER TO GEORGI

```

```

IOWA          CONTINUE
              VEE=0.
              WHENEVER M=L.MIFSEP+(INCWPT*FACTOR),TRANSFER TO RHODLI
              WHENEVER M=NE-JJQ,TRANSFER TO ARKANS
              T=DEL T*M
              PRINT FORMAT CELLU,T,M
              PRINT COMMENT $0 VAPOR CAVITY $
              EXECUTE PRTLAW.(PHK)
              PRINT FORMAT HARP,(K=SPRK,K=G.LPRK,K=G.LPRK,K*DELXC),
              (K=SPRK,IPRK,K=G.LPRK,K),(K=SPRK,IPRK,K=G.LPRK,U(K)),
              TRANSFER TO STATED
              EXECUTE PRTKUC.(PHK)
              TRANSFER TO NJERSY
              JJQ=M+(PRTCYC*FACTOR)
              PRINT COMMENT $0 FULL-FLOWING PIPE SYSTEM $
              TRANSFER TO STATER
              PRINT FORMAT FLUTE,V(1,0),V(1,1),V(1,2),V(2,0),V(2,20)
              ,V(2,40),V(2,60),V(2,80),V(2,100),(H(1,0)-ELP(1,0)),
              (H(1,1)-ELP(1,1)),(H(1,2)-ELP(1,2)),(H(2,0)-ELP(2,0)),
              (H(2,20)-ELP(2,20)),(H(2,40)-ELP(2,40)),(H(2,60)-ELP(2
              ,60)),(H(2,80)-ELP(2,80)),(H(2,100)-ELP(2,100))
              WHENEVER M=E.MARK,TRANSFER TO TEXAS
              TRANSFER TO ARKANS
              PRINT FORMAT ORGAN,V(1,0),V(1,1),V(2,0),V(2,10),
              V(2,20),V(2,30),V(2,40),V(2,50),(H(1,0)-ELP(1,0)),
              (H(1,1)-ELP(1,1)),(H(2,0)-ELP(2,0)),(H(2,10)-ELP(2,10)
              ),(H(2,20)-ELP(2,20)),(H(2,30)-ELP(2,30)),(H(2,40)-ELP
              (2,40)),(H(2,50)-ELP(2,50))
              WHENEVER M=E.MARK,TRANSFER TO TEXAS
              TRANSFER TO ARKANS
              END OF CONDITIONAL
              WHENEVER (H(1,0)-ELP(1,0)).L.(HVAPOR*1.).OR.(HHOLD-H(1,0
              )).G.10.,TRANSFER TO DELAWA
              WHENEVER M=L.PRTLIM,TRANSFER TO DELAWA
              WHENEVER M/PRTFRQ=NE.M/(PRTFRQ*1.),TRANSFER TO ARKANS
              T=DEL T*M
              PRINT FORMAT TUBA, T,M
              TRANSFER TO STATEA
              PRINT FORMAT FLUTE,V(1,0),V(1,1),V(1,2),V(2,0),V(2,20)
              ,V(2,40),V(2,60),V(2,80),V(2,100),(H(1,0)-ELP(1,0)),
              (H(1,1)-ELP(1,1)),(H(1,2)-ELP(1,2)),(H(2,0)-ELP(2,0)),
              (H(2,20)-ELP(2,20)),(H(2,40)-ELP(2,40)),(H(2,60)-ELP(2
              ,60)),(H(2,80)-ELP(2,80)),(H(2,100)-ELP(2,100))
              TRANSFER TO ARKANS
              PRINT FORMAT ORGAN,V(1,0),V(1,1),V(2,0),V(2,10),V(2,20),
              V(2,30),V(2,40),V(2,50),(H(1,0)-ELP(1,0)),(H(1,1)-ELP
              (1,1)),(H(2,0)-ELP(2,0)),(H(2,10)-ELP(2,10)),(H(2,20)-
              ELP(2,20)),(H(2,30)-ELP(2,30)),(H(2,40)-ELP(2,40)),(H(2,
              50)-ELP(2,50))
              CONTINUE
              TRANSFER TO CONNEC

```

* * * * *

PART II - PART TWO OF THIS PROGRAM IS CONCERNED WITH THE PARTIALLY FULL PIPE FLOW (OPEN-CHANNEL FLOW) ENCOUNTERED DURING THE PRESENCE OF A VACUOUS CAVITY. MORE SPECIFICALLY, IT IS CONCERNED WITH THE FORMATION AND COLLAPSE OF A VAPOR CAVITY. SEVERAL INTRODUCTORY AND DEFINITIVE STATEMENTS

```

*207
*208
*209
*210
*211
*212
*213
*214
*215
*216
*217
*218
*219
*220
*221
*222
*222
*222
*222
*222
*222
*223
*224
*225
*225
*225
*225
*226
*227
*228
*229
*229
*230
*231
*232
*233
*234
*235
*235
*235
*235
*235
*236
*237
*237
*237
*237
*238
*239

```

FOLLOW.

* * * * *

FLORID

*240
*241
*242
*243
*244
*245
*246
*247
*248
*249
*250
*251
*252
*253
*254
*255
*256
*257
*258
*259
*260
*261
*262
*263

```

MOFSEP=M
TUFSEP=MOFSEP*DELTA
PRINT FORMAT DRUM, TOFSEP, MOFSEP, TOFSLP-TOFOFF
V(1,0)=V(1,1)
H(1,0)=HVAPOR+ELP(1,0)
HP(1,0)=HVAPOR+ELP(1,0)
J=1
THROUGH NDAKOT, FOR K=0,1,K.G.INC
  Z(K)=D(1)
  U(1)=V(1,0)*ZOV
  U(2)=V(1,0)*ZUV
  PAREA=3.14159*R(1)*P.2.
  UP(0)=0.
  MINT=.015
  LAMBDA=SQRT.(PAREA*32.16/MINT)
  DELTC=FACTOR*DELTA
  DELXC=DELTC*(ABS.VHAX+ABS.LAMBDA)
  OUTFLC=DELTC*V(1,0)*ZOV*PARLA
  STATEC=RMSAS
  STATEL=OKLAHU
  COUNT=C
  YY=0.
  JHK=0

```

NDAKOT

DEFINITIONS OF INTERNAL FUNCTIONS

```

INTERNAL FUNCTION TOPWTH.(Z)=2.*SQRT.(Z*D(1))-Z.P.2.
INTERNAL FUNCTION SGADGT.(Z)=SQRT.(PEPA.(Z,J)*32.16/TOPWTH.(Z)
0 )
INTERNAL FUNCTION SOADGT.(Z)=SQRT.(PEPA.(Z,J)/(TOPWTH.(Z)*32.
0 16))
INTERNAL FUNCTION BURVOL.(X)=PARVOL.(PARK.(X,J),J)
INTERNAL FUNCTION BUBVOL.(X)=BUBVOL.(X)-OUTFLC
INTERNAL FUNCTION SURGE0.(NX)=SIMPVV.(DELXC,MK,NX,J,YY)-
0 INFLUW

```

*264
*265
*266
*267
*268
*269
*269

* * * * *

PART II - SEC.A. THIS SECTION OF THE PROGRAM CONSIDERS THE FORMATION OF THE VAPOR CAVITY. THE INITIAL GROWTH OF THE CAVITY IS CONSIDERED TO OCCUR AS A FRICTIONLESS, NEGATIVE SURGE WAVE IN A PARTIALLY FULL-FLOWING, CIRCULAR, OPEN CHANNEL. SEPARATION OF THE LIQUID AT THE TOP OF THE PIPE-WALL IS APPROXIMATED BY A PARABOLIC SURFACE.

* * * * *

```

X=BISECT.(.001*DELXC,10*DELXC,BUB00.,IOTA,VIRGNA)
KK=X/DELXC
WHENEVER KK.GE.9
  TRANSFER TO NMEXC0
OR WHENEVER KK.GE.6.AND.KK.L.9
  DELXC=3.*DELXC
  KK=X/DELXC
PRINT COMMENT $OTHE MAGNITUDE OF DELXC IS TRIPLE THE MINIMU

```

*270
*271
*272
*273
*274
*275
*276
*277

```

0 M VALUE. $
OR WHENEVER KK.GE.3.AND.KK.L.6
  DELXC=2.*DELXC
  KK=X/DELXC
  PRINT COMMENT $OTHE MAGNITUDE OF DELXC IS DOUBLE THE MINIMU
  OTHERWISE $
  PRINT COMMENT $O THE MAGNITUDE OF DELXC REMAINS THE MINIMUM
0 VALUE. $
END OF CONDITIONAL
MUCH=DELTC/DELXC
PRINT COMMENT $O GIVEN DATA AND COMPUTED VALUES PERTINENT TO
0 COMPUTATION OF FLOW FOLLOWING COLUMN SEPARATION. $
PRINT FORMAT AMOUNT,HVAPOR,DELXC,DELTC,MARK,MUCH,FACTOR,XI,
0 INC,IOTA,PAREA
SPRK=0
IPRK=1
LPRK=KK
FVA=KK
FVB=KK+1
SSUZZ=USURG.(D(J)-2.*XI*R(J),J)
ZP(O)=PARK.(X,J)+R(1)
THROUGH VRMONT, FOR K=1,1,K.G.KK
ZP(K)=PARK.(X-(K*DELXC),J)+R(1)
UP(K)=V(1,0)*ZOV+USURG.(ZP(K),J)-SSUZZ
  WHENEVER UP(K).L.0.,UP(K)=0.
THROUGH SDAKOT, FOR K=0,1,K.G.KK
  U(K)=UP(K)
  Z(K)=ZP(K)
TRANSFER TO STATEE
JJ=M+(FACTOR-1)
JJQ=JJ
VOID=OUTFLO
PRINT COMMENT $- THE INITIAL VELOCITIES AND DEPTHS IN THE VAP
  OR CAVITY ARE LISTED BELOW. $
PRINT FORMAT HARP,(K=SPRK,IPRK,K.G.LPRK,K*DELXC),(K=SPRK,IPRK
0 ,K.G.LPRK,K),(K=SPRK,IPRK,K.G.LPRK,U(K)),(K=SPRK,IPRK,K.G.LPR
1 K,Z(K))
MK=0
TRANSFER TO HAWAII

```

```

KENTUC
VRMONT
SDAKOT
OKLAHO

```

```

* * * * *
PART II - SEC.R. THIS SECTION OF THE PROGRAM TREATS THE
GROWTH AND COLLAPSE OF THE VAPOR CAVITY. AGAIN THE METHOD
OF CHARACTERISTICS IS UTILIZED, THIS TIME AS APPLIED TO
OPEN-CHANNEL FLOW, IN ORDER TO DETERMINE THE VELOCITIES AND
DEPTHS WITHIN THE CAVITY. NON-LINEAR QUANTITIES INCLUDING
FLOW RESISTANCE DUE TO FRICTION ARE INCLUDED.

```

```

* * * * *
GEORGI
MK=MK+KK
WHENEVER MK.E.0.AND.KK.E.0
  J=1
  QOUT=DELTC*(VEEE*ZOV/FACTOR)*PAREA
  OUTFLO=VOID*QOUT
  X=BISECT.(.001*DELXC,3.1*DELXC,BUBEQB.,IOTA,VIRGNA)
  KK=X/DELXC
  VOID=OUTFLO

```

```

*310
*311
*312
*313
*314
*315
*316
*317

```

```

*310
*311
*312
*313
*314
*315
*316
*317

```

```

318 PMK=MK*KK
319 COUNT=COUNT+1
320 WHENEVER COUNT.GE.3,TRANSFER TO WASH
321 STATEE=RHODCI
322 TRANSFER TO XENTUC
323 OR WHENEVER MK.LL.O.AND.KK.L.O
324 TRANSFER TO TENNSE
325 END OF CONDITIONAL
326 J=1
327 U(K+1)=U(MK)
328 Z(MK+1)=Z(MK)
329 THROUGH INDIAN, FOR K=0,1,K.G.MK-1
330 UL=U(K)
331 ZL=Z(K)
332 UM=U(K+1)
333 ZM=Z(K+1)
334 UR=U(K+2)
335 ZR=Z(K+2)
336 WHENEVER K.L.1
337 QZZL=SQAGT.(ZL)
338 UEP=UL*(UL-UM)*(UL-QZZL)*MUCH
339 ZEP=ZL*(ZL-ZM)*(UL-QZZL)*MUCH
340 ZP(K)=ZEP*(UP(K)-UEP)*SQAGT.(ZL)+FFC.(ZL,UL,J)
341 *UEP*ABS.UEP*SQAGT.(ZL)*DELTC
342 TRANSFER TO NHAMP
343 OTHERWISE
344 QZZM=SQAGT.(ZM)
345 UAL=UM*(UL-ZM)*(UM+QZZM)*MUCH
346 ZAL=ZM*(ZL-ZM)*(UM+QZZM)*MUCH
347 UEP=UM*(UM-UR)*(UM-QZZM)*MUCH
348 ZEP=ZM*(ZM-ZR)*(UM-QZZM)*MUCH
349 UALLY=UAL*ABS.UAL
350 UEPY=UEP*ABS.UEP
351 CFFQ=FFC.(ZM,UM,J)
352 VZZM=SQAGT.(ZM)
353 UP(K+1)=0.5*(UAL+UEP)+0.5*(ZAL-ZEP)/VZZM-0.5*CFFQ*UALLY
354 +UEPY)*DELTC
355 ZP(K+1)=0.5*(ZAL+ZEP)+0.5*(UAL-UEP)*VZZM-0.5*CFFQ*VZZM*
356 (UALLY-UEPY)*DELTC
357 END OF CONDITIONAL
358 THROUGH IDAHO, FOR K=0,1,K.G.MK
359 U(K)=UP(K)
360 Z(K)=ZP(K)
361 QOUT=DELTC*(VEEE*ZOV/FACTOR)*PAREA
362 VOID=VOID+QOUT
363 WHENEVER QOUT.L.O.,TRANSFER TO STATEC
364 WHENEVER YY.G.O.,TRANSFER TO OREGON
365 OUTFLO=VOID-SIMPQ.(J,DELXC,MK)
366 TRANSFER TO OHIO
367 OUTFLO=VOID-(SIMPQ.(J,DELXC,MK-1))
368 MK=MK-1
369
370 VAPOR CAVITY GROWTH IS DETERMINED BY THE FOLLOWING
371 STATEMENTS.
372
373 OHIO
374 WHENEVER OUTFLO.L.O.,TRANSFER TO UTAH
375 WHENEVER STATEC.E.NEBRSK
376 STATEC=KANSAS
377 JHK=0
378 YY=0.

```

```

*318
*319
*320
*321
*322
*323
*324
*325
*326
*327
*328
*329
*330
*331
*332
*333
*334
*335
*336
*337
*338
*339
*340
*341
*342
*343
*344
*345
*346
*347
*348
*349
*350
*351
*352
*353
*354
*355
*356
*357
*358
*359
*360
*361
*362
*363
*364
*365

```

```

*366
*367
*368
*369
*370

```

*371
 *372
 *373
 *374
 *375
 *376
 *377
 *378
 *379
 *380
 *381
 *382
 *383
 *384
 *385
 *386

```

END OF CONDITIONAL
X=BISECT.(,001*DELXC,6.1*DELXC,HJDFQR.,IOTA,VIRGNA)
WHENEVER X.LE.DELXC
  7(JK)=PARK.(X,J)+K(1)
  KK=0
  PMK=MK
  TRANSFER TO IOWA
END OF CONDITIONAL
KK=X/DELXC
THROUGH ILLNOI, FOR K=MK+1,1,K.G.M*KK
  Z(K)=PARK.(X-(DELXC*(K-MK)),J)+R(1)
  WHENEVER Z(K).L.Z(K-1).AND.K.NE.(KK+KK),Z(K)=Z(K-1)
  U(K)=V(1,0)*ZOV+USURG.(Z(K),J)-SSUZZ
  WHENEVER U(K).L.0.,U(K)=0.
  PMK=MK+KK
  TRANSFER TO IOWA
    
```

ILLNOI

```

VAPOR CAVITY SHRINKAGE IS DETERMINED BY THE SUBSEQUENT
STATEMENTS.
    
```

*387
 *388
 *389
 *390
 *391
 *392
 *393
 *394
 *395
 *396
 *397

```

WHENEVER VOID.L.0.,TRANSFER TO ILLNSE
OUTFLO=VOID-(SIMPQ.(J,DELXC,MK)-SIMPV.(DELXC,MK,YY,J,0.))
INFLOW=-OUTFLO
STATEC=NEBRSK
WHENEVER MK.L.(1+JHK),TRANSFER TO IOWA
NX=BISECT.(0.,5.1*DELXC,SURGEQ.,IOTA,WISCON)
JHK=(NX+YY)/DELXC
YY=(NX+YY)-(JHK*DELXC)
KK=-JHK
PMK=MK+KK
TRANSFER TO IOWA
    
```

NEBRSK
 UTAH

```

* * * * *
PART II - SEC.C. THIS SECTION OF THE PROGRAM RECORDS THE
COLLAPSE OF THE VAPOR CAVITY AND CARRIES OUT THE
REINITIALIZATION AND SWITCHING NECESSARY FOR CONTINUED
COMPUTATION OF THE FULL-FLOWING, TRANSIENT PRESSURES AND
VELOCITIES THROUGHOUT THE ENTIRE SYSTEM.
* * * * *
    
```

*398
 *399
 *400
 *401
 *402
 *403
 *404
 *405
 *406
 *407
 *408
 *409
 *410
 *411
 *412
 *413
 *414
 *415

```

CONTINUE
MOFCOL=M
TOFCOL=DELTA*MOFCOL
PRINT FORMAT PICCLO,TOFCOL,MOFCOL,TOFCOL-TOFSEP,TOFCOL-TOFOFF
MOFSEP=MAXLIM+2
JJ=MAXLIM+2
VP(1,0)=0.
VOID=0.
VEEE=0.
MARK=M
TRANSFER TO STATEB
PRINT COMMENT $OCOMPUTATION HAS BEEN HALTED BY CUTOFF. $
TRANSFER TO WYOMNG
PRINT COMMENT $O SUBROUTINE 'BISECT' IS UNABLE TO FIND ROOT.$
TRANSFER TO WYOMNG
PRINT COMMENT $O SUBROUTINE 'BISECT' COULD NOT FIND ROOT NX.$
TRANSFER TO WYOMNG
PRINT COMMENT $OCOMPUTATION HAS BEEN HALTED BY EXCEEDING MAXL
    
```

TENNSE
 WYIRG
 VIRGNA
 WISCON
 CONNEC

```

0 IM.
TRANSFER TO WYOMNG
PRINT COMMENT $OTHE MAGNITUDE OF KK EXCEEDS NINE TIMES DELXC
WHICH IS CONSIDERED TO BE EXCESSIVE. COMPUTATION IS BEING H
1 ALTERED FOR THIS REASON.
TRANSFER TO WYOMNG
PRINT COMMENT $OTHE VAPOR CAVITY IS OF INSUFFICIENT MAGNITUDE
TO WARRANT FURTHER INVLSIGATION. COMPUTATION IS BEING HAL
1 TED FOR THIS REASON.
CONTINUE
VECTOR VALUES CARD =$F4.2,S5,E10.4,S5,F4.2,S6,I5,S6,F6.3,
S6,F8.7,S1,F6.4
VECTOR VALUES PLAN =$F7.3,S2.6(F7.3,S3)
VECTOR VALUES PIPE1 =$E10.4,S4,F4.3,S1.3(F6.5,S4),F7.3,S3,I3
**
VECTOR VALUES PIPE2 =$E10.4,S4,F4.3,S1.3(F6.5,S4),F7.3,S3,I3
**
VECTOR VALUES QUANT = $I3,S7,F6.3,S4,F4.3,S4,I2,S4,F6.5,S4,F4
.2
VECTOR VALUES CONTRL = $2(I4,S6),(I1,S9),(I2,S8),2(I4,S6),
0 (I1,S9)
VECTOR VALUES GIVEN =$IH,S2.6HRHO = F5.3,S7.5HKA = E10.4,S6,
7HVMAX = F4.2,S6.7HHBAR = F6.3,S3.8,4HQ = F6.4
VECTOR VALUES SCHEME =$IH,S2.6HHEL = F7.3,S5.6HMEL = F7.3,
0 S8.6HHEL = F7.3,S4.7HMSEL = F7.3,S4.7HLOCI = F7.3,S4.7HLOCZ =
1 F7.3,S5.7HLOC3 = F7.3
VECTOR VALUES TUBE1 =$IH,S2.7HE(I1) = E10.4,S4.1OHZETA(I1) = F
0 4.3,S4.7HD(I1) = F6.5,S4.7HB(I1) = F6.5,S5.7HR(I1) = F6.5,S5.8HL
1 L(I1) = F7.3,S4.8HMN(I1) = I3
VECTOR VALUES TUBE2 =$IH,S2.7HE(I2) = E10.4,S4.1OHZETA(I2) = F
0 4.3,S4.7HD(I2) = F6.5,S4.7HB(I2) = F6.5,S5.7HR(I2) = F6.5,S5.8HL
1 L(I2) = F7.3,S4.8HMN(I2) = I3
VECTOR VALUES FRICT1=$I2(F5.4,S1)
VECTOR VALUES FRICT2=$I2(F5.4,S1)
VECTOR VALUES CSUR0=$F2.1,I0(S1,F6.5)
VECTOR VALUES RESFAC=$IH,S2.3,1SHREYNOLDS NO. = F6.0,S15.4HFI
0 1,I2.4H) = F5.4,S15.4HF(2,I2.4H) = F5.4**$
VECTOR VALUES MEMO =$ S11.4HH(I1,I3,4H) = F7.3,S15.4HV(I1,I3,4H
0 ) = F6.3,S15.6HELP(I1,I3,4H) = F7.3,S13.8HTHETA(I1,I3,4H) = F6.
1 3
VECTOR VALUES RANDUM =$ S11.4HH(2,I3,4H) = F7.3,S15.4HV(2,I3,
0 4H) = F6.3,S15.6HELP(2,I3,4H) = F7.3,S13.8HTHETA(2,I3,4H) = F
1 6.3
VECTOR VALUES TUBA = $IH0,S1.12HAT TIME T = F8.5,16H SECONDS,
0 AFTER 14,89H COMPLETE CYCLES OF OPERATION, THE VELOCITIES AN
1 D PRESSURES AT KEY POINTS THROUGHOUT THE /1H ,S1,35HFLOW SYST
2 EM ARE AS TABULATED BELOW.
VECTOR VALUES FLUTE = $IH0,S4.4HLOC,S7.5H(I1,0),S8.5H(I1,1),S8
0 ,5H(I1,2),S8.5H(2,0),S8.6H(2,20),S7.6H(2,40),S7.6H(2,60),S7.6H
1 (2,80),S7.7H(2,100) /1H ,S5,IHV,S6.9(S2,F8.4,S3) /1H ,S5,IH
2 H,S6.9(S2,F8.4,S3)
VECTOR VALUES ORGAN = $IH0,S4.4HLOC,S6.5H(1,0),S10.5H(1,1),S
0 10.5H(2,0),S10.6H(2,10),S9.6H(2,20),S9.6H(2,30),S9.6H(2,40),S
1 9.6H(2,50) /1H ,S5,IHV,S7.7(S2,F8.4,S5),S2,F8.4,S2 /1H ,S5,IH
2 H,S5.7(S2,F8.4,S5),S2,F8.4,S3
VECTOR VALUES OBOE = $IH-S1.83HTHE GATE VALVE AT LOCATION J
0 = 1,I = 0 HAS BEEN INSTANTANEOUSLY CLOSED AT TIME T = F8.5,
1 34H, SECONDS, OR AT OPERATION NUMBER 12,IH.
VECTOR VALUES ORDERS=$IH ,S2,3HMAXIMUM ALLOWABLE ITERATIONS
0 = 14,S3,29HCOMPUTATION CUTOFF LIMIT = 14,S3,26HINITIAL CAV

```

```

*415
*416
*417
*417
*417
*418
*419
*419
*419
*420
*421
*421
*422
*423
*423
*424
*424
*425
*425
*426
*426
*427
*427
*428
*428
*428
*428
*429
*429
*429
*430
*430
*430
*431
*432
*432
*433
*434
*434
*435
*435
*435
*436
*436
*437
*437
*437
*437
*438
*438
*438
*439
*439
*439
*439
*440
*440
*440
*441
*441

```



```

1 ITY PRINTOUT = I1,S3,22HVALVE SHUTOFF POINT = I2 /I1 ,S2,S3IHI
2 INITIAL PRINTOUT LIMIT POINT = I4,S3,29HPRINTOUT FREQUENCY CON
3 TRUL = I4,S3,26HCAVITY PRINTOUT CYCLE = I1 *$
VECTOR VALU5 DRUM=I1H-,S1,S1HCOLUMN SEPARATION HAS OCCURRED
0 AT THE GATE VALVE AT TIME T = F8.5,30H SECONDS (OPERATION CYC
1 LE NO. I4,I3H). THIS IS F8.5/I1H ,S1,40HSECONDS AFTER CLOSUR
2 E OF THE GATE VALVE. *$
VECTOR VALUES AMOUNT = I1H ,S2,9HHVAPOR = F7.4,S15,8HDELXC =
0 F7.4,S15,8HDELTC = F8.5,S10,8HMARK = I4,S12,7HHRUCH = F6.4/
1 I1 ,S2,10HFACTOR = I2,S22,5HXI = F7.4,S17,6HINC = I3,S
2 I5,7HIOTA = F5.4,S11,8HPAREA = F7.5 *$
VECTOR VALU5 PICCLG = I1H-,S1,S1,54HTHE VAPOR CAVITY HAS COMPLE
0 TELY COLLAPSED AT TIME T = F8.5,30H SECONDS (OPERATION CYCLE
1 M = I4,I3H). THIS IS F8.5,9H SECONDS /I1 ,S1,38HAFTER COLUM
2 N SEPARATION OCCURRED, AND F8.5,32H SECONDS AFTER VALVE WAS C
3 LOSED. *$
VECTOR VALUES CELLU = I1H0,S1,I2HAT TIME T = F8.5,16H SECONDS
0 , AFTER I4,87H COMPLETE CYCLES OF OPERATION, THE VELOCITIES A
1 ND DEPTHS IN THE VAPOR CAVITY AS WELL AS /I1 ,S1,89HVLLOCITIE
2 S AND PRESSURES AT KEY POINTS THROUGHOUT THE FLOW SYSTEM ARE
3 AS TABULATED BELOW. *$
VECTOR VALUES HARP = I1H0,S4,5HDIST.,S1,F6.4,*FVA*(S2,F6.4)/I
0 H ,S4,4HLDC.,*FVB*(S5,I2,S1)/I1 ,S5,I1H0,S2,*FVB*(S2,F6.3)/I1
1 ,S5,I1H,S2,*FVB*(S3,F5.3) *$
VECTOR VALU5 BASSOM = I1H-,S1,87HTHE DIRECTION OF FLOW AT TH
0 E RESERVOIR END OF THE PIPE SYSTEM HAS REVERSED AT TIME T = F
1 8.5,9H SECONDS. *$
TRANSFER TO UNITED
END OF PROGRAM

```

```

*441
*441
*442
*442
*442
*442
*443
*443
*443
*444
*444
*444
*444
*444
*445
*445
*445
*446
*446
*447
*447
*447
*448
*448
*449

```

MAD PROGRAM, TYPE 25 MAR 1964 (ALL NUMBERS ARE OCTAL)

NO. OF LOCATIONS 17735 TRA VECTOR SIZE 00026 TRA VECTOR STARTS 00352 ENTRY PT. 05657 ERASABLE STARTS 77777

VARIABLE STORAGE (A=ARRAY, C=COMMON, E=ERASABLE, P=DIGIT=MODE)

ADIM	00454	A	1	FVR	10332	CI	G3145	A	C	PIPE2	03451	A	1	UEPPY	04235	0
ALASKA	00406	4	GAP	10011	CI	LLOC1	03146	0	LLOC1	03455	A	1	UL	04236	0	
ALPHA	00765	A	0	GEORGI	00414	4	LUC2	03147	0	PMK	03456	1	UM	04237	0	
AMOUNT	01026	A	1	GIVEN	02204	A	LUC3	03150	0	PRTCYC	03457	1	UNITED	00443	4	
AOG	01031	A	0	GOA	02207	A	LPRK	10330	CI	PRTRCO	03460	1	UP	04405	A	
ARIZON	00406	4	HARS	02210	0	MAINE	00421	4	MARK	03461	1	UK	04406	0		
ARKANS	00407	4	HAL	02211	0	MARK	03151	1	MARK	03462	1	U	04553	A		
A	01034	A	0	HARP	02237	A	MARKS	03152	0	Q	03463	0	UTAH	04444	4	
B	01063	A	0	HARAR	00415	4	MAXLIM	03153	1	QUANT	03474	A	VALLY	04554	0	
CALIF	00406	4	HEL	02241	0	MEMO	03176	A	MINT	03475	0	VAL	04555	0		
CARD	01075	A	1	HEP	02242	0	MICHGN	00422	4	QZZL	03476	0	VEEE	04556	0	
CELLO	01146	A	1	HHOLD	02243	0	MINT	03177	0	RANDOM	03470	0	VEPPY	04557	0	
CFEQ	01147	0	HLQS	02246	A	MISSIP	00423	4	RELFAC	03536	A	VEP	04560	0		
CHI	01150	0	HM	02250	0	MN	03200	1	REYNU	03537	0	VIRGNA	00445	4		
COLORA	00410	4	HOLDD	02251	0	MFCOL	03203	A	RHODEI	00434	4	VL	04561	0		
CONNEC	00411	4	HP	02574	A	MUFSLP	03205	1	RHU	00434	0	VMAX	04562	0		
CONTRL	01160	A	1	HR	02575	0	MONTAN	00424	4	R	10002	ACC	VM	04563	0	
COUNT	01161	1	H	03120	A	M	03206	1	SCARU	00406	4	VUID	04564	0		
CP	01164	A	0	HVAPOR	03121	0	MUCH	03207	0	SCHEME	03565	A	VP	05107	A	
CSURG	01170	A	1	IDAHO	00406	4	MU	03212	A	SDAKOT	00406	4	VR	05110	0	
CUTOFF	01171	1	ILENDI	00406	4	NCARO	00406	4	SPRK	10326	CI	V	05433	A		
DELAWA	00412	4	INC	03122	1	NDAKOT	00406	4	SSUZZ	03567	0	VZZM	05434	0		
DELTC	01172	0	INCVPT	03123	1	NEBRSK	00425	4	STAEF	00435	4	WASH	00446	4		
DELT	01173	0	INDIAN	00406	4	NHAMP	00426	4	STAEF	00436	4	WISCON	00447	4		
DELT	01176	A	0	INFLOW	03124	0	NJERSY	00427	4	STAEF	00437	4	WSEL	05435	0	
DELXC	01177	0	IOWA	00416	4	NMEXCO	00430	4	STATED	10333	C4	WVING	00450	4		
DELX	01202	A	0	IOWA	00416	4	N	03213	1	STAEFL	00440	4	WYDMNG	00451	4	
DJM	01205	A	1	IPRK	10327	CI	NU	10010	CO	STATLS	00406	4	XI	10003	CO	
DRUM	01245	A	1	I	03126	1	NX	03214	0	SUZ	10351	ACC	X	05436	0	
D	10006	ACC	0	I	03131	A	NYORK	10334	C4	TENNSE	00441	4	YY	05437	0	
ELP	01570	A	0	JHK	03132	1	OBDE	03245	A	TEXAS	00442	4	ZAL	05440	0	
EL	02113	A	0	JJQ	03133	1	OHIO	00431	4	THETA	04112	A	ZEP	05441	0	
E	02116	A	0	JJ	03134	1	OKLAHO	00432	4	TOFCOL	04113	0	ZETA	05444	A	
FACTOR	02117	1	J	03135	1	ORDERS	03322	A	1	TOFOFF	04114	0	ZL	05445	0	
FCC	02120	0	KANSAS	00417	4	OREGON	00433	4	1	TOFSEP	04115	0	ZM	05446	0	
FLORID	00413	4	KA	03136	0	ORGAN	03363	A	1	T	04116	0	ZUV	05447	0	
FLUTE	02157	A	1	KENTUC	00420	4	OUTFLO	03364	0	TUBA	04156	A	ZP	10325	ACC	
FRIC1	02162	A	1	KK	03137	1	PAREA	10007	CO	TUBE1	04204	A	ZR	05450	0	
FRIC2	02165	A	1	K	03140	1	PENNSY	10335	C4	TUBE2	04232	A	Z	05615	A	
F	10160	ACC	0	LAMBDA	03141	0	PICCO	03433	A	1	UALY	04233	0	ZM	05616	0
FVA	10331	CI	1	LEL	03142	0	PIPEI	03442	A	1						

FUNCTION DICTIONARY

03310	00352	0	01301	00354	0	03311	00355	0	ARCSIN	00356	0
BISECT	00357	0	PCDMT	00361	0	PRINT	00362	0	PRSLT	00363	0
READ	00364	0	PARVOL	00366	0	PFFA	00367	0	PRTLAM	00370	0
PRTRUL	00371	0	SIMPW	00373	0	SIN	00374	0	SQRT	00375	0
SYSTEM	00376	0	BURVOL	00401	0	BURVOL	00401	0	SQAGDT	00402	0
SQAOGT	00403	0	TOPNTH	00405	0						

ABSOLUTE CONSTANTS

05617	+203506314631	05620	+203606314631	05621	+202614631463	05622	+000000000003	05623	+202600000000
05624	+000000000006	05625	+000000000011	05626	+167406111564	05627	+172753412172	05630	+204500000000

APPENDIX II

SUBROUTINE PROGRAMS USED WITH MAIN COMPUTER PROGRAM

A syntactical listing for each of the 11 MAD language external subroutines used in the computer program called MAIN (See Appendix I) is presented below. The subroutines are listed according to name and function:

<u>Name</u>	<u>Function</u>
1. PARK	Given a distance measured from the leading edge of the separation void, the subroutine returns the depth of flow based on the parabolic free surface (See Figure 12) described in Chapter IV.
2. PARLN	Given a depth on the free surface flow, the subroutine returns the distance to the leading edge of the separation void based on the parabolic surface (See Figure 12) described in Chapter IV.
3. PFFA	This subroutine determines the cross-sector area of a pipe flowing partially full. The computation is based on flow depth.
4. BISCT	This subroutine is used to determine the exact length of a separation void that extends at least n , but not $(n+1)$ increments of length. The exact distance of the leading edge of the void from the n -th increment is computed using equilibrium between void volume and total outflow.
5. FFC	Given the depth of flow, the velocity of flow, and the pipe segment identification, this subroutine returns the friction coefficient based upon Reynold's number. If the depth of

<u>Name</u>	<u>Function</u>
	of flow is equal to the diameter of the pipe, the coefficient is that for pipe flow; if less than the diameter of the pipe, then the coefficient is for free surface flow.
6. SIMPQ	Given the number of length increments, ΔXC , from the valve to the grid point nearest the separation void, the function returns the total volume of the void.
7. PARVOL	Given the depth of flow at a point less than an increment of length from the leading edge of the void, this subroutine returns the volume of the subincremental void determined by the parabolic surface.
8. PINTR	Given the number of increments, ΔXC , from the valve to the separation void, the subincremental distance to the leading edge of the void, and the size of the increments, the subroutine computes and returns the parabolically interpolated depth of flow from known depths.
9. SMPVL	Given the negative distance, NX , along with other controlling parameters, this function gives the incremental volume removed from the void during collapse.
10. PRINT	This function, with PRTLAW and PRTRUL providing double entry points, controls the print format to accommodate the data produced.
11. USURG	This function is used to approximate the velocity at the first grid point behind the separation void. The velocity is prorated according to depth-of-flow using the velocity ahead of the void and the free-surface propagation velocity.

07:21: 04/24/64 9 12 17.6 AM

PARK, JI

\$ COMPILE MAC,PRINT OBJECT,EXECUTE,DUMP,PUNCH OBJECT

MAD (12 MAR 1964 VERSION) PROGRAM LISTING

```

EXTERNAL FUNCTION (C,L)
INTEGER J,L
PROGRAM COMMON R(2),XI,U(2),PAKEA,ML,GAP,F(1C2,1IM),ZP(1C0),
0 SPRK,IPRK,LPRK,FVA,FVB,STATED,NYCRK,PFANSY,SUZ(11)
VECTOR VALUES DIM = 2,1,51
ENTRY TO PARK.
J=L
X=C
ALPHA = (1.-2.**XI)
K=ALPHA*R(J)-SQRT.(4.**XI*R(J)*X)
FUNCTION RETURN K
END OF FUNCTION

```

```

*CC1
*CC2
*CC3
*CC4
*CC5
*CC6
*CC7
*CC8
*CC9
*CC10
*CC11

```

370218 10/04/64 9 12 22.1 AM

PARLEVAL

\$ CCPILE MAD,PRINT OBJECT,EXECUTE,DUMP,PURCH OBJECT

MAD (12 MAR 1964 VERSION) PROGRAM LISTING

```

EXTERNAL FUNCTION (R,L)
INTEGER L,J
PROGRAM COMMON R(2),X1,D(2),PAREA,NC,GAP,F(102,DTM),ZP(100),
0 SPRK,IPRK,LPRK,FVA,FVH,STATED,NYCRK,PENASY,SUZ(11)
VECTOR VALUES DIM = 2,1,51
ENTRY TO PARLEN.
J=L
K=B
ALPHA = (1.-2.*X1)
X=(K-ALPHA*R(J)).P-2./(4.*X1*R(J))
FUNCTION RETURN X
END OF FUNCTION

```

```

*001
*002
*003
*004
*005
*006
*007
*008
*009
*010
*011

```

070218 04/04/64 12 26.5 AM

PFPA. 01

\$ COMPILE MAD,PRINT OBJECT,EXECUTE,DUMP,PUNCH OBJECT

MAD (12 MAR 1964 VERSICN) PROGRAM LISTING

```

EXTERNAL FUNCTION (P,L)
INTEGER J,L
PROGRAM COMMON R(2),XI,D(2),PAREA,NU,GAP,F(102,0:IM),ZP(100),
0 SPRK,IPRK,LPRK,FVA,FVB,STATED,NYGRK,PENNSY,SUZ(11)
VECTOR VALUES DIM = 2,1,51
ENTRY TO PFPA.
J=L
B=P
ALPHA=2.*R(J)*R(J)*ARCSIN.(SQRT.(B/(2.*R(J))))+(B-R(J))*SQR
0 T.(2.*R(J)*B-B*B)
FUNCTION RETURN ALPHA
END OF FUNCTION

```

```

*001
*002
*003
*004
*005
*006
*007
*008
*009
*010

```

07021F 04/04/64 9 12 31.1 AM

FISCT.01

\$ COMPILER MAC,PRINT OBJECT, PUNCH OBJECT, EXECUTE, DUMP

MAD (12 MAR 1964 VERSION) PROGRAM LISTING

```

EXTERNAL FUNCTION (L,R,F,LIN,K)
STATEMENT LABEL K
ENTRY TO BIsect.
XL=L
XR=R
IOTA = LIN
FL = F.(XL)
THROUGH DRUM, FOR H=XR-XL,-H/2.,H.L.(XR-XL)/32.
THROUGH DRUM, FOR X=XL,H,(X+H),G.XR
WHENEVER FL#F.(X+H).L.C, TRANSFER TO GONG
TRANSFER TO K
THROUGH TUBA, FOR H=H/2.,-H/2.,FL#F.(X+H).G.O.
WHENEVER H.L.IOTA, FUNCTION RETURN X
X=X+H
TRANSFER TO GONG
END OF FUNCTION

```

DRUM
GONG
TUBA

*001
*002
*003
*004
*005
*006
*007
*008
*009
*010
*011
*012
*013
*014
*015
*016

07)213 04/04/64 12 30.1 AM

IFC. 001

\$ COMPILER MAC, PRINT OBJECT, EXECUTE, DUMP,PUNCH OBJECT

MAD (12 MAR 1964 VERSION) PROGRAM LISTING *** **

```

EXTERNAL FUNCTION (P,V,S)
PROGRAM COMMON R(2),XI,B(2),PAREA,NU,GAP,F(102,DIM),ZP(100),
0 SPRK,IPRK,LPRK,FVA,FVB,STATED,IVGRK,PENNSV,SUZ(11)
VECTOR VALUES DIM = 2,1,51
INTEGER P,I,K,S,GAP
ENTRY TO EFC.
HZ=P
K=S
H=GAP
*WHENEVER HZ.GE.D(K)
TRANSFER TO MADRID
OR *WHENEVER FZ.GE.K(K)
METP=2.*R(K)*(3.14159-ARCCOS.((HZ-R(K))/R(K)))
OR *WHENEVER FZ.L.R(K)
METP=2.*R(K)*ARCCOS.((R(K)-HZ)/R(K))
END OF CONDITIONAL
A=PEPA.(HZ,K)
HYDRAC=A/METP
REY=HYDRAC*4.*ABS.V/NU
TRANSFER TO LAPAZ
REY=D(K)*.ABS.V/NU
*WHENEVER REY.L.64.
W = 1.
OR *WHENEVER REY.L.100.
W = 64./REY
OR *WHENEVER REY.L.35100.
I = X/H
ETA = (X-H*I)/H
*WHENEVER I.E.0
I = 1
ETA = ETA - 1.
END OF CONDITIONAL
W=F(K,I)*(ETA/2.)*(F(K,I+1)-F(K,I-1))+(ETA/2.)*ETA*(F(K,I+
0 I)+F(K,I-1)-2.*F(K,I))
OR *WHENEVER REY.GE.35100...AND.K.G.1
W = .C247
OTHERWISE
W = .C324
END OF CONDITIONAL
*WHENEVER HZ.GE.D(K)
FUNCTION RETURN W
OTHERWISE
*W=W/18.*HYDRAD)
FUNCTION RETURN W
END OF CONDITIONAL
END OF FUNCTION

```

```

*001
*002
*003
*004
*005
*006
*007
*008
*009
*010
*011
*012
*013
*014
*015
*016
*017
*018
*019
*020
*021
*022
*023
*024
*025
*026
*027
*028
*029
*030
*031
*032
*033
*034
*035
*036
*037
*038
*039
*040
*041
*042
*043
*044
*045

```

070218 04/04/64 9 12 43.3 AM

SIMPQ.C1

\$ COMPILE MAD , PRINT OBJECT, EXECUTE, DUMP, PUNCH OBJECT

MAD (12 MAR 1964 VERSION) PROGRAM LISTING

```

EXTERNAL FUNCTION (L,M,NN)
INTEGER N,IK,LK,K,MN,GAP,J,L
STATEMENT LABEL SATURN,APOLLO,AGENA
PROGRAM COMMON R(2),XI,D(2),PAREA,INC,GAP,F(102,0:IM),ZP(100),
0 SPRK,IPRK,IPRK,EVA,FVB,STATED,NYCRK,PENNSY,SUZ(11)
VECTOR VALUES DIM = 2,1,51
ENTRY TO SIMPG.
J=L
N=NN
M=M
M=M
AEVEN=0.
ADDD=0.
OAA=PAREA-PFPA.(ZP(I),J)
NAA=PAREA-PFPA.(ZP(N),J)
MFENEVER N/2.E.(N-1)/2
SATURN=APOLLO
K=1
MM=MM*0.5
OTHERWISE
SATURN=AGENA
K=2
END OF CONDITIONAL
THROUGH THOR, FOR LK=K,K,LK,G.N-1
AAA=PAREA-PFPA.(ZP(LK),J)
AEVEN=AEVEN+AAA
THROUGH ZEUS, FOR IK=1,K,IK,G.N
ZA=(ZP(IK-1)+ZP(IK))*0.5
TRANSFER TO PLUTO
TRANSFER TO PLUTO
ZA=ZP(IK)
BBB=PAREA-PFPA.(ZA,J)
ADDD=ADDD+BBB
V=(MM/3.)*(OAA+NAA+4.*ADDD+2.*AEVEN)
FUNCTION RETURN V
END OF FUNCTION

```

THOR

APOLLO

AGENA

PLUTO

ZEUS

```

*001
*002
*003
*004
*005
*006
*007
*008
*009
*010
*011
*012
*013
*014
*015
*016
*017
*018
*019
*020
*021
*022
*023
*024
*025
*026
*027
*028
*029
*030
*031
*032
*033
*034

```

9 12 4.5 AM

070213 04/04/64

PRVOL.01

\$ COMPILE MAC, PRINT OBJECT, EXECUTE, DUMP, PUNCH OBJECT

MAD (12 MAR 1964 VERSION) PROGRAM LISTING

```

EXTERNAL FUNCTION (A,L)
PROGRAM COMMON R(2),XI,D(2),PAREA,NU,GAP,F(102,DIP),ZP(100),
0 SPRK,IPRK,LPRK,FVA,FVB,STATED,NYGRK,PENNSY,SUZ(11)
VECTOR VALUES DIM = 2,1,51
DIMENSION KK(10),XX(10),AA(10)
INTEGER J,L,I,GAP
ENTRY TO PARVOL.
K=A
J=L
X=PARLEN.(K,J)
DELX=X/10.
ADD=0.
AEVEN=0.
THROUGH YUKON, FOR I=0,1,I,G.10
  XX(I)=DELX*I
  KK(I)=PARK.(XX(I),J)
  AA(I)=PAREA-PFPA.(KK(I)+R(I),J)
  WHENEVER I/2.E.(I-1)/2.AND.I.NE.0
    ADD=ADD+AA(I)
  OR WHENEVER I.NE.0.AND.I.NE.10
    AEVEN=AEVEN+AA(I)
  END OF CONDITIONAL
V=(DELX/3.)*(AA(0)+4.*ADD+2.*AEVEN+AA(10))
FUNCTION RETURN V
END OF FUNCTION

```

YUKON

```

*001
*002
*003
*004
*005
*006
*007
*008
*009
*010
*011
*012
*013
*014
*015
*016
*017
*018
*019
*020
*021
*022
*023
*024

```

07021F 04/04/64 9 12 55.0 AM

PINTR.01

\$ COMPILER MAC,PRINT OBJECT,EXECUTE,DUMP,PUNCH OBJECT

MAD (12 MAR 1964 VERSION) PROGRAM LISTING

```

EXTERNAL FUNCTION (H,I,L)
INTEGER MK,I
PROGRAM COMMON R(2),XI,D(2),PAKEA,NU,GAP,F(102,DIM),ZP(100),
0 SPRK,IPRK,LPRK,FVA,FVB,STATED,NYCRK,PENNSY,SUZ(11)
VECTOR VALUES DIM = 2,I,51
ENTRY TO PINTRP.
X=L
MK=I
DELXC=H
TH=(X/DELXC)
WHENEVER MK.E.0
  MK=I
  TH=TH-I.
END OF CONDITIONAL
Z=ZP(MK)+(TH/2.)**(ZP(MK+1)-ZP(MK-1))+TH*TH*.5*(ZP(MK+1)+ZP(M
0 K-1)-2.*ZP(MK))
FUNCTION RETURN Z
END OF FUNCTION
*001
*002
*003
*004
*005
*006
*007
*008
*009
*010
*011
*012
*013
*014
*015
*016

```

070218 04/C4/64 9 12 59.9 AM

SMPVL.01

\$ CCMPLE MAD,PRINT OBJECT,EXECUTE,DUMP,PUNCH OBJECT

MAD (12 MAR 1964 VERSION) PROGRAM LISTING

```

EXTERNAL FUNCTION (H,I,M,K,YE)
INTEGER J,K,MK,I,IMK,HK
STATEMENT LABEL SUN,EARTH,URANUS
PROGRAM COMMON R(2),XI,D(2),PAREA,NU,GAP,F(102,DIH),ZP(100),
0 SPRK,IPRK,LPRK,FVA,FVB,STATED,NYORK,PEANNSY,SUZ(11)
VECTOR VALUES DIM = 2,1,51
ENTRY TO SIMPW.
DELXC=H
MK=I
NX=M
J=K
YY=YE
WHENEVER NX.LE.0.,FUNCTION RETURN 0.
IMK=(INX+YY)/DELXC)+1.
XX=IMK*DELXC-(NX+YY)
ZZZ=PINTRP.(DELXC,MK-IMK,XX)
ZZ=PINTRP.(DELXC,MK-1,DELXC-YY)
ACCD=0.
AEVEN=0.
XYX=XX
THROUGH JUPTER,FOR HK=1,1,HK.G.9
XYX=XYX+(NX/10.)
WHENEVER XYX.G.DELXC
IMK=IMK-1
XYX=XYX-DELXC
END OF CONDITIONAL
Z=PINTRP.(DELXC,MK-IMK,XYX)
WHENEVER (HK+1)/2.E.HK/2
SUN=EARTH
OTHERWISE
SUN=URANUS
END OF CONDITIONAL
TRANSFER TO SUN
AAAA=PAREA-PFPA.(Z,J)
AEVEN=AEVEN+AAAA
TRANSFER TO JUPTER
BBBB=PAREA-PFPA.(Z,J)
ACCD=ACCD+BBBB
CONTINUE
QAA=PAREA-PFPA.(ZZZ,J)
NAA=PAREA-PFPA.(ZZ,J)
V=(NX/30.)*(QAA+6.*ACCD+2.*AEVEN+NAA)
FUNCTION RETURN V
END OF FUNCTION

```

```

*001
*002
*003
*004
*004
*005
*006
*007
*008
*009
*010
*011
*012
*013
*014
*015
*016
*017
*018
*019
*020
*021
*022
*023
*024
*025
*026
*027
*028
*029
*030
*031
*032
*033
*034
*035
*036
*037
*038
*039
*040
*041
*042
*043

```

EARTH

URANUS

JUPTER

070218 04/04/64 9 13 6.6 AM

PRINT.C1

\$ COMPILER MAC,PRINT OBJECT,EXECUTE,DUMP,PUNCH OBJECT

MAD (12 MAR 1964 VERSION) PROGRAM LISTING

```

EXTERNAL FUNCTION (M)
INTEGER M,MK,SPRK,IPRK,LPRK,FVA,FVB
STATEMENT LABEL STATED,PENNSY,NYCRK
PROGRAM COMMON R(2),XI,D(2),PAREA,NU,GAP,F(102,DIM),ZP(100),
0 SPRK,IPRK,LPRK,FVA,FVB,STATED,NYCRK,PENNSY,SUZ(11)
VECTOR VALUES DIM = 2,1,51
FORMAT VARIABLE FVA,FVB
ENTRY TO PRTLAW.
MK=M
WHENEVER MK.LE.14
  SPRK = 0
  IPRK = 1
  LPRK = MK
  FVA = MK
  FVB = MK+1
  STATED = NYCRK
  OR WHENEVER MK.G.14.AND.MK.LE.29
    SPRK = 0
    IPRK = 1
    LPRK = 14
    FVA = 14
    FVB = 15
    STATED = PENNSY
    OR WHENEVER MK.G.29.AND.MK.LE.44
      SPRK = 0
      IPRK = 2
      LPRK = 28
      FVA = 14
      FVB = 15
      STATED = PENNSY
      OR WHENEVER MK.G.44.AND.MK.LE.59
        SPRK = 0
        IPRK = 3
        LPRK = 42
        FVA = 14
        FVB = 15
        STATED = PENNSY
        OR WHENEVER MK.G.59.AND.MK.LE.74
          SPRK = 0
          IPRK = 4
          LPRK = 56
          FVA = 14
          FVB = 15
          STATED = PENNSY
          OR WHENEVER MK.G.74.AND.MK.LE.89
            SPRK = 0
            IPRK = 5
            LPRK = 70
            FVA = 14
            FVB = 15
            STATED = PENNSY
            END OF CONDITIONAL
            TRANSFER TO SCRIBE

```

```

*001
*002
*003
*004
*005
*006
*007
*008
*009
*010
*011
*012
*013
*014
*015
*016
*017
*018
*019
*020
*021
*022
*023
*024
*025
*026
*027
*028
*029
*030
*031
*032
*033
*034
*035
*036
*037
*038
*039
*040
*041
*042
*043
*044
*045
*046
*047
*048
*049
*050
*051
*052

```

```
ENTRY TO PRTRUL.  
MK = M  
WHENEVER MK.G.14.AND.MK.LE.29  
  SPRK = 15  
  LPRK = 1  
  LPRK = MK  
  FVA = MK-15  
  FVB = MK-14  
  STATED = NYORK  
OR WHENEVER MK.G.29.AND.MK.LE.44  
  SPRK = 30  
  LPRK = 1  
  LPRK = MK  
  FVA = MK-30  
  FVB = MK-29  
  STATED = NYORK  
OR WHENEVER MK.G.44.AND.MK.LE.59  
  SPRK = 45  
  LPRK = 1  
  LPRK = MK  
  FVA = MK-45  
  FVB = MK-44  
  STATED = NYORK  
OR WHENEVER MK.G.59.AND.MK.LE.74  
  SPRK = 60  
  LPRK = 1  
  LPRK = MK  
  FVA = MK-60  
  FVB = MK-59  
  STATED = NYORK  
OR WHENEVER MK.G.74.AND.MK.LE.89  
  SPRK = 75  
  LPRK = 1  
  LPRK = MK  
  FVA = MK-75  
  FVB = MK-74  
  STATED = NYORK  
END OF CONDITIONAL  
CONTINUE  
FUNCTION RETURN  
END OF FUNCTION
```

SGRIBE

*053
*054
*055
*056
*057
*058
*059
*060
*061
*062
*063
*064
*065
*066
*067
*068
*069
*070
*071
*072
*073
*074
*075
*076
*077
*078
*079
*080
*081
*082
*083
*084
*085
*086
*087
*088
*089
*090
*091
*092
*093

070218 04/24/64 9 13 15.7 AM

USUKG.01

\$ COMPILE MAD, PRINT OBJECT, EXECUTE, CUMP, PUNCH OBJECT

MAD (12 MAR 1964 VERSION) PROGRAM LISTING

```

EXTERNAL FUNCTION (Q,L)
INTEGER I,J,L
PROGRAM COMMON R(2),XI,D(2),PAREA,NU,GAP,F(102,DI*),ZF(100),
0 SPRK,IPRK,LPRK,FVA,FVB,STATED,NYCRK,PENNSY,SUZ(11)
VECTOR VALUES DIM = 2+1,51
ENTRY TO USURG.
J=L
Z=Q
DEL=D(I)/10.
THROUGH MEXICO, FOR I=0,1,DEL*(I+1).G.Z
TH=7-DEL*I
WHENEVER I.L.0
  I=1
  TH=TH-I.
END OF CONDITIONAL
U=SUZ(I)*(TH/2.)*(SUZ(I+1)-SUZ(I-1))+TH*TH*5.*(SUZ(I+1)+
0 SUZ(I-1))-2.*SUZ(I))
COEFF=2.*SQRT.(64.32*(J))
FUNCTION RETURN U*COEFF
END OF FUNCTION

```

- *001
- *002
- *003
- *004
- *005
- *006
- *007
- *008
- *009
- *010
- *011
- *012
- *013
- *014
- *015
- *016
- *017
- *018

APPENDIX III

EXPERIMENTAL DATA; RUNS NUMBERS 25 and 34

The experimental data obtained in the laboratory from Runs Numbers 25 and 34 (Group II conditions) are presented in tabular form in this appendix. Tables I and II give the pressure-rise data at the gate valve and column-separation void data, respectively, for Run Number 25. Tables III and IV provide the corresponding data for Run Number 34. Time is referenced to the moment of valve closure. Head in feet of water is measured with respect to absolute pressure conditions.

TABLE I
 EXPERIMENTAL RUN NUMBER 25
 PRESSURE-RISE DATA AT GATE VALVE

Time Seconds	Head Feet of Water	Time Seconds	Head Feet of Water
.0012	17.3	.1362	314.5
.0073	135.8	.1382	319.9
.0110	180.7	.1421	308.7
.0134	235.4	.1444	308.4
.0147	248.9	.1478	295.8
.0166	259.8	.1526	291.4
.0187	255.7	.1559	281.2
.0194	269.7	.1588	282.2
.0212	278.8	.1650	272.7
.0247	267.3	.1685	275.4
.0276	280.2	.1713	268.6
.0294	280.2	.1738	269.3
.0324	275.4	.1803	260.6
.0359	291.1	.1828	263.2
.0379	295.5	.1869	255.7
.0410	286.3	.1912	258.5
.0447	297.2	.1974	248.9
.0494	283.2	.1991	242.8
.0507	290.4	.2007	237.7
.0532	291.1	.2185	41.8
.0560	283.6	.2201	31.2
.0596	294.8	.2235	13.8
.0615	293.1	.2276	11.3
.0625	285.3	--	--
.0643	280.2	2.0524	11.3
.0667	283.2	2.0568	76.4
.0694	285.6	2.0581	67.2
.0721	282.9	2.0599	83.5
.0746	288.0	2.0631	32.9
.0769	287.3	2.0663	11.3
.0795	299.2	2.0718	16.8
.0828	295.1	2.1155	16.1
.0846	303.3	2.1188	28.2
.0868	306.7	2.1218	87.3
.0938	305.0	2.1233	111.1
.0997	310.4	2.1250	126.7
.1032	313.5	2.1259	120.2
.1079	324.3	2.1280	43.1
.1106	320.3	2.1302	83.9
.1149	327.0	2.1306	146.4
.1200	318.6	2.1324	130.1
.1221	324.7	2.1331	155.2
.1266	313.5	2.1365	119.9
.1307	319.6	2.1387	152.8

TABLE I (Cont'd)

Time Seconds	Head Feet of Water	Time Seconds	Head Feet of Water
2.1400	153.2	2.3031	151.5
2.4112	148.8	2.3080	153.6
2.1443	166.4	2.3103	152.8
2.1478	149.4	2.3118	160.9
2.1509	171.5	2.3147	165.1
2.1530	171.5	2.3178	165.1
2.1558	161.7	2.3213	154.5
2.1593	174.2	2.3374	47.9
2.1625	168.8	2.3427	34.3
2.1660	174.9	2.3488	15.5
2.1703	169.1	2.3565	11.3
2.1744	177.6	--	--
2.1777	165.7	3.3303	11.3
2.1799	169.1	3.3344	81.1
2.1821	165.7	3.3358	68.9
2.1843	167.4	3.3376	77.8
2.1865	164.0	3.3384	65.5
2.1887	174.6	3.3416	50.9
2.1909	168.6	3.3434	84.9
2.1933	174.2	3.3466	90.3
2.1958	187.8	3.3500	80.5
2.1990	182.7	3.3528	76.8
2.2024	195.3	3.3591	111.4
2.2056	188.5	3.3619	110.7
2.2088	198.0	3.3656	126.3
2.2122	188.8	3.3704	115.8
2.2159	199.4	3.3735	123.3
2.2196	198.0	3.3766	120.6
2.2230	206.5	3.3804	125.3
2.2277	201.4	3.3851	119.8
2.2312	204.7	3.3895	123.3
2.2365	202.8	3.3988	118.4
2.2391	208.2	3.4026	126.3
2.2431	202.4	3.4068	126.3
2.2449	207.5	3.4103	130.7
2.2494	206.5	3.4148	133.1
2.2537	209.2	3.4179	138.5
2.2579	208.5	3.4210	136.4
2.2609	199.4	3.4242	141.5
2.2641	201.4	3.4285	140.9
2.2681	194.9	3.4309	143.7
2.2718	196.1	3.4347	143.7
2.2750	189.9	3.4385	150.3
2.2836	191.2	3.4413	148.3
2.2879	185.8	3.4450	149.3
2.2924	174.9	3.4492	140.9

TABLE I (Cont'd)

Time Seconds	Head Feet of Water	Time Seconds	Head Feet of Water
3.4556	140.2	4.4582	109.0
3.4685	140.2	4.4651	109.7
3.4719	142.6	4.4697	112.4
3.4762	136.4	4.4790	112.1
3.4834	130.7	4.4883	104.6
3.4890	130.3	4.5000	86.3
3.4982	130.0	4.5082	108.0
3.5062	132.4	4.5184	100.9
3.5100	131.3	4.5296	85.9
3.5179	123.2	4.5365	81.5
3.5222	125.3	4.5415	83.5
3.5281	124.9	4.5481	75.1
3.5344	123.2	4.5593	49.6
3.5379	116.4	4.5678	41.8
3.5485	70.3	4.5785	35.7
3.5566	47.2	4.5932	29.5
3.5628	35.0	4.6214	21.8
3.5770	30.2	4.6644	14.4
3.6048	11.3	4.6663	11.3
--	--		
4.3460	11.3		
4.3506	62.8		
4.3519	67.6		
4.3535	76.8		
4.3566	79.1		
4.3596	83.2		
4.3623	84.2		
4.3653	66.3		
4.3675	89.3		
4.3732	93.1		
4.3776	92.0		
4.3826	96.1		
4.3863	94.8		
4.3898	99.5		
4.3954	86.1		
4.3987	98.2		
4.4009	95.1		
4.4043	99.2		
4.4076	96.1		
4.4112	101.5		
4.4117	104.9		
4.4216	103.6		
4.4251	107.7		
4.4335	102.9		
4.4419	106.3		
4.4460	110.7		

TABLE II
 EXPERIMENTAL RUN NUMBER 25
 COLUMN-SEPARATION VOID DATA

Time Seconds	Depth of Flow -- Feet			Time Seconds	Depth of Flow -- Feet		
	Gage				Gage		
	No. 1	No. 2	No. 4		No. 1	No. 2	No. 4
0.00	.083	.083	.083	1.10	.052	.066	.083
0.20	.083	.083	.083	.12	.052	.065	.083
0.30	.083	.083	.083	.14	.051	.064	.083
.32	.081	.083	.083	.16	.051	.064	.081
.34	.082	.083	.083	.18	.050	.064	.076
.36	.081	.083	.083	1.20	.050	.064	.069
.38	.080	.083	.083	.22	.049	.062	.062
0.40	.079	.083	.083	.24	.049	.060	.054
.42	.079	.083	.083	.26	.048	.060	.051
.44	.078	.080	.083	.28	.047	.060	.055
.46	.076	.078	.083	1.30	.047	.061	.065
.48	.075	.074	.083	.32	.048	.063	.064
0.50	.073	.071	.083	.34	.048	.065	.060
.52	.071	.068	.083	.36	.049	.068	.057
.54	.069	.067	.083	.38	.050	.067	.058
.56	.067	.070	.083	1.40	.051	.065	.062
.58	.064	.075	.083	.42	.052	.064	.064
0.60	.062	.069	.083	.44	.053	.063	.063
.62	.059	.067	.083	.46	.053	.064	.062
.64	.057	.063	.083	.48	.053	.065	.060
.66	.058	.055	.083	1.50	.052	.065	.056
.68	.060	.052	.083	.52	.051	.067	.054
0.70	.058	.050	.083	.54	.050	.068	.053
.72	.057	.051	.083	.56	.049	.069	.054
.74	.055	.052	.083	.58	.048	.068	.054
.76	.052	.056	.083	1.60	.048	.068	.055
.78	.050	.056	.083	.62	.048	.067	.055
0.80	.050	.053	.083	.64	.048	.064	.056
.82	.050	.056	.083	.66	.048	.062	.058
.84	.049	.056	.083	.68	.048	.062	.059
.86	.049	.059	.083	1.70	.049	.063	.060
.88	.050	.058	.083	.72	.050	.062	.061
0.90	.050	.061	.083	.74	.049	.062	.064
.92	.052	.062	.083	.76	.050	.063	.073
.94	.052	.069	.083	.78	.051	.065	.083
.96	.053	.070	.083	1.80	.051	.064	.083
.98	.053	.071	.083	.82	.050	.064	.083
1.00	.052	.071	.083	.84	.050	.069	.083
.02	.053	.071	.083	.86	.050	.075	.083
.04	.054	.068	.083	.88	.057	.083	.083
.06	.053	.067	.083	1.90	.079	.083	.083
.08	.052	.066	.083	.92	.081	.083	.083

TABLE II (Cont'd)

Time Seconds	Depth of Flow -- Feet			Time Seconds	Depth of Flow -- Feet		
	Gage				Gage		
	No. 1	No. 2	No. 4		No. 1	No. 2	No. 4
.94	.083	.083	.083	3.50	.083	.083	.083
.96	.083	.083	.083	5.00	.083	.083	.083
.98	.083	.083	.083				
2.00	.083	.083	.083				
2.10	.083	.083	.083				
2.20	.083	.083	.083				
2.30	.083	.083	.083				
2.40	.083	.083	.083				
2.50	.083	.083	.083				
2.60	.083	.083	.083				
.62	.083	.083	.083				
.64	.083	.083	.083				
.66	.082	.083	.083				
.68	.080	.083	.083				
2.70	.078	.083	.083				
.72	.076	.083	.083				
.74	.074	.083	.083				
.76	.072	.083	.083				
.78	.070	.083	.083				
2.80	.066	.083	.083				
.82	.064	.083	.083				
.84	.063	.083	.083				
.86	.064	.083	.083				
.88	.064	.083	.083				
2.90	.067	.083	.083				
.92	.069	.083	.083				
.94	.070	.083	.083				
.96	.070	.083	.083				
.98	.069	.083	.083				
3.00	.068	.083	.083				
.02	.068	.083	.083				
.04	.068	.083	.083				
.06	.068	.083	.083				
.08	.070	.083	.083				
3.10	.073	.083	.083				
.12	.076	.083	.083				
.14	.079	.083	.083				
.16	.080	.083	.083				
.18	.079	.083	.083				
3.20	.078	.083	.083				
.22	.079	.083	.083				
.24	.081	.083	.083				
.26	.083	.083	.083				
.28	.083	.083	.083				
3.30	.083	.083	.083				
3.40	.083	.083	.083				

TABLE III
 EXPERIMENTAL RUN NUMBER 34
 PRESSURE-RISE DATA AT GATE VALVE

Time Seconds	Head Feet of Water	Time Seconds	Head Feet of Water
.0028	17.6	.1260	308.2
.0074	183.8	.1314	311.1
.0105	195.6	.1350	303.1
.0121	181.7	.1385	302.2
.0140	180.3	.1404	293.3
.0156	273.5	.1429	291.9
.0186	256.3	.1449	274.9
.0211	273.2	.1474	278.3
.0237	249.8	.1494	275.0
.0273	280.9	.1519	268.2
.0308	261.7	.1542	266.4
.0337	283.0	.1554	260.8
.0364	280.9	.1600	259.0
.0392	281.5	.1633	249.5
.0412	277.7	.1659	250.4
.0436	280.6	.1705	243.0
.0462	291.9	.1739	245.4
.0490	275.9	.1774	241.5
.0523	291.9	.1808	239.2
.0555	278.9	.1833	238.6
.0592	290.1	.1846	238.3
.0635	276.5	.1879	240.7
.0658	278.6	.1900	240.7
.0692	278.6	.1910	234.1
.0712	275.6	.1929	231.2
.0733	280.9	.1941	225.0
.0763	277.4	.1962	209.9
.0782	284.5	.2046	136.4
.0821	285.7	.2128	50.9
.0839	294.0	.2147	36.6
.0871	292.5	.2171	24.5
.0899	300.5	.2206	11.3
.0942	296.9	--	--
.0987	312.3	1.8818	11.3
.1016	305.2	1.8850	87.6
.1038	314.1	1.8873	47.0
.1071	311.1	1.8908	47.6
.1109	312.6	1.8961	120.2
.1154	321.2	1.8995	122.2
.1187	312.6	1.9005	133.5
.1210	317.0	1.9031	133.5

TABLE III (Cont'd)

Time Seconds	Head Feet of Water	Time Seconds	Head Feet of Water
1.9046	142.1	2.0921	83.7
1.9066	145.0	2.0969	60.9
1.9092	140.3	2.1046	39.6
1.9108	148.3	2.1149	24.5
1.9130	155.4	2.1303	11.3
1.9145	159.2	--	--
1.9168	156.3	2.9938	11.3
1.9256	163.1	2.9977	79.3
1.9290	167.8	3.0024	80.2
1.9315	166.6	3.0048	90.5
1.9336	169.9	3.0101	90.5
1.9354	167.5	3.0160	97.4
1.9380	166.0	3.0227	93.8
1.9484	159.5	3.0256	97.9
1.9569	161.9	3.0333	92.9
1.9572	166.0	3.0409	92.0
1.9642	172.0	3.0499	95.0
1.9687	169.6	3.0596	98.2
1.9735	167.5	3.0687	106.8
1.9780	175.2	3.0711	107.7
1.9800	172.9	3.0759	112.7
1.9858	183.8	3.0792	114.2
1.9879	182.6	3.0816	118.7
1.9944	190.9	3.0910	120.1
2.0021	188.2	3.0965	123.7
2.0043	190.0	3.1096	124.6
2.0159	192.7	3.1192	121.0
2.0232	189.1	3.1286	115.7
2.0264	181.4	3.1363	111.0
2.0321	72.0	3.1391	113.3
2.0341	72.6	3.1477	113.0
2.0400	167.0	3.1545	113.0
2.0446	164.3	3.1609	118.7
2.0497	162.2	3.1718	121.9
2.0539	160.0	3.1756	121.6
2.0585	154.8	3.1872	100.6
2.0611	148.3	3.2052	55.9
2.0640	141.5	3.2173	38.7
2.0676	134.7	3.2256	32.5
2.0719	133.5	3.2468	27.2
2.0752	133.5	3.2602	11.3
2.0775	133.5	--	--
2.0835	131.1	3.8050	11.3
2.0868	118.7	3.8056	16.5

TABLE III (Cont'd)

Time Seconds	Head Feet of Water	Time Seconds	Head Feet of Water
3.8274	11.3	4.0872	93.2
3.8582	11.3	4.0912	89.4
3.8659	20.9	4.0958	80.2
3.8723	45.5	4.0986	73.7
3.8813	29.8	4.0136	65.4
3.8864	50.6	4.1124	57.7
3.8942	44.9	4.1229	51.5
3.9009	63.6	4.1299	42.3
3.9069	59.4	4.1389	41.4
3.9095	66.9	4.1423	41.4
3.9208	73.1	4.1507	34.6
3.9232	71.3	4.1714	29.8
3.9262	67.4	4.1799	30.7
3.9282	68.0	4.1900	19.5
3.9303	71.6	4.1984	11.3
3.9344	76.0	--	--
3.9353	74.3	4.6409	11.3
3.9376	71.9	4.6426	16.9
3.9399	73.4	4.6567	24.5
3.9426	76.0	4.6759	14.8
3.9454	75.1	4.6785	27.0
3.9491	74.8	4.6939	35.8
3.9517	78.4	4.7003	47.3
3.9550	76.3	4.7144	44.0
3.9591	79.0	4.7208	50.9
3.9593	84.0	4.7516	57.1
3.9659	81.7	4.7580	64.5
3.9711	79.1	4.7772	66.6
3.9775	81.1	4.7875	70.4
3.9813	84.6	4.7958	73.1
3.9870	81.7	4.7982	70.7
3.9912	87.0	4.8018	71.9
3.9951	84.9	4.8057	72.5
4.0000	88.2	4.8105	73.7
4.0053	86.1	4.8151	71.9
4.0120	88.5	4.8208	74.8
4.0174	66.7	4.8239	74.3
4.0217	90.8	4.8303	75.5
4.0279	90.2	4.8342	78.1
4.0298	93.5	4.8469	82.0
4.0446	90.5	4.8531	80.2
4.0467	88.2	4.8627	80.2
4.0540	87.6	4.8799	79.3
4.0657	92.6	4.8913	74.8
4.0708	93.5	4.9009	71.9
4.0809	95.6	4.9113	72.5

TABLE III (Cont'd)

Time Seconds	Head Feet of Water	Time Seconds	Head Feet of Water
4.9156	70.1		
4.9210	62.4		
4.9318	55.3		
4.9432	50.0		
4.9515	44.6		
4.9613	44.6		
4.9675	41.1		
4.9762	40.5		
4.9878	36.7		
5.0000	19.8		
5.0118	27.8		
5.0285	25.4		
5.0439	18.0		
5.0618	13.0		
5.0740	11.3		

TABLE IV

EXPERIMENTAL RUN NUMBER 34
COLUMN-SEPARATION VOID DATA

Time Seconds	Depth of Flow -- Feet			Time Seconds	Depth of Flow -- Feet		
	Gage				Gage		
	No. 1	No. 4	No. 5		No. 1	No. 4	No. 5
0.00	.083	.083	.083	.98	.048	.079	.083
0.20	.083	.083	.083	1.00	.048	.073	.081
.22	.083	.083	.083	.02	.047	.065	.079
.24	.083	.083	.083	.04	.047	.054	.079
.26	.083	.083	.083	.06	.046	.051	.078
.28	.080	.083	.083	.08	.045	.050	.078
0.30	.078	.083	.083	1.10	.045	.056	.078
.32	.076	.083	.083	.12	.045	.067	.077
.34	.073	.083	.083	.14	.044	.063	.077
.36	.071	.083	.083	.16	.043	.057	.073
.38	.073	.083	.083	.18	.043	.053	.068
0.40	.076	.083	.083	1.20	.043	.053	.063
.42	.077	.083	.083	.22	.042	.052	.061
.44	.073	.083	.083	.24	.043	.052	.058
.46	.070	.083	.083	.26	.043	.053	.052
.48	.068	.083	.083	.28	.043	.055	.052
0.50	.064	.083	.083	1.30	.043	.058	.059
.52	.059	.083	.083	.32	.043	.064	.062
.54	.054	.083	.083	.34	.044	.063	.061
.56	.051	.083	.083	.36	.044	.062	.056
.58	.049	.083	.083	.38	.043	.057	.054
0.60	.049	.083	.083	1.40	.044	.058	.051
.62	.051	.083	.083	.42	.044	.054	.051
.64	.051	.083	.083	.44	.044	.052	.052
.66	.050	.083	.083	.46	.043	.050	.052
.68	.049	.083	.083	.48	.043	.046	.053
0.70	.048	.083	.083	1.50	.043	.049	.054
.72	.046	.083	.083	.52	.043	.049	.055
.74	.045	.083	.083	.54	.043	.054	.056
.76	.044	.083	.083	.56	.043	.054	.056
.78	.044	.083	.083	.58	.043	.052	.068
0.80	.043	.083	.083	1.60	.043	.054	.083
.82	.043	.083	.083	.62	.043	.055	.083
.84	.042	.083	.083	.64	.044	.058	.083
.86	.043	.083	.083	.66	.044	.072	.083
.88	.043	.083	.083	.68	.044	.083	.083
0.90	.044	.081	.083	1.70	.044	.083	.083
.92	.045	.081	.083	.72	.044	.083	.083
.94	.047	.081	.083	.74	.044	.083	.083
.96	.048	.080	.083	.76	.044	.083	.083

TABLE IV (Cont'd)

Time Seconds	Depth of Flow -- Feet			Time Seconds	Depth of Flow -- Feet		
	Gage				Gage		
	No. 1	No. 4	No. 5		No. 1	No. 4	No. 5
1.78	.044	.083	.083	.06	.079	.083	.083
1.80	.045	.083	.083	.08	.079	.083	.083
.82	.052	.083	.083	3.10	.082	.083	.083
.84	.071	.083	.083	.12	.083	.083	.083
.86	.081	.083	.083	.14	.083	.083	.083
.88	.083	.083	.083	.16	.083	.083	.083
1.90	.083	.083	.083	.18	.083	.083	.083
2.00	.083	.083	.083	3.20	.083	.083	.083
2.10	.083	.083	.083	3.30	.083	.083	.083
2.20	.083	.083	.083	3.40	.083	.083	.083
2.30	.083	.083	.083	3.50	.083	.083	.083
2.40	.083	.083	.083	5.00	.083	.083	.083
.42	.081	.083	.083				
.44	.079	.083	.083				
.46	.077	.083	.083				
.48	.075	.083	.083				
2.50	.074	.083	.083				
.52	.072	.083	.083				
.54	.070	.083	.083				
.56	.068	.083	.083				
.58	.063	.083	.083				
2.60	.057	.083	.083				
.62	.058	.083	.083				
.64	.060	.083	.083				
.66	.060	.083	.083				
.68	.061	.083	.083				
2.70	.063	.083	.083				
.72	.063	.083	.083				
.74	.063	.083	.083				
.76	.063	.083	.083				
.78	.063	.083	.083				
2.80	.063	.083	.083				
.82	.063	.083	.083				
.84	.064	.083	.083				
.86	.064	.083	.083				
.88	.065	.083	.083				
2.90	.065	.083	.083				
.92	.064	.083	.083				
.94	.064	.083	.083				
.96	.063	.083	.083				
.98	.063	.083	.083				
3.00	.063	.083	.083				
.02	.065	.083	.083				
.04	.069	.083	.083				

APPENDIX IV

COMPUTER SIMULATED RESULTS

The results obtained from digital computer simulation of column separation accompanying transient pipe flow for Group II laboratory conditions are presented in this appendix. Photo reduced copies of the line-printer output list the data in sequence with respect to time. However, only the first 2,000 cycles (3.704 seconds of the simulated phenomena) are presented.

Certain events which occur during the course of the simulation are of particular interest. These events are identified according to time and to cycle number:

<u>Time in Seconds</u>	<u>Cycle No.</u>	<u>Event</u>
0	-	Computation starts while steady-state conditions prevail.
.00557	3	Gate valve is instantaneously closed.
.10299	55	High pressure wave reaches reservoir; direction of flow at reservoir reverses.
.03711-.18557	-	At valve, pressure continues to increase slightly as pipe is "packed".
.19299	104	Direction of flow at valve reverses and pressure begins to decrease.
.20413	110	Negative absolute pressure occurs at gate valve and initial separation void forms. Free-surface flow throughout void is toward reservoir.

<u>Time in Seconds</u>	<u>Cycle No.</u>	<u>Event</u>
1.16723	629	Flow within void reverses direction at point 0.384 foot from gate valve. Reversal propagates in both directions from this point with subsequent cycles.
1.48270	799	Column separation void reaches its maximum extent, 2.30 + feet measured from gate valve, and hovers at this approximate distance.
1.62837	869	Flow direction at reservoir reverses. Flow starts toward valve.
2.11363	1139	Void starts to retreat from its maximum extent.
3.13426	1689	Initial void collapses. Second high pressure rise occurs.
3.23540	1743	High pressure wave reaches reservoir; direction of flow at reservoir reverses.
3.15468-3.32911	-	Pressure continues to increase at valve as pipe is "packed".
3.33468	1797	Negative absolute pressure occurs at the gate valve and the second separation voids forms.

GIVEN INFORMATION

GIVEN PHYSICAL DATA AND CONSTANTS
 RHO = 1.930 KA = .4860E 08 VMAX = 3.50 HBAR = 33.224 G = -.0107 LCC3 = 444.000
 DIMENSIONAL DATA DESCRIBING ANALYTIC MODEL LEL = 22.078 WSEL = 22.574 LGC1 = 18.000 LCC2 = 44.000
 HEL = 34.719 MEL = 26.328

PIPE CHARACTERISTICS AND RELATED DATA
 E(1) = .5112E 08 ZETA(1) = .280 R(1) = .04139 LL(1) = .0.771 MN(1) = 1
 E(2) = .2448E 10 ZETA(2) = .300 R(2) = .04678 R(2) = .04146 LL(2) = 43.187 MN(2) = 50

PROGRAM OPERATION AND CONTROL DATA
 MAXIMUM ALLOWABLE ITERATIONS = 4000 COMPUTATION CUTOFF LIMIT = 1600 INITIAL CAVITY PRINTOUT = 4 VALVE SHUT-OFF POINT = 3
 INITIAL PRINTOUT LIMIT POINT = 4 PRINTOUT FREQUENCY CONTROL = 10 CAVITY PRINTOUT CYCLE = 2

FRICITION VALUES FOR CONSECUTIVE REYNOLDS NUMBERS FROM 100 TO 35100 IN INCREMENTS OF 1000.

REYNOLDS NO. = 100	F(1, 0) = .7000	F(2, 0) = .8400
REYNOLDS NO. = 1100	F(1, 1) = .1400	F(2, 1) = .0865
REYNOLDS NO. = 2100	F(1, 2) = .0925	F(2, 2) = .0560
REYNOLDS NO. = 3100	F(1, 3) = .0735	F(2, 3) = .0445
REYNOLDS NO. = 4100	F(1, 4) = .0630	F(2, 4) = .0385
REYNOLDS NO. = 5100	F(1, 5) = .0570	F(2, 5) = .0350
REYNOLDS NO. = 6100	F(1, 6) = .0525	F(2, 6) = .0328
REYNOLDS NO. = 7100	F(1, 7) = .0490	F(2, 7) = .0318
REYNOLDS NO. = 8100	F(1, 8) = .0470	F(2, 8) = .0312
REYNOLDS NO. = 9100	F(1, 9) = .0454	F(2, 9) = .0311
REYNOLDS NO. = 10100	F(1,10) = .0438	F(2,10) = .0309
REYNOLDS NO. = 11100	F(1,11) = .0422	F(2,11) = .0306
REYNOLDS NO. = 12100	F(1,12) = .0412	F(2,12) = .0302
REYNOLDS NO. = 13100	F(1,13) = .0402	F(2,13) = .0299
REYNOLDS NO. = 14100	F(1,14) = .0393	F(2,14) = .0296
REYNOLDS NO. = 15100	F(1,15) = .0386	F(2,15) = .0292
REYNOLDS NO. = 16100	F(1,16) = .0380	F(2,16) = .0289
REYNOLDS NO. = 17100	F(1,17) = .0374	F(2,17) = .0287
REYNOLDS NO. = 18100	F(1,18) = .0368	F(2,18) = .0284
REYNOLDS NO. = 19100	F(1,19) = .0362	F(2,19) = .0280
REYNOLDS NO. = 20100	F(1,20) = .0357	F(2,20) = .0278
REYNOLDS NO. = 21100	F(1,21) = .0352	F(2,21) = .0275
REYNOLDS NO. = 22100	F(1,22) = .0348	F(2,22) = .0272
REYNOLDS NO. = 23100	F(1,23) = .0345	F(2,23) = .0270
REYNOLDS NO. = 24100	F(1,24) = .0342	F(2,24) = .0268
REYNOLDS NO. = 25100	F(1,25) = .0339	F(2,25) = .0266
REYNOLDS NO. = 26100	F(1,26) = .0337	F(2,26) = .0263
REYNOLDS NO. = 27100	F(1,27) = .0334	F(2,27) = .0261
REYNOLDS NO. = 28100	F(1,28) = .0332	F(2,28) = .0259
REYNOLDS NO. = 29100	F(1,29) = .0330	F(2,29) = .0257
REYNOLDS NO. = 30100	F(1,30) = .0329	F(2,30) = .0255
REYNOLDS NO. = 31100	F(1,31) = .0328	F(2,31) = .0253
REYNOLDS NO. = 32100	F(1,32) = .0327	F(2,32) = .0251
REYNOLDS NO. = 33100	F(1,33) = .0326	F(2,33) = .0249
REYNOLDS NO. = 34100	F(1,34) = .0325	F(2,34) = .0248
REYNOLDS NO. = 35100	F(1,35) = .0324	F(2,35) = .0247

COMPUTED RESULTS

COMPUTED VALUES OF RELATIVE PRESSURE HEAD, VELOCITY, ELEVATION, AND ANGLE OF PIPE INCLINATION AT TIME T = 0.			
H(1, 0)	= 46.246	V(1, 0)	= -1.988
H(1, 1)	= 46.491	V(1, 1)	= -1.988
H(2, 0)	= 46.491	V(2, 0)	= -1.981
H(2, 1)	= 46.677	V(2, 1)	= -1.981
H(2, 2)	= 46.863	V(2, 2)	= -1.981
H(2, 3)	= 47.049	V(2, 3)	= -1.981
H(2, 4)	= 47.236	V(2, 4)	= -1.981
H(2, 5)	= 47.422	V(2, 5)	= -1.961
H(2, 6)	= 47.608	V(2, 6)	= -1.981
H(2, 7)	= 47.794	V(2, 7)	= -1.981
H(2, 8)	= 47.980	V(2, 8)	= -1.981
H(2, 9)	= 48.166	V(2, 9)	= -1.981
H(2, 10)	= 48.352	V(2, 10)	= -1.981
H(2, 11)	= 48.539	V(2, 11)	= -1.981
H(2, 12)	= 48.725	V(2, 12)	= -1.981
H(2, 13)	= 48.911	V(2, 13)	= -1.981
H(2, 14)	= 49.097	V(2, 14)	= -1.981
H(2, 15)	= 49.283	V(2, 15)	= -1.981
H(2, 16)	= 49.469	V(2, 16)	= -1.981
H(2, 17)	= 49.655	V(2, 17)	= -1.981
H(2, 18)	= 49.841	V(2, 18)	= -1.981
H(2, 19)	= 50.028	V(2, 19)	= -1.981
H(2, 20)	= 50.214	V(2, 20)	= -1.981
H(2, 21)	= 50.400	V(2, 21)	= -1.981
H(2, 22)	= 50.586	V(2, 22)	= -1.981
H(2, 23)	= 50.772	V(2, 23)	= -1.981
H(2, 24)	= 50.958	V(2, 24)	= -1.981
H(2, 25)	= 51.144	V(2, 25)	= -1.981
H(2, 26)	= 51.331	V(2, 26)	= -1.981
H(2, 27)	= 51.517	V(2, 27)	= -1.981
H(2, 28)	= 51.703	V(2, 28)	= -1.981
H(2, 29)	= 51.889	V(2, 29)	= -1.981
H(2, 30)	= 52.075	V(2, 30)	= -1.981
H(2, 31)	= 52.261	V(2, 31)	= -1.981
H(2, 32)	= 52.447	V(2, 32)	= -1.981
H(2, 33)	= 52.634	V(2, 33)	= -1.981
H(2, 34)	= 52.820	V(2, 34)	= -1.981
H(2, 35)	= 53.006	V(2, 35)	= -1.981
H(2, 36)	= 53.192	V(2, 36)	= -1.981
H(2, 37)	= 53.378	V(2, 37)	= -1.981
H(2, 38)	= 53.564	V(2, 38)	= -1.981
H(2, 39)	= 53.750	V(2, 39)	= -1.981
H(2, 40)	= 53.937	V(2, 40)	= -1.981
H(2, 41)	= 54.123	V(2, 41)	= -1.981
H(2, 42)	= 54.309	V(2, 42)	= -1.981
H(2, 43)	= 54.495	V(2, 43)	= -1.981
H(2, 44)	= 54.681	V(2, 44)	= -1.981
H(2, 45)	= 54.867	V(2, 45)	= -1.981
H(2, 46)	= 55.053	V(2, 46)	= -1.981
H(2, 47)	= 55.240	V(2, 47)	= -1.981
H(2, 48)	= 55.426	V(2, 48)	= -1.981
H(2, 49)	= 55.612	V(2, 49)	= -1.981
H(2, 50)	= 55.798	V(2, 50)	= -1.981
CLP(1, 0)	= 34.719	THETA(1, 0)	= .000
ELP(1, 1)	= 34.719	THETA(1, 1)	= .000
LLP(2, 0)	= 34.719	THETA(2, 0)	= .000
ELP(2, 1)	= 34.719	THETA(2, 1)	= .000
ELP(2, 2)	= 29.193	THETA(2, 2)	= .329
ELP(2, 3)	= 26.338	THETA(2, 3)	= .329
ELP(2, 4)	= 26.236	THETA(2, 4)	= .011
ELP(2, 5)	= 26.142	THETA(2, 5)	= .011
ELP(2, 6)	= 26.049	THETA(2, 6)	= .011
ELP(2, 7)	= 25.956	THETA(2, 7)	= .011
ELP(2, 8)	= 25.862	THETA(2, 8)	= .011
ELP(2, 9)	= 25.769	THETA(2, 9)	= .011
ELP(2, 10)	= 25.676	THETA(2, 10)	= .011
ELP(2, 11)	= 25.582	THETA(2, 11)	= .011
ELP(2, 12)	= 25.489	THETA(2, 12)	= .011
ELP(2, 13)	= 25.396	THETA(2, 13)	= .011
ELP(2, 14)	= 25.302	THETA(2, 14)	= .011
ELP(2, 15)	= 25.209	THETA(2, 15)	= .011
ELP(2, 16)	= 25.116	THETA(2, 16)	= .011
ELP(2, 17)	= 24.929	THETA(2, 17)	= .011
ELP(2, 18)	= 24.836	THETA(2, 18)	= .011
ELP(2, 19)	= 24.742	THETA(2, 19)	= .011
ELP(2, 20)	= 24.649	THETA(2, 20)	= .011
ELP(2, 21)	= 24.556	THETA(2, 21)	= .011
ELP(2, 22)	= 24.462	THETA(2, 22)	= .011
ELP(2, 23)	= 24.369	THETA(2, 23)	= .011
ELP(2, 24)	= 24.276	THETA(2, 24)	= .011
ELP(2, 25)	= 24.182	THETA(2, 25)	= .011
ELP(2, 26)	= 24.089	THETA(2, 26)	= .011
ELP(2, 27)	= 23.996	THETA(2, 27)	= .011
ELP(2, 28)	= 23.902	THETA(2, 28)	= .011
ELP(2, 29)	= 23.809	THETA(2, 29)	= .011
ELP(2, 30)	= 23.716	THETA(2, 30)	= .011
ELP(2, 31)	= 23.623	THETA(2, 31)	= .011
ELP(2, 32)	= 23.529	THETA(2, 32)	= .011
ELP(2, 33)	= 23.436	THETA(2, 33)	= .011
ELP(2, 34)	= 23.343	THETA(2, 34)	= .011
ELP(2, 35)	= 23.249	THETA(2, 35)	= .011
ELP(2, 36)	= 23.156	THETA(2, 36)	= .011
ELP(2, 37)	= 23.063	THETA(2, 37)	= .011
ELP(2, 38)	= 22.969	THETA(2, 38)	= .011
ELP(2, 39)	= 22.876	THETA(2, 39)	= .011
ELP(2, 40)	= 22.783	THETA(2, 40)	= .011
ELP(2, 41)	= 22.689	THETA(2, 41)	= .011
ELP(2, 42)	= 22.596	THETA(2, 42)	= .011
ELP(2, 43)	= 22.503	THETA(2, 43)	= .011
ELP(2, 44)	= 22.409	THETA(2, 44)	= .011
ELP(2, 45)	= 22.316	THETA(2, 45)	= .011
ELP(2, 46)	= 22.223	THETA(2, 46)	= .011
ELP(2, 47)	= 22.129	THETA(2, 47)	= .011
ELP(2, 48)	= 22.036	THETA(2, 48)	= .011
ELP(2, 49)	= 21.943	THETA(2, 49)	= .011
ELP(2, 50)	= 21.850	THETA(2, 50)	= .000

VALUES OF KEY VARIABLES USED THROUGHOUT THE COMPUTATIONS IN PART I.

A(1) = 2449.843175, A(2) = 4729.905945, DELX(1) = 8.771030, DELX(2) = 8.783710
 DELT(1) = 3.575114E-03, DELT(2) = 1.855691E-03, MU(1) = 2.115712E-4
 MU(2) = 2.112644E-04, CP(1) = .827193, CP(2) = .810101, AGG(1) = 76.176371
 AGG(2) = 147.074190, GOA(1) = .913127, GOA(2) = 6.799289E-03

AT TIME T = .00186 SECONDS, AFTER FLOW SYSTEM ARE AS TABULATED BELOW.

LOC.	(1,0)	(1,1)	(2,0)	(2,10)	(2,20)	(2,30)	(2,40)	(2,50)
V	-1.9881	-1.9881	-1.9814	-1.9814	-1.9814	-1.9814	-1.9814	-1.9814
H	17.6737	17.9216	17.9216	22.0037	24.8080	27.6124	30.4168	33.1790

AT TIME T = .00371 SECONDS, AFTER FLOW SYSTEM ARE AS TABULATED BELOW.

LOC.	(1,0)	(1,1)	(2,0)	(2,10)	(2,20)	(2,30)	(2,40)	(2,50)
V	-1.9881	-1.9881	-1.9814	-1.9814	-1.9814	-1.9814	-1.9814	-1.9814
H	17.6738	17.9217	17.9217	22.0038	24.8082	27.6125	30.4169	33.1790

→ THE GATE VALVE AT LOCATION J = 1, I = 0 HAS BEEN INSTANTANEOUSLY CLOSED AT TIME T = .00557 SECONDS, OR AT OPERATION NUMBER 3. ←

AT TIME T = .00557 SECONDS, AFTER FLOW SYSTEM ARE AS TABULATED BELOW.

LOC.	(1,0)	(1,1)	(2,0)	(2,10)	(2,20)	(2,30)	(2,40)	(2,50)
V	.0000	-1.9881	-1.9814	-1.9814	-1.9814	-1.9814	-1.9814	-1.9814
H	169.1229	17.9218	17.9218	22.0039	24.8083	27.6127	30.4170	33.1790

AT TIME T = .01856 SECONDS, AFTER FLOW SYSTEM ARE AS TABULATED BELOW.

LOC.	(1,0)	(1,1)	(2,0)	(2,10)	(2,20)	(2,30)	(2,40)	(2,50)
V	.0000	-2.2578	-2.2569	-1.9814	-1.9814	-1.9614	-1.9814	-1.9814
H	277.4224	271.9850	271.9850	22.0053	24.8091	27.6135	30.4178	33.1790

AT TIME T = .03711 SECONDS, AFTER FLOW SYSTEM ARE AS TABULATED BELOW.

LOC.	(1,0)	(1,1)	(2,0)	(2,10)	(2,20)	(2,30)	(2,40)	(2,50)
V	.0000	-0.219	-0.218	-2637	-1.9814	-1.9814	-1.9814	-1.9814
H	307.8768	307.4795	307.4795	275.0641	24.8108	27.6146	30.4178	33.1790

AT TIME T = .05567 SECONDS, AFTER FLOW SYSTEM ARE AS TABULATED BELOW.

LOC.	(1,0)	(1,1)	(2,0)	(2,10)	(2,20)	(2,30)	(2,40)	(2,50)
V	.0000	-0.040	-0.039	-0.0282	-1.9814	-1.9814	-1.9814	-1.9814
H	311.0562	311.0418	311.0418	310.6210	276.8696	27.6152	30.4179	33.1790

AT TIME T = .07423 SECONDS, AFTER FLOW SYSTEM ARE AS TABULATED BELOW.

LOC.	(1,0)	(1,1)	(2,0)	(2,10)	(2,20)	(2,30)	(2,40)	(2,50)
V	.0000	-0.026	-0.026	-0.0103	-1.9814	-1.9814	-1.9814	-1.9814
H	311.0562	311.0418	311.0418	310.6210	276.8696	27.6152	30.4179	33.1790

H 312.1615 312.1759 312.1759 314.1860 312.6951 278.6736 30.4184 33.1790

AT TIME T = .09278 SECONDS, AFTER 50 COMPLETE CYCLES OF OPERATION, THE VELOCITIES AND PRESSURES AT KEY POINTS THROUGHOUT THE FLOW SYSTEM ARE AS TABULATED BELOW.

LOC. (1,0) (2,0) (2,20) (2,30) (2,40) (2,50)

V .0000 -.0025 -.0152 -.0409 -.0784 (2,40)

H 313.1086 313.1248 313.1248 315.3199 316.318 317.9177 318.2143 33.1790

→ THE DIRECTION OF FLOW AT THE RESERVOIR END OF THE PIPE SYSTEM HAS REVERSED AT TIME T = .10299 SECONDS. ←

LOC. (1,0) (1,1) (2,0) (2,10) (2,20) (2,30) (2,40) (2,50)

V .0000 -.0025 -.0025 -.0085 -.0152 -.0230 -.0473 (2,40)

H 314.6418 314.6378 314.0578 316.2669 317.1845 317.9177 318.2143 33.1790

AT TIME T = .12990 SECONDS, AFTER 70 COMPLETE CYCLES OF OPERATION, THE VELOCITIES AND PRESSURES AT KEY POINTS THROUGHOUT THE FLOW SYSTEM ARE AS TABULATED BELOW.

LOC. (1,0) (1,1) (2,0) (2,10) (2,20) (2,30) (2,40) (2,50)

V .0000 -.0025 -.0024 -.0088 -.0151 -.0216 (2,40)

H 314.9730 314.9886 314.9886 317.1995 318.1314 319.0495 319.4492 33.1790

AT TIME T = .14846 SECONDS, AFTER 80 COMPLETE CYCLES OF OPERATION, THE VELOCITIES AND PRESSURES AT KEY POINTS THROUGHOUT THE FLOW SYSTEM ARE AS TABULATED BELOW.

LOC. (1,0) (1,1) (2,0) (2,10) (2,20) (2,30) (2,40) (2,50)

V .0000 -.0025 -.0024 -.0085 -.0151 (2,40)

H 315.9036 315.9188 315.9188 318.1297 319.0628 319.8625 36.9225 33.1790

AT TIME T = .16701 SECONDS, AFTER 90 COMPLETE CYCLES OF OPERATION, THE VELOCITIES AND PRESSURES AT KEY POINTS THROUGHOUT THE FLOW SYSTEM ARE AS TABULATED BELOW.

LOC. (1,0) (1,1) (2,0) (2,10) (2,20) (2,30) (2,40) (2,50)

V .0000 -.0024 -.0024 -.0086 -.0151 (2,40)

H 316.8337 316.8485 316.8485 319.0588 319.2625 37.8110 34.3139 33.1790

AT TIME T = .18557 SECONDS, AFTER 100 COMPLETE CYCLES OF OPERATION, THE VELOCITIES AND PRESSURES AT KEY POINTS THROUGHOUT THE FLOW SYSTEM ARE AS TABULATED BELOW.

LOC. (1,0) (1,1) (2,0) (2,10) (2,20) (2,30) (2,40) (2,50)

V .0000 -.0024 -.0024 -.0086 (2,40)

H 317.7625 317.7769 317.7769 319.0599 38.6820 35.1923 34.1157 33.1790

AT TIME T = .19485 SECONDS, AFTER 105 COMPLETE CYCLES OF OPERATION, THE VELOCITIES AND PRESSURES AT KEY POINTS THROUGHOUT THE FLOW SYSTEM ARE AS TABULATED BELOW.

LOC. (1,0) (1,1) (2,0) (2,10) (2,20) (2,30) (2,40) (2,50)

V .0000 1.2830 1.2786 1.8467 1.9115 (2,40)

H 259.2695 220.2949 220.2949 47.0015 36.6331 35.0356 34.1033 33.1790

AT TIME T = .19670 SECONDS, AFTER 106 COMPLETE CYCLES OF OPERATION, THE VELOCITIES AND PRESSURES AT KEY POINTS THROUGHOUT THE FLOW SYSTEM ARE AS TABULATED BELOW.

LOC. (1,0) (1,1) (2,0) (2,10) (2,20) (2,30) (2,40) (2,50)

V .0000 1.4479 1.4430 1.8627 1.9126 (2,40)

H 188.4125 177.1988 177.1988 44.6576 36.4565 35.0225 34.1024 33.1790

AT TIME T = .19856 SECONDS, AFTER 107 COMPLETE CYCLES OF OPERATION, THE VELOCITIES AND PRESSURES AT KEY POINTS THROUGHOUT THE FLOW SYSTEM ARE AS TABULATED BELOW.

LOC.	(1,0)	(1,1)	(2,0)	(2,10)	(2,30)	(2,40)	(2,50)
V	.0000	1.4354	1.4305	1.9137	1.9166	1.9168	1.9169
H	125.4320	126.6930	126.6930	36.3190	35.0116	34.1013	33.1790

AT TIME T = .20041 SECONDS, AFTER 108 COMPLETE CYCLES OF OPERATION, THE VELOCITIES AND PRESSURES AT KEY POINTS THROUGHOUT THE FLOW SYSTEM ARE AS TABULATED BELOW.

LOC.	(1,0)	(1,1)	(2,0)	(2,10)	(2,30)	(2,40)	(2,50)
V	.0000	1.5430	1.3335	1.9144	1.9166	1.9168	1.9168
H	69.4124	76.2915	76.2915	36.2138	35.0039	34.1008	33.1790

AT TIME T = .20227 SECONDS, AFTER 109 COMPLETE CYCLES OF OPERATION, THE VELOCITIES AND PRESSURES AT KEY POINTS THROUGHOUT THE FLOW SYSTEM ARE AS TABULATED BELOW.

LOC.	(1,0)	(1,1)	(2,0)	(2,10)	(2,30)	(2,40)	(2,50)
V	.0000	1.2163	1.2122	1.9150	1.9168	1.9169	1.9169
H	19.9497	29.2550	29.2550	36.1313	34.9972	34.1001	33.1790

→ COLUMN SEPARATION HAS OCCURRED AT THE GATE VALVE AT TIME T = .20413 SECONDS (OPERATION CYCLE NO. 110). THIS IS ←

THE MAGNITUDE OF DELXC REMAINS THE MINIMUM VALUE.

GIVEN DATA AND COMPUTED VALUES PERTINENT TO COMPUTATION OF FLOW FOLLOWING COLUMN SEPARATION.

HVAPOR = 11.3000	DELXC = .0640	DELTC = .00928	MARK = 0	MUCH = .1852
FACTOR = 5	XI = .0250	INC = 90	LOTA = .0001	PAREA = .00538

THE INITIAL VELOCITIES AND DEPTHS IN THE VAPOR CAVITY ARE LISTED BELOW.

DIST.	.0000	.0640
LOC.	0	1
U	.000	1.053
Z	.061	.070

THE VELOCITIES AND ABSOLUTE HEADS THROUGHOUT THE REMAINDER OF THE FULL-FLOWING PIPE SYSTEM ARE AS LISTED BELOW.

LOC.	(1,0)	(1,1)	(2,0)	(2,10)	(2,30)	(2,40)	(2,50)
V	1.0935	1.2728	1.2685	1.8976	1.9168	1.9169	1.9169
H	11.3000	15.5826	15.5826	39.5523	36.0688	34.9927	33.1790

AT TIME T = .21155 SECONDS, AFTER 114 COMPLETE CYCLES OF OPERATION, THE VELOCITIES AND DEPTHS IN THE VAPOR CAVITY AS WELL AS VELOCITIES AND PRESSURES AT KEY POINTS THROUGHOUT THE FLOW SYSTEM ARE AS TABULATED BELOW.

VAPOR CAVITY

DIST.	.0000	.0640
LOC.	0	1
U	.000	.812
Z	.054	.066

FULL-FLOWING PIPE SYSTEM

LOC.	(1,0)	(1,1)	(2,0)	(2,10)	(2,30)	(2,40)	(2,50)
V	1.3537	1.4227	1.4179	2.0872	1.9170	1.9170	1.9170
H	11.3000	11.3000	11.3000	63.7753	35.9304	34.9820	33.1790

AT TIME T = .22083 SECONDS, AFTER 119 COMPLETE CYCLES OF OPERATION, THE VELOCITIES AND DEPTHS IN THE VAPOR CAVITY AS WELL AS VELOCITIES AND PRESSURES AT KEY POINTS THROUGHOUT THE FLOW SYSTEM ARE AS TABULATED BELOW.

VAPOR CAVITY

DIST. .0000 .0640 .1280
 LOC. 0 1 2
 U .000 .635 1.296
 Z .051 .038 .067

FULL-FLOWING PIPE SYSTEM

LOC. (1,0) (1,1) (2,0) (2,10) (2,20) (2,30) (2,40) (2,50)
 V 1.4594 1.4696 1.4647 1.7330 1.9171 1.9173 1.9173 1.9173
 H 11.3000 11.3000 11.3000 11.3000 35.8734 34.9768 34.0979 33.1790

AT TIME T = .23011 SECONDS, AFTER 124 COMPLETE CYCLES OF OPERATION, THE VELOCITIES AND DEPTHS IN THE VAPOR CAVITY AS WELL AS VELOCITIES AND PRESSURES AT KEY POINTS THROUGHOUT THE FLOW SYSTEM ARE AS TABULATED BELOW.

VAPOR CAVITY

DIST. .0000 .0640 .1280 .1920
 LOC. 0 1 2 3
 U .000 .543 1.120 1.501
 Z .048 .052 .058 .076

FULL-FLOWING PIPE SYSTEM

LOC. (1,0) (1,1) (2,0) (2,10) (2,20) (2,30) (2,40) (2,50)
 V 1.5011 1.5325 1.5273 1.7275 2.0926 1.9174 1.9174 1.9174
 H 11.3000 11.3000 11.3000 11.3000 61.6408 34.9756 34.0981 33.1790

AT TIME T = .23938 SECONDS, AFTER 129 COMPLETE CYCLES OF OPERATION, THE VELOCITIES AND DEPTHS IN THE VAPOR CAVITY AS WELL AS VELOCITIES AND PRESSURES AT KEY POINTS THROUGHOUT THE FLOW SYSTEM ARE AS TABULATED BELOW.

VAPOR CAVITY

DIST. .0000 .0640 .1280 .1920
 LOC. 0 1 2 3
 U .000 .479 .988 1.328
 Z .046 .048 .053 .066

FULL-FLOWING PIPE SYSTEM

LOC. (1,0) (1,1) (2,0) (2,10) (2,20) (2,30) (2,40) (2,50)
 V 1.5418 1.5404 1.5352 1.7120 1.7491 1.9176 1.9176 1.9176
 H 11.3000 11.3245 11.3245 11.3000 11.3000 34.9742 34.0977 33.1790

AT TIME T = .25794 SECONDS, AFTER 139 COMPLETE CYCLES OF OPERATION, THE VELOCITIES AND DEPTHS IN THE VAPOR CAVITY AS WELL AS VELOCITIES AND PRESSURES AT KEY POINTS THROUGHOUT THE FLOW SYSTEM ARE AS TABULATED BELOW.

VAPOR CAVITY

DIST. .0000 .0640 .1280 .1920 .2560
 LOC. 0 1 2 3 4
 U .000 .392 .798 1.082 1.304
 Z .042 .043 .046 .058 .069

FULL-FLOWING PIPE SYSTEM

LOC. (1,0) (1,1) (2,0) (2,10) (2,20) (2,30) (2,40) (2,50)
 V 1.5839 1.5766 1.5749 1.6978 1.7449 1.7555 1.9179
 H 11.3000 11.3867 11.3000 11.3000 11.3000 11.3000 34.0973 33.1790

AT TIME T = .27650 SECONDS, AFTER 149 COMPLETE CYCLES OF OPERATION, THE VELOCITIES AND DEPTHS IN THE VAPOR CAVITY AS WELL AS VELOCITIES AND PRESSURES AT KEY POINTS THROUGHOUT THE FLOW SYSTEM ARE AS TABULATED BELOW.

VAPOR CAVITY

DIST. .0000 .0640 .1280 .1920 .2560 .3200
 LOC. 0 1 2 3 4 5
 U .000 .333 .665 .897 1.142 1.453
 Z .039 .039 .042 .051 .060 .072

FULL-FLOWING PIPE SYSTEM

LOC. (1,0) (1,1) (2,0) (2,10) (2,20) (2,30) (2,40) (2,50)
 V 1.6156 1.6139 1.6085 1.6897 1.7400 1.7516 1.7618 1.9182
 H 11.3000 11.3809 11.3809 11.3000 11.3000 11.3000 11.3000 33.1790

AT TIME T = .29505 SECONDS, AFTER 159 COMPLETE CYCLES OF OPERATION, THE VELOCITIES AND DEPTHS IN THE VAPOR CAVITY AS WELL AS VELOCITIES AND PRESSURES AT KEY POINTS THROUGHOUT THE FLOW SYSTEM ARE AS TABULATED BELOW.

VAPOR CAVITY

DIST. .0000 .0640 .1280 .1920 .2560 .3200 .3840
 LOC. 0 1 2 3 4 5 6
 U .000 .288 .564 .761 .979 1.227 1.475
 Z .036 .037 .039 .046 .054 .062 .072

FULL-FLOWING PIPE SYSTEM

LOC. (1,0) (1,1) (2,0) (2,10) (2,20) (2,30) (2,40) (2,50)
 V 1.6376 1.6361 1.6306 1.6855 1.7347 1.7478 1.7579 1.8718
 H 11.3000 11.3676 11.3676 11.3000 11.3000 11.3000 11.3000 33.1790

AT TIME T = .31361 SECONDS, AFTER 169 COMPLETE CYCLES OF OPERATION, THE VELOCITIES AND DEPTHS IN THE VAPOR CAVITY AS WELL AS VELOCITIES AND PRESSURES AT KEY POINTS THROUGHOUT THE FLOW SYSTEM ARE AS TABULATED BELOW.

VAPOR CAVITY

DIST. .0000 .0640 .1280 .1920 .2560 .3200 .3840 .4479
 LOC. 0 1 2 3 4 5 6 7
 U .000 .252 .485 .657 .851 1.067 1.280 1.491
 Z .034 .035 .037 .043 .049 .055 .063 .074

FULL-FLOWING PIPE SYSTEM

LOC. (1,0) (1,1) (2,0) (2,10) (2,20) (2,30) (2,40) (2,50)
 V 1.6540 1.6527 1.6472 1.6839 1.7293 1.7440 1.7369 1.6356
 H 11.3000 11.3574 11.3574 11.3000 11.3000 11.3000 13.8824 33.1790

AT TIME T = .33217 SECONDS, AFTER 179 COMPLETE CYCLES OF OPERATION, THE VELOCITIES AND DEPTHS IN THE VAPOR CAVITY AS WELL AS VELOCITIES AND PRESSURES AT KEY POINTS THROUGHOUT THE FLOW SYSTEM ARE AS TABULATED BELOW.

VAPOR CAVITY

DIST. .0000 .0640 .1280 .1920 .2560 .3200 .3840 .4479 .5119
 LOC. 0 1 2 3 4 5 6 7 8
 U .000 .221 .420 .573 .747 .942 1.131 1.319 1.504

Z .032 .033 .035 .040 .045 .051 .057 .063 .074

FULL-FLOWING PIPE SYSTEM

LOC.	(1,0)	(1,1)	(2,0)	(2,10)	(2,20)	(2,30)	(2,40)	(2,50)
V	1.662	1.6652	1.6595	1.6845	1.7240	1.7276	1.6144	1.6527
H	11.3000	11.3472	11.3472	11.3000	11.3000	12.9934	30.4613	33.1790

AT TIME T = .35073 SECONDS, AFTER 189 COMPLETE CYCLES OF OPERATION, THE VELOCITIES AND DEPTHS IN THE VAPOR CAVITY AS WELL AS VELOCITIES AND PRESSURES AT KEY POINTS THROUGHOUT THE FLOW SYSTEM ARE AS TABULATED BELOW.

VAPOR CAVITY

DIST.	.0000	.0640	.1280	.1920	.2560	.3200	.3840	.4479	.5119	.5759
LOC.	0	1	2	3	4	5	6	7	8	9
U	.000	.194	.366	.504	.662	.839	1.012	1.187	1.335	1.675
Z	.031	.032	.034	.038	.042	.047	.052	.058	.065	.077

FULL-FLOWING PIPE SYSTEM

LOC.	(1,0)	(1,1)	(2,0)	(2,10)	(2,20)	(2,30)	(2,40)	(2,50)
V	1.6753	1.6745	1.6688	1.6874	1.7145	1.6053	1.5940	1.5934
H	11.3000	11.3368	11.3368	11.3000	11.3560	29.4638	32.2588	33.1790

AT TIME T = .36928 SECONDS, AFTER 199 COMPLETE CYCLES OF OPERATION, THE VELOCITIES AND DEPTHS IN THE VAPOR CAVITY AS WELL AS VELOCITIES AND PRESSURES AT KEY POINTS THROUGHOUT THE FLOW SYSTEM ARE AS TABULATED BELOW.

VAPOR CAVITY

DIST.	.0000	.0640	.1280	.1920	.2560	.3200	.3840	.4479	.5119	.5759	.6399
LOC.	0	1	2	3	4	5	6	7	8	9	10
U	.000	.171	.321	.446	.591	.752	.912	1.074	1.212	1.440	1.682
Z	.030	.031	.033	.036	.040	.044	.049	.053	.060	.064	.078

FULL-FLOWING PIPE SYSTEM

LOC.	(1,0)	(1,1)	(2,0)	(2,10)	(2,20)	(2,30)	(2,40)	(2,50)
V	1.6822	1.6815	1.6758	1.6923	1.5893	1.5816	1.5845	1.5853
H	11.3000	11.3295	11.3295	11.4256	27.4391	30.7421	32.2148	33.1790

AT TIME T = .38784 SECONDS, AFTER 209 COMPLETE CYCLES OF OPERATION, THE VELOCITIES AND DEPTHS IN THE VAPOR CAVITY AS WELL AS VELOCITIES AND PRESSURES AT KEY POINTS THROUGHOUT THE FLOW SYSTEM ARE AS TABULATED BELOW.

VAPOR CAVITY

DIST.	.0000	.0640	.1280	.1920	.2560	.3200	.3840	.4479	.5119	.5759	.6399
LOC.	0	1	2	3	4	5	6	7	8	9	10
U	.000	.150	.282	.396	.531	.679	.826	.977	1.108	1.309	1.446
Z	.029	.030	.032	.035	.038	.042	.046	.050	.055	.058	.066

FULL-FLOWING PIPE SYSTEM

LOC.	(1,0)	(1,1)	(2,0)	(2,10)	(2,20)	(2,30)	(2,40)	(2,50)
V	1.6874	1.6868	1.6811	1.5880	1.5691	1.5687	1.5730	1.5756
H	11.3000	11.3215	11.3215	27.5549	29.2013	30.1870	31.7095	33.1790

AT TIME T = .40640 SECONDS, AFTER 219 COMPLETE CYCLES OF OPERATION, THE VELOCITIES AND DEPTHS IN THE VAPOR CAVITY AS WELL AS VELOCITIES AND PRESSURES AT KEY POINTS THROUGHOUT THE FLOW SYSTEM ARE AS TABULATED BELOW.

VAPOR CAVITY

DIST.	.0000	.0640	.1280	.1920	.2560	.3200	.3840	.4479	.5119	.5759	.6399	.7039
LOC.	0	1	2	3	4	5	6	7	8	9	10	11
U	.000	.131	.248	.354	.479	.615	.753	.892	1.031	1.203	1.316	1.358
Z	.028	.029	.031	.034	.037	.040	.043	.047	.052	.054	.061	.067

FULL-FLOWING PIPE SYSTEM

LOC.	(1,0)	(1,1)	(2,0)	(2,10)	(2,20)	(2,30)	(2,40)	(2,50)
V	1.4891	1.4970	1.4919	1.5666	1.5875	1.5807	1.5599	1.5678
H	11.3000	12.4187	12.4187	29.1074	30.2893	30.1734	31.1983	33.1793

AT TIME T = .42495 SECONDS, AFTER 229 COMPLETE CYCLES OF OPERATION, THE VELOCITIES AND DEPTHS IN THE VAPOR CAVITY IS WELL AS VELOCITIES AND PRESSURES AT KEY POINTS THROUGHOUT THE FLOW SYSTEM ARE AS TABULATED BELOW.

VAPOR CAVITY

DIST.	.0000	.0640	.1280	.1920	.2560	.3200	.3840	.4479	.5119	.5759	.6399	.7039
LOC.	0	1	2	3	4	5	6	7	8	9	10	12
U	.000	.114	.219	.317	.434	.560	.688	.818	.939	1.112	1.242	1.277
Z	.028	.028	.030	.033	.035	.038	.041	.045	.049	.051	.057	.064

FULL-FLOWING PIPE SYSTEM

LOC.	(1,0)	(1,1)	(2,0)	(2,10)	(2,20)	(2,30)	(2,40)	(2,50)
V	1.4592	1.4587	1.4537	1.4719	1.5582	1.5588	1.5486	1.5444
H	11.3000	11.4113	11.4113	16.4861	30.0760	31.2931	31.6835	33.1793

AT TIME T = .44351 SECONDS, AFTER 249 COMPLETE CYCLES OF OPERATION, THE VELOCITIES AND DEPTHS IN THE VAPOR CAVITY IS WELL AS VELOCITIES AND PRESSURES AT KEY POINTS THROUGHOUT THE FLOW SYSTEM ARE AS TABULATED BELOW.

VAPOR CAVITY

DIST.	.0000	.0640	.1280	.1920	.2560	.3200	.3840	.4479	.5119	.5759	.6399	.7039
LOC.	0	1	2	3	4	5	6	7	8	9	10	12
U	.000	.100	.194	.285	.394	.512	.631	.752	.869	1.031	1.182	1.178
Z	.027	.028	.029	.032	.034	.037	.040	.043	.046	.048	.053	.060

FULL-FLOWING PIPE SYSTEM

LOC.	(1,0)	(1,1)	(2,0)	(2,10)	(2,20)	(2,30)	(2,40)	(2,50)
V	1.4495	1.4494	1.4446	1.4459	1.4637	1.4462	1.5434	1.5365
H	11.3000	11.5042	11.3042	13.7304	17.5533	31.5763	33.3069	33.1790

AT TIME T = .46207 SECONDS, AFTER 249 COMPLETE CYCLES OF OPERATION, THE VELOCITIES AND DEPTHS IN THE VAPOR CAVITY IS WELL AS VELOCITIES AND PRESSURES AT KEY POINTS THROUGHOUT THE FLOW SYSTEM ARE AS TABULATED BELOW.

VAPOR CAVITY

DIST.	.0000	.0640	.1280	.1920	.2560	.3200	.3840	.4479	.5119	.5759	.6399	.7039
LOC.	0	1	2	3	4	5	6	7	8	9	10	12
U	.000	.087	.171	.258	.359	.469	.581	.694	.807	.958	1.041	1.093
Z	.027	.027	.029	.031	.033	.035	.038	.041	.044	.046	.051	.057

FULL-FLOWING PIPE SYSTEM

LOC.	(1,0)	(1,1)	(2,0)	(2,10)	(2,20)	(2,30)	(2,40)	(2,50)
V	1.4423	1.4422	1.4373	1.4365	1.4345	1.4489	1.5342	1.5423
H	11.3000	11.3037	11.3037	13.6583	15.2969	19.6201	33.1056	33.1790

AT TIME T = .48062 SECONDS, AFTER 259 COMPLETE CYCLES OF OPERATION, THE VELOCITIES AND DEPTHS IN THE VAPOR CAVITY IS WELL AS VELOCITIES AND PRESSURES AT KEY POINTS THROUGHOUT THE FLOW SYSTEM ARE AS TABULATED BELOW.

VELOCITIES AND PRESSURES AT KEY POINTS THROUGHOUT THE FLOW SYSTEM ARE AS TABULATED BELOW.

VAPOR CAVITY

DIST.	.0000	.0640	.1280	.1920	.2560	.3200	.3840	.4479	.5119	.5759	.6399	.7039	.7679	.8319	.8959
LOC.	0	1	2	3	4	5	6	7	8	9	10	11	12	13	14
U	.000	.076	.152	.233	.328	.430	.535	.642	.752	.892	.966	1.071	1.071	1.157	1.322
Z	.026	.027	.028	.030	.032	.034	.037	.039	.042	.044	.048	.054	.060	.063	.071

FULL-FLOWING PIPE SYSTEM

LOC.	(1,0)	(1,1)	(2,0)	(2,10)	(2,20)	(2,30)	(2,40)	(2,50)
V	1.4342	1.4337	1.4288	1.4261	1.4218	1.4230	1.4283	1.4318
H	11.3000	11.3401	11.3401	14.1434	15.7289	16.8922	19.5991	33.1790

AT TIME T = .49918 SECONDS, AFTER 269 COMPLETE CYCLES OF OPERATION, THE VELOCITIES AND DEPTHS IN THE VAPOR CAVITY AS WELL AS VELOCITIES AND PRESSURES AT KEY POINTS THROUGHOUT THE FLOW SYSTEM ARE AS TABULATED BELOW.

VAPOR CAVITY

DIST.	.0000	.0640	.1280	.1920	.2560	.3200	.3840	.4479	.5119	.5759	.6399	.7039	.7679	.8319	.8959
LOC.	0	1	2	3	4	5	6	7	8	9	10	11	12	13	14
U	.000	.066	.134	.211	.300	.396	.495	.596	.702	.833	.902	.964	1.002	1.072	1.238
Z	.026	.027	.028	.029	.031	.033	.035	.038	.040	.042	.046	.052	.057	.061	.064

DIST. .9599

LOC. 15

U 1.422

Z .075

FULL-FLOWING PIPE SYSTEM

LOC.	(1,0)	(1,1)	(2,0)	(2,10)	(2,20)	(2,30)	(2,40)	(2,50)
V	1.4224	1.4207	1.4159	1.4182	1.4147	1.4213	1.4212	1.4351
H	11.3000	11.4422	11.4422	14.6826	15.7351	15.7213	17.0824	33.1790

AT TIME T = .51774 SECONDS, AFTER 279 COMPLETE CYCLES OF OPERATION, THE VELOCITIES AND DEPTHS IN THE VAPOR CAVITY AS WELL AS VELOCITIES AND PRESSURES AT KEY POINTS THROUGHOUT THE FLOW SYSTEM ARE AS TABULATED BELOW.

VAPOR CAVITY

DIST.	.0000	.0640	.1280	.1920	.2560	.3200	.3840	.4479	.5119	.5759	.6399	.7039	.7679	.8319	.8959
LOC.	0	1	2	3	4	5	6	7	8	9	10	11	12	13	14
U	.000	.058	.120	.192	.275	.365	.458	.554	.657	.778	.841	.879	.937	1.078	1.130
Z	.026	.026	.027	.029	.031	.032	.034	.037	.039	.041	.045	.050	.055	.058	.061

DIST. .9599

LOC. 15

U 1.266

Z .065

FULL-FLOWING PIPE SYSTEM

LOC.	(1,0)	(1,1)	(2,0)	(2,10)	(2,20)	(2,30)	(2,40)	(2,50)
V	1.4065	1.4053	1.4006	1.4046	1.4138	1.4129	1.4287	1.4315
H	11.3000	11.4560	11.4560	14.3098	14.6786	15.9303	29.2934	33.1790

AT TIME T = .53629 SECONDS, AFTER 289 COMPLETE CYCLES OF OPERATION, THE VELOCITIES AND DEPTHS IN THE VAPOR CAVITY AS WELL AS VELOCITIES AND PRESSURES AT KEY POINTS THROUGHOUT THE FLOW SYSTEM ARE AS TABULATED BELOW.

VAPOR CAVITY

DIST.	.0000	.0640	.1280	.1920	.2560	.3200	.3840	.4479	.5119	.5759	.6399	.7039	.7679	.8319	.8959
LOC.	0	1	2	3	4	5	6	7	8	9	10	11	12	13	14
U	.000	.051	.107	.174	.253	.337	.425	.517	.616	.727	.844	.920	.878	.908	1.066
Z	.026	.026	.027	.028	.030	.032	.033	.036	.038	.039	.043	.048	.053	.056	.058

DIST.	.9599	1.0239
LOC.	15	16
U	1.173	1.190
Z	.062	.068

FULL-FLOWING PIPE SYSTEM

LOC.	(1,0)	(1,1)	(2,0)	(2,10)	(2,30)	(2,40)	(2,50)
V	1.3968	1.3961	1.3914	1.4002	1.4029	1.4037	1.4024
H	11.3000	11.3402	11.3402	12.7375	14.5118	28.1920	33.1795

AT TIME T = .59485 SECONDS, AFTER 299 COMPLETE CYCLES OF OPERATION, THE VELOCITIES AND DEPTHS IN THE VAPOR CAVITY AS WELL AS VELOCITIES AND PRESSURES AT KEY POINTS THROUGHOUT THE FLOW SYSTEM ARE AS TABULATED BELOW.

VAPOR CAVITY

DIST.	.0000	.0640	.1280	.1920	.2560	.3200	.3840	.4479	.5119	.5759	.6399	.7039	.7679	.8319	.8959
LOC.	0	1	2	3	4	5	6	7	8	9	10	11	12	13	14
U	.000	.045	.095	.158	.233	.312	.395	.483	.578	.680	.731	.765	.823	.912	1.007
Z	.025	.026	.027	.028	.029	.031	.033	.035	.036	.038	.042	.047	.051	.053	.056

DIST.	.9599	1.0239	1.0879
LOC.	15	16	17
U	1.099	1.129	1.233
Z	.059	.064	.073

FULL-FLOWING PIPE SYSTEM

LOC.	(1,0)	(1,1)	(2,0)	(2,10)	(2,30)	(2,40)	(2,50)
V	1.3959	1.3954	1.3907	1.3930	1.2942	1.2954	1.2960
H	11.3000	11.3219	11.3219	13.1104	26.1967	32.1145	33.1795

AT TIME T = .57341 SECONDS, AFTER 309 COMPLETE CYCLES OF OPERATION, THE VELOCITIES AND DEPTHS IN THE VAPOR CAVITY AS WELL AS VELOCITIES AND PRESSURES AT KEY POINTS THROUGHOUT THE FLOW SYSTEM ARE AS TABULATED BELOW.

VAPOR CAVITY

DIST.	.0000	.0640	.1280	.1920	.2560	.3200	.3840	.4479	.5119	.5759	.6399	.7039	.7679	.8319	.8959
LOC.	0	1	2	3	4	5	6	7	8	9	10	11	12	13	14
U	.000	.039	.086	.144	.214	.289	.368	.452	.543	.636	.682	.714	.772	.859	.951
Z	.025	.026	.026	.027	.029	.030	.032	.034	.035	.037	.041	.045	.049	.052	.054

DIST.	.9599	1.0239	1.0879	1.1519
LOC.	15	16	17	18
U	1.035	1.070	1.145	1.394
Z	.057	.062	.064	.076

FULL-FLOWING PIPE SYSTEM

LOC.	(1,0)	(1,1)	(2,0)	(2,10)	(2,30)	(2,40)	(2,50)
V	1.3948	1.3939	1.3892	1.3866	1.2825	1.2865	1.2885
H	11.3000	11.3595	11.3595	25.8330	30.1181	31.7431	33.1790

AT TIME T = .59197 SECONDS, AFTER 319 COMPLETE CYCLES OF OPERATION, THE VELOCITIES AND DEPTHS IN THE VAPOR CAVITY AS WELL AS VELOCITIES AND PRESSURES AT KEY POINTS THROUGHOUT THE FLOW SYSTEM ARE AS TABULATED BELOW.

VAPOR CAVITY															
DIST.	.0000	.0640	.1280	.1920	.2560	.3200	.3840	.4479	.5119	.5759	.6399	.7039	.7679	.8319	.8959
LOC.	0	1	2	3	4	5	6	7	8	9	10	11	12	13	14
U	.000	.035	.077	.132	.198	.269	.343	.424	.511	.595	.636	.667	.725	.810	.899
Z	.025	.025	.026	.027	.028	.030	.031	.033	.034	.036	.040	.044	.047	.050	.052
DIST.	.9599	1.0239	1.0879	1.1519											
LOC.	15	16	17	18											
U	.977	1.014	1.090	1.215											
Z	.055	.059	.062	.067											

FULL-FLOWING PIPE SYSTEM															
LOC.	(1,0)	(1,1)	(2,0)	(2,10)	(2,20)	(2,30)	(2,40)	(2,50)	(2,60)	(2,70)	(2,80)	(2,90)	(2,100)	(2,110)	(2,120)
V	1.2292	1.2372	1.2340	1.2817	1.2806	1.2773	1.2756	1.2771	1.2756	1.2738	1.2738	1.2680	1.2680	1.2628	1.2628
H	11.3000	13.6268	13.6268	28.4951	29.7469	30.2834	31.2286	31.2286	31.2286	30.8549	30.8549	31.7614	31.7614	33.1790	33.1790

AT TIME T = .61052 SECONDS, AFTER 329 COMPLETE CYCLES OF OPERATION, THE VELOCITIES AND DEPTHS IN THE VAPOR CAVITY AS WELL AS VELOCITIES AND PRESSURES AT KEY POINTS THROUGHOUT THE FLOW SYSTEM ARE AS TABULATED BELOW.

VAPOR CAVITY															
DIST.	.0000	.0640	.1280	.1920	.2560	.3200	.3840	.4479	.5119	.5759	.6399	.7039	.7679	.8319	.8959
LOC.	0	1	2	3	4	5	6	7	8	9	10	11	12	13	14
U	.000	.031	.070	.121	.182	.250	.321	.398	.480	.556	.593	.624	.682	.765	.850
Z	.025	.025	.026	.027	.028	.029	.031	.032	.034	.035	.039	.043	.046	.048	.050
DIST.	.9599	1.0239	1.0879	1.1519	1.2159										
LOC.	15	16	17	18	19										
U	.922	.961	1.036	1.127	1.179										
Z	.053	.057	.060	.063	.075										

FULL-FLOWING PIPE SYSTEM															
LOC.	(1,0)	(1,1)	(2,0)	(2,10)	(2,20)	(2,30)	(2,40)	(2,50)	(2,60)	(2,70)	(2,80)	(2,90)	(2,100)	(2,110)	(2,120)
V	1.1796	1.1794	1.1759	1.2074	1.2741	1.2738	1.2680	1.2680	1.2680	1.2680	1.2680	1.2680	1.2680	1.2628	1.2628
H	11.3000	11.4860	11.4860	18.8599	29.7135	30.8549	31.7614	31.7614	31.7614	30.8549	30.8549	31.7614	31.7614	33.1790	33.1790

AT TIME T = .62908 SECONDS, AFTER 339 COMPLETE CYCLES OF OPERATION, THE VELOCITIES AND DEPTHS IN THE VAPOR CAVITY AS WELL AS VELOCITIES AND PRESSURES AT KEY POINTS THROUGHOUT THE FLOW SYSTEM ARE AS TABULATED BELOW.

VAPOR CAVITY															
DIST.	.0000	.0640	.1280	.1920	.2560	.3200	.3840	.4479	.5119	.5759	.6399	.7039	.7679	.8319	.8959
LOC.	0	1	2	3	4	5	6	7	8	9	10	11	12	13	14
U	.000	.028	.064	.111	.168	.233	.300	.374	.452	.520	.552	.583	.642	.722	.804
Z	.025	.025	.026	.026	.027	.029	.030	.031	.033	.035	.038	.042	.044	.047	.049
DIST.	.9599	1.0239	1.0879	1.1519	1.2159										
LOC.	15	16	17	18	19										
U	.871	.911	.985	1.057	1.089										
Z	.052	.056	.058	.061	.067										

FULL-FLOWING PIPE SYSTEM															
LOC.	(1,0)	(1,1)	(2,0)	(2,10)	(2,20)	(2,30)	(2,40)	(2,50)	(2,60)	(2,70)	(2,80)	(2,90)	(2,100)	(2,110)	(2,120)
V	1.1796	1.1794	1.1759	1.2074	1.2741	1.2738	1.2680	1.2680	1.2680	1.2680	1.2680	1.2680	1.2680	1.2628	1.2628
H	11.3000	11.4860	11.4860	18.8599	29.7135	30.8549	31.7614	31.7614	31.7614	30.8549	30.8549	31.7614	31.7614	33.1790	33.1790

V 1.1704 1.1702 1.1663 1.1686 1.2010 1.2649 1.2611 1.2589
 H 11.3000 11.3108 11.3108 14.0419 20.0131 31.1863 32.8408 33.1790

AT TIME T = .64764 SECONDS, AFTER 349 COMPLETE CYCLES OF OPERATION, THE VELOCITIES AND DEPTHS IN THE VAPOR CAVITY AS WELL AS VELOCITIES AND PRESSURES AT KEY POINTS THROUGHOUT THE FLOW SYSTEM ARE AS TABULATED BELOW.

VAPOR CAVITY

DIST.	.0000	.0640	.1280	.1920	.2560	.3200	.3840	.4479	.5119	.5759	.6399	.7039	.7679	.8319	.8959
LOC.	0	1	2	3	4	5	6	7	8	9	10	11	12	13	14
U	.000	.025	.058	.102	.156	.217	.282	.352	.425	.485	.514	.546	.609	.663	.760
Z	.025	.025	.025	.026	.027	.028	.029	.031	.032	.034	.037	.041	.043	.045	.048
DIST.	.9599	1.0239	1.0879	1.1519	1.2159	1.2799									
LOC.	15	16	17	18	19	20									
U	.823	.865	.937	.999	1.029	1.002									
Z	.050	.054	.056	.059	.064	.074									

FULL-FLOWING PIPE SYSTEM

LOC.	(1,0)	(1,1)	(2,0)	(2,10)	(2,20)	(2,30)	(2,40)	(2,50)
V	1.1646	1.1644	1.1605	1.1600	1.1600	1.1886	1.2559	1.2594
H	11.3000	11.3082	11.3082	13.7555	15.5715	22.0399	32.6405	33.1790

AT TIME T = .66619 SECONDS, AFTER 359 COMPLETE CYCLES OF OPERATION, THE VELOCITIES AND DEPTHS IN THE VAPOR CAVITY AS WELL AS VELOCITIES AND PRESSURES AT KEY POINTS THROUGHOUT THE FLOW SYSTEM ARE AS TABULATED BELOW.

VAPOR CAVITY

DIST.	.0000	.0640	.1280	.1920	.2560	.3200	.3840	.4479	.5119	.5759	.6399	.7039	.7679	.8319	.8959
LOC.	0	1	2	3	4	5	6	7	8	9	10	11	12	13	14
U	.000	.023	.053	.094	.144	.202	.265	.331	.399	.452	.479	.511	.570	.645	.719
Z	.025	.025	.025	.026	.027	.028	.029	.030	.032	.034	.037	.040	.042	.044	.046
DIST.	.9599	1.0239	1.0879	1.1519	1.2159	1.2799									
LOC.	15	16	17	18	19	20									
U	.778	.821	.890	.946	.966	.950									
Z	.049	.052	.055	.058	.062	.066									

FULL-FLOWING PIPE SYSTEM

LOC.	(1,0)	(1,1)	(2,0)	(2,10)	(2,20)	(2,30)	(2,40)	(2,50)
V	1.1581	1.1578	1.1539	1.1518	1.1479	1.1514	1.1873	1.2528
H	11.3000	11.3260	11.3260	14.1139	15.7920	17.0812	22.4666	33.1790

AT TIME T = .68475 SECONDS, AFTER 369 COMPLETE CYCLES OF OPERATION, THE VELOCITIES AND DEPTHS IN THE VAPOR CAVITY AS WELL AS VELOCITIES AND PRESSURES AT KEY POINTS THROUGHOUT THE FLOW SYSTEM ARE AS TABULATED BELOW.

VAPOR CAVITY

DIST.	.0000	.0640	.1280	.1920	.2560	.3200	.3840	.4479	.5119	.5759	.6399	.7039	.7679	.8319	.8959
LOC.	0	1	2	3	4	5	6	7	8	9	10	11	12	13	14
U	.000	.022	.049	.087	.134	.189	.249	.312	.374	.421	.446	.479	.538	.610	.680
Z	.025	.025	.025	.026	.026	.027	.028	.030	.031	.033	.036	.039	.041	.043	.045
DIST.	.9599	1.0239	1.0879	1.1519	1.2159	1.2799	1.3438								
LOC.	15	16	17	18	19	20	21								
U	.736	.780	.846	.896	.913	.917	1.060								
Z	.048	.051	.053	.056	.061	.065	.068								

FULL-FLOWING PIPE SYSTEM

LOC.	(1,0)	(1,1)	(2,0)	(2,10)	(2,20)	(2,30)	(2,40)	(2,50)
V	1.1483	1.1477	1.1438	1.1418	1.1433	1.1466	1.1488	1.1158
H	11.3000	11.3983	11.3983	14.6361	15.6215	16.2337	17.7232	33.1790

AT TIME T = .70331 SECONDS, AFTER 379 COMPLETE CYCLES OF OPERATION, THE VELOCITIES AND DEPTHS IN THE VAPOR CAVITY AS WELL AS VELOCITIES AND PRESSURES AT KEY POINTS THROUGHOUT THE FLOW SYSTEM ARE AS TABULATED BELOW.

VAPOR CAVITY

DIST.	.0000	.0640	.1280	.1920	.2560	.3200	.3840	.4479	.5119	.5759	.6399	.7039	.7679	.8319	.8959
LOC.	0	1	2	3	4	5	6	7	8	9	10	11	12	13	14
U	.000	.020	.046	.081	.125	.176	.234	.294	.350	.392	.415	.449	.507	.577	.645
Z	.025	.025	.025	.025	.026	.027	.028	.029	.031	.033	.035	.038	.040	.042	.044
DIST.	.9599	1.0239	1.0879	1.1519	1.2159	1.2799	1.3438	1.4078							
LOC.	15	16	17	18	19	20	21	22							
U	.696	.741	.803	.848	.885	.885	.987	1.134							
Z	.047	.050	.052	.055	.059	.063	.065	.077							

FULL-FLOWING PIPE SYSTEM

LOC.	(1,0)	(1,1)	(2,0)	(2,10)	(2,20)	(2,30)	(2,40)	(2,50)
V	1.1348	1.1343	1.1305	1.1354	1.1406	1.1407	1.0756	1.0456
H	11.3000	11.4250	11.4250	14.1822	15.0792	16.2673	26.9541	33.1790

AT TIME T = .72186 SECONDS, AFTER 389 COMPLETE CYCLES OF OPERATION, THE VELOCITIES AND DEPTHS IN THE VAPOR CAVITY AS WELL AS VELOCITIES AND PRESSURES AT KEY POINTS THROUGHOUT THE FLOW SYSTEM ARE AS TABULATED BELOW.

VAPOR CAVITY

DIST.	.0000	.0640	.1280	.1920	.2560	.3200	.3840	.4479	.5119	.5759	.6399	.7039	.7679	.8319	.8959
LOC.	0	1	2	3	4	5	6	7	8	9	10	11	12	13	14
U	.000	.019	.043	.075	.116	.165	.220	.276	.328	.364	.386	.422	.479	.546	.608
Z	.024	.025	.025	.025	.026	.027	.028	.029	.030	.032	.035	.037	.039	.041	.043
DIST.	.9599	1.0239	1.0879	1.1519	1.2159	1.2799	1.3438	1.4078							
LOC.	15	16	17	18	19	20	21	22							
U	.658	.704	.763	.802	.817	.849	.930	1.009							
Z	.046	.048	.051	.054	.058	.061	.063	.067							

FULL-FLOWING PIPE SYSTEM

LOC.	(1,0)	(1,1)	(2,0)	(2,10)	(2,20)	(2,30)	(2,40)	(2,50)
V	1.1290	1.1285	1.1247	1.1294	1.1328	1.0699	1.0379	1.0355
H	11.3000	11.3318	11.3318	13.1504	14.8322	25.7526	31.7118	33.1790

AT TIME T = .74042 SECONDS, AFTER 399 COMPLETE CYCLES OF OPERATION, THE VELOCITIES AND DEPTHS IN THE VAPOR CAVITY AS WELL AS VELOCITIES AND PRESSURES AT KEY POINTS THROUGHOUT THE FLOW SYSTEM ARE AS TABULATED BELOW.

VAPOR CAVITY

DIST.	.0000	.0640	.1280	.1920	.2560	.3200	.3840	.4479	.5119	.5759	.6399	.7039	.7679	.8319	.8959
LOC.	0	1	2	3	4	5	6	7	8	9	10	11	12	13	14
U	.000	.018	.040	.071	.109	.155	.207	.260	.306	.337	.359	.396	.452	.516	.575
Z	.024	.024	.025	.025	.026	.026	.027	.028	.030	.032	.034	.037	.039	.040	.042
DIST.	.9599	1.0239	1.0879	1.1519	1.2159	1.2799	1.3438	1.4078	1.4718						
LOC.	15	16	17	18	19	20	21	22	23						

U .623 .668 .723 .759 .774 .812 .886 .951 .966
 Z .045 .047 .050 .053 .057 .060 .061 .064 .074

FULL-FLOWING PIPE SYSTEM

LOC. (1,0) (1,1) (2,0) (2,10) (2,20) (2,30) (2,40) (2,50)
 V 1.1287 1.1282 1.1244 1.1253 1.0591 1.0305 1.0299 1.0313
 H 11.3000 11.3259 11.3259 13.4314 23.7803 30.2245 32.0139 33.1790

AT TIME T = .79898 SECONDS, AFTER 409 COMPLETE CYCLES OF OPERATION, THE VELOCITIES AND DEPTHS IN THE VAPOR CAVITY AS WELL AS VELOCITIES AND PRESSURES AT KEY POINTS THROUGHOUT THE FLOW SYSTEM ARE AS TABULATED BELOW.

VAPOR CAVITY

DIST. .0000 .0640 .1280 .1920 .2560 .3200 .3840 .4479 .5119 .5759 .6399 .7039 .7679 .8319 .8959
 LOC. 0 1 2 3 4 5 6 7 8 9 10 11 12 13 14
 U .000 .017 .038 .066 .102 .145 .194 .244 .285 .312 .334 .371 .427 .488 .544
 Z .024 .024 .025 .025 .025 .026 .027 .028 .029 .031 .034 .036 .038 .039 .041

DIST. .9599 1.0239 1.0879 1.1519 1.2159 1.2799 1.3438 1.4078 1.4718
 LOC. 15 16 17 18 19 20 21 22 23
 U .589 .634 .686 .717 .734 .777 .846 .897 .912
 Z .044 .046 .048 .052 .055 .058 .060 .063 .065

FULL-FLOWING PIPE SYSTEM

LOC. (1,0) (1,1) (2,0) (2,10) (2,20) (2,30) (2,40) (2,50)
 V 1.1258 1.1253 1.1215 1.0564 1.0233 1.0192 1.0229 1.0244
 H 11.3000 11.3302 11.3302 22.9968 28.7725 30.0390 31.7349 33.1790

AT TIME T = .77753 SECONDS, AFTER 419 COMPLETE CYCLES OF OPERATION, THE VELOCITIES AND DEPTHS IN THE VAPOR CAVITY AS WELL AS VELOCITIES AND PRESSURES AT KEY POINTS THROUGHOUT THE FLOW SYSTEM ARE AS TABULATED BELOW.

VAPOR CAVITY

DIST. .0000 .0640 .1280 .1920 .2560 .3200 .3840 .4479 .5119 .5759 .6399 .7039 .7679 .8319 .8959
 LOC. 0 1 2 3 4 5 6 7 8 9 10 11 12 13 14
 U .000 .016 .036 .063 .096 .136 .182 .228 .265 .288 .310 .349 .403 .461 .514
 Z .024 .024 .024 .025 .025 .026 .027 .028 .029 .031 .033 .035 .037 .039 .041

DIST. .9599 1.0239 1.0879 1.1519 1.2159 1.2799 1.3438 1.4078 1.4718 1.5358
 LOC. 15 16 17 18 19 20 21 22 23 24
 U .558 .602 .649 .677 .697 .743 .808 .854 .874 .900
 Z .043 .045 .048 .051 .054 .057 .058 .061 .064 .068

FULL-FLOWING PIPE SYSTEM

LOC. (1,0) (1,1) (2,0) (2,10) (2,20) (2,30) (2,40) (2,50)
 V 1.0110 1.0118 1.0084 1.0200 1.0166 1.0158 1.0137 1.0155
 H 11.3000 14.2594 14.2594 27.8842 29.2493 30.2844 31.2491 33.1790

AT TIME T = .79609 SECONDS, AFTER 429 COMPLETE CYCLES OF OPERATION, THE VELOCITIES AND DEPTHS IN THE VAPOR CAVITY AS WELL AS VELOCITIES AND PRESSURES AT KEY POINTS THROUGHOUT THE FLOW SYSTEM ARE AS TABULATED BELOW.

VAPOR CAVITY

DIST. .0000 .0640 .1280 .1920 .2560 .3200 .3840 .4479 .5119 .5759 .6399 .7039 .7679 .8319 .8959
 LOC. 0 1 2 3 4 5 6 7 8 9 10 11 12 13 14
 U .000 .016 .035 .059 .090 .128 .171 .213 .245 .266 .288 .327 .380 .436 .485
 Z .024 .024 .024 .025 .025 .026 .026 .027 .029 .031 .033 .035 .036 .038 .043

DIST.	.9599	1.0239	1.0879	1.1519	1.2159	1.2799	1.3438	1.4078	1.4718	1.5358
LOC.	15	16	17	18	19	20	21	22	23	24
U	.528	.571	.614	.640	.662	.710	.771	.812	.835	.862
Z	.042	.044	.047	.050	.053	.055	.057	.060	.063	.065

FULL-FLOWING PIPE SYSTEM

LOC.	(1,0)	(1,1)	(2,0)	(2,10)	(2,20)	(2,30)	(2,40)	(2,50)
V	.9232	.9239	.9208	.9688	1.0125	1.0111	1.0084	1.0031
H	11.3000	11.5783	11.5783	21.8117	29.3944	30.4585	31.7708	33.1790

AT TIME T = .81465 SECONDS, AFTER 439 COMPLETE CYCLES OF OPERATION, THE VELOCITIES AND DEPTHS IN THE VAPOR CAVITY AS WELL AS VELOCITIES AND PRESSURES AT KEY POINTS THROUGHOUT THE FLOW SYSTEM ARE AS TABULATED BELOW.

VAPOR CAVITY

DIST.	.0000	.0640	.1280	.1920	.2560	.3200	.3840	.4479	.5119	.5759	.6399	.7039	.7679	.8319	.8959
LOC.	0	1	2	3	4	5	6	7	8	9	10	11	12	13	14
U	.000	.015	.033	.056	.085	.121	.160	.197	.226	.246	.268	.307	.359	.411	.458
Z	.024	.024	.024	.024	.025	.025	.026	.027	.029	.031	.033	.034	.036	.037	.039
DIST.	.9599	1.0239	1.0879	1.1519	1.2159	1.2799	1.3438	1.4078	1.4718	1.5358	1.5998	1.6638	1.7278	1.7918	1.8558
LOC.	15	16	17	18	19	20	21	22	23	24	25	26	27	28	29
U	.499	.541	.580	.604	.629	.678	.735	.773	.798	.823	.857	.887	.917	.947	.977
Z	.041	.044	.046	.049	.052	.054	.056	.059	.062	.065	.069	.072	.075	.078	.081

FULL-FLOWING PIPE SYSTEM

LOC.	(1,0)	(1,1)	(2,0)	(2,10)	(2,20)	(2,30)	(2,40)	(2,50)
V	.9126	.9125	.9094	.9136	.9635	1.0052	1.0006	1.0014
H	11.3000	11.3163	11.3163	14.4106	23.0477	30.8779	32.4266	33.1790

AT TIME T = .83321 SECONDS, AFTER 449 COMPLETE CYCLES OF OPERATION, THE VELOCITIES AND DEPTHS IN THE VAPOR CAVITY AS WELL AS VELOCITIES AND PRESSURES AT KEY POINTS THROUGHOUT THE FLOW SYSTEM ARE AS TABULATED BELOW.

VAPOR CAVITY

DIST.	.0000	.0640	.1280	.1920	.2560	.3200	.3840	.4479	.5119	.5759	.6399	.7039	.7679	.8319	.8959
LOC.	0	1	2	3	4	5	6	7	8	9	10	11	12	13	14
U	.000	.015	.032	.054	.081	.113	.149	.183	.208	.226	.250	.288	.338	.388	.432
Z	.024	.024	.024	.024	.025	.025	.026	.027	.028	.030	.032	.034	.035	.037	.039
DIST.	.9599	1.0239	1.0879	1.1519	1.2159	1.2799	1.3438	1.4078	1.4718	1.5358	1.5998	1.6638	1.7278	1.7918	1.8558
LOC.	15	16	17	18	19	20	21	22	23	24	25	26	27	28	29
U	.472	.511	.547	.570	.598	.647	.700	.735	.761	.785	.809	.833	.857	.881	.905
Z	.041	.043	.045	.048	.051	.053	.055	.058	.061	.064	.068	.071	.074	.077	.080

FULL-FLOWING PIPE SYSTEM

LOC.	(1,0)	(1,1)	(2,0)	(2,10)	(2,20)	(2,30)	(2,40)	(2,50)
V	.9079	.9078	.9047	.9043	.9067	.9532	.9982	.9980
H	11.3000	11.3128	11.3128	13.8469	15.9368	25.0393	32.3248	33.1790

AT TIME T = .85176 SECONDS, AFTER 459 COMPLETE CYCLES OF OPERATION, THE VELOCITIES AND DEPTHS IN THE VAPOR CAVITY AS WELL AS VELOCITIES AND PRESSURES AT KEY POINTS THROUGHOUT THE FLOW SYSTEM ARE AS TABULATED BELOW.

VAPOR CAVITY

DIST.	.0000	.0640	.1280	.1920	.2560	.3200	.3840	.4479	.5119	.5759	.6399	.7039	.7679	.8319	.8959
LOC.	0	1	2	3	4	5	6	7	8	9	10	11	12	13	14
U	.000	.015	.032	.054	.081	.113	.149	.183	.208	.226	.250	.288	.338	.388	.432
Z	.024	.024	.024	.024	.025	.025	.026	.027	.028	.030	.032	.034	.035	.037	.039
DIST.	.9599	1.0239	1.0879	1.1519	1.2159	1.2799	1.3438	1.4078	1.4718	1.5358	1.5998	1.6638	1.7278	1.7918	1.8558
LOC.	15	16	17	18	19	20	21	22	23	24	25	26	27	28	29
U	.472	.511	.547	.570	.598	.647	.700	.735	.761	.785	.809	.833	.857	.881	.905
Z	.041	.043	.045	.048	.051	.053	.055	.058	.061	.064	.068	.071	.074	.077	.080

FULL-FLOWING PIPE SYSTEM															
AT TIME T = .87032 SECONDS, AFTER 469 COMPLETE CYCLES OF OPERATION, THE VELOCITIES AND DEPTHS IN THE VAPOR CAVITY AS WELL AS VELOCITIES AND PRESSURES AT KEY POINTS THROUGHOUT THE FLOW SYSTEM ARE AS TABULATED BELOW.															
VAPOR CAVITY															
DIST.	.0000	.0640	.1280	.1920	.2560	.3200	.3840	.4479	.5119	.5759	.6399	.7039	.7679	.8319	.8959
LOC.	0	1	2	3	4	5	6	7	8	9	10	11	12	13	14
U	.000	.014	.031	.051	.077	.107	.139	.168	.190	.208	.232	.271	.318	.370	.427
Z	.024	.024	.024	.024	.025	.025	.026	.027	.028	.030	.032	.033	.035	.038	.038
DIST.	.9599	1.0239	1.0879	1.1519	1.2159	1.2799	1.3438	1.4078	1.4718	1.5358	1.5998	1.6638			
LOC.	15	16	17	18	19	20	21	22	23	24	25	26	27	28	29
U	.446	.403	.516	.538	.569	.617	.667	.700	.751	.781	.902				
Z	.040	.042	.045	.047	.050	.052	.054	.057	.060	.062	.064	.0675			
FULL-FLOWING PIPE SYSTEM															
AT TIME T = .87032 SECONDS, AFTER 469 COMPLETE CYCLES OF OPERATION, THE VELOCITIES AND DEPTHS IN THE VAPOR CAVITY AS WELL AS VELOCITIES AND PRESSURES AT KEY POINTS THROUGHOUT THE FLOW SYSTEM ARE AS TABULATED BELOW.															
VAPOR CAVITY															

FULL-FLOWING PIPE SYSTEM															
AT TIME T = .88888 SECONDS, AFTER 479 COMPLETE CYCLES OF OPERATION, THE VELOCITIES AND DEPTHS IN THE VAPOR CAVITY AS WELL AS VELOCITIES AND PRESSURES AT KEY POINTS THROUGHOUT THE FLOW SYSTEM ARE AS TABULATED BELOW.															
VAPOR CAVITY															
DIST.	.0000	.0640	.1280	.1920	.2560	.3200	.3840	.4479	.5119	.5759	.6399	.7039	.7679	.8319	.8959
LOC.	0	1	2	3	4	5	6	7	8	9	10	11	12	13	14
U	.000	.014	.030	.049	.073	.100	.129	.154	.173	.190	.216	.254	.299	.354	.38*
Z	.024	.024	.024	.024	.024	.025	.026	.027	.028	.030	.031	.033	.034	.036	.038
DIST.	.9599	1.0239	1.0879	1.1519	1.2159	1.2799	1.3438	1.4078	1.4718	1.5358	1.5998	1.6638			
LOC.	15	16	17	18	19	20	21	22	23	24	25	26	27	28	29
U	.420	.456	.486	.508	.541	.588	.634	.665	.690	.718	.745	.802			
Z	.040	.042	.044	.047	.049	.051	.053	.056	.059	.061	.064	.068			
FULL-FLOWING PIPE SYSTEM															
AT TIME T = .90743 SECONDS, AFTER 489 COMPLETE CYCLES OF OPERATION, THE VELOCITIES AND DEPTHS IN THE VAPOR CAVITY AS WELL AS VELOCITIES AND PRESSURES AT KEY POINTS THROUGHOUT THE FLOW SYSTEM ARE AS TABULATED BELOW.															
VAPOR CAVITY															

FULL-FLOWING PIPE SYSTEM															
AT TIME T = .90743 SECONDS, AFTER 489 COMPLETE CYCLES OF OPERATION, THE VELOCITIES AND DEPTHS IN THE VAPOR CAVITY AS WELL AS VELOCITIES AND PRESSURES AT KEY POINTS THROUGHOUT THE FLOW SYSTEM ARE AS TABULATED BELOW.															
VAPOR CAVITY															
DIST.	.0000	.0640	.1280	.1920	.2560	.3200	.3840	.4479	.5119	.5759	.6399	.7039	.7679	.8319	.8959
LOC.	0	1	2	3	4	5	6	7	8	9	10	11	12	13	14
U	.000	.014	.029	.047	.069	.094	.119	.140	.157	.174	.200	.238	.282	.324	.361
Z	.024	.024	.024	.024	.024	.025	.025	.026	.028	.030	.031	.033	.034	.035	.037
DIST.	.9599	1.0239	1.0879	1.1519	1.2159	1.2799	1.3438	1.4078	1.4718	1.5358	1.5998	1.6638	1.7278		
LOC.	15	16	17	18	19	20	21	22	23	24	25	26	27	28	29
U	.396	.429	.457	.480	.514	.560	.603	.632	.657	.685	.715	.759	.882		
Z	.039	.041	.043	.046	.048	.050	.052	.055	.058	.060	.063	.065	.077		
FULL-FLOWING PIPE SYSTEM															
AT TIME T = .90743 SECONDS, AFTER 489 COMPLETE CYCLES OF OPERATION, THE VELOCITIES AND DEPTHS IN THE VAPOR CAVITY AS WELL AS VELOCITIES AND PRESSURES AT KEY POINTS THROUGHOUT THE FLOW SYSTEM ARE AS TABULATED BELOW.															
VAPOR CAVITY															

FULL-FLOWING PIPE SYSTEM															
AT TIME T = .90743 SECONDS, AFTER 489 COMPLETE CYCLES OF OPERATION, THE VELOCITIES AND DEPTHS IN THE VAPOR CAVITY AS WELL AS VELOCITIES AND PRESSURES AT KEY POINTS THROUGHOUT THE FLOW SYSTEM ARE AS TABULATED BELOW.															
VAPOR CAVITY															
DIST.	.0000	.0640	.1280	.1920	.2560	.3200	.3840	.4479	.5119	.5759	.6399	.7039	.7679	.8319	.8959
LOC.	0	1	2	3	4	5	6	7	8	9	10	11	12	13	14
U	.000	.014	.029	.047	.069	.094	.119	.140	.157	.174	.200	.238	.282	.324	.361
Z	.024	.024	.024	.024	.024	.025	.025	.026	.028	.030	.031	.033	.034	.035	.037
DIST.	.9599	1.0239	1.0879	1.1519	1.2159	1.2799	1.3438	1.4078	1.4718	1.5358	1.5998	1.6638	1.7278		
LOC.	15	16	17	18	19	20	21	22	23	24	25	26	27	28	29
U	.396	.429	.457	.480	.514	.560	.603	.632	.657	.685	.715	.759	.882		
Z	.039	.041	.043	.046	.048	.050	.052	.055	.058	.060	.063	.065	.077		
FULL-FLOWING PIPE SYSTEM															
AT TIME T = .90743 SECONDS, AFTER 489 COMPLETE CYCLES OF OPERATION, THE VELOCITIES AND DEPTHS IN THE VAPOR CAVITY AS WELL AS VELOCITIES AND PRESSURES AT KEY POINTS THROUGHOUT THE FLOW SYSTEM ARE AS TABULATED BELOW.															
VAPOR CAVITY															

FULL-FLOWING PIPE SYSTEM															
AT TIME T = .90743 SECONDS, AFTER 489 COMPLETE CYCLES OF OPERATION, THE VELOCITIES AND DEPTHS IN THE VAPOR CAVITY AS WELL AS VELOCITIES AND PRESSURES AT KEY POINTS THROUGHOUT THE FLOW SYSTEM ARE AS TABULATED BELOW.															
VAPOR CAVITY															
DIST.	.0000	.0640	.1280	.1920	.2560	.3200	.3840	.4479	.5119	.5759	.6399	.7039	.7679	.8319	.8959
LOC.	0	1	2	3	4	5	6	7	8	9	10	11	12	13	14
U	.000	.014	.029	.047	.069	.094	.119	.140	.157	.174	.200	.238	.282	.324	.361
Z	.024	.024	.024	.024	.024	.025	.025	.026	.028	.030	.031	.033	.034	.035	.037
DIST.	.9599	1.0239	1.0879	1.1519	1.2159	1.2799	1.3438	1.4078	1.4718	1.5358	1.5998	1.6638	1.7278		
LOC.	15	16	17	18	19	20	21	22	23	24	25	26	27	28	29
U	.396	.429	.457	.480	.514	.560	.603	.632	.657	.685	.715	.759	.882		
Z	.039	.041	.043	.046	.048	.050	.052	.055	.058	.060	.063	.065	.077		
FULL-FLOWING PIPE SYSTEM															
AT TIME T = .90743 SECONDS, AFTER 489 COMPLETE CYCLES OF OPERATION, THE VELOCITIES AND DEPTHS IN THE VAPOR CAVITY AS WELL AS VELOCITIES AND PRESSURES AT KEY POINTS THROUGHOUT THE FLOW SYSTEM ARE AS TABULATED BELOW.															
VAPOR CAVITY															

DIST.	.0000	.0640	.1280	.1920	.2560	.3200	.3840	.4479	.5119	.5759	.6399	.7039	.7679	.8319	.8959
LOC.	0	1	2	3	4	5	6	7	8	9	10	11	12	13	14
U	.000	.014	.028	.045	.065	.087	.109	.127	.141	.158	.185	.223	.264	.314	.372
Z	.024	.024	.024	.024	.024	.025	.025	.026	.028	.029	.031	.032	.033	.034	.037
DIST.	.9599	1.0239	1.0879	1.1519	1.2159	1.2799	1.3438	1.4078	1.4718	1.5358	1.5998	1.6638	1.7278		
LOC.	15	16	17	18	19	20	21	22	23	24	25	26	27		
U	.373	.404	.429	.453	.488	.533	.572	.600	.625	.653	.683	.725	.785		
Z	.038	.041	.043	.045	.047	.049	.051	.054	.057	.059	.062	.064	.068		

FULL-FLOWING PIPE SYSTEM

LOC.	(1,0)	(1,1)	(2,0)	(2,10)	(2,20)	(2,30)	(2,40)	(2,50)
V	.8797	.8793	.8763	.8777	.8820	.8409	.7913	.7872
H	11.3000	11.3236	11.3236	13.5408	15.0965	22.7689	31.3638	33.1793

AT TIME T = .92599 SECONDS, AFTER 499 COMPLETE CYCLES OF OPERATION, THE VELOCITIES AND DEPTHS IN THE VAPOR CAVITY AS WELL AS VELOCITIES AND PRESSURES AT KEY POINTS THROUGHOUT THE FLOW SYSTEM ARE AS TABULATED BELOW.

VAPOR CAVITY

DIST.	.0000	.0640	.1280	.1920	.2560	.3200	.3840	.4479	.5119	.5759	.6399	.7039	.7679	.8319	.8959
LOC.	0	1	2	3	4	5	6	7	8	9	10	11	12	13	14
U	.000	.013	.028	.044	.062	.081	.100	.114	.127	.144	.171	.208	.248	.282	.319
Z	.024	.024	.024	.024	.024	.025	.025	.026	.028	.029	.031	.032	.033	.035	.039
DIST.	.9599	1.0239	1.0879	1.1519	1.2159	1.2799	1.3438	1.4078	1.4718	1.5358	1.5998	1.6638	1.7278	1.7918	
LOC.	15	16	17	18	19	20	21	22	23	24	25	26	27	28	
U	.350	.379	.403	.428	.463	.506	.543	.569	.594	.623	.655	.689	.746	.878	
Z	.038	.040	.042	.045	.047	.049	.051	.053	.056	.058	.061	.063	.065	.077	

FULL-FLOWING PIPE SYSTEM

LOC.	(1,0)	(1,1)	(2,0)	(2,10)	(2,20)	(2,30)	(2,40)	(2,50)
V	.8786	.8780	.8750	.8749	.8318	.7853	.7826	.7828
H	11.3000	11.3375	11.3375	13.5147	20.8342	29.8760	31.9428	33.1790

AT TIME T = .94455 SECONDS, AFTER 509 COMPLETE CYCLES OF OPERATION, THE VELOCITIES AND DEPTHS IN THE VAPOR CAVITY AS WELL AS VELOCITIES AND PRESSURES AT KEY POINTS THROUGHOUT THE FLOW SYSTEM ARE AS TABULATED BELOW.

VAPOR CAVITY

DIST.	.0000	.0640	.1280	.1920	.2560	.3200	.3840	.4479	.5119	.5759	.6399	.7039	.7679	.8319	.8959
LOC.	0	1	2	3	4	5	6	7	8	9	10	11	12	13	14
U	.000	.013	.027	.042	.058	.075	.090	.102	.113	.130	.158	.194	.232	.267	.293
Z	.024	.024	.024	.024	.024	.024	.025	.026	.028	.029	.030	.031	.033	.034	.036
DIST.	.9599	1.0239	1.0879	1.1519	1.2159	1.2799	1.3438	1.4078	1.4718	1.5358	1.5998	1.6638	1.7278	1.7918	
LOC.	15	16	17	18	19	20	21	22	23	24	25	26	27	28	
U	.328	.355	.378	.403	.438	.480	.514	.539	.564	.593	.626	.661	.698	.766	
Z	.038	.040	.042	.044	.046	.048	.050	.052	.055	.057	.060	.062	.064	.068	

FULL-FLOWING PIPE SYSTEM

LOC.	(1,0)	(1,1)	(2,0)	(2,10)	(2,20)	(2,30)	(2,40)	(2,50)
V	.8756	.8753	.8723	.8293	.7785	.7735	.7768	.7780
H	11.3000	11.3239	11.3239	19.8778	28.2585	30.0019	31.7341	33.1790

AT TIME T = .96310 SECONDS, AFTER 519 COMPLETE CYCLES OF OPERATION, THE VELOCITIES AND DEPTHS IN THE VAPOR CAVITY AS WELL AS VELOCITIES AND PRESSURES AT KEY POINTS THROUGHOUT THE FLOW SYSTEM ARE AS TABULATED BELOW.

VAPOR CAVITY

DIST.	.0000	.0640	.1280	.1920	.2560	.3200	.3840	.4479	.5119	.5759	.6399	.7039	.7679	.8319	.8959
LOC.	0	1	2	3	4	5	6	7	8	9	10	11	12	13	14
U	.000	.013	.026	.040	.055	.069	.081	.090	.100	.117	.145	.180	.217	.250	.279
Z	.024	.024	.024	.024	.024	.024	.025	.026	.027	.029	.030	.031	.032	.034	.035
DIST.	.9599	1.0239	1.0879	1.1519	1.2159	1.2799	1.3438	1.4078	1.4718	1.5358	1.5998	1.6638	1.7278	1.7918	1.8558
LOC.	15	16	17	18	19	20	21	22	23	24	25	26	27	28	29
U	.307	.331	.354	.380	.416	.455	.486	.511	.536	.565	.598	.633	.669	.706	.744
Z	.037	.039	.041	.043	.045	.047	.049	.052	.054	.056	.059	.061	.063	.065	.078

FULL-FLOWING PIPE SYSTEM

LOC.	(1,C)	(1,1)	(2,0)	(2,10)	(2,20)	(2,30)	(2,40)	(2,50)
V	.8070	.8031	.8004	.7762	.7711	.7700	.7690	.7709
H	11.3000	13.7947	13.7947	27.3066	29.0369	30.1183	31.2820	33.1790

AT TIME T = .98166 SECONDS, AFTER 529 COMPLETE CYCLES OF OPERATION, THE VELOCITIES AND DEPTHS IN THE VAPOR CAVITY AS WELL AS VELOCITIES AND PRESSURES AT KEY POINTS THROUGHOUT THE FLOW SYSTEM ARE AS TABULATED BELOW.

VAPOR CAVITY

DIST.	.0000	.0640	.1280	.1920	.2560	.3200	.3840	.4479	.5119	.5759	.6399	.7039	.7679	.8319	.8959
LOC.	0	1	2	3	4	5	6	7	8	9	10	11	12	13	14
U	.000	.013	.025	.038	.051	.063	.072	.079	.088	.105	.133	.167	.201	.235	.260
Z	.024	.024	.024	.024	.024	.024	.025	.026	.027	.029	.030	.031	.032	.034	.035
DIST.	.9599	1.0239	1.0879	1.1519	1.2159	1.2799	1.3438	1.4078	1.4718	1.5358	1.5998	1.6638	1.7278	1.7918	1.8558
LOC.	15	16	17	18	19	20	21	22	23	24	25	26	27	28	29
U	.286	.309	.331	.358	.394	.430	.459	.483	.508	.538	.571	.606	.641	.674	.718
Z	.037	.039	.041	.043	.045	.047	.049	.051	.053	.056	.058	.060	.062	.064	.072

FULL-FLOWING PIPE SYSTEM

LOC.	(1,0)	(1,1)	(2,0)	(2,10)	(2,20)	(2,30)	(2,40)	(2,50)
V	.6839	.6861	.6838	.7424	.7677	.7666	.7641	.7660
H	11.3000	11.8018	11.8018	24.1979	29.1653	30.3164	31.6060	33.1790

AT TIME T = 1.00022 SECONDS, AFTER 539 COMPLETE CYCLES OF OPERATION, THE VELOCITIES AND DEPTHS IN THE VAPOR CAVITY AS WELL AS VELOCITIES AND PRESSURES AT KEY POINTS THROUGHOUT THE FLOW SYSTEM ARE AS TABULATED BELOW.

VAPOR CAVITY

DIST.	.0000	.0640	.1280	.1920	.2560	.3200	.3840	.4479	.5119	.5759	.6399	.7039	.7679	.8319	.8959
LOC.	0	1	2	3	4	5	6	7	8	9	10	11	12	13	14
U	.000	.012	.025	.037	.048	.057	.064	.069	.077	.094	.121	.154	.187	.216	.242
Z	.023	.023	.024	.024	.024	.024	.025	.026	.027	.028	.029	.031	.032	.033	.035
DIST.	.9599	1.0239	1.0879	1.1519	1.2159	1.2799	1.3438	1.4078	1.4718	1.5358	1.5998	1.6638	1.7278	1.7918	1.8558
LOC.	15	16	17	18	19	20	21	22	23	24	25	26	27	28	29
U	.266	.287	.310	.337	.372	.406	.433	.457	.482	.512	.545	.579	.612	.635	.663
Z	.037	.038	.040	.042	.044	.046	.048	.050	.053	.055	.057	.059	.061	.064	.068

FULL-FLOWING PIPE SYSTEM

LOC.	(1,0)	(1,1)	(2,0)	(2,10)	(2,20)	(2,30)	(2,40)	(2,50)
V	.6704	.6706	.6683	.6755	.7380	.7618	.7577	.7600
H	11.3000	11.3493	11.3493	14.9698	25.4916	30.6508	32.2528	33.1790

AT TIME T = 1.01877 SECONDS, AFTER 549 COMPLETE CYCLES OF OPERATION, THE VELOCITIES AND DEPTHS IN THE VAPOR CAVITY AS WELL AS VELOCITIES AND PRESSURES AT KEY POINTS THROUGHOUT THE FLOW SYSTEM ARE AS TABULATED BELOW.

VAPOR CAVITY

DIST.	.0000	.0640	.1280	.1920	.2560	.3200	.3840	.4479	.5119	.5759	.6399	.7039	.7679	.8319	.8959
LOC.	0	1	2	3	4	5	6	7	8	9	10	11	12	13	14
U	.000	.012	.024	.035	.044	.051	.055	.059	.066	.083	.113	.141	.172	.230	.225
Z	.023	.023	.024	.024	.024	.024	.025	.026	.027	.028	.029	.030	.032	.033	.035
DIST.	.9599	1.0239	1.0879	1.1519	1.2159	1.2799	1.3438	1.4078	1.4718	1.5358	1.5998	1.6638	1.7278	1.7918	1.8558
LOC.	15	16	17	18	19	20	21	22	23	24	25	26	27	28	29
U	.247	.267	.289	.317	.350	.382	.408	.431	.457	.487	.520	.553	.583	.61	.627
Z	.036	.038	.040	.042	.044	.045	.048	.050	.052	.054	.056	.058	.060	.063	.065

FULL-FLOWING PIPE SYSTEM

LOC.	(1,0)	(1,1)	(2,0)	(2,10)	(2,20)	(2,30)	(2,40)	(2,50)
V	.6664	.6663	.6640	.6640	.6699	.7292	.7551	.7553
H	11.3000	11.3205	11.3205	13.9370	16.4854	27.4400	32.2629	33.1790

AT TIME T = 1.03733 SECONDS, AFTER 559 COMPLETE CYCLES OF OPERATION, THE VELOCITIES AND DEPTHS IN THE VAPOR CAVITY AS WELL AS VELOCITIES AND PRESSURES AT KEY POINTS THROUGHOUT THE FLOW SYSTEM ARE AS TABULATED BELOW.

VAPOR CAVITY

DIST.	.0000	.1280	.2560	.3840	.5119	.6399	.7679	.8959	1.0239	1.1519	1.2799	1.4078	1.5358	1.6638	1.7918
LOC.	0	2	4	6	8	10	12	14	16	18	20	22	24	26	28
U	.000	.023	.040	.047	.057	.089	.158	.207	.247	.297	.359	.407	.463	.527	.573
Z	.023	.023	.024	.025	.027	.029	.031	.034	.038	.041	.045	.049	.053	.057	.062

DIST.	1.9198
LOC.	30
U	.605
Z	.071

FULL-FLOWING PIPE SYSTEM

LOC.	(1,0)	(1,1)	(2,0)	(2,10)	(2,20)	(2,30)	(2,40)	(2,50)
V	.6620	.6619	.6597	.6584	.6554	.6634	.7270	.7528
H	11.3000	11.3340	11.3340	14.1129	15.8997	18.1262	28.4228	33.1790

AT TIME T = 1.05589 SECONDS, AFTER 569 COMPLETE CYCLES OF OPERATION, THE VELOCITIES AND DEPTHS IN THE VAPOR CAVITY AS WELL AS VELOCITIES AND PRESSURES AT KEY POINTS THROUGHOUT THE FLOW SYSTEM ARE AS TABULATED BELOW.

VAPOR CAVITY

DIST.	.0000	.1280	.2560	.3840	.5119	.6399	.7679	.8959	1.0239	1.1519	1.2799	1.4078	1.5358	1.6638	1.7918
LOC.	0	2	4	6	8	10	12	14	16	18	20	22	24	26	28
U	.000	.021	.036	.039	.048	.089	.144	.190	.229	.278	.337	.383	.440	.502	.541
Z	.023	.023	.024	.025	.027	.029	.031	.034	.038	.041	.045	.049	.053	.057	.061

DIST.	1.9198
LOC.	30
U	.560
Z	.068

FULL-FLOWING PIPE SYSTEM

LOC.	(1,0)	(1,1)	(2,0)	(2,10)	(2,20)	(2,30)	(2,40)	(2,50)
------	-------	-------	-------	--------	--------	--------	--------	--------

V .0554 .6554 .6514 .6533 .6520 .6510 .6532 .6524 .6514 .6534
 H 11.3000 11.3805 11.3805 14.5726 15.7521 16.8989 16.8989 19.1162 19.1162 3.1713

AT TIME T = 1.07445 SECONDS, AFTER 579 COMPLETE CYCLES OF OPERATION, THE VELOCITIES AND DEPTHS IN THE VAPOR CAVITY AS WELL AS VELOCITIES AND PRESSURES AT KEY POINTS THROUGHOUT THE FLOW SYSTEM ARE AS TABULATED BELOW.

VAPOR CAVITY

DIST. .0600 .1280 .2560 .3840 .5119 .6399 .7679 .8959 1.0239 1.1519 1.2799 1.4078 1.5358 1.6638 1.7918
 LOC. 0 2 4 6 8 10 12 14 16 18 20 22 24 26 28
 U .000 .020 .032 .044 .056 .068 .080 .092 .104 .116 .128 .140 .152 .164 .176
 Z .023 .023 .024 .025 .027 .029 .031 .034 .037 .041 .044 .048 .052 .056 .061

DIST. 1.9198
 LOC. 30
 U .538
 Z .065

FULL-FLOWING PIPE SYSTEM

LOC. (1,0) (1,1) (2,0) (2,10) (2,20) (2,30) (2,40) (2,50)
 V .6453 .6453 .6431 .6468 .6489 .6499 .6253 .5773
 H 11.3000 11.4289 11.4289 14.2962 15.3721 16.7433 21.6973 33.1790

AT TIME T = 1.09300 SECONDS, AFTER 589 COMPLETE CYCLES OF OPERATION, THE VELOCITIES AND DEPTHS IN THE VAPOR CAVITY AS WELL AS VELOCITIES AND PRESSURES AT KEY POINTS THROUGHOUT THE FLOW SYSTEM ARE AS TABULATED BELOW.

VAPOR CAVITY

DIST. .0600 .1280 .2560 .3840 .5119 .6399 .7679 .8959 1.0239 1.1519 1.2799 1.4078 1.5358 1.6638 1.7918
 LOC. 0 2 4 6 8 10 12 14 16 18 20 22 24 26 28
 U .000 .019 .028 .034 .042 .050 .057 .065 .073 .081 .089 .097 .105 .113 .121
 Z .023 .023 .024 .025 .027 .029 .031 .034 .037 .040 .044 .048 .051 .055 .059

DIST. 1.9198 1.9838
 LOC. 30 31
 U .513 .585
 Z .065 .069

FULL-FLOWING PIPE SYSTEM

LOC. (1,0) (1,1) (2,0) (2,10) (2,20) (2,30) (2,40) (2,50)
 V .6430 .6423 .6402 .6410 .6448 .6212 .5590 .5521
 H 11.3000 11.3465 11.3465 13.7081 15.2893 20.3551 30.8202 33.1790

AT TIME T = 1.11156 SECONDS, AFTER 599 COMPLETE CYCLES OF OPERATION, THE VELOCITIES AND DEPTHS IN THE VAPOR CAVITY AS WELL AS VELOCITIES AND PRESSURES AT KEY POINTS THROUGHOUT THE FLOW SYSTEM ARE AS TABULATED BELOW.

VAPOR CAVITY

DIST. .0600 .1280 .2560 .3840 .5119 .6399 .7679 .8959 1.0239 1.1519 1.2799 1.4078 1.5358 1.6638 1.7918
 LOC. 0 2 4 6 8 10 12 14 16 18 20 22 24 26 28
 U .000 .017 .024 .031 .038 .045 .052 .060 .067 .074 .081 .089 .097 .105 .113
 Z .023 .023 .024 .025 .027 .028 .031 .033 .037 .040 .043 .047 .051 .055 .060

DIST. 1.9198 1.9838
 LOC. 30 31
 U .490 .535
 Z .064 .066

FULL-FLOWING PIPE SYSTEM

LOC.	(1,0)	(1,1)	(2,0)	(2,10)	(2,20)	(2,30)	(2,40)	(2,50)
V	.6408	.6404	.6383	.6382	.6133	.5541	.5479	.5473
H	11.3000	11.3257	11.3257	13.6195	18.4772	29.3393	31.8684	33.1795

AT TIME T = 1.13012 SECONDS, AFTER 609 COMPLETE CYCLES OF OPERATION, THE VELOCITIES AND DEPTHS IN THE VAPOR CAVITY AS WELL AS VELOCITIES AND PRESSURES AT KEY POINTS THROUGHOUT THE FLOW SYSTEM ARE AS TABULATED BELOW.

VAPOR CAVITY

DIST.	.0000	.1280	.2560	.3840	.5119	.6399	.7679	.8959	1.0239	1.1519	1.2799	1.4078	1.5358	1.6638	1.7918
LOC.	0	2	4	6	8	10	12	14	16	18	20	22	24	26	28
U	.000	.016	.019	.011	.017	.051	.091	.126	.161	.208	.254	.298	.353	.4.2	.427
Z	.023	.023	.024	.025	.027	.028	.030	.033	.036	.040	.043	.047	.050	.054	.059

DIST.	1.9198	1.9838	2.0478
LOC.	30	31	32
U	.471	.510	.638
Z	.063	.065	.076

FULL-FLOWING PIPE SYSTEM

LOC.	(1,0)	(1,1)	(2,0)	(2,10)	(2,20)	(2,30)	(2,40)	(2,50)
V	.6384	.6381	.6360	.6107	.5477	.5402	.5428	.5438
H	11.3000	11.3204	11.3204	17.3568	27.6433	29.9815	31.7420	33.1795

AT TIME T = 1.14867 SECONDS, AFTER 619 COMPLETE CYCLES OF OPERATION, THE VELOCITIES AND DEPTHS IN THE VAPOR CAVITY AS WELL AS VELOCITIES AND PRESSURES AT KEY POINTS THROUGHOUT THE FLOW SYSTEM ARE AS TABULATED BELOW.

VAPOR CAVITY

DIST.	.0000	.1280	.2560	.3840	.5119	.6399	.7679	.8959	1.0239	1.1519	1.2799	1.4078	1.5358	1.6638	1.7918
LOC.	0	2	4	6	8	10	12	14	16	18	20	22	24	26	28
U	.000	.014	.014	.005	.011	.042	.078	.110	.145	.192	.235	.279	.332	.377	.402
Z	.023	.023	.024	.025	.027	.028	.030	.033	.036	.039	.043	.046	.050	.054	.059

DIST.	1.9198	1.9838	2.0478
LOC.	30	31	32
U	.451	.477	.543
Z	.063	.064	.069

FULL-FLOWING PIPE SYSTEM

LOC.	(1,0)	(1,1)	(2,0)	(2,10)	(2,20)	(2,30)	(2,40)	(2,50)
V	.6007	.5963	.5943	.5457	.5376	.5365	.5361	.5379
H	11.3000	12.9274	12.9274	26.5941	28.8506	30.0483	31.3356	33.1790

AT TIME T = 1.16723 SECONDS, AFTER 629 COMPLETE CYCLES OF OPERATION, THE VELOCITIES AND DEPTHS IN THE VAPOR CAVITY AS WELL AS VELOCITIES AND PRESSURES AT KEY POINTS THROUGHOUT THE FLOW SYSTEM ARE AS TABULATED BELOW.

VAPOR CAVITY

DIST.	.0000	.1280	.2560	.3840	.5119	.6399	.7679	.8959	1.0239	1.1519	1.2799	1.4078	1.5358	1.6638	1.7918
LOC.	0	2	4	6	8	10	12	14	16	18	20	22	24	26	28
U	.000	.011	.010	.001	.005	.033	.066	.095	.130	.175	.217	.260	.312	.353	.379
Z	.023	.023	.024	.025	.027	.028	.030	.033	.036	.039	.042	.046	.049	.053	.058

DIST.	1.9198	1.9838	2.0478
LOC.	30	31	32

U .429 .453 .499
Z .062 .064 .067

FULL-FLOWING PIPE SYSTEM

LOC.	(1,0)	(1,1)	(2,0)	(2,10)	(2,30)	(2,40)	(2,50)
V	.4605	.4642	.4626	.5345	.5326	.5316	.5284
H	11.3000	12.3306	25.6961	28.9998	30.2044	31.5278	33.1790

AT TIME T = 1.18579 SECONDS, AFTER 659 COMPLETE CYCLES OF OPERATION, THE VELOCITIES AND DEPTHS IN THE VAPOR CAVITY AS WELL AS VELOCITIES AND PRESSURES AT KEY POINTS THROUGHOUT THE FLOW SYSTEM ARE AS TABULATED BELOW.

VAPOR CAVITY

DIST.	.0000	.1280	.2560	.3840	.5119	.6399	.7679	.8959	1.0239	1.1519	1.2799	1.4078	1.5358	1.6638	1.7918
LOC.	0	2	4	6	8	10	12	14	16	18	20	22	24	26	28
V	.0000	.0399	.005	-.007	-.001	.025	.028	.030	.036	.039	.042	.046	.049	.053	.057
Z	.023	.023	.024	.025	.026	.028	.030	.033	.036	.039	.042	.046	.049	.053	.057

DIST.	1.9198	1.9838	2.0478
LOC.	30	31	32
V	.4394	.431	.467
Z	.061	.063	.066

FULL-FLOWING PIPE SYSTEM

LOC.	(1,0)	(1,1)	(2,0)	(2,10)	(2,30)	(2,40)	(2,50)
V	.4394	.4396	.4382	.4516	.5173	.5296	.5252
H	11.3000	11.3992	11.3992	16.0394	27.0570	30.4780	33.1790

AT TIME T = 1.20434 SECONDS, AFTER 649 COMPLETE CYCLES OF OPERATION, THE VELOCITIES AND DEPTHS IN THE VAPOR CAVITY AS WELL AS VELOCITIES AND PRESSURES AT KEY POINTS THROUGHOUT THE FLOW SYSTEM ARE AS TABULATED BELOW.

VAPOR CAVITY

DIST.	.0000	.1280	.2560	.3840	.5119	.6399	.7679	.8959	1.0239	1.1519	1.2799	1.4078	1.5358	1.6638	1.7918
LOC.	0	2	4	6	8	10	12	14	16	18	20	22	24	26	28
V	.0000	.007	.000	-.013	-.007	.017	.042	.067	.101	.143	.182	.224	.272	.316	.337
Z	.023	.023	.024	.025	.026	.028	.030	.033	.036	.039	.042	.045	.049	.053	.057

DIST.	1.9198	1.9838	2.0478
LOC.	30	31	32
V	.386	.409	.441
Z	.061	.062	.065

FULL-FLOWING PIPE SYSTEM

LOC.	(1,0)	(1,1)	(2,0)	(2,10)	(2,30)	(2,40)	(2,50)
V	.4352	.4352	.4337	.4343	.5097	.5233	.5234
H	11.3000	11.3296	11.3296	14.0531	17.5409	28.9463	33.1790

AT TIME T = 1.22290 SECONDS, AFTER 659 COMPLETE CYCLES OF OPERATION, THE VELOCITIES AND DEPTHS IN THE VAPOR CAVITY AS WELL AS VELOCITIES AND PRESSURES AT KEY POINTS THROUGHOUT THE FLOW SYSTEM ARE AS TABULATED BELOW.

VAPOR CAVITY

DIST.	.0000	.1280	.2560	.3840	.5119	.6399	.7679	.8959	1.0239	1.1519	1.2799	1.4078	1.5358	1.6638	1.7918
LOC.	0	2	4	6	8	10	12	14	16	18	20	22	24	26	28
V	.0000	.004	-.005	-.018	-.013	.008	.031	.054	.087	.127	.165	.207	.252	.284	.316
Z	.023	.023	.024	.025	.026	.028	.030	.033	.035	.038	.042	.045	.048	.052	.056

DIST. 1.9198 1.9838 2.0478 2.1118
 LOC. 30 31 32 33
 U .365 .388 .397 .395
 Z .060 .062 .065 .070

FULL-FLOWING PIPE SYSTEM

LOC. (1,0) (1,1) (2,0) (2,10) (2,20) (2,30) (2,40) (2,50)
 V .4315 .4314 .4300 .4293 .4268 .4407 .5073 .5213
 H 11.3000 11.3400 11.3400 14.1068 15.9561 19.2552 30.0867 33.1790

AT TIME T = 1.24146 SECONDS, AFTER 609 COMPLETE CYCLES OF OPERATION, THE VELOCITIES AND DEPTHS IN THE VAPOR CAVITY AS WELL AS VELOCITIES AND PRESSURES AT KEY POINTS THROUGHOUT THE FLOW SYSTEM ARE AS TABULATED BELOW.

VAPOR CAVITY

DIST. .0000 .1280 .2560 .3840 .5119 .6399 .7679 .8959 1.0239 1.1519 1.2799 1.4078 1.5358 1.6638 1.7918
 LOC. 0 2 4 6 8 10 12 14 16 18 20 22 24 26 28
 U .000 .001 .009 .023 .041 .060 .073 .091 .112 .149 .191 .233 .252 .277 .297
 Z .023 .023 .024 .025 .026 .028 .030 .032 .035 .038 .041 .044 .048 .052 .056

DIST. 1.9198 1.9838 2.0478 2.1118
 LOC. 30 31 32 33
 U .345 .362 .356 .358
 Z .059 .061 .065 .068

FULL-FLOWING PIPE SYSTEM

LOC. (1,0) (1,1) (2,0) (2,10) (2,20) (2,30) (2,40) (2,50)
 V .4261 .4261 .4246 .4229 .4228 .4245 .4389 .4913
 H 11.3000 11.3779 11.3779 14.5192 15.8187 17.1117 20.3308 33.1790

AT TIME T = 1.26001 SECONDS, AFTER 679 COMPLETE CYCLES OF OPERATION, THE VELOCITIES AND DEPTHS IN THE VAPOR CAVITY AS WELL AS VELOCITIES AND PRESSURES AT KEY POINTS THROUGHOUT THE FLOW SYSTEM ARE AS TABULATED BELOW.

VAPOR CAVITY

DIST. .0000 .1280 .2560 .3840 .5119 .6399 .7679 .8959 1.0239 1.1519 1.2799 1.4078 1.5358 1.6638 1.7918
 LOC. 0 2 4 6 8 10 12 14 16 18 20 22 24 26 28
 U .000 .001 .014 .027 .024 .028 .030 .029 .030 .038 .041 .044 .048 .052 .055
 Z .023 .023 .024 .025 .026 .028 .030 .032 .035 .038 .041 .044 .048 .052 .055

DIST. 1.9198 1.9838 2.0478 2.1118
 LOC. 30 31 32 33
 U .323 .333 .327 .338
 Z .059 .061 .064 .066

FULL-FLOWING PIPE SYSTEM

LOC. (1,0) (1,1) (2,0) (2,10) (2,20) (2,30) (2,40) (2,50)
 V .4172 .4172 .4158 .4185 .4202 .4216 .4086 .3569
 H 11.3000 11.4333 11.4333 14.3670 15.6751 16.8955 20.2929 33.1790

AT TIME T = 1.27857 SECONDS, AFTER 689 COMPLETE CYCLES OF OPERATION, THE VELOCITIES AND DEPTHS IN THE VAPOR CAVITY AS WELL AS VELOCITIES AND PRESSURES AT KEY POINTS THROUGHOUT THE FLOW SYSTEM ARE AS TABULATED BELOW.

VAPOR CAVITY

DIST. .0000 .1280 .2560 .3840 .5119 .6399 .7679 .8959 1.0239 1.1519 1.2799 1.4078 1.5358 1.6638 1.7918
 LOC. 0 2 4 6 8 10 12 14 16 18 20 22 24 26 28

U	.000	-.004	-.019	-.032	-.029	-.016	-.002	.017	.047	.082	.118	.158	.195	.272	.379
Z	.023	.023	.024	.025	.026	.028	.030	.032	.035	.038	.041	.044	.047	.051	.055
DIST. 1.9198 1.9838 2.0478 2.1118															
LOC. 30 31 32 33															
U	.299	.305	.306	.324											
Z	.059	.061	.064	.065											

FULL-FLOWING PIPE SYSTEM

LOC.	(1,0)	(1,1)	(2,0)	(2,10)	(2,20)	(2,30)	(2,40)	(2,50)
V	.4138	.4134	.4120	.4134	.4167	.4044	.3391	.3261
H	11.3000	11.3260	11.3260	13.8683	15.4423	18.8085	29.7597	33.1790

AT TIME T = 1.29713 SECONDS, AFTER 699 COMPLETE CYCLES OF OPERATION, THE VELOCITIES AND DEPTHS IN THE VAPOR CAVITY AS WELL AS VELOCITIES AND PRESSURES AT KEY POINTS THROUGHOUT THE FLOW SYSTEM ARE AS TABULATED BELOW.

VAPOR CAVITY

DIST.	.0000	.1280	.2560	.3840	.5119	.6399	.7679	.8959	1.0239	1.1519	1.2799	1.4078	1.5358	1.6638	1.7918
LOC.	0	2	4	6	8	10	12	14	16	18	20	22	24	26	28
U	.000	-.007	-.023	-.036	-.034	-.024	-.013	.005	.034	.067	.102	.142	.176	.213	.241
Z	.023	.023	.024	.025	.026	.028	.030	.032	.035	.038	.041	.044	.047	.051	.054

DIST.	1.9198	1.9838	2.0478	2.1118	2.1757
LOC.	30	31	32	33	34
U	.275	.280	.290	.300	.362
Z	.058	.061	.063	.065	.072

FULL-FLOWING PIPE SYSTEM

LOC.	(1,0)	(1,1)	(2,0)	(2,10)	(2,20)	(2,30)	(2,40)	(2,50)
V	.4120	.4117	.4133	.4103	.3977	.3349	.3220	.3214
H	11.3000	11.3203	11.3203	13.6808	16.9951	28.2870	31.7649	33.1790

AT TIME T = 1.31569 SECONDS, AFTER 709 COMPLETE CYCLES OF OPERATION, THE VELOCITIES AND DEPTHS IN THE VAPOR CAVITY AS WELL AS VELOCITIES AND PRESSURES AT KEY POINTS THROUGHOUT THE FLOW SYSTEM ARE AS TABULATED BELOW.

VAPOR CAVITY

DIST.	.0000	.1280	.2560	.3840	.5119	.6399	.7679	.8959	1.0239	1.1519	1.2799	1.4078	1.5358	1.6638	1.7918
LOC.	0	2	4	6	8	10	12	14	16	18	20	22	24	26	28
U	.000	-.011	-.028	-.040	-.039	-.032	-.023	-.006	.022	.053	.088	.126	.158	.185	.223
Z	.023	.023	.024	.025	.026	.028	.030	.032	.035	.037	.040	.043	.047	.051	.054

DIST.	1.9198	1.9838	2.0478	2.1118	2.1757
LOC.	30	31	32	33	34
U	.252	.257	.268	.274	.312
Z	.058	.060	.063	.065	.068

FULL-FLOWING PIPE SYSTEM

LOC.	(1,0)	(1,1)	(2,0)	(2,10)	(2,20)	(2,30)	(2,40)	(2,50)
V	.4100	.4098	.4084	.3947	.3287	.3154	.3172	.3170
H	11.3000	11.3211	11.3211	15.7171	26.5036	29.9410	31.7518	33.1790

AT TIME T = 1.33424 SECONDS, AFTER 719 COMPLETE CYCLES OF OPERATION, THE VELOCITIES AND DEPTHS IN THE VAPOR CAVITY AS WELL AS VELOCITIES AND PRESSURES AT KEY POINTS THROUGHOUT THE FLOW SYSTEM ARE AS TABULATED BELOW.

VAPOR CAVITY

DIST.	.0000	.1280	.2560	.3840	.5119	.6399	.7679	.8959	1.0239	1.1519	1.2799	1.4078	1.5358	1.6638	1.7918
LOC.	0	2	4	6	8	10	12	14	16	18	20	22	24	26	28
U	.000	-.014	-.032	-.044	-.044	-.033	-.033	-.017	.009	.040	.073	.110	.140	.167	.234
Z	.023	.023	.024	.025	.026	.028	.030	.032	.035	.037	.040	.043	.047	.050	.054
DIST.	1.9198	1.9838	2.0478	2.1118	2.1757										
LOC.	30	31	32	33	34										
U	.229	.235	.246	.258	.290										
Z	.058	.060	.062	.064	.065										

FULL-FLOWING PIPE SYSTEM

LOC.	(1,0)	(1,1)	(2,0)	(2,10)	(2,20)	(2,30)	(2,40)	(2,50)
V	.3900	.3868	.3855	.3270	.3125	.3109	.3113	.3130
H	11.3000	12.2530	12.2530	25.3990	28.6512	29.9721	31.3982	33.1790

AT TIME T = 1.35280 SECONDS, AFTER 729 COMPLETE CYCLES OF OPERATION, THE VELOCITIES AND DEPTHS IN THE VAPOR CAVITY AS WELL AS VELOCITIES AND PRESSURES AT KEY POINTS THROUGHOUT THE FLOW SYSTEM ARE AS TABULATED BELOW.

VAPOR CAVITY

DIST.	.0000	.1280	.2560	.3840	.5119	.6399	.7679	.8959	1.0239	1.1519	1.2799	1.4078	1.5358	1.6638	1.7918
LOC.	0	2	4	6	8	10	12	14	16	18	20	22	24	26	28
U	.000	-.017	-.036	-.048	-.050	-.047	-.043	-.028	-.003	.026	.059	.094	.122	.150	.185
Z	.023	.024	.024	.025	.026	.028	.030	.032	.034	.037	.040	.043	.046	.050	.053
DIST.	1.9198	1.9838	2.0478	2.1118	2.1757	2.2397									
LOC.	30	31	32	33	34	35									
U	.207	.214	.226	.246	.252	.279									
Z	.058	.060	.062	.064	.066	.070									

FULL-FLOWING PIPE SYSTEM

LOC.	(1,0)	(1,1)	(2,0)	(2,10)	(2,20)	(2,30)	(2,40)	(2,50)
V	.2547	.2580	.2571	.3034	.3092	.3084	.3067	.3048
H	11.3000	12.9740	12.9740	26.4569	28.8703	30.1084	31.4416	33.1790

AT TIME T = 1.37136 SECONDS, AFTER 739 COMPLETE CYCLES OF OPERATION, THE VELOCITIES AND DEPTHS IN THE VAPOR CAVITY AS WELL AS VELOCITIES AND PRESSURES AT KEY POINTS THROUGHOUT THE FLOW SYSTEM ARE AS TABULATED BELOW.

VAPOR CAVITY

DIST.	.0000	.1280	.2560	.3840	.5119	.6399	.7679	.8959	1.0239	1.1519	1.2799	1.4078	1.5358	1.6638	1.7918
LOC.	0	2	4	6	8	10	12	14	16	18	20	22	24	26	28
U	.000	-.020	-.040	-.052	-.055	-.055	-.052	-.038	-.014	.013	.045	.078	.105	.133	.166
Z	.023	.024	.024	.025	.026	.028	.030	.032	.034	.037	.040	.043	.046	.050	.053
DIST.	1.9198	1.9838	2.0478	2.1118	2.1757	2.2397									
LOC.	30	31	32	33	34	35									
U	.185	.194	.208	.224	.229	.216									
Z	.057	.060	.061	.063	.066	.075									

FULL-FLOWING PIPE SYSTEM

LOC.	(1,0)	(1,1)	(2,0)	(2,10)	(2,20)	(2,30)	(2,40)	(2,50)
V	.2165	.2169	.2161	.2395	.2993	.3051	.3018	.3005
H	11.3000	11.4523	11.4523	17.7517	27.9177	30.3390	31.9299	33.1790

AT TIME T = 1.38991 SECONDS, AFTER 749 COMPLETE CYCLES OF OPERATION, THE VELOCITIES AND DEPTHS IN THE VAPOR CAVITY AS WELL AS VELOCITIES AND PRESSURES AT KEY POINTS THROUGHOUT THE FLOW SYSTEM ARE AS TABULATED BELOW.

VAPOR CAVITY

DIST.	.0000	.1280	.2560	.3840	.5119	.6399	.7679	.8959	1.0239	1.1519	1.2799	1.4078	1.5358	1.6638	1.7918
LOC.	0	2	4	6	8	10	12	14	16	18	20	22	24	26	28
U	.000	-.023	-.044	-.056	-.063	-.063	-.061	-.048	-.026	.001	.032	.063	.088	.117	.147
Z	.023	.024	.024	.025	.026	.028	.030	.032	.034	.037	.040	.043	.046	.049	.053

DIST.	1.9198	1.9838	2.0478	2.1118	2.1757	2.2397
LOC.	30	31	32	33	34	35
U	.165	.175	.189	.200	.189	.187
Z	.057	.059	.061	.063	.066	.072

FULL-FLOWING PIPE SYSTEM

LOC.	(1,0)	(1,1)	(2,0)	(2,10)	(2,20)	(2,30)	(2,40)	(2,50)
V	.2116	.2116	.2109	.2123	.2355	.2928	.2988	.2989
H	11.3000	11.3398	11.3398	14.2229	19.2499	29.7417	32.1175	33.1790

AT TIME T = 1.40847 SECONDS, AFTER 759 COMPLETE CYCLES OF OPERATION, THE VELOCITIES AND DEPTHS IN THE VAPOR CAVITY AS WELL AS VELOCITIES AND PRESSURES AT KEY POINTS THROUGHOUT THE FLOW SYSTEM ARE AS TABULATED BELOW.

VAPOR CAVITY

DIST.	.0000	.1280	.2560	.3840	.5119	.6399	.7679	.8959	1.0239	1.1519	1.2799	1.4078	1.5358	1.6638	1.7918
LOC.	0	2	4	6	8	10	12	14	16	18	20	22	24	26	28
U	.000	-.026	-.048	-.060	-.065	-.070	-.070	-.058	-.037	-.012	.018	.047	.071	.100	.128
Z	.023	.024	.025	.025	.026	.028	.030	.032	.034	.037	.039	.042	.046	.049	.053

DIST.	1.9198	1.9838	2.0478	2.1118	2.1757	2.2397
LOC.	30	31	32	33	34	35
U	.145	.156	.169	.171	.161	.168
Z	.057	.059	.061	.063	.066	.069

FULL-FLOWING PIPE SYSTEM

LOC.	(1,0)	(1,1)	(2,0)	(2,10)	(2,20)	(2,30)	(2,40)	(2,50)
V	.2085	.2085	.2078	.2070	.2060	.2295	.2899	.2971
H	11.3000	11.3470	11.3470	14.1206	16.0774	21.0602	31.0366	33.1790

AT TIME T = 1.42703 SECONDS, AFTER 769 COMPLETE CYCLES OF OPERATION, THE VELOCITIES AND DEPTHS IN THE VAPOR CAVITY AS WELL AS VELOCITIES AND PRESSURES AT KEY POINTS THROUGHOUT THE FLOW SYSTEM ARE AS TABULATED BELOW.

VAPOR CAVITY

DIST.	.0000	.1280	.2560	.3840	.5119	.6399	.7679	.8959	1.0239	1.1519	1.2799	1.4078	1.5358	1.6638	1.7918
LOC.	0	2	4	6	8	10	12	14	16	18	20	22	24	26	28
U	.000	-.029	-.051	-.064	-.071	-.077	-.079	-.068	-.048	-.024	.005	.032	.055	.084	.109
Z	.023	.024	.025	.025	.026	.028	.030	.032	.034	.037	.039	.042	.046	.049	.053

DIST.	1.9198	1.9838	2.0478	2.1118	2.1757	2.2397
LOC.	30	31	32	33	34	35
U	.126	.137	.146	.144	.141	.155
Z	.057	.059	.061	.063	.066	.067

FULL-FLOWING PIPE SYSTEM

LOC.	(1,0)	(1,1)	(2,0)	(2,10)	(2,20)	(2,30)	(2,40)	(2,50)
V	.2041	.2040	.2034	.2015	.2010	.2033	.2281	.2809
H	11.3000	11.3776	11.3776	14.4783	15.9325	17.4039	22.1983	33.1790

AT TIME T = 1.44558 SECONDS, AFTER 779 COMPLETE CYCLES OF OPERATION, THE VELOCITIES AND DEPTHS IN THE VAPOR CAVITY AS WELL AS VELOCITIES AND PRESSURES AT KEY POINTS THROUGHOUT THE FLOW SYSTEM ARE AS TABULATED BELOW.

VAPOR CAVITY

DIST.	.0000	.1280	.2560	.3840	.5119	.6399	.7679	.8959	1.0239	1.1519	1.2799	1.4078	1.5358	1.6638	1.7918
LOC.	0	2	4	6	8	10	12	14	16	18	20	22	24	26	28
U	.000	-.031	-.055	-.076	-.085	-.087	-.087	-.077	-.059	-.036	-.008	.017	.040	.058	.090
Z	.024	.024	.025	.025	.026	.028	.030	.032	.034	.037	.039	.042	.045	.049	.052

DIST.	1.9198	1.9838	2.0478	2.1118	2.1757	2.2397
LOC.	30	31	32	33	34	35
U	.107	.117	.122	.126	.126	.146
Z	.056	.058	.061	.063	.065	.066

FULL-FLOWING PIPE SYSTEM

LOC.	(1,0)	(1,1)	(2,0)	(2,10)	(2,20)	(2,30)	(2,40)	(2,50)
V	.1965	.1965	.1958	.1974	.1988	.1996	.1946	.1595
H	11.3000	11.4337	11.4337	14.4673	15.8046	17.0710	19.6157	33.1790

AT TIME T = 1.46414 SECONDS, AFTER 789 COMPLETE CYCLES OF OPERATION, THE VELOCITIES AND DEPTHS IN THE VAPOR CAVITY AS WELL AS VELOCITIES AND PRESSURES AT KEY POINTS THROUGHOUT THE FLOW SYSTEM ARE AS TABULATED BELOW.

VAPOR CAVITY

DIST.	.0000	.1280	.2560	.3840	.5119	.6399	.7679	.8959	1.0239	1.1519	1.2799	1.4078	1.5358	1.6638	1.7918
LOC.	0	2	4	6	8	10	12	14	16	18	20	22	24	26	28
U	.000	-.034	-.058	-.071	-.082	-.092	-.095	-.087	-.070	-.047	-.021	.002	.025	.051	.071
Z	.024	.024	.025	.025	.027	.028	.030	.032	.034	.036	.039	.042	.045	.049	.052

DIST.	1.9198	1.9838	2.0478	2.1118	2.1757	2.2397
LOC.	30	31	32	33	34	35
U	.088	.096	.098	.100	.115	.138
Z	.056	.058	.061	.063	.065	.065

FULL-FLOWING PIPE SYSTEM

LOC.	(1,0)	(1,1)	(2,0)	(2,10)	(2,20)	(2,30)	(2,40)	(2,50)
V	.1918	.1916	.1909	.1931	.1959	.1901	.1309	.1083
H	11.3000	11.3168	11.3168	14.0380	15.6060	18.0134	28.0898	33.1790

AT TIME T = 1.48270 SECONDS, AFTER 799 COMPLETE CYCLES OF OPERATION, THE VELOCITIES AND DEPTHS IN THE VAPOR CAVITY AS WELL AS VELOCITIES AND PRESSURES AT KEY POINTS THROUGHOUT THE FLOW SYSTEM ARE AS TABULATED BELOW.

VAPOR CAVITY

DIST.	.0000	.1280	.2560	.3840	.5119	.6399	.7679	.8959	1.0239	1.1519	1.2799	1.4078	1.5358	1.6638	1.7918
LOC.	0	2	4	6	8	10	12	14	16	18	20	22	24	26	28
U	.000	-.036	-.061	-.075	-.087	-.099	-.103	-.096	-.080	-.059	-.035	-.013	.010	.035	.053
Z	.024	.024	.025	.026	.027	.028	.030	.032	.034	.036	.039	.042	.045	.048	.052

DIST.	1.9198	1.9838	2.0478	2.1118	2.1757	2.2397
LOC.	30	31	32	33	34	35
U	.068	.074	.077	.083	.106	.131
Z	.056	.058	.060	.063	.064	.064

FULL-FLOWING PIPE SYSTEM

LOC.	(1,0)	(1,1)	(2,0)	(2,10)	(2,20)	(2,30)	(2,40)	(2,50)
------	-------	-------	-------	--------	--------	--------	--------	--------

V .1904 .1903 .1895 .1844 .1275 .1037 .1122
 H 11.5000 11.5220 11.7328 10.2447 26.6277 31.6333 33.1790

AT TIME T = 1.56125 SECONDS, AFTER 809 COMPLETE CYCLES OF OPERATION, THE VELOCITIES AND DEPTHS IN THE VAPOR CAVITY AS WELL AS VELOCITIES AND PRESSURES AT KEY POINTS THROUGHOUT THE FLOW SYSTEM ARE AS TABULATED BELOW.

VAPOR CAVITY

DIST. .0000 .1280 .2560 .3840 .5119 .6399 .7679 .8959 1.0239 1.1519 1.2799 1.4078 1.5358 1.6638 1.7918
 LOC. 0 2 4 6 8 10 12 14 16 18 20 22 24 26 28
 U .000 -0.038 -0.064 -0.079 -0.093 -0.106 -0.111 -0.105 -0.090 -0.070 -0.048 -0.027 -0.005 .018 .035
 Z .024 .024 .025 .026 .027 .028 .030 .032 .034 .036 .039 .042 .045 .048 .052

DIST. 1.9198 1.9838 2.0478 2.1118 2.1757 2.2397 2.3037
 LOC. 30 31 32 33 34 35 36
 U .049 .053 .057 .070 .092 .088 .122
 Z .056 .058 .060 .062 .064 .066 .071

FULL-FLOWING PIPE SYSTEM

LOC. (1,0) (1,1) (2,0) (2,10) (2,20) (2,30) (2,40) (2,50)
 V .1889 .1888 .1881 .1809 .1206 .0979 .0984 .0947
 H 11.3000 11.3265 11.3265 14.8038 24.7568 29.8796 31.7699 33.1790

AT TIME T = 1.51981 SECONDS, AFTER 819 COMPLETE CYCLES OF OPERATION, THE VELOCITIES AND DEPTHS IN THE VAPOR CAVITY AS WELL AS VELOCITIES AND PRESSURES AT KEY POINTS THROUGHOUT THE FLOW SYSTEM ARE AS TABULATED BELOW.

VAPOR CAVITY

DIST. .0000 .1280 .2560 .3840 .5119 .6399 .7679 .8959 1.0239 1.1519 1.2799 1.4078 1.5358 1.6638 1.7918
 LOC. 0 2 4 6 8 10 12 14 16 18 20 22 24 26 28
 U .000 -0.040 -0.067 -0.083 -0.098 -0.112 -0.118 -0.113 -0.100 -0.081 -0.061 -0.041 -0.020 .012 .037
 Z .024 .024 .025 .026 .027 .028 .030 .032 .034 .036 .039 .042 .045 .048 .052

DIST. 1.9198 1.9838 2.0478 2.1118 2.1757 2.2397 2.3037
 LOC. 30 31 32 33 34 35 36
 U .029 .033 .040 .055 .070 .066 .093
 Z .056 .058 .060 .062 .064 .066 .068

FULL-FLOWING PIPE SYSTEM

LOC. (1,0) (1,1) (2,0) (2,10) (2,20) (2,30) (2,40) (2,50)
 V .1783 .1763 .1757 .1194 .0943 .0919 .0932 .0947
 H 11.5000 11.8291 11.8291 23.6314 28.4522 29.9089 31.4685 33.1790

AT TIME T = 1.53837 SECONDS, AFTER 829 COMPLETE CYCLES OF OPERATION, THE VELOCITIES AND DEPTHS IN THE VAPOR CAVITY AS WELL AS VELOCITIES AND PRESSURES AT KEY POINTS THROUGHOUT THE FLOW SYSTEM ARE AS TABULATED BELOW.

VAPOR CAVITY

DIST. .0000 .1280 .2560 .3840 .5119 .6399 .7679 .8959 1.0239 1.1519 1.2799 1.4078 1.5358 1.6638 1.7918
 LOC. 0 2 4 6 8 10 12 14 16 18 20 22 24 26 28
 U .000 -0.042 -0.070 -0.087 -0.104 -0.119 -0.126 -0.122 -0.110 -0.092 -0.073 -0.055 -0.034 -0.019 -0.001
 Z .024 .024 .025 .026 .027 .028 .030 .032 .034 .036 .039 .042 .045 .048 .052

DIST. 1.9198 1.9838 2.0478 2.1118 2.1757 2.2397 2.3037
 LOC. 30 31 32 33 34 35 36
 U .009 .014 .024 .038 .048 .053 .078
 Z .056 .058 .060 .062 .064 .066 .068

FULL-FLOWING PIPE SYSTEM

LOC.	(1,0)	(1,1)	(2,0)	(2,10)	(2,20)	(2,30)	(2,40)	(2,50)
V	.0634	.0647	.0645	.0890	.0895	.0896	.0882	.0874
H	11.5000	13.3542	13.3542	26.7703	28.7427	30.2414	31.3603	31.1790

AT TIME T = 1.55694 SECONDS, AFTER 849 COMPLETE CYCLES OF OPERATION, THE VELOCITIES AND DEPTHS IN THE VAPOR CAVITY AS WELL AS VELOCITIES AND PRESSURES AT KEY POINTS THROUGHOUT THE FLOW SYSTEM ARE AS TABULATED BELOW.

VAPOR CAVITY

DIST.	.0000	.1280	.2560	.3840	.5119	.6399	.7679	.8959	1.0239	1.1519	1.2799	1.4078	1.5358	1.6638	1.7918
LOC.	0	2	4	6	8	10	12	14	16	18	20	22	24	26	28
U	.000	-.043	-.072	-.091	-.139	-.126	-.130	-.130	-.129	-.103	-.086	-.069	-.049	-.031	-.019
Z	.024	.024	.025	.026	.027	.028	.030	.032	.034	.036	.039	.042	.045	.048	.052
DIST.	1.9198	1.9838	2.0478	2.1118	2.1757	2.2397	2.3037								
LOC.	30	31	32	33	34	35	36								
U	-.010	-.003	.007	.020	.029	.040	.064								
Z	.056	.058	.060	.061	.063	.065	.067								

FULL-FLOWING PIPE SYSTEM

LOC.	(1,0)	(1,1)	(2,0)	(2,10)	(2,20)	(2,30)	(2,40)	(2,50)
V	-.0005	.0004	.0034	.0356	.0844	.0867	.0839	.0817
H	11.5000	11.5429	11.5429	19.8177	28.3019	30.2434	31.7929	31.1790

AT TIME T = 1.57548 SECONDS, AFTER 849 COMPLETE CYCLES OF OPERATION, THE VELOCITIES AND DEPTHS IN THE VAPOR CAVITY AS WELL AS VELOCITIES AND PRESSURES AT KEY POINTS THROUGHOUT THE FLOW SYSTEM ARE AS TABULATED BELOW.

VAPOR CAVITY

DIST.	.0000	.1280	.2560	.3840	.5119	.6399	.7679	.8959	1.0239	1.1519	1.2799	1.4078	1.5358	1.6638	1.7918
LOC.	0	2	4	6	8	10	12	14	16	18	20	22	24	26	28
U	.000	-.045	-.075	-.095	-.115	-.132	-.141	-.139	-.129	-.114	-.098	-.082	-.063	-.048	-.037
Z	.024	.025	.025	.026	.027	.028	.030	.032	.034	.036	.039	.042	.045	.048	.052
DIST.	1.9198	1.9838	2.0478	2.1118	2.1757	2.2397	2.3037								
LOC.	30	31	32	33	34	35	36								
U	-.028	-.020	-.009	.002	.012	.022	.045								
Z	.056	.058	.059	.061	.063	.065	.068								

FULL-FLOWING PIPE SYSTEM

LOC.	(1,0)	(1,1)	(2,0)	(2,10)	(2,20)	(2,30)	(2,40)	(2,50)
V	-.0071	-.0070	-.0070	-.0041	.0320	.0786	.0802	.0803
H	11.5000	11.5497	11.5497	14.4270	21.2862	30.1146	32.1040	31.1790

AT TIME T = 1.59404 SECONDS, AFTER 859 COMPLETE CYCLES OF OPERATION, THE VELOCITIES AND DEPTHS IN THE VAPOR CAVITY AS WELL AS VELOCITIES AND PRESSURES AT KEY POINTS THROUGHOUT THE FLOW SYSTEM ARE AS TABULATED BELOW.

VAPOR CAVITY

DIST.	.0000	.1280	.2560	.3840	.5119	.6399	.7679	.8959	1.0239	1.1519	1.2799	1.4078	1.5358	1.6638	1.7918
LOC.	0	2	4	6	8	10	12	14	16	18	20	22	24	26	28
U	.000	-.046	-.077	-.099	-.120	-.138	-.148	-.147	-.139	-.125	-.111	-.095	-.078	-.064	-.055
Z	.025	.025	.025	.026	.027	.028	.030	.032	.034	.036	.039	.042	.045	.048	.052
DIST.	1.9198	1.9838	2.0478	2.1118	2.1757	2.2397	2.3037								
LOC.	30	31	32	33	34	35	36								

U -.045 -.037 -.026 -.015 -.005 .001 .025
 Z .056 .057 .059 .061 .063 .065 .068

FULL-FLOWING PIPE SYSTEM

LOC. (1,0) (1,1) (2,0) (2,10) (2,20) (2,30) (2,40) (2,50)
 V -.0101 -.0101 -.0100 -.0098 -.0256 .0751 .0783
 H 11.3000 11.3478 11.3478 14.0930 16.1931 23.1648 31.5450 33.1790

AT TIME T = 1.61260 SECONDS, AFTER 869 COMPLETE CYCLES OF OPERATION, THE VELOCITIES AND DEPTHS IN THE VAPOR CAVITY AS WELL AS VELOCITIES AND PRESSURES AT KEY POINTS THROUGHOUT THE FLOW SYSTEM ARE AS TABULATED BELOW.

VAPOR CAVITY

DIST. .0000 .1280 .2560 .3840 .5119 .6399 .7679 .8959 1.0239 1.1519 1.2799 1.4078 1.5358 1.6636 1.7918
 LOC. 0 2 4 6 8 10 12 14 16 18 20 22 24 26 28
 U .000 -.047 -.080 -.104 -.126 -.145 -.155 -.148 -.136 -.123 -.108 -.093 -.081 -.073
 Z .025 .025 .025 .026 .027 .029 .030 .032 .034 .036 .039 .042 .045 .048 .052

DIST. 1.9198 1.9838 2.0478 2.1118 2.1757 2.2397 2.3037
 LOC. 30 31 32 33 34 35 36
 U -.062 -.053 -.042 -.032 -.024 -.019 .004
 Z .055 .057 .059 .061 .063 .065 .068

FULL-FLOWING PIPE SYSTEM

LOC. (1,0) (1,1) (2,0) (2,10) (2,20) (2,30) (2,40) (2,50)
 V -.0140 -.0141 -.0140 -.0157 -.0170 .0243 .0699
 H 11.3000 11.3723 11.3723 14.3902 15.9682 17.6377 24.3009 33.1790

→ THE DIRECTION OF FLOW AT THE RESERVOIR END OF THE PIPE SYSTEM HAS REVERSED AT TIME T = 1.62837 SECONDS.

AT TIME T = 1.63115 SECONDS, AFTER 879 COMPLETE CYCLES OF OPERATION, THE VELOCITIES AND DEPTHS IN THE VAPOR CAVITY AS WELL AS VELOCITIES AND PRESSURES AT KEY POINTS THROUGHOUT THE FLOW SYSTEM ARE AS TABULATED BELOW.

VAPOR CAVITY

DIST. .0000 .1280 .2560 .3840 .5119 .6399 .7679 .8959 1.0239 1.1519 1.2799 1.4078 1.5358 1.6638 1.7918
 LOC. 0 2 4 6 8 10 12 14 16 18 20 22 24 26 28
 U .000 -.048 -.082 -.108 -.132 -.151 -.162 -.163 -.157 -.147 -.135 -.121 -.107 -.097 -.090
 Z .025 .025 .025 .026 .027 .029 .030 .032 .034 .036 .039 .042 .045 .048 .052

DIST. 1.9198 1.9838 2.0478 2.1118 2.1757 2.2397 2.3037
 LOC. 30 31 32 33 34 35 36
 U -.078 -.069 -.059 -.050 -.043 -.039 -.015
 Z .055 .057 .059 .061 .063 .065 .068

FULL-FLOWING PIPE SYSTEM

LOC. (1,0) (1,1) (2,0) (2,10) (2,20) (2,30) (2,40) (2,50)
 V -.0208 -.0208 -.0208 -.0204 -.0183 .0183 .0183
 H 11.3000 11.4253 11.4253 14.5249 15.8343 17.1009 19.3257 33.1790

AT TIME T = 1.64971 SECONDS, AFTER 889 COMPLETE CYCLES OF OPERATION, THE VELOCITIES AND DEPTHS IN THE VAPOR CAVITY AS WELL AS VELOCITIES AND PRESSURES AT KEY POINTS THROUGHOUT THE FLOW SYSTEM ARE AS TABULATED BELOW.

VAPOR CAVITY

DIST. .0000 .1280 .2560 .3840 .5119 .6399 .7679 .8959 1.0239 1.1519 1.2799 1.4078 1.5358 1.6638 1.7918

LOC.	0	2	4	6	8	10	12	14	16	18	20	22	24	26	28
U	.000	-.049	-.112	-.137	-.157	-.169	-.171	-.171	-.166	-.158	-.147	-.134	-.122	-.114	-.117
Z	.025	.025	.026	.027	.029	.030	.032	.032	.034	.036	.039	.042	.045	.048	.052

DIST.	1.9198	1.9838	2.0478	2.1118	2.1757	2.2397	2.3037
LOC.	0	31	32	33	34	35	36
U	-.094	-.085	-.076	-.068	-.058	-.033	
Z	.055	.057	.059	.061	.063	.065	.067

FULL-FLOWING PIPE SYSTEM

LOC.	(1,0)	(1,1)	(2,0)	(2,10)	(2,20)	(2,30)	(2,40)	(2,50)
V	-.0272	-.0272	-.0271	-.0242	-.0217	-.0242	-.0724	-.1063
H	11.3000	11.3258	11.3258	14.1481	15.0581	17.5199	26.0000	33.1790

AT TIME T = 1.66827 SECONDS, AFTER 899 COMPLETE CYCLES OF OPERATION, THE VELOCITIES AND DEPTHS IN THE VAPOR CAVITY AS WELL AS VELOCITIES AND PRESSURES AT KEY POINTS THROUGHOUT THE FLOW SYSTEM ARE AS TABULATED BELOW.

VAPOR CAVITY

DIST.	.0000	.1280	.2560	.3840	.5119	.6399	.7679	.8959	1.0239	1.1519	1.2799	1.4078	1.5358	1.6638	1.7918
LOC.	0	2	4	6	8	10	12	14	16	18	20	22	24	26	28
U	.000	-.050	-.087	-.116	-.143	-.163	-.176	-.179	-.176	-.168	-.159	-.147	-.137	-.130	-.123
Z	.025	.025	.026	.026	.027	.029	.030	.032	.034	.036	.039	.042	.045	.048	.052

DIST.	1.9198	1.9838	2.0478	2.1118	2.1757	2.2397	2.3037
LOC.	0	31	32	33	34	35	36
U	-.110	-.101	-.093	-.086	-.081	-.074	-.050
Z	.055	.057	.059	.061	.063	.065	.067

FULL-FLOWING PIPE SYSTEM

LOC.	(1,0)	(1,1)	(2,0)	(2,10)	(2,20)	(2,30)	(2,40)	(2,50)
V	-.0284	-.0284	-.0283	-.0284	-.0293	-.0757	-.1121	-.1150
H	11.3000	11.3249	11.3249	13.7378	15.8326	24.5375	31.4009	33.1790

AT TIME T = 1.66862 SECONDS, AFTER 909 COMPLETE CYCLES OF OPERATION, THE VELOCITIES AND DEPTHS IN THE VAPOR CAVITY AS WELL AS VELOCITIES AND PRESSURES AT KEY POINTS THROUGHOUT THE FLOW SYSTEM ARE AS TABULATED BELOW.

VAPOR CAVITY

DIST.	.0000	.1280	.2560	.3840	.5119	.6399	.7679	.8959	1.0239	1.1519	1.2799	1.4078	1.5358	1.6638	1.7918
LOC.	0	2	4	6	8	10	12	14	16	18	20	22	24	26	28
U	.000	-.050	-.090	-.121	-.148	-.170	-.183	-.187	-.185	-.179	-.171	-.161	-.152	-.146	-.139
Z	.025	.025	.026	.026	.028	.029	.030	.032	.034	.036	.039	.042	.045	.048	.052

DIST.	1.9198	1.9838	2.0478	2.1118	2.1757	2.2397	2.3037
LOC.	0	31	32	33	34	35	36
U	-.125	-.117	-.110	-.104	-.098	-.089	-.064
Z	.055	.057	.059	.061	.063	.064	.066

FULL-FLOWING PIPE SYSTEM

LOC.	(1,0)	(1,1)	(2,0)	(2,10)	(2,20)	(2,30)	(2,40)	(2,50)
V	-.0298	-.0298	-.0297	-.0334	-.0822	-.1171	-.1183	-.1179
H	11.3000	11.3268	11.3268	14.2852	22.5982	29.7017	31.7650	33.1790

AT TIME T = 1.70538 SECONDS, AFTER 919 COMPLETE CYCLES OF OPERATION, THE VELOCITIES AND DEPTHS IN THE VAPOR CAVITY AS WELL AS VELOCITIES AND PRESSURES AT KEY POINTS THROUGHOUT THE FLOW SYSTEM ARE AS TABULATED BELOW.

VAPOR CAVITY

DIST.	.0000	.1280	.2560	.3840	.5119	.6399	.7679	.8959	1.0239	1.1519	1.2799	1.4078	1.5358	1.6638	1.7918
LOC.	0	2	4	6	8	10	12	14	16	18	20	22	24	26	28
U	.000	-.051	-.092	-.125	-.154	-.176	-.189	-.195	-.194	-.190	-.183	-.174	-.167	-.152	-.152
Z	.025	.025	.026	.026	.028	.029	.030	.032	.034	.036	.039	.042	.045	.048	.052
DIST.	1.9198	1.9838	2.0478	2.1118	2.1757	2.2397	2.3037								
LOC.	30	31	32	33	34	35	36								
U	-.141	-.133	-.127	-.121	-.114	-.101	-.077								
Z	.055	.057	.059	.061	.062	.064	.066								

FULL-FLOWING PIPE SYSTEM

LOC.	(1,0)	(1,1)	(2,0)	(2,10)	(2,20)	(2,30)	(2,40)	(2,50)
V	-.0356	-.0367	-.0366	-.0834	-.1211	-.1249	-.1229	-.1216
H	11.3000	11.5838	11.5838	21.4450	28.1431	29.6333	31.5236	33.1790

AT TIME T = 1.72394 SECONDS, AFTER 929 COMPLETE CYCLES OF OPERATION, THE VELOCITIES AND DEPTHS IN THE VAPOR CAVITY AS WELL AS VELOCITIES AND PRESSURES AT KEY POINTS THROUGHOUT THE FLOW SYSTEM ARE AS TABULATED BELOW.

VAPOR CAVITY

DIST.	.0000	.1280	.2560	.3840	.5119	.6399	.7679	.8959	1.0239	1.1519	1.2799	1.4078	1.5358	1.6638	1.7918
LOC.	0	2	4	6	8	10	12	14	16	18	20	22	24	26	28
U	.000	-.051	-.094	-.129	-.159	-.182	-.196	-.203	-.204	-.201	-.195	-.187	-.182	-.178	-.170
Z	.025	.026	.026	.027	.028	.029	.030	.032	.034	.036	.039	.042	.045	.048	.052
DIST.	1.9198	1.9838	2.0478	2.1118	2.1757	2.2397	2.3037								
LOC.	30	31	32	33	34	35	36								
U	-.157	-.150	-.144	-.137	-.128	-.112	-.088								
Z	.055	.057	.059	.061	.062	.064	.065								

FULL-FLOWING PIPE SYSTEM

LOC.	(1,0)	(1,1)	(2,0)	(2,10)	(2,20)	(2,30)	(2,40)	(2,50)
V	-.1225	-.1234	-.1230	-.1243	-.1261	-.1269	-.1282	-.1279
H	11.3000	13.3604	13.3604	26.7100	28.6886	29.9662	31.2889	33.1790

AT TIME T = 1.74249 SECONDS, AFTER 939 COMPLETE CYCLES OF OPERATION, THE VELOCITIES AND DEPTHS IN THE VAPOR CAVITY AS WELL AS VELOCITIES AND PRESSURES AT KEY POINTS THROUGHOUT THE FLOW SYSTEM ARE AS TABULATED BELOW.

VAPOR CAVITY

DIST.	.0000	.1280	.2560	.3840	.5119	.6399	.7679	.8959	1.0239	1.1519	1.2799	1.4078	1.5358	1.6638	1.7918
LOC.	0	2	4	6	8	10	12	14	16	18	20	22	24	26	28
U	.000	-.052	-.097	-.134	-.164	-.188	-.203	-.211	-.211	-.213	-.207	-.201	-.197	-.194	-.186
Z	.026	.026	.026	.027	.028	.029	.031	.032	.034	.036	.039	.042	.045	.048	.052
DIST.	1.9198	1.9838	2.0478	2.1118	2.1757	2.2397	2.3037								
LOC.	30	31	32	33	34	35	36								
U	-.173	-.166	-.160	-.152	-.141	-.127	-.102								
Z	.055	.057	.059	.060	.062	.064	.067								

FULL-FLOWING PIPE SYSTEM

LOC.	(1,0)	(1,1)	(2,0)	(2,10)	(2,20)	(2,30)	(2,40)	(2,50)
V	-.2133	-.2114	-.2107	-.1658	-.1301	-.1295	-.1319	-.1348
H	11.3000	11.7681	11.7681	21.8961	28.5358	30.1442	31.6630	33.1790

AT TIME T = 1.76105 SECONDS, AFTER 949 COMPLETE CYCLES OF OPERATION, THE VELOCITIES AND DEPTHS IN THE VAPOR CAVITY AS WELL AS VELOCITIES AND PRESSURES AT KEY POINTS THROUGHOUT THE FLOW SYSTEM ARE AS TABULATED BELOW.

VAPOR CAVITY

DIST.	.0000	.1280	.2560	.3840	.5119	.6399	.7679	.8959	1.0239	1.1519	1.2799	1.4078	1.5358	1.6638	1.7918
LOC.	0	2	4	6	8	10	12	14	16	18	20	22	24	26	28
U	.000	-.052	-.099	-.138	-.170	-.194	-.210	-.219	-.223	-.222	-.219	-.214	-.212	-.209	-.201
Z	.026	.026	.026	.027	.028	.029	.031	.032	.034	.037	.039	.042	.045	.048	.052

DIST.	1.9198	1.9838	2.0478	2.1118	2.1757	2.2397	2.3037
LOC.	30	31	32	33	34	35	36
U	-.188	-.182	-.176	-.167	-.155	-.149	-.123
Z	.055	.057	.059	.060	.062	.064	.068

FULL-FLOWING PIPE SYSTEM

LOC.	(1,0)	(1,1)	(2,0)	(2,10)	(2,20)	(2,30)	(2,40)	(2,50)
V	-.2231	-.2230	-.2223	-.2166	-.1691	-.1351	-.1361	-.136
H	11.3000	11.3692	11.3692	14.8627	23.3541	30.2334	32.0771	33.1790

AT TIME T = 1.77961 SECONDS, AFTER 959 COMPLETE CYCLES OF OPERATION, THE VELOCITIES AND DEPTHS IN THE VAPOR CAVITY AS WELL AS VELOCITIES AND PRESSURES AT KEY POINTS THROUGHOUT THE FLOW SYSTEM ARE AS TABULATED BELOW.

VAPOR CAVITY

DIST.	.0000	.1280	.2560	.3840	.5119	.6399	.7679	.8959	1.0239	1.1519	1.2799	1.4078	1.5358	1.6638	1.7918
LOC.	0	2	4	6	8	10	12	14	16	18	20	22	24	26	28
U	.000	-.053	-.101	-.142	-.175	-.200	-.217	-.227	-.232	-.233	-.231	-.228	-.227	-.224	-.216
Z	.026	.026	.026	.027	.028	.029	.031	.032	.034	.037	.039	.042	.045	.048	.052

DIST.	1.9198	1.9838	2.0478	2.1118	2.1757	2.2397	2.3037
LOC.	30	31	32	33	34	35	36
U	-.204	-.198	-.190	-.181	-.173	-.177	-.150
Z	.055	.057	.059	.060	.062	.064	.070

FULL-FLOWING PIPE SYSTEM

LOC.	(1,0)	(1,1)	(2,0)	(2,10)	(2,20)	(2,30)	(2,40)	(2,50)
V	-.2262	-.2262	-.2254	-.2257	-.2217	-.1757	-.1392	-.1373
H	11.3000	11.3494	11.3494	14.0925	16.5508	25.2894	31.7929	33.1790

AT TIME T = 1.79816 SECONDS, AFTER 969 COMPLETE CYCLES OF OPERATION, THE VELOCITIES AND DEPTHS IN THE VAPOR CAVITY AS WELL AS VELOCITIES AND PRESSURES AT KEY POINTS THROUGHOUT THE FLOW SYSTEM ARE AS TABULATED BELOW.

VAPOR CAVITY

DIST.	.0000	.1280	.2560	.3840	.5119	.6399	.7679	.8959	1.0239	1.1519	1.2799	1.4078	1.5358	1.6638	1.7918
LOC.	0	2	4	6	8	10	12	14	16	18	20	22	24	26	28
U	.000	-.054	-.104	-.146	-.181	-.206	-.224	-.235	-.242	-.243	-.243	-.242	-.242	-.239	-.230
Z	.026	.026	.026	.027	.028	.029	.031	.032	.034	.037	.039	.042	.045	.048	.052

DIST.	1.9198	1.9838	2.0478	2.1118	2.1757	2.2397	2.3037
LOC.	30	31	32	33	34	35	36
U	-.219	-.213	-.205	-.197	-.195	-.208	-.178
Z	.055	.057	.058	.060	.062	.065	.070

FULL-FLOWING PIPE SYSTEM

LOC.	(1,0)	(1,1)	(2,0)	(2,10)	(2,20)	(2,30)	(2,40)	(2,50)
------	-------	-------	-------	--------	--------	--------	--------	--------

V -0.2298 -0.2299 -0.2291 -0.2305 -0.2323 -0.2258 -0.1769 -0.1424
 H 11.3000 11.3689 11.3689 14.3138 16.0177 18.1034 26.4348 33.1790

AT TIME T = 1.81672 SECONDS, AFTER 979 COMPLETE CYCLES OF OPERATION, THE VELOCITIES AND DEPTHS IN THE VAPOR CAVITY AS WELL AS VELOCITIES AND PRESSURES AT KEY POINTS THROUGHOUT THE FLOW SYSTEM ARE AS TABULATED BELOW.

VAPOR CAVITY

DIST.	0.000	0.1280	0.2560	0.3840	0.5119	0.6399	0.7679	0.8959	1.0239	1.1519	1.2799	1.4078	1.5358	1.6638	1.7918
LOC.	0	2	4	6	8	10	12	14	16	18	20	22	24	26	28
U	0.000	-0.054	-0.106	-0.151	-0.186	-0.212	-0.231	-0.243	-0.251	-0.254	-0.255	-0.255	-0.256	-0.253	-0.245
Z	0.026	0.026	0.027	0.027	0.028	0.030	0.031	0.033	0.035	0.037	0.039	0.042	0.045	0.049	0.052

DIST.	1.9198	1.9838	2.0478	2.1118	2.1757	2.2397	2.3037
LOC.	30	31	32	33	34	35	36
U	-0.234	-0.227	-0.220	-0.215	-0.221	-0.237	-0.207
Z	0.055	0.057	0.058	0.060	0.063	0.065	0.070

FULL-FLOWING PIPE SYSTEM

LOC.	(1,0)	(1,1)	(2,0)	(2,10)	(2,20)	(2,30)	(2,40)	(2,50)
V	-0.2358	-0.2358	-0.2351	-0.2357	-0.2346	-0.2336	-0.2290	-0.2166
H	11.3000	11.4168	11.4168	14.5704	15.8665	17.1563	19.5244	33.1790

AT TIME T = 1.83528 SECONDS, AFTER 989 COMPLETE CYCLES OF OPERATION, THE VELOCITIES AND DEPTHS IN THE VAPOR CAVITY AS WELL AS VELOCITIES AND PRESSURES AT KEY POINTS THROUGHOUT THE FLOW SYSTEM ARE AS TABULATED BELOW.

VAPOR CAVITY

DIST.	0.000	0.1280	0.2560	0.3840	0.5119	0.6399	0.7679	0.8959	1.0239	1.1519	1.2799	1.4078	1.5358	1.6638	1.7918
LOC.	0	2	4	6	8	10	12	14	16	18	20	22	24	26	28
U	0.000	-0.055	-0.108	-0.155	-0.191	-0.218	-0.238	-0.252	-0.260	-0.265	-0.267	-0.269	-0.271	-0.267	-0.259
Z	0.026	0.026	0.027	0.027	0.028	0.030	0.031	0.033	0.035	0.037	0.039	0.042	0.045	0.049	0.052

DIST.	1.9198	1.9838	2.0478	2.1118	2.1757	2.2397	2.3037
LOC.	30	31	32	33	34	35	36
U	-0.248	-0.242	-0.236	-0.237	-0.248	-0.264	-0.233
Z	0.055	0.057	0.059	0.061	0.063	0.066	0.070

FULL-FLOWING PIPE SYSTEM

LOC.	(1,0)	(1,1)	(2,0)	(2,10)	(2,20)	(2,30)	(2,40)	(2,50)
V	-0.2433	-0.2431	-0.2423	-0.2391	-0.2370	-0.2378	-0.2731	-0.3155
H	11.3000	11.3702	11.3702	14.2479	15.7102	17.2875	23.9181	33.1790

AT TIME T = 1.85384 SECONDS, AFTER 999 COMPLETE CYCLES OF OPERATION, THE VELOCITIES AND DEPTHS IN THE VAPOR CAVITY AS WELL AS VELOCITIES AND PRESSURES AT KEY POINTS THROUGHOUT THE FLOW SYSTEM ARE AS TABULATED BELOW.

VAPOR CAVITY

DIST.	0.000	0.1280	0.2560	0.3840	0.5119	0.6399	0.7679	0.8959	1.0239	1.1519	1.2799	1.4078	1.5358	1.6638	1.7918
LOC.	0	2	4	6	8	10	12	14	16	18	20	22	24	26	28
U	0.000	-0.056	-0.111	-0.159	-0.197	-0.225	-0.245	-0.260	-0.270	-0.276	-0.279	-0.283	-0.285	-0.281	-0.273
Z	0.027	0.027	0.027	0.028	0.029	0.030	0.031	0.033	0.035	0.037	0.040	0.042	0.046	0.049	0.052

DIST.	1.9198	1.9838	2.0478	2.1118	2.1757	2.2397	2.3037
LOC.	30	31	32	33	34	35	36
U	-0.263	-0.257	-0.255	-0.261	-0.274	-0.287	-0.255
Z	0.055	0.057	0.059	0.061	0.064	0.066	0.070

FULL-FLOWING PIPE SYSTEM

LOC.	(1,C)	(1,1)	(2,0)	(2,10)	(2,20)	(2,30)	(2,40)	(2,50)
V	-.2446	-.2446	-.2438	-.2435	-.2423	-.2762	-.3240	-.3294
H	11.3000	11.3279	11.3279	13.7911	15.6695	22.4424	30.9519	33.1791

AT TIME T = 1.87239 SECONDS, AFTER 1009 COMPLETE CYCLES OF OPERATION, THE VELOCITIES AND DEPTHS IN THE VAPOR CAVITY AS WELL AS VELOCITIES AND PRESSURES AT KEY POINTS THROUGHOUT THE FLOW SYSTEM ARE AS TABULATED BELOW.

VAPOR CAVITY

DIST.	.0000	.1280	.2560	.3840	.5119	.6399	.7679	.8959	1.0239	1.1519	1.2799	1.4078	1.5358	1.6638	1.7918
LOC.	0	2	4	6	8	10	12	14	16	18	20	22	24	26	28
U	.000	-.037	-.113	-.163	-.202	-.231	-.252	-.268	-.279	-.286	-.291	-.296	-.298	-.295	-.287
Z	.027	.027	.027	.028	.029	.030	.031	.033	.035	.037	.040	.043	.046	.049	.052

DIST.	1.9198	1.9838	2.0478	2.1118	2.1757	2.2397	2.3037
LOC.	30	31	32	33	34	35	36
U	-.277	-.274	-.276	-.285	-.299	-.306	-.275
Z	.055	.057	.059	.061	.064	.066	.069

FULL-FLOWING PIPE SYSTEM

LOC.	(1,0)	(1,1)	(2,0)	(2,10)	(2,20)	(2,30)	(2,40)	(2,50)
V	-.2459	-.2459	-.2450	-.2469	-.2825	-.3282	-.3326	-.3325
H	11.3000	11.3279	11.3279	14.0277	20.4983	29.3040	31.7436	33.1790

AT TIME T = 1.89095 SECONDS, AFTER 1019 COMPLETE CYCLES OF OPERATION, THE VELOCITIES AND DEPTHS IN THE VAPOR CAVITY AS WELL AS VELOCITIES AND PRESSURES AT KEY POINTS THROUGHOUT THE FLOW SYSTEM ARE AS TABULATED BELOW.

VAPOR CAVITY

DIST.	.0000	.1280	.2560	.3840	.5119	.6399	.7679	.8959	1.0239	1.1519	1.2799	1.4078	1.5358	1.6638	1.7918
LOC.	0	2	4	6	8	10	12	14	16	18	20	22	24	26	28
U	.000	-.058	-.115	-.167	-.207	-.237	-.259	-.276	-.289	-.297	-.304	-.310	-.312	-.319	-.301
Z	.027	.027	.027	.028	.029	.030	.031	.033	.035	.037	.040	.043	.046	.049	.052

DIST.	1.9198	1.9838	2.0478	2.1118	2.1757	2.2397	2.3037
LOC.	30	31	32	33	34	35	36
U	-.293	-.293	-.298	-.310	-.320	-.291	-.291
Z	.055	.057	.059	.062	.064	.066	.069

FULL-FLOWING PIPE SYSTEM

LOC.	(1,0)	(1,1)	(2,0)	(2,10)	(2,20)	(2,30)	(2,40)	(2,50)
V	-.2494	-.2494	-.2491	-.2838	-.3326	-.3388	-.3367	-.3357
H	11.3000	11.4574	11.4574	19.2867	27.6346	29.7982	31.5748	33.1790

AT TIME T = 1.90951 SECONDS, AFTER 1029 COMPLETE CYCLES OF OPERATION, THE VELOCITIES AND DEPTHS IN THE VAPOR CAVITY AS WELL AS VELOCITIES AND PRESSURES AT KEY POINTS THROUGHOUT THE FLOW SYSTEM ARE AS TABULATED BELOW.

VAPOR CAVITY

DIST.	.0000	.1280	.2560	.3840	.5119	.6399	.7679	.8959	1.0239	1.1519	1.2799	1.4078	1.5358	1.6638	1.7918
LOC.	0	2	4	6	8	10	12	14	16	18	20	22	24	26	28
U	.000	-.059	-.118	-.171	-.213	-.243	-.267	-.285	-.298	-.307	-.316	-.323	-.325	-.322	-.315
Z	.027	.027	.027	.028	.029	.030	.032	.033	.035	.037	.040	.043	.046	.049	.052

DIST.	1.9198	1.9838	2.0478	2.1118	2.1757	2.2397	2.3037
LOC.	30	31	32	33	34	35	36
U	-.277	-.274	-.276	-.285	-.299	-.306	-.275
Z	.055	.057	.059	.061	.064	.066	.069

U -0.310 -0.313 -0.321 -0.332 -0.338 -0.332 -0.304
 Z .056 .058 .066 .062 .065 .066 .069

FULL-FLOWING PIPE SYSTEM

LOC. (1,0) (1,1) (2,0) (2,10) (2,20) (2,30) (2,40) (2,50)
 V -0.3093 -0.3116 -0.3155 -0.3346 -0.3402 -0.3411 -0.3419 -0.341
 H 11.3000 13.0638 13.5638 26.3355 28.5846 29.9665 31.2765 33.1790

AT TIME T = 1.92806 SECONDS, AFTER 1039 COMPLETE CYCLES OF OPERATION, THE VELOCITIES AND DEPTHS IN THE VAPOR CAVITY AS WELL AS VELOCITIES AND PRESSURES AT KEY POINTS THROUGHOUT THE FLOW SYSTEM ARE AS TABULATED BELOW.

VAPOR CAVITY

DIST. 0.0000 .1280 .2560 .3840 .5119 .6399 .7679 .8959 1.0239 1.1519 1.2799 1.4078 1.5358 1.6638 1.7918
 LOC. 0 2 4 6 8 10 12 14 16 18 20 22 24 26 28
 U .000 -0.060 -0.120 -0.175 -0.218 -0.250 -0.274 -0.293 -0.307 -0.318 -0.326 -0.336 -0.339 -0.335 -0.329
 Z .027 .027 .028 .028 .029 .030 .032 .033 .035 .038 .040 .043 .046 .049 .052

DIST. 1.9198 1.9838 2.0478 2.1118 2.1757 2.2397 2.3037
 LOC. 30 31 32 33 34 35 36
 U -0.328 -0.334 -0.344 -0.352 -0.353 -0.348 -0.319
 Z .056 .058 .060 .063 .065 .066 .071

FULL-FLOWING PIPE SYSTEM

LOC. (1,0) (1,1) (2,0) (2,10) (2,20) (2,30) (2,40) (2,50)
 V -0.4192 -0.4167 -0.4152 -0.3668 -0.3431 -0.3433 -0.3454 -0.3482
 H 11.3000 12.1458 12.1458 23.6475 28.5887 30.0617 31.5522 33.1790

AT TIME T = 1.94662 SECONDS, AFTER 1049 COMPLETE CYCLES OF OPERATION, THE VELOCITIES AND DEPTHS IN THE VAPOR CAVITY AS WELL AS VELOCITIES AND PRESSURES AT KEY POINTS THROUGHOUT THE FLOW SYSTEM ARE AS TABULATED BELOW.

VAPOR CAVITY

DIST. 0.0000 .1280 .2560 .3840 .5119 .6399 .7679 .8959 1.0239 1.1519 1.2799 1.4078 1.5358 1.6638 1.7918
 LOC. 0 2 4 6 8 10 12 14 16 18 20 22 24 26 28
 U .000 -0.061 -0.123 -0.179 -0.223 -0.256 -0.281 -0.301 -0.316 -0.329 -0.341 -0.349 -0.352 -0.349 -0.344
 Z .027 .027 .028 .028 .029 .030 .032 .033 .035 .038 .040 .043 .046 .049 .052

DIST. 1.9198 1.9838 2.0478 2.1118 2.1757 2.2397 2.3037
 LOC. 30 31 32 33 34 35 36
 U -0.347 -0.355 -0.365 -0.370 -0.377 -0.377 -0.344
 Z .056 .058 .061 .063 .065 .067 .074

FULL-FLOWING PIPE SYSTEM

LOC. (1,0) (1,1) (2,0) (2,10) (2,20) (2,30) (2,40) (2,50)
 V -0.4358 -0.4357 -0.4342 -0.4236 -0.3698 -0.3474 -0.3495 -0.3497
 H 11.3000 11.3997 11.3997 15.7186 25.1366 30.2342 32.0049 33.1790

AT TIME T = 1.96518 SECONDS, AFTER 1059 COMPLETE CYCLES OF OPERATION, THE VELOCITIES AND DEPTHS IN THE VAPOR CAVITY AS WELL AS VELOCITIES AND PRESSURES AT KEY POINTS THROUGHOUT THE FLOW SYSTEM ARE AS TABULATED BELOW.

VAPOR CAVITY

DIST. 0.0000 .1280 .2560 .3840 .5119 .6399 .7679 .8959 1.0239 1.1519 1.2799 1.4078 1.5358 1.6638 1.7918
 LOC. 0 2 4 6 8 10 12 14 16 18 20 22 24 26 28
 U .000 -0.062 -0.125 -0.183 -0.229 -0.262 -0.289 -0.309 -0.326 -0.341 -0.353 -0.362 -0.364 -0.362 -0.359
 Z .028 .028 .028 .029 .029 .031 .032 .034 .036 .038 .041 .043 .046 .049 .053

DIST.	1.9198	1.9838	2.0478	2.1118	2.1757	2.2397	2.3037
LOC.	0	31	32	33	34	35	36
U	-.367	-.376	-.384	-.388	-.415	-.377	
Z	.056	.059	.061	.063	.065	.068	.075

FULL-FLOWING PIPE SYSTEM

LOC.	(1,0)	(1,1)	(2,0)	(2,10)	(2,20)	(2,30)	(2,40)	(2,50)
V	-.4388	-.4388	-.4373	-.4371	-.4277	-.3759	-.3517	-.3588
H	11.3000	11.3578	11.3578	14.1744	17.3844	27.0906	31.9033	33.1790

AT TIME T = 1.98373 SECONDS, AFTER 1069 COMPLETE CYCLES OF OPERATION, THE VELOCITIES AND DEPTHS IN THE VAPOR CAVITY AS WELL AS VELOCITIES AND PRESSURES AT KEY POINTS THROUGHOUT THE FLOW SYSTEM ARE AS TABULATED BELOW.

VAPOR CAVITY

DIST.	.0000	.1280	.2560	.3840	.5119	.6399	.7679	.8959	1.0239	1.1519	1.2799	1.4078	1.5358	1.6638	1.7918
LOC.	0	2	4	6	8	10	12	14	16	18	20	22	24	26	28
U	.000	-.063	-.128	-.187	-.234	-.269	-.296	-.317	-.336	-.352	-.366	-.375	-.377	-.375	-.375
Z	.028	.028	.028	.029	.030	.031	.032	.034	.036	.038	.041	.044	.047	.050	.053

DIST.	1.9198	1.9838	2.0478	2.1118	2.1757	2.2397	2.3037
LOC.	0	31	32	33	34	35	36
U	-.388	-.397	-.403	-.409	-.424	-.450	-.410
Z	.057	.059	.061	.063	.066	.069	.075

FULL-FLOWING PIPE SYSTEM

LOC.	(1,0)	(1,1)	(2,0)	(2,10)	(2,20)	(2,30)	(2,40)	(2,50)
V	-.4417	-.4418	-.4403	-.4414	-.4432	-.4319	-.3771	-.3537
H	11.3000	11.3729	11.3729	14.2967	16.1354	19.0744	28.3190	33.1790

AT TIME T = 2.00229 SECONDS, AFTER 1079 COMPLETE CYCLES OF OPERATION, THE VELOCITIES AND DEPTHS IN THE VAPOR CAVITY AS WELL AS VELOCITIES AND PRESSURES AT KEY POINTS THROUGHOUT THE FLOW SYSTEM ARE AS TABULATED BELOW.

VAPOR CAVITY

DIST.	.0000	.1280	.2560	.3840	.5119	.6399	.7679	.8959	1.0239	1.1519	1.2799	1.4078	1.5358	1.6638	1.7918
LOC.	0	2	4	6	8	10	12	14	16	18	20	22	24	26	28
U	.000	-.065	-.130	-.191	-.239	-.275	-.303	-.326	-.345	-.363	-.378	-.387	-.390	-.389	-.393
Z	.028	.028	.028	.029	.030	.031	.032	.034	.036	.038	.041	.044	.047	.050	.053

DIST.	1.9198	1.9838	2.0478	2.1118	2.1757	2.2397	2.3037
LOC.	0	31	32	33	34	35	36
U	-.408	-.416	-.424	-.436	-.456	-.480	-.439
Z	.057	.059	.062	.064	.067	.070	.073

FULL-FLOWING PIPE SYSTEM

LOC.	(1,0)	(1,1)	(2,0)	(2,10)	(2,20)	(2,30)	(2,40)	(2,50)
V	-.4465	-.4466	-.4451	-.4463	-.4456	-.4444	-.4337	-.4033
H	11.3000	11.4138	11.4138	14.6107	15.9865	17.3721	20.4129	33.1790

AT TIME T = 2.02085 SECONDS, AFTER 1089 COMPLETE CYCLES OF OPERATION, THE VELOCITIES AND DEPTHS IN THE VAPOR CAVITY AS WELL AS VELOCITIES AND PRESSURES AT KEY POINTS THROUGHOUT THE FLOW SYSTEM ARE AS TABULATED BELOW.

VAPOR CAVITY

DIST.	.0000	.1280	.2560	.3840	.5119	.6399	.7679	.8959	1.0239	1.1519	1.2799	1.4078	1.5358	1.6638	1.7918
LOC.	0	2	4	6	8	10	12	14	16	18	20	22	24	26	28
U	.000	-.063	-.128	-.187	-.234	-.269	-.296	-.317	-.336	-.352	-.366	-.375	-.377	-.375	-.375
Z	.028	.028	.028	.029	.030	.031	.032	.034	.036	.038	.041	.044	.047	.050	.053

U .000 -.066 -.133 -.195 -.244 -.282 -.310 -.334 -.355 -.375 -.390 -.399 -.402 -.411
 Z .028 .028 .029 .029 .030 .031 .032 .034 .036 .039 .041 .044 .047 .050 .053

DIST. 1.9198 1.9838 2.0478 2.1118 2.1757 2.2397 2.3037
 LOC. 30 31 32 33 34 35 36
 U -.428 -.437 -.448 -.465 -.485 -.491 -.456
 Z .058 .060 .062 .065 .068 .070 .072

FULL-FLOWING PIPE SYSTEM

LOC. (1,0) (1,1) (2,0) (2,10) (2,20) (2,30) (2,40) (2,50)
 V -.4538 -.4537 -.4522 -.4493 -.4475 -.4475 -.4704 -.5134
 H 11.3000 11.4108 11.4108 14.3797 15.8478 17.3228 22.2716 33.1790

AT TIME T = 2.03940 SECONDS, AFTER 1099 COMPLETE CYCLES OF OPERATION, THE VELOCITIES AND DEPTHS IN THE VAPOR CAVITY AS WELL AS VELOCITIES AND PRESSURES AT KEY POINTS THROUGHOUT THE FLOW SYSTEM ARE AS TABULATED BELOW.

VAPOR CAVITY

DIST. .0000 .1280 .2560 .3840 .5119 .6399 .7679 .8959 1.0239 1.1519 1.2799 1.4078 1.5358 1.6638 1.7918
 LOC. 0 2 4 6 8 10 12 14 16 18 20 22 24 26 28
 U .000 -.068 -.136 -.199 -.250 -.288 -.317 -.343 -.366 -.386 -.402 -.412 -.415 -.418 -.429
 Z .028 .028 .029 .029 .030 .031 .033 .034 .036 .039 .041 .044 .047 .050 .054

DIST. 1.9198 1.9838 2.0478 2.1118 2.1757 2.2397 2.3037
 LOC. 30 31 32 33 34 35 36
 U -.448 -.459 -.474 -.493 -.504 -.499 -.468
 Z .058 .060 .063 .066 .068 .070 .072

FULL-FLOWING PIPE SYSTEM

LOC. (1,0) (1,1) (2,0) (2,10) (2,20) (2,30) (2,40) (2,50)
 V -.4556 -.4556 -.4541 -.4533 -.4511 -.4735 -.5270 -.5374
 H 11.3000 11.3328 11.3328 13.9271 15.7162 20.7366 30.1073 33.1790

AT TIME T = 2.05796 SECONDS, AFTER 1109 COMPLETE CYCLES OF OPERATION, THE VELOCITIES AND DEPTHS IN THE VAPOR CAVITY AS WELL AS VELOCITIES AND PRESSURES AT KEY POINTS THROUGHOUT THE FLOW SYSTEM ARE AS TABULATED BELOW.

VAPOR CAVITY

DIST. .0000 .1280 .2560 .3840 .5119 .6399 .7679 .8959 1.0239 1.1519 1.2799 1.4078 1.5358 1.6638 1.7918
 LOC. 0 2 4 6 8 10 12 14 16 18 20 22 24 26 28
 U .000 -.069 -.138 -.203 -.255 -.294 -.325 -.351 -.376 -.398 -.414 -.424 -.434 -.448
 Z .029 .029 .029 .030 .030 .031 .033 .035 .037 .039 .042 .044 .047 .050 .054

DIST. 1.9198 1.9838 2.0478 2.1118 2.1757 2.2397 2.3037
 LOC. 30 31 32 33 34 35 36
 U -.470 -.484 -.501 -.515 -.517 -.505 -.477
 Z .059 .061 .064 .066 .068 .070 .071

FULL-FLOWING PIPE SYSTEM

LOC. (1,0) (1,1) (2,0) (2,10) (2,20) (2,30) (2,40) (2,50)
 V -.4565 -.4565 -.4549 -.4559 -.4792 -.5305 -.5403 -.5407
 H 11.3000 11.3359 11.3359 13.9471 18.8064 28.4793 31.6749 33.1790

AT TIME T = 2.07652 SECONDS, AFTER 1119 COMPLETE CYCLES OF OPERATION, THE VELOCITIES AND DEPTHS IN THE VAPOR CAVITY AS WELL AS VELOCITIES AND PRESSURES AT KEY POINTS THROUGHOUT THE FLOW SYSTEM ARE AS TABULATED BELOW.

VAPOR CAVITY

DIST.	.0000	.1280	.2560	.3840	.5119	.6399	.7679	.8959	1.0239	1.1519	1.2799	1.4078	1.5358	1.6638	1.7918
LOC.	0	2	4	6	8	10	12	14	16	18	20	22	24	26	28
U	.000	-.071	-.141	-.207	-.260	-.301	-.332	-.360	-.386	-.409	-.426	-.436	-.441	-.450	-.468
Z	.029	.029	.029	.030	.030	.032	.033	.035	.037	.039	.042	.045	.048	.051	.055
DIST.	1.9198	1.9838	2.0478	2.1118	2.1757	2.2397	2.3037								
LOC.	30	31	32	33	34	35	36								
U	-.493	-.509	-.525	-.532	-.527	-.511	-.485								
Z	.059	.062	.064	.066	.068	.069	.071								

FULL-FLOWING PIPE SYSTEM

LOC.	(1,0)	(1,1)	(2,0)	(2,10)	(2,20)	(2,30)	(2,40)	(2,50)
V	-.4585	-.4587	-.4572	-.4807	-.5351	-.5460	-.5461	-.5433
H	11.3000	11.4010	11.4010	17.4818	26.8883	29.7345	31.5942	33.1790

AT TIME T = 2.09508 SECONDS, AFTER 1129 COMPLETE CYCLES OF OPERATION, THE VELOCITIES AND DEPTHS IN THE VAPOR CAVITY AS WELL AS VELOCITIES AND PRESSURES AT KEY POINTS THROUGHOUT THE FLOW SYSTEM ARE AS TABULATED BELOW.

VAPOR CAVITY

DIST.	.0000	.1280	.2560	.3840	.5119	.6399	.7679	.8959	1.0239	1.1519	1.2799	1.4078	1.5358	1.6638	1.7918
LOC.	0	2	4	6	8	10	12	14	16	18	20	22	24	26	28
U	.000	-.072	-.144	-.211	-.266	-.307	-.340	-.370	-.397	-.421	-.438	-.448	-.455	-.467	-.488
Z	.029	.029	.029	.030	.031	.032	.033	.035	.037	.039	.042	.045	.048	.051	.055
DIST.	1.9198	1.9838	2.0478	2.1118	2.1757	2.2397	2.3037								
LOC.	30	31	32	33	34	35	36								
U	-.517	-.533	-.544	-.545	-.533	-.516	-.492								
Z	.060	.062	.065	.067	.068	.069	.070								

FULL-FLOWING PIPE SYSTEM

LOC.	(1,0)	(1,1)	(2,0)	(2,10)	(2,20)	(2,30)	(2,40)	(2,50)
V	-.4968	-.4993	-.4976	-.5363	-.5475	-.5487	-.5489	-.5476
H	11.3000	12.6260	12.6260	25.3979	28.3979	29.8040	31.2817	33.1790

AT TIME T = 2.11363 SECONDS, AFTER 1139 COMPLETE CYCLES OF OPERATION, THE VELOCITIES AND DEPTHS IN THE VAPOR CAVITY AS WELL AS VELOCITIES AND PRESSURES AT KEY POINTS THROUGHOUT THE FLOW SYSTEM ARE AS TABULATED BELOW.

VAPOR CAVITY

DIST.	.0000	.1280	.2560	.3840	.5119	.6399	.7679	.8959	1.0239	1.1519	1.2799	1.4078	1.5358	1.6638	1.7918
LOC.	0	2	4	6	8	10	12	14	16	18	20	22	24	26	28
U	.000	-.074	-.146	-.214	-.271	-.313	-.347	-.379	-.408	-.432	-.449	-.460	-.469	-.485	-.509
Z	.029	.029	.030	.030	.031	.032	.033	.035	.037	.040	.042	.045	.048	.052	.056
DIST.	1.9198	1.9838	2.0478	2.1118	2.1757	2.2397	2.3037								
LOC.	30	31	32	33	34	35	36								
U	-.541	-.554	-.560	-.554	-.539	-.521	-.499								
Z	.060	.063	.065	.067	.068	.069	.070								

FULL-FLOWING PIPE SYSTEM

LOC.	(1,0)	(1,1)	(2,0)	(2,10)	(2,20)	(2,30)	(2,40)	(2,50)
V	-.6116	-.6092	-.6071	-.5642	-.5499	-.5504	-.5522	-.5545
H	11.3000	12.5776	12.5776	24.8170	28.5141	29.9445	31.4307	33.1790

AT TIME T = 2.13219 SECONDS, AFTER 1149 COMPLETE CYCLES OF OPERATION, THE VELOCITIES AND DEPTHS IN THE VAPOR CAVITY AS WELL AS VELOCITIES AND PRESSURES AT KEY POINTS THROUGHOUT THE FLOW SYSTEM ARE AS TABULATED BELOW.

VAPOR CAVITY

DIST.	.0000	.1280	.2560	.3840	.5119	.6399	.7679	.8959	1.0239	1.1519	1.2799	1.4078	1.5358	1.6638	1.7918
LOC.	0	2	4	6	8	10	12	14	16	18	20	22	24	26	28
U	.000	-.075	-.149	-.218	-.276	-.319	-.355	-.388	-.418	-.443	-.461	-.473	-.485	-.494	-.502
Z	.029	.030	.030	.030	.031	.032	.034	.035	.038	.040	.043	.045	.048	.052	.056

DIST.	1.9198	1.9838	2.0478	2.1118	2.1757	2.2397
LOC.	30	31	32	33	34	35
U	-.563	-.572	-.572	-.561	-.544	-.525
Z	.061	.063	.065	.066	.068	.069

FULL-FLOWING PIPE SYSTEM

LOC.	(1,0)	(1,1)	(2,0)	(2,10)	(2,20)	(2,30)	(2,40)	(2,50)
V	-.6411	-.6408	-.6386	-.6205	-.5671	-.5333	-.5559	-.5567
H	11.3000	11.4443	11.4443	16.9970	26.3724	30.1402	31.8823	33.1790

AT TIME T = 2.15075 SECONDS, AFTER 1159 COMPLETE CYCLES OF OPERATION, THE VELOCITIES AND DEPTHS IN THE VAPOR CAVITY AS WELL AS VELOCITIES AND PRESSURES AT KEY POINTS THROUGHOUT THE FLOW SYSTEM ARE AS TABULATED BELOW.

VAPOR CAVITY

DIST.	.0000	.1280	.2560	.3840	.5119	.6399	.7679	.8959	1.0239	1.1519	1.2799	1.4078	1.5358	1.6638	1.7918
LOC.	0	2	4	6	8	10	12	14	16	18	20	22	24	26	28
U	.000	-.077	-.152	-.222	-.281	-.326	-.364	-.398	-.429	-.455	-.473	-.486	-.500	-.503	-.509
Z	.030	.030	.030	.031	.031	.032	.034	.036	.038	.040	.043	.046	.049	.052	.057

DIST.	1.9198	1.9838	2.0478	2.1118	2.1757	2.2397
LOC.	30	31	32	33	34	35
U	-.583	-.587	-.581	-.567	-.549	-.530
Z	.061	.063	.065	.066	.067	.068

FULL-FLOWING PIPE SYSTEM

LOC.	(1,0)	(1,1)	(2,0)	(2,10)	(2,20)	(2,30)	(2,40)	(2,50)
V	-.6444	-.6444	-.6422	-.6414	-.6236	-.5725	-.5579	-.5574
H	11.3000	11.3694	11.3694	14.2936	18.6477	28.3178	31.9302	33.1790

AT TIME T = 2.16930 SECONDS, AFTER 1169 COMPLETE CYCLES OF OPERATION, THE VELOCITIES AND DEPTHS IN THE VAPOR CAVITY AS WELL AS VELOCITIES AND PRESSURES AT KEY POINTS THROUGHOUT THE FLOW SYSTEM ARE AS TABULATED BELOW.

VAPOR CAVITY

DIST.	.0000	.1280	.2560	.3840	.5119	.6399	.7679	.8959	1.0239	1.1519	1.2799	1.4078	1.5358	1.6638	1.7918
LOC.	0	2	4	6	8	10	12	14	16	18	20	22	24	26	28
U	.000	-.079	-.155	-.226	-.286	-.332	-.372	-.408	-.440	-.466	-.484	-.499	-.517	-.524	-.527
Z	.030	.030	.030	.031	.032	.033	.034	.036	.038	.041	.043	.046	.049	.053	.057

DIST.	1.9198	1.9838	2.0478	2.1118	2.1757	2.2397
LOC.	30	31	32	33	34	35
U	-.599	-.598	-.587	-.571	-.553	-.534
Z	.062	.064	.065	.066	.067	.068

FULL-FLOWING PIPE SYSTEM

LOC.	(1,0)	(1,1)	(2,0)	(2,10)	(2,20)	(2,30)	(2,40)	(2,50)
V	-.6467	-.6467	-.6445	-.6454	-.6467	-.6282	-.5740	-.5590
H	11.3000	11.3794	11.3794	14.2968	16.2542	20.4626	29.6657	33.1790

AT TIME T = 2.16786 SECONDS, AFTER 1179 COMPLETE CYCLES OF OPERATION, THE VELOCITIES AND DEPTHS IN THE VAPOR CAVITY AS WELL AS VELOCITIES AND PRESSURES AT KEY POINTS THROUGHOUT THE FLOW SYSTEM ARE AS TABULATED BELOW.

VAPOR CAVITY

DIST.	.0000	.1280	.2560	.3840	.5119	.6399	.7679	.8959	1.0239	1.1519	1.2799	1.4078	1.5358	1.6638	1.7918
LOC.	0	2	4	6	8	10	12	14	16	18	20	22	24	26	28
U	.000	-.080	-.158	-.230	-.291	-.339	-.381	-.418	-.451	-.477	-.496	-.513	-.535	-.565	-.598
Z	.030	.030	.031	.031	.032	.033	.034	.036	.038	.041	.043	.046	.050	.054	.058

DIST.	1.9198	1.9838	2.0478	2.1118	2.1757
LOC.	30	31	32	33	34
U	-.612	-.606	-.593	-.576	-.557
Z	.062	.064	.065	.066	.067

FULL-FLOWING PIPE SYSTEM

LOC.	(1,0)	(1,1)	(2,0)	(2,10)	(2,20)	(2,30)	(2,40)	(2,50)
V	-.6505	-.6506	-.6484	-.6499	-.6498	-.6480	-.6291	-.5904
H	11.3000	11.4136	11.4136	14.6165	16.1107	17.6190	21.7788	33.1790

AT TIME T = 2.20642 SECONDS, AFTER 1189 COMPLETE CYCLES OF OPERATION, THE VELOCITIES AND DEPTHS IN THE VAPOR CAVITY AS WELL AS VELOCITIES AND PRESSURES AT KEY POINTS THROUGHOUT THE FLOW SYSTEM ARE AS TABULATED BELOW.

VAPOR CAVITY

DIST.	.0000	.1280	.2560	.3840	.5119	.6399	.7679	.8959	1.0239	1.1519	1.2799	1.4078	1.5358	1.6638	1.7918
LOC.	0	2	4	6	8	10	12	14	16	18	20	22	24	26	28
U	.000	-.082	-.161	-.234	-.296	-.346	-.389	-.428	-.462	-.489	-.509	-.528	-.553	-.587	-.618
Z	.030	.031	.031	.031	.032	.033	.035	.036	.039	.041	.044	.047	.050	.054	.059

DIST.	1.9198	1.9838	2.0478	2.1118	2.1757
LOC.	30	31	32	33	34
U	-.623	-.613	-.597	-.579	-.560
Z	.062	.064	.065	.066	.067

FULL-FLOWING PIPE SYSTEM

LOC.	(1,0)	(1,1)	(2,0)	(2,10)	(2,20)	(2,30)	(2,40)	(2,50)
V	-.6571	-.6570	-.6548	-.6527	-.6512	-.6508	-.6642	-.6989
H	11.3000	11.4375	11.4375	14.5052	15.9816	17.4266	21.1833	33.1790

AT TIME T = 2.22497 SECONDS, AFTER 1199 COMPLETE CYCLES OF OPERATION, THE VELOCITIES AND DEPTHS IN THE VAPOR CAVITY AS WELL AS VELOCITIES AND PRESSURES AT KEY POINTS THROUGHOUT THE FLOW SYSTEM ARE AS TABULATED BELOW.

VAPOR CAVITY

DIST.	.0000	.1280	.2560	.3840	.5119	.6399	.7679	.8959	1.0239	1.1519	1.2799	1.4078	1.5358	1.6638	1.7918
LOC.	0	2	4	6	8	10	12	14	16	18	20	22	24	26	28
U	.000	-.084	-.164	-.238	-.301	-.353	-.398	-.439	-.473	-.500	-.521	-.543	-.573	-.608	-.639
Z	.031	.031	.031	.032	.032	.033	.035	.037	.039	.041	.044	.047	.051	.055	.059

DIST.	1.9198	1.9838	2.0478	2.1118	2.1757
LOC.	30	31	32	33	34
U	-.631	-.618	-.601	-.583	-.564
Z	.062	.063	.064	.065	.066

FULL-FLOWING PIPE SYSTEM

LOC.	(1,0)	(1,1)	(2,0)	(2,10)	(2,20)	(2,30)	(2,40)	(2,50)
------	-------	-------	-------	--------	--------	--------	--------	--------

V - .6598 - .6575 - .6561 - .6537 - .6673 - .7203 - .7379
H 11.3000 11.3434 14.0820 15.8217 19.5380 20.8432 33.1790

AT TIME T = 2.24353 SECONDS, AFTER 1209 COMPLETE CYCLES OF OPERATION, THE VELOCITIES AND DEPTHS IN THE VAPOR CAVITY AS WELL AS VELOCITIES AND PRESSURES AT KEY POINTS THROUGHOUT THE FLOW SYSTEM ARE AS TABULATED BELOW.

VAPOR CAVITY

DIST.	.0000	.1280	.2560	.3840	.5119	.6399	.7679	.8959	1.0239	1.1519	1.2799	1.4078	1.5358	1.6638	1.7918
LOC.	0	2	4	6	8	10	12	14	16	18	20	22	24	26	28
U	.000	-.085	-.167	-.242	-.306	-.360	-.408	-.449	-.484	-.511	-.534	-.560	-.593	-.629	-.669
Z	.031	.031	.031	.032	.032	.034	.035	.037	.039	.042	.044	.047	.051	.055	.059

DIST.	1.9198	1.9838	2.0478	2.1118
LOC.	30	31	32	33
U	-.637	-.622	-.605	-.586
Z	.062	.063	.064	.065

FULL-FLOWING PIPE SYSTEM

LOC.	(1,0)	(1,1)	(2,0)	(2,10)	(2,30)	(2,50)
V	-.6602	-.6602	-.6580	-.6722	-.7230	-.7408
H	11.3000	11.3476	11.3476	17.6319	27.2133	33.1790

AT TIME T = 2.26209 SECONDS, AFTER 1219 COMPLETE CYCLES OF OPERATION, THE VELOCITIES AND DEPTHS IN THE VAPOR CAVITY AS WELL AS VELOCITIES AND PRESSURES AT KEY POINTS THROUGHOUT THE FLOW SYSTEM ARE AS TABULATED BELOW.

VAPOR CAVITY

DIST.	.0000	.1280	.2560	.3840	.5119	.6399	.7679	.8959	1.0239	1.1519	1.2799	1.4078	1.5358	1.6638	1.7918
LOC.	0	2	4	6	8	10	12	14	16	18	20	22	24	26	28
U	.000	-.087	-.170	-.246	-.311	-.368	-.417	-.459	-.495	-.523	-.548	-.577	-.613	-.648	-.685
Z	.031	.031	.032	.032	.033	.034	.035	.037	.040	.042	.045	.048	.052	.056	.060

DIST.	1.9198	1.9838	2.0478	2.1118
LOC.	30	31	32	33
U	-.642	-.626	-.608	-.589
Z	.062	.063	.064	.065

FULL-FLOWING PIPE SYSTEM

LOC.	(1,0)	(1,1)	(2,0)	(2,10)	(2,30)	(2,50)
V	-.6612	-.6614	-.6592	-.7277	-.7455	-.7444
H	11.3000	11.3800	11.3800	25.3051	29.6309	33.1790

AT TIME T = 2.28064 SECONDS, AFTER 1229 COMPLETE CYCLES OF OPERATION, THE VELOCITIES AND DEPTHS IN THE VAPOR CAVITY AS WELL AS VELOCITIES AND PRESSURES AT KEY POINTS THROUGHOUT THE FLOW SYSTEM ARE AS TABULATED BELOW.

VAPOR CAVITY

DIST.	.0000	.1280	.2560	.3840	.5119	.6399	.7679	.8959	1.0239	1.1519	1.2799	1.4078	1.5358	1.6638	1.7918
LOC.	0	2	4	6	8	10	12	14	16	18	20	22	24	26	28
U	.000	-.088	-.173	-.250	-.317	-.376	-.426	-.470	-.506	-.535	-.563	-.595	-.634	-.666	-.670
Z	.032	.032	.032	.032	.033	.034	.036	.038	.040	.042	.045	.048	.052	.057	.060

DIST.	1.9198	1.9838	2.0478	2.1118
LOC.	30	31	32	33
U	-.646	-.629	-.611	-.592
Z	.062	.063	.064	.065

FULL-FLOWING PIPE SYSTEM

LOC.	(1,0)	(1,1)	(2,0)	(2,10)	(2,20)	(2,30)	(2,40)	(2,50)
V	-.6842	-.6864	-.6840	-.7282	-.7472	-.7490	-.7484	-.7471
H	11.3000	12.2208	12.2208	23.9988	28.1455	29.6797	31.2974	33.1790

AT TIME T = 2.29920 SECONDS, AFTER 1239 COMPLETE CYCLES OF OPERATION, THE VELOCITIES AND DEPTHS IN THE VAPOR CAVITY AS WELL AS VELOCITIES AND PRESSURES AT KEY POINTS THROUGHOUT THE FLOW SYSTEM ARE AS TABULATED BELOW.

VAPOR CAVITY

DIST.	.0000	.1280	.2560	.3840	.5119	.6399	.7679	.8959	1.0239	1.1519	1.2799	1.4078	1.5358	1.6638	1.7918
LOC.	0	2	4	6	8	10	12	14	16	18	20	22	24	26	28
U	.000	-.090	-.176	-.254	-.322	-.383	-.436	-.481	-.517	-.548	-.578	-.615	-.655	-.681	-.677
Z	.032	.032	.032	.033	.033	.034	.036	.038	.040	.043	.046	.049	.053	.057	.060

DIST.	1.9198	1.9838	2.0478
LOC.	30	31	32
U	-.649	-.632	-.614
Z	.062	.063	.064

FULL-FLOWING PIPE SYSTEM

LOC.	(1,0)	(1,1)	(2,0)	(2,10)	(2,20)	(2,30)	(2,40)	(2,50)
V	-.7906	-.7891	-.7865	-.7570	-.7495	-.7501	-.7517	-.7531
H	11.3000	12.9027	12.9027	25.4628	28.3708	29.8115	31.3115	33.1790

AT TIME T = 2.31776 SECONDS, AFTER 1249 COMPLETE CYCLES OF OPERATION, THE VELOCITIES AND DEPTHS IN THE VAPOR CAVITY AS WELL AS VELOCITIES AND PRESSURES AT KEY POINTS THROUGHOUT THE FLOW SYSTEM ARE AS TABULATED BELOW.

VAPOR CAVITY

DIST.	.0000	.1280	.2560	.3840	.5119	.6399	.7679	.8959	1.0239	1.1519	1.2799	1.4078	1.5358	1.6638	1.7918
LOC.	0	2	4	6	8	10	12	14	16	18	20	22	24	26	28
U	.000	-.092	-.178	-.258	-.328	-.392	-.446	-.491	-.528	-.561	-.594	-.634	-.674	-.693	-.682
Z	.032	.032	.033	.033	.034	.035	.036	.038	.041	.043	.046	.050	.054	.057	.060

DIST.	1.9198	1.9838	2.0478
LOC.	30	31	32
U	-.652	-.634	-.616
Z	.062	.063	.064

FULL-FLOWING PIPE SYSTEM

LOC.	(1,0)	(1,1)	(2,0)	(2,10)	(2,20)	(2,30)	(2,40)	(2,50)
V	-.8380	-.8372	-.8344	-.8076	-.7599	-.7522	-.7548	-.7562
H	11.3000	11.5367	11.5367	18.5778	27.1348	30.0018	31.7335	33.1790

AT TIME T = 2.33632 SECONDS, AFTER 1259 COMPLETE CYCLES OF OPERATION, THE VELOCITIES AND DEPTHS IN THE VAPOR CAVITY AS WELL AS VELOCITIES AND PRESSURES AT KEY POINTS THROUGHOUT THE FLOW SYSTEM ARE AS TABULATED BELOW.

VAPOR CAVITY

DIST.	.0000	.1280	.2560	.3840	.5119	.6399	.7679	.8959	1.0239	1.1519	1.2799	1.4078	1.5358	1.6638	1.7918
LOC.	0	2	4	6	8	10	12	14	16	18	20	22	24	26	28
U	.000	-.093	-.181	-.262	-.334	-.400	-.456	-.502	-.540	-.574	-.612	-.655	-.691	-.703	-.687
Z	.033	.033	.033	.033	.034	.035	.037	.039	.041	.043	.047	.050	.054	.058	.060

DIST.	1.9198	1.9838
LOC.	30	31

U -.655 -.637
Z .062 .063

FULL-FLOWING PIPE SYSTEM

LOC.	(1,0)	(1,1)	(2,0)	(2,10)	(2,20)	(2,30)	(2,40)	(2,50)
V	-.8419	-.8418	-.8390	-.8371	-.8101	-.7665	-.7567	-.7564
H	11.3000	11.3862	11.3862	14.5126	20.2363	29.0617	31.9103	35.1790

AT TIME T = 2.35487 SECONDS, AFTER 1269 COMPLETE CYCLES OF OPERATION, THE VELOCITIES AND DEPTHS IN THE VAPOR CAVITY AS WELL AS VELOCITIES AND PRESSURES AT KEY POINTS THROUGHOUT THE FLOW SYSTEM ARE AS TABULATED BELOW.

VAPOR CAVITY

DIST.	.0000	.1280	.2560	.3840	.5119	.6399	.7679	.8959	1.0239	1.1519	1.2799	1.4078	1.5358	1.6638	1.7918
LOC.	0	2	4	6	8	10	12	14	16	18	20	22	24	26	28
U	.000	-.095	-.184	-.266	-.341	-.408	-.466	-.513	-.552	-.589	-.630	-.674	-.707	-.711	-.690
Z	.033	.033	.033	.034	.034	.035	.037	.039	.041	.044	.047	.051	.055	.058	.060

DIST. 1.9198 1.9838
LOC. 30 31
U -.657 -.639
Z .062 .062

FULL-FLOWING PIPE SYSTEM

LOC.	(1,0)	(1,1)	(2,0)	(2,10)	(2,20)	(2,30)	(2,40)	(2,50)
V	-.8436	-.8436	-.8407	-.8414	-.8114	-.8144	-.7661	-.7572
H	11.3000	11.3881	11.3881	14.3262	16.4645	22.1720	30.5557	33.1790

AT TIME T = 2.37343 SECONDS, AFTER 1279 COMPLETE CYCLES OF OPERATION, THE VELOCITIES AND DEPTHS IN THE VAPOR CAVITY AS WELL AS VELOCITIES AND PRESSURES AT KEY POINTS THROUGHOUT THE FLOW SYSTEM ARE AS TABULATED BELOW.

VAPOR CAVITY

DIST.	.0000	.1280	.2560	.3840	.5119	.6399	.7679	.8959	1.0239	1.1519	1.2799	1.4078	1.5358	1.6638	1.7918
LOC.	0	2	4	6	8	10	12	14	16	18	20	22	24	26	28
U	.000	-.096	-.187	-.271	-.347	-.417	-.476	-.524	-.564	-.604	-.649	-.693	-.720	-.717	-.693
Z	.033	.033	.034	.034	.034	.036	.037	.039	.042	.044	.048	.051	.055	.058	.060

DIST. 1.9198
LOC. 30
U -.659
Z .061

FULL-FLOWING PIPE SYSTEM

LOC.	(1,0)	(1,1)	(2,0)	(2,10)	(2,20)	(2,30)	(2,40)	(2,50)
V	-.8464	-.8465	-.8436	-.8451	-.8457	-.8429	-.8147	-.7757
H	11.3000	11.4159	11.4159	14.6162	16.2652	17.9853	23.5111	33.1790

AT TIME T = 2.39199 SECONDS, AFTER 1289 COMPLETE CYCLES OF OPERATION, THE VELOCITIES AND DEPTHS IN THE VAPOR CAVITY AS WELL AS VELOCITIES AND PRESSURES AT KEY POINTS THROUGHOUT THE FLOW SYSTEM ARE AS TABULATED BELOW.

VAPOR CAVITY

DIST.	.0000	.1280	.2560	.3840	.5119	.6399	.7679	.8959	1.0239	1.1519	1.2799	1.4078	1.5358	1.6638	1.7918
LOC.	0	2	4	6	8	10	12	14	16	18	20	22	24	26	28
U	.000	-.097	-.190	-.275	-.354	-.426	-.486	-.535	-.578	-.621	-.668	-.711	-.731	-.722	-.695
Z	.034	.034	.034	.034	.035	.036	.038	.040	.042	.045	.048	.052	.055	.058	.060

DIST. 1.9198
 LOC. 30
 U -0.660
 Z .061

FULL-FLOWING PIPE SYSTEM

LOC.	(1,C)	(1,1)	(2,0)	(2,10)	(2,20)	(2,30)	(2,40)	(2,50)
V	-0.8519	-0.8519	-0.8490	-0.8479	-0.8465	-0.8459	-0.8522	-0.8718
H	11.3000	11.4521	11.4521	14.6320	16.1370	17.6091	20.6720	33.1790

AT TIME T = 2.41054 SECONDS, AFTER 1299 COMPLETE CYCLES OF OPERATION, THE VELOCITIES AND DEPTHS IN THE VAPOR CAVITY AS WELL AS VELOCITIES AND PRESSURES AT KEY POINTS THROUGHOUT THE FLOW SYSTEM ARE AS TABULATED BELOW.

VAPOR CAVITY

DIST.	0.0000	0.640	1.280	1.920	2.560	3.200	3.840	4.479	5.119	5.759	6.399	7.039	7.679	8.319	8.959
LOC.	0	1	2	3	4	5	6	7	8	9	10	11	12	13	14
V	0.00	-0.050	-0.099	-0.147	-0.193	-0.237	-0.280	-0.321	-0.361	-0.399	-0.435	-0.467	-0.496	-0.523	-0.547
Z	0.034	0.034	0.034	0.034	0.034	0.034	0.034	0.035	0.035	0.036	0.036	0.037	0.038	0.039	0.040
DIST.	0.9599	1.0239	1.0879	1.1519	1.2159	1.2799	1.3438	1.4078	1.4718	1.5358	1.5998	1.6638	1.7278	1.7918	1.8558
LOC.	15	16	17	18	19	20	21	22	23	24	25	26	27	28	29
V	-0.569	-0.591	-0.614	-0.638	-0.663	-0.688	-0.710	-0.727	-0.737	-0.740	-0.736	-0.726	-0.712	-0.696	-0.679
Z	0.041	0.042	0.044	0.045	0.047	0.049	0.051	0.053	0.054	0.056	0.057	0.058	0.059	0.060	0.060

FULL-FLOWING PIPE SYSTEM

LOC.	(1,0)	(1,1)	(2,0)	(2,10)	(2,20)	(2,30)	(2,40)	(2,50)
V	-0.8555	-0.8554	-0.8525	-0.8504	-0.8481	-0.8558	-0.9028	-0.9284
H	11.3000	11.3669	11.3669	14.2522	15.9768	18.8183	27.2958	31.1790

AT TIME T = 2.42910 SECONDS, AFTER 1309 COMPLETE CYCLES OF OPERATION, THE VELOCITIES AND DEPTHS IN THE VAPOR CAVITY AS WELL AS VELOCITIES AND PRESSURES AT KEY POINTS THROUGHOUT THE FLOW SYSTEM ARE AS TABULATED BELOW.

VAPOR CAVITY

DIST.	0.0000	0.640	1.280	1.920	2.560	3.200	3.840	4.479	5.119	5.759	6.399	7.039	7.679	8.319	8.959
LOC.	0	1	2	3	4	5	6	7	8	9	10	11	12	13	14
V	0.00	-0.051	-0.100	-0.149	-0.196	-0.241	-0.284	-0.327	-0.368	-0.407	-0.444	-0.477	-0.507	-0.534	-0.559
Z	0.034	0.034	0.034	0.034	0.035	0.035	0.035	0.035	0.036	0.036	0.037	0.038	0.038	0.039	0.040
DIST.	0.9599	1.0239	1.0879	1.1519	1.2159	1.2799	1.3438	1.4078	1.4718	1.5358	1.5998	1.6638	1.7278	1.7918	1.8558
LOC.	15	16	17	18	19	20	21	22	23	24	25	26	27	28	29
V	-0.582	-0.606	-0.631	-0.656	-0.682	-0.706	-0.727	-0.741	-0.748	-0.747	-0.740	-0.728	-0.714	-0.698	-0.681
Z	0.042	0.043	0.044	0.046	0.048	0.050	0.051	0.053	0.055	0.056	0.057	0.058	0.059	0.059	0.060

FULL-FLOWING PIPE SYSTEM

LOC.	(1,0)	(1,1)	(2,0)	(2,10)	(2,20)	(2,30)	(2,40)	(2,50)
V	-0.8554	-0.8554	-0.8525	-0.8527	-0.8597	-0.9048	-0.9318	-0.9337
H	11.3000	11.3609	11.3609	13.9909	16.9296	25.6358	31.3362	33.1790

AT TIME T = 2.44766 SECONDS, AFTER 1319 COMPLETE CYCLES OF OPERATION, THE VELOCITIES AND DEPTHS IN THE VAPOR CAVITY AS WELL AS VELOCITIES AND PRESSURES AT KEY POINTS THROUGHOUT THE FLOW SYSTEM ARE AS TABULATED BELOW.

VAPOR CAVITY

DIST.	0.0000	0.640	1.280	1.920	2.560	3.200	3.840	4.479	5.119	5.759	6.399	7.039	7.679	8.319	8.959
LOC.	0	1	2	3	4	5	6	7	8	9	10	11	12	13	14

U	.000	-.051	-.102	-.151	-.199	-.245	-.289	-.333	-.376	-.416	-.453	-.487	-.518	-.545	-.571
Z	.035	.035	.035	.035	.035	.035	.035	.036	.036	.036	.037	.038	.039	.040	.041
DIST.	.9599	1.0239	1.0879	1.1519	1.2159	1.2799	1.3438	1.4078	1.4718	1.5358	1.5998	1.6638	1.7278	1.7918	1.8558
LOC.	15	16	17	18	19	20	21	22	23	24	25	26	27	28	29
U	-.596	-.622	-.648	-.675	-.701	-.724	-.742	-.753	-.756	-.752	-.743	-.730	-.715	-.699	-.682
Z	.042	.043	.045	.047	.048	.050	.052	.053	.055	.056	.057	.058	.059	.059	.060

FULL-FLOWING PIPE SYSTEM

LOC.	(1,0)	(1,1)	(2,0)	(2,10)	(2,20)	(2,30)	(2,40)	(2,50)
V	-.8556	-.8557	-.8528	-.8617	-.9091	-.9354	-.9456	-.9352
H	11.3000	11.3765	11.3765	15.3105	23.6230	29.4179	31.5529	33.1790

AT TIME T = 2.46621 SECONDS, AFTER 1329 COMPLETE CYCLES OF OPERATION, THE VELOCITIES AND DEPTHS IN THE VAPOR CAVITY AS WELL AS VELOCITIES AND PRESSURES AT KEY POINTS THROUGHOUT THE FLOW SYSTEM ARE AS TABULATED BELOW.

VAPOR CAVITY

DIST.	.0000	.0640	.1280	.1920	.2560	.3200	.3840	.4479	.5119	.5759	.6399	.7039	.7679	.8319	.8959
LOC.	0	1	2	3	4	5	6	7	8	9	10	11	12	13	14
U	.000	-.052	-.103	-.153	-.202	-.249	-.295	-.339	-.383	-.424	-.463	-.497	-.529	-.557	-.584
Z	.035	.035	.035	.035	.035	.035	.036	.036	.036	.037	.038	.038	.039	.040	.041
DIST.	.9599	1.0239	1.0879	1.1519	1.2159	1.2799	1.3438	1.4078	1.4718	1.5358	1.5998	1.6638	1.7278	1.7918	
LOC.	15	16	17	18	19	20	21	22	23	24	25	26	27	28	
U	-.611	-.638	-.666	-.694	-.719	-.741	-.756	-.763	-.763	-.756	-.746	-.732	-.716	-.700	
Z	.043	.044	.046	.047	.049	.051	.052	.054	.055	.056	.057	.058	.058	.059	

FULL-FLOWING PIPE SYSTEM

LOC.	(1,0)	(1,1)	(2,0)	(2,10)	(2,20)	(2,30)	(2,40)	(2,50)
V	-.8685	-.8700	-.8671	-.9091	-.9372	-.9599	-.9388	-.9375
H	11.3000	11.9074	11.9074	22.2577	27.7677	29.5328	31.3038	33.1790

AT TIME T = 2.48477 SECONDS, AFTER 1339 COMPLETE CYCLES OF OPERATION, THE VELOCITIES AND DEPTHS IN THE VAPOR CAVITY AS WELL AS VELOCITIES AND PRESSURES AT KEY POINTS THROUGHOUT THE FLOW SYSTEM ARE AS TABULATED BELOW.

VAPOR CAVITY

DIST.	.0000	.0640	.1280	.1920	.2560	.3200	.3840	.4479	.5119	.5759	.6399	.7039	.7679	.8319	.8959
LOC.	0	1	2	3	4	5	6	7	8	9	10	11	12	13	14
U	.000	-.052	-.104	-.155	-.205	-.253	-.300	-.346	-.391	-.433	-.472	-.508	-.540	-.570	-.598
Z	.036	.036	.036	.036	.036	.036	.036	.036	.037	.037	.038	.039	.040	.041	.042
DIST.	.9599	1.0239	1.0879	1.1519	1.2159	1.2799	1.3438	1.4078	1.4718	1.5358	1.5998	1.6638	1.7278	1.7918	
LOC.	15	16	17	18	19	20	21	22	23	24	25	26	27	28	
U	-.627	-.655	-.684	-.712	-.737	-.756	-.767	-.771	-.768	-.759	-.747	-.733	-.717	-.701	
Z	.043	.045	.046	.048	.050	.051	.053	.054	.055	.056	.057	.058	.058	.059	

FULL-FLOWING PIPE SYSTEM

LOC.	(1,0)	(1,1)	(2,0)	(2,10)	(2,20)	(2,30)	(2,40)	(2,50)
V	-.9573	-.9571	-.9539	-.9423	-.9398	-.9405	-.9418	-.9423
H	11.3000	13.0125	13.0125	25.6151	28.1583	29.6531	31.2018	33.1790

AT TIME T = 2.50333 SECONDS, AFTER 1349 COMPLETE CYCLES OF OPERATION, THE VELOCITIES AND DEPTHS IN THE VAPOR CAVITY AS WELL AS VELOCITIES AND PRESSURES AT KEY POINTS THROUGHOUT THE FLOW SYSTEM ARE AS TABULATED BELOW.

VAPOR CAVITY

DIST.	.0000	.0640	.1280	.1920	.2560	.3200	.3840	.4479	.5119	.5759	.6399	.7039	.7679	.8319	.8959
LOC.	0	1	2	3	4	5	6	7	8	9	10	11	12	13	14
U	.000	-.053	-.106	-.158	-.208	-.253	-.306	-.353	-.399	-.442	-.482	-.518	-.552	-.583	-.613
Z	.036	.036	.036	.036	.036	.036	.036	.037	.037	.038	.038	.039	.040	.041	.042
DIST.	.9599	1.0239	1.0879	1.1519	1.2159	1.2799	1.3438	1.4078	1.4718	1.5358	1.5998	1.6638	1.7278		
LOC.	15	16	17	18	19	20	21	22	23	24	25	26	27		
U	-.643	-.673	-.703	-.730	-.753	-.768	-.776	-.777	-.771	-.761	-.749	-.734	-.718		
Z	.044	.045	.047	.049	.050	.052	.053	.054	.055	.056	.057	.058	.058		

FULL-FLOWING PIPE SYSTEM

LOC.	(1,0)	(1,1)	(2,0)	(2,10)	(2,20)	(2,30)	(2,40)	(2,50)
V	-1.0232	-1.0219	-1.0185	-0.9843	-0.9457	-0.9417	-0.9441	-0.9460
H	11.3000	11.7135	11.7135	20.2098	27.5041	29.8263	31.5689	33.1790

AT TIME T = 2.52188 SECONDS, AFTER 1359 COMPLETE CYCLES OF OPERATION, THE VELOCITIES AND DEPTHS IN THE VAPOR CAVITY AS WELL AS VELOCITIES AND PRESSURES AT KEY POINTS THROUGHOUT THE FLOW SYSTEM ARE AS TABULATED BELOW.

VAPOR CAVITY

DIST.	.0000	.0640	.1280	.1920	.2560	.3200	.3840	.4479	.5119	.5759	.6399	.7039	.7679	.8319	.8959
LOC.	0	1	2	3	4	5	6	7	8	9	10	11	12	13	14
U	.000	-.054	-.107	-.160	-.212	-.263	-.312	-.360	-.407	-.451	-.492	-.530	-.564	-.597	-.629
Z	.036	.036	.036	.036	.036	.037	.037	.037	.038	.038	.039	.040	.041	.042	.043
DIST.	.9599	1.0239	1.0879	1.1519	1.2159	1.2799	1.3438	1.4078	1.4718	1.5358	1.5998	1.6638	1.7278		
LOC.	15	16	17	18	19	20	21	22	23	24	25	26	27		
U	-.660	-.692	-.721	-.747	-.767	-.779	-.783	-.781	-.774	-.763	-.749	-.734	-.718		
Z	.044	.046	.048	.049	.051	.052	.053	.054	.055	.056	.057	.057	.058		

FULL-FLOWING PIPE SYSTEM

LOC.	(1,0)	(1,1)	(2,0)	(2,10)	(2,20)	(2,30)	(2,40)	(2,50)
V	-1.0291	-1.0290	-1.0256	-1.0215	-0.9860	-0.9492	-0.9459	-0.9458
H	11.3000	11.4079	11.4079	14.9158	21.9053	29.4225	31.8437	33.1790

AT TIME T = 2.54044 SECONDS, AFTER 1369 COMPLETE CYCLES OF OPERATION, THE VELOCITIES AND DEPTHS IN THE VAPOR CAVITY AS WELL AS VELOCITIES AND PRESSURES AT KEY POINTS THROUGHOUT THE FLOW SYSTEM ARE AS TABULATED BELOW.

VAPOR CAVITY

DIST.	.0000	.0640	.1280	.1920	.2560	.3200	.3840	.4479	.5119	.5759	.6399	.7039	.7679	.8319	.8959
LOC.	0	1	2	3	4	5	6	7	8	9	10	11	12	13	14
U	.000	-.054	-.109	-.162	-.215	-.267	-.318	-.368	-.416	-.461	-.502	-.541	-.577	-.611	-.645
Z	.037	.037	.037	.037	.037	.037	.037	.038	.038	.039	.039	.040	.041	.042	.043
DIST.	.9599	1.0239	1.0879	1.1519	1.2159	1.2799	1.3438	1.4078	1.4718	1.5358	1.5998	1.6638			
LOC.	15	16	17	18	19	20	21	22	23	24	25	26			
U	-.678	-.710	-.739	-.762	-.779	-.788	-.789	-.785	-.776	-.764	-.750	-.734			
Z	.045	.047	.048	.050	.051	.052	.054	.054	.055	.056	.057	.057			

FULL-FLOWING PIPE SYSTEM

LOC.	(1,0)	(1,1)	(2,0)	(2,10)	(2,20)	(2,30)	(2,40)	(2,50)
V	-1.0302	-1.0302	-1.0268	-1.0272	-1.0248	-0.9900	-0.9509	-0.9458
H	11.3000	11.3991	11.3991	14.3929	16.8689	23.9492	31.0785	33.1790

AT TIME T = 2.55900 SECONDS, AFTER 1379 COMPLETE CYCLES OF OPERATION, THE VELOCITIES AND DEPTHS IN THE VAPOR CAVITY AS WELL AS VELOCITIES AND PRESSURES AT KEY POINTS THROUGHOUT THE FLOW SYSTEM ARE AS TABULATED BELOW.

VAPOR CAVITY

DIST.	.0000	.1280	.1920	.2560	.3200	.3840	.4479	.5119	.5759	.6399	.7039	.7679	.8319	.8959
LOC.	0	1	2	3	4	5	6	7	8	9	10	11	12	13
U	.000	-.055	-.110	-.165	-.219	-.272	-.324	-.375	-.424	-.470	-.513	-.559	-.607	-.662
Z	.037	.037	.037	.037	.037	.038	.038	.039	.039	.040	.041	.042	.043	.044

DIST. .9599 1.0239 1.0879 1.1519 1.2159 1.2799 1.3438 1.4078 1.4718 1.5358 1.5998

LOC. 15 16 17 18 19 20 21 22 23 24 25

U -.696 -.728 -.755 -.776 -.789 -.794 -.793 -.787 -.777 -.764 -.750

Z .046 .047 .049 .050 .052 .053 .054 .055 .055 .056 .057

FULL-FLOWING PIPE SYSTEM

LOC.	(1,0)	(1,1)	(2,0)	(2,10)	(2,20)	(2,30)	(2,40)	(2,50)
V	-1.0321	-1.0321	-1.0286	-1.0300	-1.0311	-1.0262	-0.9897	-0.9559
H	11.3000	11.4213	11.4213	14.6286	16.4476	18.5609	25.3549	33.1790

AT TIME T = 2.57756 SECONDS, AFTER 1389 COMPLETE CYCLES OF OPERATION, THE VELOCITIES AND DEPTHS IN THE VAPOR CAVITY AS WELL AS VELOCITIES AND PRESSURES AT KEY POINTS THROUGHOUT THE FLOW SYSTEM ARE AS TABULATED BELOW.

VAPOR CAVITY

DIST.	.0000	.0640	.1280	.1920	.2560	.3200	.3840	.4479	.5119	.5759	.6399	.7039	.7679	.8319	.8959
LOC.	0	1	2	3	4	5	6	7	8	9	10	11	12	13	14
U	.000	-.056	-.112	-.168	-.223	-.278	-.331	-.383	-.433	-.480	-.524	-.566	-.605	-.643	-.680
Z	.038	.038	.038	.038	.038	.038	.038	.039	.039	.040	.040	.041	.042	.043	.045

DIST. .9599 1.0239 1.0879 1.1519 1.2159 1.2799 1.3438 1.4078 1.4718 1.5358 1.5998

LOC. 15 16 17 18 19 20 21 22 23 24 25

U -.715 -.745 -.770 -.788 -.797 -.796 -.796 -.788 -.777 -.764 -.749

Z .046 .048 .049 .051 .052 .053 .054 .055 .055 .056 .057

FULL-FLOWING PIPE SYSTEM

LOC.	(1,0)	(1,1)	(2,0)	(2,10)	(2,20)	(2,30)	(2,40)	(2,50)
V	-1.0363	-1.0363	-1.0328	-1.0326	-1.0314	-1.0307	-1.0310	-1.0333
H	11.3000	11.4606	11.4606	14.7526	16.3205	17.8663	20.7364	33.1790

AT TIME T = 2.59611 SECONDS, AFTER 1399 COMPLETE CYCLES OF OPERATION, THE VELOCITIES AND DEPTHS IN THE VAPOR CAVITY AS WELL AS VELOCITIES AND PRESSURES AT KEY POINTS THROUGHOUT THE FLOW SYSTEM ARE AS TABULATED BELOW.

VAPOR CAVITY

DIST.	.0000	.0640	.1280	.1920	.2560	.3200	.3840	.4479	.5119	.5759	.6399	.7039	.7679	.8319	.8959
LOC.	0	1	2	3	4	5	6	7	8	9	10	11	12	13	14
U	.000	-.057	-.113	-.170	-.227	-.283	-.338	-.391	-.442	-.491	-.536	-.580	-.621	-.660	-.698
Z	.038	.038	.038	.038	.038	.038	.039	.039	.040	.040	.041	.042	.043	.044	.045

DIST. .9599 1.0239 1.0879 1.1519 1.2159 1.2799 1.3438 1.4078 1.4718 1.5358

LOC. 15 16 17 18 19 20 21 22 23 24 25

U -.732 -.761 -.783 -.797 -.804 -.803 -.798 -.789 -.777 -.764

Z .047 .048 .050 .051 .052 .053 .054 .055 .055 .056 .056

FULL-FLOWING PIPE SYSTEM

LOC.	(1,0)	(1,1)	(2,0)	(2,10)	(2,20)	(2,30)	(2,40)	(2,50)
V	-1.0402	-1.0401	-1.0366	-1.0342	-1.0321	-1.0361	-1.0739	-1.1055
H	11.3000	11.4010	11.4010	14.4315	16.1123	18.4930	25.7190	33.1790

AT TIME T = 2.61467 SECONDS, AFTER 1409 COMPLETE CYCLES OF OPERATION, THE VELOCITIES AND DEPTHS IN THE VAPOR CAVITY AS WELL AS VELOCITIES AND PRESSURES AT KEY POINTS THROUGHOUT THE FLOW SYSTEM ARE AS TABULATED BELOW.

VAPOR CAVITY

DIST.	.0000	.0640	.1280	.1920	.2560	.3200	.3840	.4479	.5119	.5759	.6399	.7039	.7679	.8319	.8959
LOC.	0	1	2	3	4	5	6	7	8	9	10	11	12	13	14
U	.000	-.057	-.115	-.173	-.232	-.289	-.345	-.400	-.452	-.502	-.549	-.594	-.637	-.678	-.718
Z	.039	.039	.039	.039	.039	.039	.039	.040	.040	.041	.041	.042	.043	.045	.046
DIST.	.9599	1.0239	1.0879	1.1519	1.2159	1.2799	1.3438	1.4078	1.4718	1.5358					
LOC.	15	16	17	18	19	20	21	22	23	24					
U	-.749	-.775	-.794	-.805	-.808	-.806	-.799	-.789	-.777	-.763					
Z	.048	.049	.050	.051	.052	.053	.054	.055	.055	.056					

FULL-FLOWING PIPE SYSTEM

LOC.	(1,0)	(1,1)	(2,0)	(2,10)	(2,20)	(2,30)	(2,40)	(2,50)
V	-1.0397	-1.0397	-1.0362	-1.0362	-1.0389	-1.0752	-1.1164	-1.1144
H	11.3000	11.3745	11.3745	14.1007	16.6621	23.9989	30.9378	33.1790

AT TIME T = 2.63323 SECONDS, AFTER 1419 COMPLETE CYCLES OF OPERATION, THE VELOCITIES AND DEPTHS IN THE VAPOR CAVITY AS WELL AS VELOCITIES AND PRESSURES AT KEY POINTS THROUGHOUT THE FLOW SYSTEM ARE AS TABULATED BELOW.

VAPOR CAVITY

DIST.	.0000	.0640	.1280	.1920	.2560	.3200	.3840	.4479	.5119	.5759	.6399	.7039	.7679	.8319	.8959
LOC.	0	1	2	3	4	5	6	7	8	9	10	11	12	13	14
U	.000	-.058	-.117	-.177	-.236	-.295	-.352	-.408	-.462	-.513	-.562	-.609	-.654	-.696	-.733
Z	.039	.039	.039	.039	.039	.039	.040	.040	.041	.041	.042	.043	.044	.045	.047
DIST.	.9599	1.0239	1.0879	1.1519	1.2159	1.2799	1.3438	1.4078	1.4718						
LOC.	15	16	17	18	19	20	21	22	23						
U	-.764	-.788	-.803	-.811	-.812	-.808	-.800	-.789	-.777						
Z	.048	.049	.051	.052	.053	.053	.054	.054	.055						

FULL-FLOWING PIPE SYSTEM

LOC.	(1,0)	(1,1)	(2,0)	(2,10)	(2,20)	(2,30)	(2,40)	(2,50)
V	-1.0393	-1.0394	-1.0359	-1.0409	-1.0790	-1.1129	-1.1155	-1.1153
H	11.3000	11.3828	11.3828	14.8199	21.9025	29.0682	31.4830	33.1790

AT TIME T = 2.65178 SECONDS, AFTER 1429 COMPLETE CYCLES OF OPERATION, THE VELOCITIES AND DEPTHS IN THE VAPOR CAVITY AS WELL AS VELOCITIES AND PRESSURES AT KEY POINTS THROUGHOUT THE FLOW SYSTEM ARE AS TABULATED BELOW.

VAPOR CAVITY

DIST.	.0000	.0640	.1280	.1920	.2560	.3200	.3840	.4479	.5119	.5759	.6399	.7039	.7679	.8319	.8959
LOC.	0	1	2	3	4	5	6	7	8	9	10	11	12	13	14
U	.000	-.059	-.119	-.180	-.241	-.301	-.360	-.417	-.472	-.525	-.576	-.625	-.671	-.713	-.749
Z	.040	.040	.040	.040	.040	.040	.040	.041	.041	.042	.043	.044	.045	.046	.047
DIST.	.9599	1.0239	1.0879	1.1519	1.2159	1.2799	1.3438	1.4078	1.4718						
LOC.	15	16	17	18	19	20	21	22	23						
U	-.778	-.799	-.811	-.815	-.814	-.809	-.800	-.789	-.776						
Z	.049	.050	.051	.052	.053	.053	.054	.054	.055						

FULL-FLOWING PIPE SYSTEM

LOC.	(1,0)	(1,1)	(2,0)	(2,10)	(2,20)	(2,30)	(2,40)	(2,50)
V	-1.0393	-1.0394	-1.0359	-1.0409	-1.0790	-1.1129	-1.1155	-1.1153
H	11.3000	11.3828	11.3828	14.8199	21.9025	29.0682	31.4830	33.1790

V -1.0458 -1.0468 -1.0478 -1.1146 -1.1177 -1.1167
H 11.3000 11.6970 11.6970 27.1862 29.3701 31.1701

AT TIME T = 2.67034 SECONDS, AFTER 1439 COMPLETE CYCLES OF OPERATION, THE VELOCITIES AND DEPTHS IN THE VAPOR CAVITY AS WELL AS VELOCITIES AND PRESSURES AT KEY POINTS THROUGHOUT THE FLOW SYSTEM ARE AS TABULATED BELOW.

VAPOR CAVITY

DIST.	.0600	.6640	.1280	.1920	.2560	.3200	.3840	.4479	.5119	.5759	.6399	.7039	.7679	.8319	.8959
LOC.	0	1	2	3	4	5	6	7	8	9	10	11	12	13	14
U	.000	-.061	-.122	-.184	-.246	-.307	-.368	-.429	-.490	-.552	-.613	-.675	-.736	-.797	-.858
Z	.040	.040	.040	.040	.040	.041	.041	.041	.042	.042	.043	.044	.045	.045	.044

DIST.	.9599	1.0239	1.0879	1.1519	1.2159	1.2799	1.3438	1.4078
LOC.	15	16	17	18	19	20	21	22
U	-.790	-.807	-.816	-.819	-.816	-.809	-.798	-.786
Z	.049	.050	.051	.052	.053	.053	.054	.054

FULL-FLOWING PIPE SYSTEM

LOC.	(1,0)	(1,1)	(2,0)	(2,10)	(2,40)	(2,30)	(2,40)	(2,50)
V	-1.1135	-1.1143	-1.1136	-1.1167	-1.1186	-1.1194	-1.1203	-1.1211
H	11.3000	12.9082	12.9082	25.3032	27.0836	29.4664	31.1096	33.1790

AT TIME T = 2.68890 SECONDS, AFTER 1449 COMPLETE CYCLES OF OPERATION, THE VELOCITIES AND DEPTHS IN THE VAPOR CAVITY AS WELL AS VELOCITIES AND PRESSURES AT KEY POINTS THROUGHOUT THE FLOW SYSTEM ARE AS TABULATED BELOW.

VAPOR CAVITY

DIST.	.0000	.0640	.1280	.1920	.2560	.3200	.3840	.4479	.5119	.5759	.6399	.7039	.7679	.8319	.8959
LOC.	0	1	2	3	4	5	6	7	8	9	10	11	12	13	14
U	.000	-.062	-.124	-.188	-.251	-.314	-.376	-.436	-.495	-.552	-.607	-.658	-.705	-.746	-.777
Z	.041	.041	.041	.041	.041	.041	.041	.042	.042	.043	.044	.045	.046	.047	.049

DIST.	.9599	1.0239	1.0879	1.1519	1.2159	1.2799	1.3438	1.4078
LOC.	15	16	17	18	19	20	21	22
U	-.800	-.814	-.820	-.821	-.816	-.809	-.798	-.786
Z	.050	.051	.051	.052	.053	.053	.054	.054

FULL-FLOWING PIPE SYSTEM

LOC.	(1,0)	(1,1)	(2,0)	(2,10)	(2,40)	(2,30)	(2,40)	(2,50)
V	-1.1935	-1.1918	-1.1878	-1.1503	-1.1215	-1.1197	-1.1218	-1.1239
H	11.3000	11.9708	11.9708	21.6408	27.5861	29.6221	31.3970	33.1790

AT TIME T = 2.70745 SECONDS, AFTER 1459 COMPLETE CYCLES OF OPERATION, THE VELOCITIES AND DEPTHS IN THE VAPOR CAVITY AS WELL AS VELOCITIES AND PRESSURES AT KEY POINTS THROUGHOUT THE FLOW SYSTEM ARE AS TABULATED BELOW.

VAPOR CAVITY

DIST.	.0000	.0640	.1280	.1920	.2560	.3200	.3840	.4479	.5119	.5759	.6399	.7039	.7679	.8319	.8959
LOC.	0	1	2	3	4	5	6	7	8	9	10	11	12	13	14
U	.000	-.063	-.127	-.192	-.257	-.321	-.385	-.447	-.507	-.566	-.623	-.675	-.722	-.750	-.789
Z	.041	.041	.041	.042	.042	.042	.042	.043	.043	.044	.045	.046	.047	.048	.049

DIST.	.9599	1.0239	1.0879	1.1519	1.2159	1.2799	1.3438
LOC.	15	16	17	18	19	20	21
U	-.808	-.819	-.823	-.822	-.816	-.808	-.797
Z	.050	.051	.052	.052	.053	.053	.054

U -0.823 -0.627 -0.826 -0.821 -0.813
 Z .051 .051 .052 .052 .053

FULL-FLOWING PIPE SYSTEM

LOC. (1,0) (1,1) (2,0) (2,10) (2,20) (2,30) (2,40) (2,50)
 V -1.2083 -1.2083 -1.2042 -1.2047 -1.2039 -1.2029 -1.1973 -1.1847
 H 11.3000 11.4657 11.4657 14.8571 16.5298 18.1965 21.3343 23.1790

AT TIME T = 2.76168 SECONDS, AFTER 1499 COMPLETE CYCLES OF OPERATION, THE VELOCITIES AND DEPTHS IN THE VAPOR CAVITY AS WELL AS VELOCITIES AND PRESSURES AT KEY POINTS THROUGHOUT THE FLOW SYSTEM ARE AS TABULATED BELOW.

VAPOR CAVITY

DIST. .0000 .0640 .1280 .1920 .2560 .3200 .3840 .4479 .5119 .5759 .6399 .7039 .7679 .8319 .8959
 LOC. 0 1 2 3 4 5 6 7 8 9 10 11 12 13 14
 U .000 -0.070 -0.140 -0.211 -0.282 -0.353 -0.425 -0.495 -0.564 -0.628 -0.686 -0.735 -0.773 -0.800 -0.817
 Z .044 .044 .044 .044 .044 .045 .045 .046 .046 .047 .048 .049 .049 .050 .051

DIST. .9599 1.0239 1.0879 1.1519 1.2159
 LOC. 15 16 17 18 19
 U -0.825 -0.828 -0.825 -0.820 -0.811
 Z .051 .052 .052 .052 .053

FULL-FLOWING PIPE SYSTEM

LOC. (1,0) (1,1) (2,0) (2,10) (2,20) (2,30) (2,40) (2,50)
 V -1.2121 -1.2119 -1.2079 -1.2055 -1.2037 -1.2036 -1.2335 -1.2660
 H 11.3000 11.4361 11.4361 14.8131 16.5261 18.4507 24.3569 33.1790

AT TIME T = 2.80024 SECONDS, AFTER 1509 COMPLETE CYCLES OF OPERATION, THE VELOCITIES AND DEPTHS IN THE VAPOR CAVITY AS WELL AS VELOCITIES AND PRESSURES AT KEY POINTS THROUGHOUT THE FLOW SYSTEM ARE AS TABULATED BELOW.

VAPOR CAVITY

DIST. .0000 .0640 .1280 .1920 .2560 .3200 .3840 .4479 .5119 .5759 .6399 .7039 .7679 .8319 .8959
 LOC. 0 1 2 3 4 5 6 7 8 9 10 11 12 13 14
 U .000 -0.072 -0.144 -0.217 -0.289 -0.363 -0.437 -0.509 -0.579 -0.643 -0.700 -0.746 -0.781 -0.805 -0.820
 Z .045 .045 .045 .045 .045 .045 .046 .046 .047 .048 .048 .049 .050 .050 .051

DIST. .9599 1.0239 1.0879 1.1519
 LOC. 15 16 17 18
 U -0.826 -0.827 -0.824 -0.818
 Z .051 .052 .052 .052

FULL-FLOWING PIPE SYSTEM

LOC. (1,0) (1,1) (2,0) (2,10) (2,20) (2,30) (2,40) (2,50)
 V -1.2115 -1.2115 -1.2074 -1.2069 -1.2072 -1.2341 -1.2745 -1.2819
 H 11.3000 11.3880 11.3880 14.2556 16.5336 22.5453 30.2957 33.1790

AT TIME T = 2.81879 SECONDS, AFTER 1519 COMPLETE CYCLES OF OPERATION, THE VELOCITIES AND DEPTHS IN THE VAPOR CAVITY AS WELL AS VELOCITIES AND PRESSURES AT KEY POINTS THROUGHOUT THE FLOW SYSTEM ARE AS TABULATED BELOW.

VAPOR CAVITY

DIST. .0000 .0640 .1280 .1920 .2560 .3200 .3840 .4479 .5119 .5759 .6399 .7039 .7679 .8319 .8959
 LOC. 0 1 2 3 4 5 6 7 8 9 10 11 12 13 14
 U .000 -0.074 -0.148 -0.223 -0.297 -0.373 -0.449 -0.523 -0.594 -0.657 -0.712 -0.755 -0.787 -0.809 -0.821
 Z .045 .045 .046 .046 .046 .046 .047 .047 .048 .049 .049 .050 .050 .051 .051

DIST. .9599 1.0239 1.0879 1.1519
 LOC. 15 16 17 18
 U -.827 -.827 -.823 -.816
 Z .051 .052 .052 .052

FULL-FLOWING PIPE SYSTEM

LOC. (1,0) (1,1) (2,0) (2,10) (2,20) (2,30) (2,40) (2,50)
 V -1.2104 -1.2104 -1.2063 -1.2090 -1.2071 -1.2756 -1.2823 -1.2824
 H 11.3000 11.3939 11.3939 14.5853 20.3851 28.3468 31.3833 33.1790

AT TIME T = 2.83735 SECONDS, AFTER 1529 COMPLETE CYCLES OF OPERATION, THE VELOCITIES AND DEPTHS IN THE VAPOR CAVITY AS WELL AS VELOCITIES AND PRESSURES AT KEY POINTS THROUGHOUT THE FLOW SYSTEM ARE AS TABULATED BELOW.

VAPOR CAVITY

DIST. .0000 .0640 .1280 .1920 .2560 .3200 .3840 .4479 .5119 .5759 .6399 .7039 .7679 .8319 .8959
 LOC. 0 1 2 3 4 5 6 7 8 9 10 11 12 13 14
 U .000 -.076 -.152 -.229 -.306 -.384 -.462 -.537 -.608 -.670 -.722 -.763 -.792 -.811 -.822
 Z .046 .046 .046 .047 .047 .047 .048 .048 .049 .049 .050 .050 .051 .051 .051

DIST. .9599 1.0239 1.0879
 LOC. 15 16 17
 U -.826 -.825 -.820
 Z .051 .052 .052

FULL-FLOWING PIPE SYSTEM

LOC. (1,0) (1,1) (2,0) (2,10) (2,20) (2,30) (2,40) (2,50)
 V -1.2129 -1.2135 -1.2094 -1.2364 -1.2774 -1.2852 -1.2837 -1.2828
 H 11.3000 11.5704 11.5704 18.7790 26.3465 29.1987 31.2601 33.1790

AT TIME T = 2.85591 SECONDS, AFTER 1539 COMPLETE CYCLES OF OPERATION, THE VELOCITIES AND DEPTHS IN THE VAPOR CAVITY AS WELL AS VELOCITIES AND PRESSURES AT KEY POINTS THROUGHOUT THE FLOW SYSTEM ARE AS TABULATED BELOW.

VAPOR CAVITY

DIST. .0000 .0640 .1280 .1920 .2560 .3200 .3840 .4479 .5119 .5759 .6399 .7039 .7679 .8319 .8959
 LOC. 0 1 2 3 4 5 6 7 8 9 10 11 12 13 14
 U .000 -.078 -.157 -.236 -.315 -.395 -.475 -.551 -.621 -.682 -.731 -.769 -.795 -.813 -.822
 Z .047 .047 .047 .047 .048 .048 .049 .049 .050 .050 .050 .051 .051 .051 .051

DIST. .9599 1.0239
 LOC. 15 16
 U -.825 -.823
 Z .051 .052

FULL-FLOWING PIPE SYSTEM

LOC. (1,0) (1,1) (2,0) (2,10) (2,20) (2,30) (2,40) (2,50)
 V -1.2604 -1.2618 -1.2576 -1.2775 -1.2842 -1.2852 -1.2856 -1.2850
 H 11.3000 12.6650 12.6650 24.5675 27.5657 29.2671 31.0381 33.1790

AT TIME T = 2.87447 SECONDS, AFTER 1549 COMPLETE CYCLES OF OPERATION, THE VELOCITIES AND DEPTHS IN THE VAPOR CAVITY AS WELL AS VELOCITIES AND PRESSURES AT KEY POINTS THROUGHOUT THE FLOW SYSTEM ARE AS TABULATED BELOW.

VAPOR CAVITY

DIST. .0000 .0640 .1280 .1920 .2560 .3200 .3840 .4479 .5119 .5759 .6399 .7039 .7679 .8319 .8959
 LOC. 0 1 2 3 4 5 6 7 8 9 10 11 12 13 14

U .000 -.001 -.162 -.243 -.325 -.407 -.488 -.564 -.633 -.691 -.738 -.773 -.797 -.813 -.821
 Z .048 .048 .048 .048 .049 .049 .050 .050 .050 .051 .051 .051 .051 .051

DIST. .9599 1.0239
 LOC. 15 16
 U -.823 -.820
 Z .051 .052

FULL-FLOWING PIPE SYSTEM

LOC. (1,0) (1,1) (2,0) (2,10) (2,20) (2,30) (2,40) (2,50)
 V -1.3466 -1.3448 -1.3403 -1.3051 -1.2853 -1.2847 -1.2865 -1.2884
 H 11.3000 12.2553 12.2553 22.7221 27.4858 29.4040 31.2278 33.1790

AT TIME T = 2.89302 SECONDS, AFTER 1569 COMPLETE CYCLES OF OPERATION, THE VELOCITIES AND DEPTHS IN THE VAPOR CAVITY AS WELL AS VELOCITIES AND PRESSURES AT KEY POINTS THROUGHOUT THE FLOW SYSTEM ARE AS TABULATED BELOW.

VAPOR CAVITY

DIST. .0000 .0640 .1280 .1920 .2560 .3200 .3840 .4479 .5119 .5759 .6399 .7039 .7679 .8319 .8959
 LOC. 0 1 2 3 4 5 6 7 8 9 10 11 12 13 14
 U .000 -.083 -.167 -.251 -.336 -.419 -.501 -.576 -.643 -.699 -.743 -.775 -.798 -.812 -.819
 Z .049 .049 .049 .049 .050 .050 .051 .051 .051 .051 .051 .051 .051 .051 .051

DIST. .9599
 LOC. 15
 U -.820
 Z .051

FULL-FLOWING PIPE SYSTEM

LOC. (1,0) (1,1) (2,0) (2,10) (2,20) (2,30) (2,40) (2,50)
 V -1.3652 -1.3650 -1.3604 -1.3478 -1.3054 -1.2865 -1.2874 -1.2879
 H 11.3000 11.4732 11.4732 16.4923 24.5791 29.4463 31.5843 33.1790

AT TIME T = 2.91158 SECONDS, AFTER 1569 COMPLETE CYCLES OF OPERATION, THE VELOCITIES AND DEPTHS IN THE VAPOR CAVITY AS WELL AS VELOCITIES AND PRESSURES AT KEY POINTS THROUGHOUT THE FLOW SYSTEM ARE AS TABULATED BELOW.

VAPOR CAVITY

DIST. .0000 .0640 .1280 .1920 .2560 .3200 .3840 .4479 .5119 .5759 .6399 .7039 .7679 .8319 .8959
 LOC. 0 1 2 3 4 5 6 7 8 9 10 11 12 13 14
 U .000 -.086 -.173 -.260 -.346 -.432 -.513 -.587 -.651 -.704 -.746 -.776 -.797 -.810 -.816
 Z .050 .050 .050 .050 .051 .051 .052 .052 .052 .052 .052 .052 .052 .051 .051

FULL-FLOWING PIPE SYSTEM

LOC. (1,0) (1,1) (2,0) (2,10) (2,20) (2,30) (2,40) (2,50)
 V -1.3655 -1.3655 -1.3609 -1.3605 -1.3487 -1.3080 -1.2880 -1.2865
 H 11.3000 11.4255 11.4255 14.6376 18.4959 26.7764 31.4396 33.1790

AT TIME T = 2.93014 SECONDS, AFTER 1579 COMPLETE CYCLES OF OPERATION, THE VELOCITIES AND DEPTHS IN THE VAPOR CAVITY AS WELL AS VELOCITIES AND PRESSURES AT KEY POINTS THROUGHOUT THE FLOW SYSTEM ARE AS TABULATED BELOW.

VAPOR CAVITY

DIST. .0000 .0640 .1280 .1920 .2560 .3200 .3840 .4479 .5119 .5759 .6399 .7039 .7679 .8319 .8959
 LOC. 0 1 2 3 4 5 6 7 8 9 10 11 12 13 14
 U .000 -.090 -.179 -.269 -.357 -.443 -.524 -.596 -.658 -.708 -.747 -.776 -.796 -.812 -.813
 Z .051 .051 .051 .052 .052 .052 .053 .053 .053 .052 .052 .052 .052 .052 .051

FULL-FLOWING PIPE SYSTEM

LOC.	(1,C)	(1,1)	(2,0)	(2,10)	(2,20)	(2,30)	(2,40)	(2,50)
V	-1.3655	-1.3655	-1.3609	-1.3618	-1.3629	-1.3699	-1.3670	-1.3680
H	11.3000	11.4372	11.4372	14.7094	16.8631	20.5323	28.4325	33.1790

AT TIME T = 2.94869 SECONDS, AFTER 1539 COMPLETE CYCLES OF OPERATION, THE VELOCITIES AND DEPTHS IN THE VAPOR CAVITY AS WELL AS VELOCITIES AND PRESSURES AT KEY POINTS THROUGHOUT THE FLOW SYSTEM ARE AS TABULATED BELOW.

VAPOR CAVITY

DIST.	.0000	.0640	.1280	.1920	.2560	.3200	.3840	.4479	.5119	.5759	.6399	.7039	.7679	.8319
LOC.	0	1	2	3	4	5	6	7	8	9	10	11	12	13
U	.000	-.093	-.186	-.278	-.368	-.454	-.533	-.603	-.662	-.710	-.747	-.775	-.793	-.804
Z	.052	.052	.052	.053	.053	.053	.054	.053	.053	.053	.052	.052	.052	.052

FULL-FLOWING PIPE SYSTEM

LOC.	(1,0)	(1,1)	(2,0)	(2,10)	(2,20)	(2,30)	(2,40)	(2,50)
V	-1.3670	-1.3671	-1.3624	-1.3633	-1.3629	-1.3617	-1.3496	-1.3272
H	11.3000	11.4694	11.4694	14.9386	16.7486	18.5498	22.3570	33.1790

AT TIME T = 2.96725 SECONDS, AFTER 1599 COMPLETE CYCLES OF OPERATION, THE VELOCITIES AND DEPTHS IN THE VAPOR CAVITY AS WELL AS VELOCITIES AND PRESSURES AT KEY POINTS THROUGHOUT THE FLOW SYSTEM ARE AS TABULATED BELOW.

VAPOR CAVITY

DIST.	.0000	.0640	.1280	.1920	.2560	.3200	.3840	.4479	.5119	.5759	.6399	.7039	.7679
LOC.	0	1	2	3	4	5	6	7	8	9	10	11	12
U	.000	-.097	-.193	-.287	-.378	-.464	-.541	-.608	-.665	-.711	-.746	-.772	-.790
Z	.054	.054	.054	.054	.054	.054	.054	.054	.054	.053	.053	.052	.052

FULL-FLOWING PIPE SYSTEM

LOC.	(1,0)	(1,1)	(2,0)	(2,10)	(2,20)	(2,30)	(2,40)	(2,50)
V	-1.3702	-1.3701	-1.3659	-1.3636	-1.3620	-1.3627	-1.3816	-1.4107
H	11.3000	11.4652	11.4652	14.7863	16.6261	18.5765	23.3525	33.1790

AT TIME T = 2.98581 SECONDS, AFTER 1609 COMPLETE CYCLES OF OPERATION, THE VELOCITIES AND DEPTHS IN THE VAPOR CAVITY AS WELL AS VELOCITIES AND PRESSURES AT KEY POINTS THROUGHOUT THE FLOW SYSTEM ARE AS TABULATED BELOW.

VAPOR CAVITY

DIST.	.0000	.0640	.1280	.1920	.2560	.3200	.3840	.4479	.5119	.5759	.6399	.7039
LOC.	0	1	2	3	4	5	6	7	8	9	10	11
U	.000	-.100	-.200	-.296	-.388	-.472	-.547	-.612	-.666	-.710	-.744	-.769
Z	.055	.055	.055	.055	.056	.056	.055	.055	.054	.054	.053	.052

FULL-FLOWING PIPE SYSTEM

LOC.	(1,0)	(1,1)	(2,0)	(2,10)	(2,20)	(2,30)	(2,40)	(2,50)
V	-1.3698	-1.3698	-1.3652	-1.3642	-1.3633	-1.3818	-1.4234	-1.4355
H	11.3000	11.4037	11.4037	14.4329	16.6148	21.4132	29.4021	33.1790

AT TIME T = 3.00436 SECONDS, AFTER 1619 COMPLETE CYCLES OF OPERATION, THE VELOCITIES AND DEPTHS IN THE VAPOR CAVITY AS WELL AS VELOCITIES AND PRESSURES AT KEY POINTS THROUGHOUT THE FLOW SYSTEM ARE AS TABULATED BELOW.

VAPOR CAVITY

DIST.	.0000	.0640	.1280	.1920	.2560	.3200	.3840	.4479	.5119	.5759	.6399	.7039
-------	-------	-------	-------	-------	-------	-------	-------	-------	-------	-------	-------	-------

LOC. 0 1 2 3 4 5 6 7 8 9 10 11

U .000 -.104 -.206 -.304 -.396 -.478 -.551 -.613 -.665 -.707 -.740 -.763

Z .056 .056 .057 .057 .057 .057 .056 .056 .055 .054 .053 .053

FULL-FLOWING PIPE SYSTEM

LOC. (1,0) (1,1) (2,0) (2,10) (2,20) (2,30) (2,40) (2,50)

V -1.3680 -1.3680 -1.3634 -1.3649 -1.3839 -1.4237 -1.4355 -1.4361

H 11.3000 11.4067 11.4067 14.5105 19.2061 27.3993 31.2485 33.1793

AT TIME T = 3.02292 SECONDS, AFTER 1629 COMPLETE CYCLES OF OPERATION, THE VELOCITIES AND DEPTHS IN THE VAPOR CAVITY AS WELL AS VELOCITIES AND PRESSURES AT KEY POINTS THROUGHOUT THE FLOW SYSTEM ARE AS TABULATED BELOW.

VAPOR CAVITY

WIST. 0.000 .0640 .1280 .1920 .2560 .3200 .3840 .4479 .5119 .5759 .6399

LOC. 0 1 2 3 4 5 6 7 8 9 10

U .000 -.107 -.212 -.311 -.402 -.482 -.552 -.612 -.662 -.703 -.734

Z .658 .058 .058 .058 .058 .058 .057 .056 .055 .054 .053

FULL-FLOWING PIPE SYSTEM

LOC. (1,0) (1,1) (2,0) (2,10) (2,20) (2,30) (2,40) (2,50)

V -1.3682 -1.3685 -1.3639 -1.3830 -1.4250 -1.4374 -1.4363 -1.4356

H 11.3000 11.5021 11.5021 17.4414 25.2543 29.0100 31.2125 33.1740

AT TIME T = 3.04148 SECONDS, AFTER 1639 COMPLETE CYCLES OF OPERATION, THE VELOCITIES AND DEPTHS IN THE VAPOR CAVITY AS WELL AS VELOCITIES AND PRESSURES AT KEY POINTS THROUGHOUT THE FLOW SYSTEM ARE AS TABULATED BELOW.

VAPOR CAVITY

DIST. 0.000 .0640 .1280 .1920 .2560 .3200 .3840 .4479 .5119 .5759

LOC. 0 1 2 3 4 5 6 7 8 9

U .000 -.111 -.217 -.317 -.406 -.484 -.551 -.609 -.658 -.696

Z .060 .060 .060 .059 .059 .059 .058 .057 .056 .055

FULL-FLOWING PIPE SYSTEM

LOC. (1,0) (1,1) (2,0) (2,10) (2,20) (2,30) (2,40) (2,50)

V -1.3990 -1.4005 -1.3958 -1.4237 -1.4362 -1.4375 -1.4374 -1.4365

H 11.3000 12.3746 12.3746 23.4820 27.2115 29.0619 30.9842 33.1790

AT TIME T = 3.06003 SECONDS, AFTER 1649 COMPLETE CYCLES OF OPERATION, THE VELOCITIES AND DEPTHS IN THE VAPOR CAVITY AS WELL AS VELOCITIES AND PRESSURES AT KEY POINTS THROUGHOUT THE FLOW SYSTEM ARE AS TABULATED BELOW.

VAPOR CAVITY

DIST. 0.000 .0640 .1280 .1920 .2560 .3200 .3840 .4479 .5119

LOC. 0 1 2 3 4 5 6 7 8

U .000 -.113 -.221 -.320 -.407 -.483 -.549 -.604 -.650

Z .061 .061 .061 .061 .060 .060 .059 .057 .056

FULL-FLOWING PIPE SYSTEM

LOC. (1,0) (1,1) (2,0) (2,10) (2,20) (2,30) (2,40) (2,50)

V -1.4827 -1.4814 -1.4764 -1.4487 -1.4362 -1.4363 -1.4378 -1.4392

H 11.3000 12.4905 12.4905 23.4025 27.2831 29.1846 31.0707 33.1790

AT TIME T = 3.07859 SECONDS, AFTER 1659 COMPLETE CYCLES OF OPERATION, THE VELOCITIES AND DEPTHS IN THE VAPOR CAVITY AS WELL AS VELOCITIES AND PRESSURES AT KEY POINTS THROUGHOUT THE FLOW SYSTEM ARE AS TABULATED BELOW.

VAPOR CAVITY

DIST.	.0000	.0640	.1280	.1920	.2560	.3200	.3840	.4479
LOC.	0	1	2	3	4	5	6	7
U	.000	-.114	-.223	-.321	-.406	-.480	-.543	-.596
Z	.063	.063	.063	.062	.062	.060	.059	.058

FULL-FLOWING PIPE SYSTEM

LOC.	(1,0)	(1,1)	(2,0)	(2,10)	(2,20)	(2,30)	(2,40)	(2,50)
V	-1.5125	-1.5120	-1.5069	-1.4885	-1.4487	-1.4365	-1.4381	-1.4390
H	11.3000	11.3465	11.5465	17.6046	25.3887	29.2911	31.4192	33.1790

AT TIME T = 3.09715 SECONDS, AFTER 1669 COMPLETE CYCLES OF OPERATION, THE VELOCITIES AND DEPTHS IN THE VAPOR CAVITY AS WELL AS VELOCITIES AND PRESSURES AT KEY POINTS THROUGHOUT THE FLOW SYSTEM ARE AS TABULATED BELOW.

VAPOR CAVITY

DIST.	.0000	.0640	.1280	.1920	.2560	.3200
LOC.	0	1	2	3	4	5
U	.000	-.114	-.222	-.318	-.402	-.474
Z	.065	.065	.065	.064	.063	.061

FULL-FLOWING PIPE SYSTEM

LOC.	(1,0)	(1,1)	(2,0)	(2,10)	(2,20)	(2,30)	(2,40)	(2,50)
V	-1.5129	-1.5129	-1.5078	-1.5066	-1.4885	-1.4504	-1.4377	-1.4369
H	11.3000	11.4427	11.4427	14.8464	19.6534	27.6347	31.4404	33.1790

AT TIME T = 3.11571 SECONDS, AFTER 1679 COMPLETE CYCLES OF OPERATION, THE VELOCITIES AND DEPTHS IN THE VAPOR CAVITY AS WELL AS VELOCITIES AND PRESSURES AT KEY POINTS THROUGHOUT THE FLOW SYSTEM ARE AS TABULATED BELOW.

VAPOR CAVITY

DIST.	.0000	.0640	.1280	.1920
LOC.	0	1	2	3
U	.000	-.112	-.218	-.313
Z	.068	.067	.067	.065

FULL-FLOWING PIPE SYSTEM

LOC.	(1,0)	(1,1)	(2,0)	(2,10)	(2,20)	(2,30)	(2,40)	(2,50)
V	-1.5121	-1.5121	-1.5070	-1.5077	-1.5081	-1.4895	-1.4492	-1.4364
H	11.3000	11.4483	11.4483	14.7761	17.1268	21.8428	29.4501	33.1790

← THE VAPOR CAVITY HAS COMPLETELY COLLAPSED AT TIME T = 3.13426 SECONDS (OPERATION CYCLE M = 1689). THIS IS 2.93014 SECONDS ← AFTER COLUMN SEPARATION OCCURRED, AND 3.12870 SECONDS AFTER VALVE WAS CLOSED.

VAPOR CAVITY

LOC.	(1,0)	(1,1)	(2,0)	(2,10)	(2,20)	(2,30)	(2,40)	(2,50)
V	-1.5125	-1.5125	-1.5074	-1.5085	-1.5086	-1.5066	-1.4879	-1.4613
H	11.3000	11.4752	11.4752	15.0048	16.9719	18.9788	23.6648	33.1790

AT TIME T = 3.13612 SECONDS, AFTER 1690 COMPLETE CYCLES OF OPERATION, THE VELOCITIES AND PRESSURES AT KEY POINTS THROUGHOUT THE FLOW SYSTEM ARE AS TABULATED BELOW.

VAPOR CAVITY

LOC.	(1,0)	(1,1)	(2,0)	(2,10)	(2,20)	(2,30)	(2,40)	(2,50)
V	.0000	-1.5127	-1.5076	-1.5085	-1.5084	-1.5068	-1.4916	-1.4673
H	126.5298	11.4788	11.4788	15.0196	16.9606	18.9115	23.1907	33.1790

AT TIME T = 3.15468 SECONDS, AFTER 1700 COMPLETE CYCLES OF OPERATION, THE VELOCITIES AND PRESSURES AT KEY POINTS THROUGHOUT THE FLOW SYSTEM ARE AS TABULATED BELOW.

LOC.	(1,0)	(1,1)	(2,0)	(2,10)	(2,20)	(2,30)	(2,40)	(2,50)
V	.0000	-.0916	-.0916	-1.5083	-1.5069	-1.5217	-1.5217	-1.5457
H	222.3961	220.4687	226.4687	14.9212	16.8446	18.8398	23.1672	33.1790

AT TIME T = 3.17323 SECONDS, AFTER 1710 COMPLETE CYCLES OF OPERATION, THE VELOCITIES AND PRESSURES AT KEY POINTS THROUGHOUT THE FLOW SYSTEM ARE AS TABULATED BELOW.

LOC.	(1,0)	(1,1)	(2,0)	(2,10)	(2,20)	(2,30)	(2,40)	(2,50)
V	.0000	-.0077	-.0677	-.0939	-1.5070	-1.5217	-1.5610	-1.5756
H	233.3888	233.2271	233.2271	222.9844	16.8032	21.0872	28.8351	35.1790

AT TIME T = 3.19179 SECONDS, AFTER 1720 COMPLETE CYCLES OF OPERATION, THE VELOCITIES AND PRESSURES AT KEY POINTS THROUGHOUT THE FLOW SYSTEM ARE AS TABULATED BELOW.

LOC.	(1,0)	(1,1)	(2,0)	(2,10)	(2,20)	(2,30)	(2,40)	(2,50)
V	.0000	-.0011	-.0611	-.0103	-.1127	-1.5605	-1.5753	-1.5761
H	234.4422	234.4238	234.4238	235.8169	226.6305	26.7563	31.1035	33.1790

AT TIME T = 3.21035 SECONDS, AFTER 1730 COMPLETE CYCLES OF OPERATION, THE VELOCITIES AND PRESSURES AT KEY POINTS THROUGHOUT THE FLOW SYSTEM ARE AS TABULATED BELOW.

LOC.	(1,0)	(1,1)	(2,0)	(2,10)	(2,20)	(2,30)	(2,40)	(2,50)
V	.0000	-.0017	-.0917	-.0196	-.0676	-1.5756	-1.5756	-1.5753
H	234.8549	234.8720	234.8720	239.3619	245.1795	235.9953	31.1333	33.1790

AT TIME T = 3.22890 SECONDS, AFTER 1740 COMPLETE CYCLES OF OPERATION, THE VELOCITIES AND PRESSURES AT KEY POINTS THROUGHOUT THE FLOW SYSTEM ARE AS TABULATED BELOW.

LOC.	(1,0)	(1,1)	(2,0)	(2,10)	(2,20)	(2,30)	(2,40)	(2,50)
V	.0000	-.0150	-.0150	-.0589	-.0770	-.0868	-.1745	-1.5751
H	237.6604	237.8206	237.8206	245.4985	248.7567	248.9576	237.4697	33.1790

→ THE DIRECTION OF FLOW AT THE RESERVOIR END OF THE PIPE SYSTEM HAS REVERSED AT TIME T = 3.23540 SECONDS. ←

AT TIME T = 3.24746 SECONDS, AFTER 1750 COMPLETE CYCLES OF OPERATION, THE VELOCITIES AND PRESSURES AT KEY POINTS THROUGHOUT THE FLOW SYSTEM ARE AS TABULATED BELOW.

LOC.	(1,0)	(1,1)	(2,0)	(2,10)	(2,20)	(2,30)	(2,40)	(2,50)
V	.0000	-.0288	-.0287	-.0724	-.0781	-.0808	-.0904	1.2190
H	247.7477	247.7045	247.7045	248.4821	249.2789	250.2749	250.4436	33.1790

AT TIME T = 3.26602 SECONDS, AFTER 1760 COMPLETE CYCLES OF OPERATION, THE VELOCITIES AND PRESSURES AT KEY POINTS THROUGHOUT THE FLOW SYSTEM ARE AS TABULATED BELOW.

LOC.	(1,0)	(1,1)	(2,0)	(2,10)	(2,20)	(2,30)	(2,40)	(2,50)
V	.0000	-.0104	-.0104	-.0479	-.0762	-.0816	1.3095	1.5883
H	255.5118	255.3711	255.3711	252.7516	249.9986	250.7663	46.5190	33.1790

AT TIME T = 3.28457 SECONDS, AFTER 1770 COMPLETE CYCLES OF OPERATION, THE VELOCITIES AND PRESSURES AT KEY POINTS THROUGHOUT THE FLOW SYSTEM ARE AS TABULATED BELOW.

LOC.	(1,0)	(1,1)	(2,0)	(2,10)	(2,20)	(2,30)	(2,40)	(2,50)
V	.0000	-.0021	-.0021	-.0143	-.0516	1.3108	1.3936	1.3998
H	257.3105	257.2807	257.2807	258.1508	254.2275	46.7309	34.0492	33.1790

AT TIME T = 3.30313 SECONDS, AFTER 1780 COMPLETE CYCLES OF OPERATION, THE VELOCITIES AND PRESSURES AT KEY POINTS THROUGHOUT THE FLOW SYSTEM ARE AS TABULATED BELOW.

FLOW SYSTEM ARE AS TABULATED BELOW.

LOC.	(1,0)	(1,1)	(2,0)	(2,10)	(2,20)	(2,30)	(2,40)	(2,50)
V	.0000	-.0012	-.0012	-.0057	1.3692	1.4201	1.4610	1.3989
H	257.8703	257.8616	257.8616	260.0297	55.3635	38.0023	33.4494	33.1790

AT TIME T = 3.32169 SECONDS, AFTER 1790 COMPLETE CYCLES OF OPERATION, THE VELOCITIES AND PRESSURES AT KEY POINTS THROUGHOUT THE FLOW SYSTEM ARE AS TABULATED BELOW.

LOC.	(1,0)	(1,1)	(2,0)	(2,10)	(2,20)	(2,30)	(2,40)	(2,50)
V	.0000	-.0016	-.0016	1.3787	1.4622	1.4589	1.4252	1.4022
H	258.4284	258.4250	258.4250	56.8706	44.3148	42.0606	37.1541	33.1790

AT TIME T = 3.32540 SECONDS, AFTER 1792 COMPLETE CYCLES OF OPERATION, THE VELOCITIES AND PRESSURES AT KEY POINTS THROUGHOUT THE FLOW SYSTEM ARE AS TABULATED BELOW.

LOC.	(1,0)	(1,1)	(2,0)	(2,10)	(2,20)	(2,30)	(2,40)	(2,50)
V	.0000	.9842	.9809	1.4153	1.4652	1.4623	1.4330	1.4067
H	211.3071	183.4390	183.4390	51.4954	43.9692	42.5557	38.3408	33.1790

AT TIME T = 3.32725 SECONDS, AFTER 1793 COMPLETE CYCLES OF OPERATION, THE VELOCITIES AND PRESSURES AT KEY POINTS THROUGHOUT THE FLOW SYSTEM ARE AS TABULATED BELOW.

LOC.	(1,0)	(1,1)	(2,0)	(2,10)	(2,20)	(2,30)	(2,40)	(2,50)
V	.0000	1.1050	1.1013	1.4276	1.4661	1.4635	1.4368	1.4098
H	158.0020	149.7719	149.7719	49.6803	43.8552	42.7476	38.9261	33.1790

AT TIME T = 3.32911 SECONDS, AFTER 1794 COMPLETE CYCLES OF OPERATION, THE VELOCITIES AND PRESSURES AT KEY POINTS THROUGHOUT THE FLOW SYSTEM ARE AS TABULATED BELOW.

LOC.	(1,0)	(1,1)	(2,0)	(2,10)	(2,20)	(2,30)	(2,40)	(2,50)
V	.0000	1.0954	1.0917	1.4372	1.4669	1.4646	1.4406	1.4138
H	110.1061	111.0738	111.0738	48.2775	43.7719	42.9110	39.4920	33.1790

AT TIME T = 3.33097 SECONDS, AFTER 1795 COMPLETE CYCLES OF OPERATION, THE VELOCITIES AND PRESSURES AT KEY POINTS THROUGHOUT THE FLOW SYSTEM ARE AS TABULATED BELOW.

LOC.	(1,0)	(1,1)	(2,0)	(2,10)	(2,20)	(2,30)	(2,40)	(2,50)
V	.0000	1.0256	1.0222	1.4445	1.4674	1.4653	1.4442	1.4184
H	67.3567	72.5709	72.5709	47.1905	43.7079	43.0444	40.0207	33.1790

AT TIME T = 3.33282 SECONDS, AFTER 1796 COMPLETE CYCLES OF OPERATION, THE VELOCITIES AND PRESSURES AT KEY POINTS THROUGHOUT THE FLOW SYSTEM ARE AS TABULATED BELOW.

LOC.	(1,0)	(1,1)	(2,0)	(2,10)	(2,20)	(2,30)	(2,40)	(2,50)
V	.0000	.9293	.9262	1.4502	1.4678	1.4660	1.4477	1.4238
H	29.5638	36.6482	36.6482	46.3516	43.6630	43.1578	40.5059	33.1790

→ COLUMN SEPARATION HAS OCCURRED AT THE GATE VALVE AT TIME T = 3.33468 SECONDS (OPERATION CYCLE NO. 1797). THIS IS 3.32911 SECONDS AFTER CLOSURE OF THE GATE VALVE. ←

THE MAGNITUDE OF DELXC REMAINS THE MINIMUM VALUE.

GIVEN DATA AND COMPUTED VALUES PERTINENT TO COMPUTATION OF FLOW FOLLOWING COLUMN SEPARATION.
 HVAPOR = 11.3000 DELXC = .0640 MARK = 1689 MUCH = .1450
 FACTOR = 5 XI = .0250 INC = 90 IOTA = .0001 PAREA = .00538

THE INITIAL VELOCITIES AND DEPTHS IN THE VAPOR CAVITY ARE LISTED BELOW.

DIST. .0000 .0640
 LOC. 0 1
 U .000 .757
 Z .063 .074

THE VELOCITIES AND ABSOLUTE HEADS THROUGHOUT THE REMAINDER OF THE FULL-FLOWING PIPE SYSTEM ARE AS LISTED BELOW.

LOC.	(1,0)	(1,1)	(2,0)	(2,10)	(2,30)	(2,40)	(2,50)
V	.7565	.9453	.9421	1.4680	1.4664	1.4569	1.4290
H	11.3000	22.2504	22.2504	43.6285	43.2483	40.9318	33.1790

AT TIME T = 3.34210 SECONDS, AFTER 1801 COMPLETE CYCLES OF OPERATION, THE VELOCITIES AND DEPTHS IN THE VAPOR CAVITY AS WELL AS VELOCITIES AND PRESSURES AT KEY POINTS THROUGHOUT THE FLOW SYSTEM ARE AS TABULATED BELOW.

VAPOR CAVITY

DIST. .0000 .0640
 LOC. 0 1
 U .000 .589
 Z .058 .068

FULL-FLOWING PIPE SYSTEM

LOC.	(1,0)	(1,1)	(2,0)	(2,10)	(2,30)	(2,40)	(2,50)
V	.9856	1.0475	1.0440	1.4683	1.4672	1.4626	1.4591
H	11.3000	11.3000	11.3000	43.5751	43.4822	41.9209	33.1790

AT TIME T = 3.35138 SECONDS, AFTER 1806 COMPLETE CYCLES OF OPERATION, THE VELOCITIES AND DEPTHS IN THE VAPOR CAVITY AS WELL AS VELOCITIES AND PRESSURES AT KEY POINTS THROUGHOUT THE FLOW SYSTEM ARE AS TABULATED BELOW.

VAPOR CAVITY

DIST. .0000 .0640 .1280
 LOC. 0 1 2
 U .000 .468 .906
 Z .056 .062 .071

FULL-FLOWING PIPE SYSTEM

LOC.	(1,0)	(1,1)	(2,0)	(2,10)	(2,30)	(2,40)	(2,50)
V	1.0693	1.0797	1.0761	1.4625	1.4675	1.4777	1.4963
H	11.3000	11.3000	11.3000	43.3000	43.5579	41.2864	33.1790

AT TIME T = 3.36066 SECONDS, AFTER 1811 COMPLETE CYCLES OF OPERATION, THE VELOCITIES AND DEPTHS IN THE VAPOR CAVITY AS WELL AS VELOCITIES AND PRESSURES AT KEY POINTS THROUGHOUT THE FLOW SYSTEM ARE AS TABULATED BELOW.

VAPOR CAVITY

DIST. .0000 .0640 .1280
 LOC. 0 1 2
 U .000 .400 .791
 Z .053 .058 .066

FULL-FLOWING PIPE SYSTEM

LOC.	(1,0)	(1,1)	(2,0)	(2,10)	(2,30)	(2,40)	(2,50)
V	1.1003	1.1181	1.1143	1.2398	1.4701	1.4969	1.5206
H	11.3000	11.3000	11.3000	64.3438	43.1690	38.9629	31.1790

AT TIME T = 3.36994 SECONDS, AFTER 1816 COMPLETE CYCLES OF OPERATION, THE VELOCITIES AND DEPTHS IN THE VAPOR CAVITY AS WELL AS

VELOCITIES AND PRESSURES AT KEY POINTS THROUGHOUT THE FLOW SYSTEM ARE AS TABULATED BELOW.

VAPOR CAVITY

DIST. .0000 .0640 .1280 .1920
 LOC. 0 1 2 3
 U .000 .349 .694 .965
 Z .051 .055 .062 .072

FULL-FLOWING PIPE SYSTEM

LOC. (1,0) (1,1) (2,0) (2,10) (2,20) (2,30) (2,40) (2,50)
 V 1.1277 1.1310 1.1272 1.2327 1.2479 1.4797 1.5158 1.5312
 H 11.3000 11.3000 11.3000 11.3000 11.4358 41.7385 36.3103 33.1790

AT TIME T = 3.38849 SECONDS, AFTER 1826 COMPLETE CYCLES OF OPERATION, THE VELOCITIES AND DEPTHS IN THE VAPOR CAVITY AS WELL AS VELOCITIES AND PRESSURES AT KEY POINTS THROUGHOUT THE FLOW SYSTEM ARE AS TABULATED BELOW.

VAPOR CAVITY

DIST. .0000 .0640 .1280 .1920 .2560
 LOC. 0 1 2 3 4
 U .000 .276 .555 .799 1.000
 Z .048 .050 .056 .063 .074

FULL-FLOWING PIPE SYSTEM

LOC. (1,0) (1,1) (2,0) (2,10) (2,20) (2,30) (2,40) (2,50)
 V 1.1623 1.1638 1.1599 1.2277 1.2503 1.3299 1.5329 1.5352
 H 11.3000 11.3000 11.3000 11.3000 11.3000 11.3000 33.7061 33.1790

AT TIME T = 3.40705 SECONDS, AFTER 1836 COMPLETE CYCLES OF OPERATION, THE VELOCITIES AND DEPTHS IN THE VAPOR CAVITY AS WELL AS VELOCITIES AND PRESSURES AT KEY POINTS THROUGHOUT THE FLOW SYSTEM ARE AS TABULATED BELOW.

VAPOR CAVITY

DIST. .0000 .0640 .1280 .1920 .2560
 LOC. 0 1 2 3 4
 U .000 .227 .458 .670 .849
 Z .046 .047 .052 .058 .065

FULL-FLOWING PIPE SYSTEM

LOC. (1,0) (1,1) (2,0) (2,10) (2,20) (2,30) (2,40) (2,50)
 V 1.1873 1.1881 1.1840 1.2268 1.2542 1.3283 1.3836 1.5346
 H 11.3000 11.3000 11.3000 11.3000 11.3000 11.3000 11.3000 33.1790

AT TIME T = 3.42561 SECONDS, AFTER 1846 COMPLETE CYCLES OF OPERATION, THE VELOCITIES AND DEPTHS IN THE VAPOR CAVITY AS WELL AS VELOCITIES AND PRESSURES AT KEY POINTS THROUGHOUT THE FLOW SYSTEM ARE AS TABULATED BELOW.

VAPOR CAVITY

DIST. .0000 .0640 .1280 .1920 .2560 .3200
 LOC. 0 1 2 3 4 5
 U .000 .191 .385 .570 .741 .951
 Z .044 .045 .049 .054 .060 .065

FULL-FLOWING PIPE SYSTEM

LOC. (1,0) (1,1) (2,0) (2,10) (2,20) (2,30) (2,40) (2,50)

V 1.2069 1.2063 1.2022 1.2289 1.2579 1.3272 1.3810 1.4471
 H 11.3000 11.3000 11.3000 11.3000 11.3000 11.3000 11.3000 11.3000

AT TIME T = 3.44416 SECONDS, AFTER 1856 COMPLETE CYCLES OF OPERATION, THE VELOCITIES AND DEPTHS IN THE VAPOR CAVITY AS WELL AS VELOCITIES AND PRESSURES AT KEY POINTS THROUGHOUT THE FLOW SYSTEM ARE AS TABULATED BELOW.

VAPOR CAVITY

DIST.	.0000	.0640	.1280	.1920	.2560	.3200	.3840
LOC.	0	1	2	3	4	5	6
V	.000	.163	.328	.491	.654	.816	.977
Z	.043	.044	.046	.051	.056	.060	.068

FULL-FLOWING PIPE SYSTEM

LOC.	(1,0)	(1,1)	(2,0)	(2,10)	(2,20)	(2,30)	(2,40)
V	1.2200	1.2202	1.2161	1.2351	1.2612	1.3265	1.3980
H	11.3000	11.3000	11.3000	11.3000	11.3000	11.3000	17.1039

AT TIME T = 3.46272 SECONDS, AFTER 1866 COMPLETE CYCLES OF OPERATION, THE VELOCITIES AND DEPTHS IN THE VAPOR CAVITY AS WELL AS VELOCITIES AND PRESSURES AT KEY POINTS THROUGHOUT THE FLOW SYSTEM ARE AS TABULATED BELOW.

VAPOR CAVITY

DIST.	.0000	.0640	.1280	.1920	.2560	.3200	.3840
LOC.	0	1	2	3	4	5	6
V	.000	.140	.282	.427	.579	.741	1.006
Z	.041	.042	.045	.048	.053	.057	.063

FULL-FLOWING PIPE SYSTEM

LOC.	(1,0)	(1,1)	(2,0)	(2,10)	(2,20)	(2,30)	(2,40)
V	1.2308	1.2310	1.2268	1.2436	1.2641	1.3091	1.2306
H	11.3000	11.3000	11.3000	11.3296	11.3000	12.7346	29.4578

AT TIME T = 3.48128 SECONDS, AFTER 1876 COMPLETE CYCLES OF OPERATION, THE VELOCITIES AND DEPTHS IN THE VAPOR CAVITY AS WELL AS VELOCITIES AND PRESSURES AT KEY POINTS THROUGHOUT THE FLOW SYSTEM ARE AS TABULATED BELOW.

VAPOR CAVITY

DIST.	.0000	.0640	.1280	.1920	.2560	.3200	.3840
LOC.	0	1	2	3	4	5	6
V	.000	.121	.245	.375	.515	.661	.819
Z	.040	.041	.043	.046	.050	.054	.059

FULL-FLOWING PIPE SYSTEM

LOC.	(1,0)	(1,1)	(2,0)	(2,10)	(2,20)	(2,30)	(2,40)
V	1.2395	1.2398	1.2356	1.2511	1.2669	1.1998	1.2007
H	11.3000	11.3000	11.3000	11.6535	11.3000	24.7443	28.8404

AT TIME T = 3.49983 SECONDS, AFTER 1886 COMPLETE CYCLES OF OPERATION, THE VELOCITIES AND DEPTHS IN THE VAPOR CAVITY AS WELL AS VELOCITIES AND PRESSURES AT KEY POINTS THROUGHOUT THE FLOW SYSTEM ARE AS TABULATED BELOW.

VAPOR CAVITY

DIST.	.0000	.0640	.1280	.1920	.2560	.3200	.3840
LOC.	0	1	2	3	4	5	6
V	.000	.106	.215	.332	.460	.593	.718
Z	.039	.040	.042	.045	.048	.051	.056

FULL-FLOWING PIPE SYSTEM

LOC.	(1,0)	(1,1)	(2,0)	(2,10)	(2,20)	(2,30)	(2,40)	(2,50)
V	1.2470	1.2474	1.2432	1.2581	1.1826	1.1755	1.1756	1.1724
H	11.3000	11.3000	11.3000	11.7124	22.0072	24.9259	28.5106	33.1793

AT TIME T = 3.51839 SECONDS, AFTER 1896 COMPLETE CYCLES OF OPERATION, THE VELOCITIES AND DEPTHS IN THE VAPOR CAVITY AS WELL AS VELOCITIES AND PRESSURES AT KEY POINTS THROUGHOUT THE FLOW SYSTEM ARE AS TABULATED BELOW.

VAPOR CAVITY

DIST.	.0000	.0640	.1280	.1920	.2560	.3200	.3840	.4479	.5119	.5759
LOC.	0	1	2	3	4	5	6	7	8	9
U	.000	.092	.190	.296	.413	.534	.655	.795	.892	1.021
Z	.039	.039	.041	.043	.046	.049	.053	.056	.061	.065

FULL-FLOWING PIPE SYSTEM

LOC.	(1,0)	(1,1)	(2,0)	(2,10)	(2,20)	(2,30)	(2,40)	(2,50)
V	1.2540	1.2545	1.2502	1.1896	1.1734	1.1586	1.1475	1.1453
H	11.3000	11.3000	11.3000	22.8171	24.3702	25.7683	29.2960	33.1793

AT TIME T = 3.53695 SECONDS, AFTER 1906 COMPLETE CYCLES OF OPERATION, THE VELOCITIES AND DEPTHS IN THE VAPOR CAVITY AS WELL AS VELOCITIES AND PRESSURES AT KEY POINTS THROUGHOUT THE FLOW SYSTEM ARE AS TABULATED BELOW.

VAPOR CAVITY

DIST.	.0000	.0640	.1280	.1920	.2560	.3200	.3840	.4479	.5119	.5759	.6399
LOC.	0	1	2	3	4	5	6	7	8	9	10
U	.000	.081	.169	.265	.372	.484	.600	.725	.822	.941	1.100
Z	.038	.039	.040	.042	.045	.047	.051	.054	.058	.062	.072

FULL-FLOWING PIPE SYSTEM

LOC.	(1,0)	(1,1)	(2,0)	(2,10)	(2,20)	(2,30)	(2,40)	(2,50)
V	1.1254	1.1317	1.1278	1.1732	1.1657	1.1454	1.1285	1.1227
H	11.3000	12.2281	12.2281	24.1137	26.5588	28.7198	30.4703	33.1793

AT TIME T = 3.55500 SECONDS, AFTER 1916 COMPLETE CYCLES OF OPERATION, THE VELOCITIES AND DEPTHS IN THE VAPOR CAVITY AS WELL AS VELOCITIES AND PRESSURES AT KEY POINTS THROUGHOUT THE FLOW SYSTEM ARE AS TABULATED BELOW.

VAPOR CAVITY

DIST.	.0000	.0640	.1280	.1920	.2560	.3200	.3840	.4479	.5119	.5759	.6399
LOC.	0	1	2	3	4	5	6	7	8	9	10
U	.000	.072	.151	.238	.337	.441	.550	.664	.759	.867	.977
Z	.038	.038	.039	.041	.043	.046	.049	.052	.056	.059	.065

FULL-FLOWING PIPE SYSTEM

LOC.	(1,0)	(1,1)	(2,0)	(2,10)	(2,20)	(2,30)	(2,40)	(2,50)
V	1.1010	1.1012	1.0975	1.1043	1.1454	1.1356	1.1207	1.1118
H	11.3000	11.4200	11.4200	17.2708	28.4421	31.2384	32.8376	33.1793

AT TIME T = 3.57406 SECONDS, AFTER 1926 COMPLETE CYCLES OF OPERATION, THE VELOCITIES AND DEPTHS IN THE VAPOR CAVITY AS WELL AS VELOCITIES AND PRESSURES AT KEY POINTS THROUGHOUT THE FLOW SYSTEM ARE AS TABULATED BELOW.

VAPOR CAVITY

DIST.	.0000	.0640	.1280	.1920	.2560	.3200	.3840	.4479	.5119	.5759	.6399	.7039
-------	-------	-------	-------	-------	-------	-------	-------	-------	-------	-------	-------	-------

FULL-FLOWING PIPE SYSTEM

LOC.	0	1	2	3	4	5	6	7	8	9	10	11
U	.000	.064	.135	.216	.306	.402	.505	.616	.701	.802	.887	.893
Z	.037	.037	.038	.040	.042	.044	.047	.050	.054	.057	.062	.067

AT TIME T = 3.59262 SECONDS, AFTER 1936 COMPLETE CYCLES OF OPERATION, THE VELOCITIES AND DEPTHS IN THE VAPOR CAVITY AS WELL AS VELOCITIES AND PRESSURES AT KEY POINTS THROUGHOUT THE FLOW SYSTEM ARE AS TABULATED BELOW.

VAPOR CAVITY

DIST.	.0000	.0640	.1280	.1920	.2560	.3200	.3840	.4479	.5119	.5759	.6399	.7039
LOC.	0	1	2	3	4	5	6	7	8	9	10	11
U	.000	.058	.122	.196	.279	.369	.465	.561	.649	.742	.814	.890
Z	.037	.037	.038	.039	.041	.043	.046	.048	.052	.055	.059	.064

FULL-FLOWING PIPE SYSTEM

LOC.	(1,0)	(1,1)	(2,0)	(2,10)	(2,20)	(2,30)	(2,40)
V	1.0523	1.0494	1.0458	1.0472	1.0458	1.0562	1.1160
H	11.3000	11.8259	11.8259	17.5866	20.7893	24.7340	32.9348

AT TIME T = 3.61118 SECONDS, AFTER 1946 COMPLETE CYCLES OF OPERATION, THE VELOCITIES AND DEPTHS IN THE VAPOR CAVITY AS WELL AS VELOCITIES AND PRESSURES AT KEY POINTS THROUGHOUT THE FLOW SYSTEM ARE AS TABULATED BELOW.

VAPOR CAVITY

DIST.	.0000	.0640	.1280	.1920	.2560	.3200	.3840	.4479	.5119	.5759	.6399	.7039
LOC.	0	1	2	3	4	5	6	7	8	9	10	11
U	.000	.052	.111	.179	.255	.339	.428	.518	.601	.686	.749	.824
Z	.036	.037	.037	.039	.040	.042	.044	.047	.050	.053	.057	.063

FULL-FLOWING PIPE SYSTEM

LOC.	(1,0)	(1,1)	(2,0)	(2,20)	(2,30)	(2,40)
V	1.0219	1.0213	1.0178	1.0310	1.0441	1.0655
H	11.3000	11.5916	11.5916	20.3508	21.6104	24.0208

AT TIME T = 3.62973 SECONDS, AFTER 1956 COMPLETE CYCLES OF OPERATION, THE VELOCITIES AND DEPTHS IN THE VAPOR CAVITY AS WELL AS VELOCITIES AND PRESSURES AT KEY POINTS THROUGHOUT THE FLOW SYSTEM ARE AS TABULATED BELOW.

VAPOR CAVITY

DIST.	.0000	.0640	.1280	.1920	.2560	.3200	.3840	.4479	.5119	.5759	.6399	.7039
LOC.	0	1	2	3	4	5	6	7	8	9	10	11
U	.000	.047	.101	.163	.234	.312	.395	.478	.557	.634	.689	.781
Z	.036	.036	.037	.038	.039	.041	.043	.046	.048	.051	.056	.064

FULL-FLOWING PIPE SYSTEM

LOC.	(1,0)	(1,1)	(2,0)	(2,20)	(2,30)	(2,40)
V	.9986	.9988	1.0018	1.0201	1.0384	1.0444
H	11.3000	11.5046	15.6446	17.6866	19.6543	21.9354

AT TIME T = 3.64829 SECONDS, AFTER 1966 COMPLETE CYCLES OF OPERATION, THE VELOCITIES AND DEPTHS IN THE VAPOR CAVITY AS WELL AS VELOCITIES AND PRESSURES AT KEY POINTS THROUGHOUT THE FLOW SYSTEM ARE AS TABULATED BELOW.

VAPOR CAVITY

DIST.	.0000	.0640	.1280	.1920	.2560	.3200	.3840	.4479	.5119	.5759	.6399	.7039
LOC.	0	1	2	3	4	5	6	7	8	9	10	11
U	.000	.047	.101	.163	.234	.312	.395	.478	.557	.634	.689	.781
Z	.036	.036	.037	.038	.039	.041	.043	.046	.048	.051	.056	.064

FULL-FLOWING PIPE SYSTEM

LOC.	(1,0)	(1,1)	(2,0)	(2,20)	(2,30)	(2,40)
V	.9986	.9988	1.0018	1.0201	1.0384	1.0444
H	11.3000	11.5046	15.6446	17.6866	19.6543	21.9354

VAPOR CAVITY

DIST.	.0000	.0640	.1280	.1920	.2560	.3200	.3840	.4479	.5119	.5759	.6399	.7039	.7679	.8319	.8959
LOC.	0	1	2	3	4	5	6	7	8	9	10	11	12	13	14
U	.000	.043	.092	.150	.216	.288	.365	.442	.516	.586	.635	.678	.740	.816	.896
Z	.036	.036	.037	.037	.039	.040	.042	.044	.047	.050	.054	.059	.062	.065	.074

FULL-FLOWING PIPE SYSTEM

LOC.	(1,0)	(1,1)	(2,0)	(2,10)	(2,10)	(2,20)	(2,30)	(2,40)	(2,50)
V	.9885	.9876	.9843	.9939	.9933	1.0092	1.0205	.9780	.9705
H	11.3000	11.3625	11.3625	13.4266	12.2039	14.7675	18.0243	23.0318	33.1790

AT TIME T = 3.66885 SECONDS, AFTER 1976 COMPLETE CYCLES OF OPERATION, THE VELOCITIES AND DEPTHS IN THE VAPOR CAVITY AS WELL AS VELOCITIES AND PRESSURES AT KEY POINTS THROUGHOUT THE FLOW SYSTEM ARE AS TABULATED BELOW.

VAPOR CAVITY

DIST.	.0000	.0640	.1280	.1920	.2560	.3200	.3840	.4479	.5119	.5759	.6399	.7039	.7679	.8319	.8959
LOC.	0	1	2	3	4	5	6	7	8	9	10	11	12	13	14
U	.000	.040	.085	.138	.199	.266	.338	.409	.478	.540	.585	.630	.697	.779	.853
Z	.035	.036	.036	.037	.038	.040	.041	.043	.046	.049	.053	.057	.060	.063	.068

FULL-FLOWING PIPE SYSTEM

LOC.	(1,0)	(1,1)	(2,0)	(2,10)	(2,10)	(2,20)	(2,30)	(2,40)	(2,50)
V	.9882	.9881	.9847	.9933	.9933	.9945	.9498	.9469	.9519
H	11.3000	11.3006	11.3006	12.2039	12.2039	13.7745	24.1265	29.2893	33.1790

AT TIME T = 3.68540 SECONDS, AFTER 1986 COMPLETE CYCLES OF OPERATION, THE VELOCITIES AND DEPTHS IN THE VAPOR CAVITY AS WELL AS VELOCITIES AND PRESSURES AT KEY POINTS THROUGHOUT THE FLOW SYSTEM ARE AS TABULATED BELOW.

VAPOR CAVITY

DIST.	.0000	.0640	.1280	.1920	.2560	.3200	.3840	.4479	.5119	.5759	.6399	.7039	.7679	.8319	.8959
LOC.	0	1	2	3	4	5	6	7	8	9	10	11	12	13	14
U	.000	.037	.079	.128	.185	.247	.313	.379	.442	.498	.539	.587	.655	.729	.803
Z	.035	.035	.036	.036	.038	.039	.041	.043	.045	.048	.052	.055	.058	.061	.064

FULL-FLOWING PIPE SYSTEM

LOC.	(1,0)	(1,1)	(2,0)	(2,10)	(2,10)	(2,20)	(2,30)	(2,40)	(2,50)
V	.9917	.9920	.9886	.9927	.9927	.9942	.9212	.9232	.9235
H	11.3000	11.3000	11.3000	13.0802	13.0802	21.3382	25.0180	23.5210	33.1790

AT TIME T = 3.70396 SECONDS, AFTER 1996 COMPLETE CYCLES OF OPERATION, THE VELOCITIES AND DEPTHS IN THE VAPOR CAVITY AS WELL AS VELOCITIES AND PRESSURES AT KEY POINTS THROUGHOUT THE FLOW SYSTEM ARE AS TABULATED BELOW.

VAPOR CAVITY

DIST.	.0000	.0640	.1280	.1920	.2560	.3200	.3840	.4479	.5119	.5759	.6399	.7039	.7679	.8319	.8959
LOC.	0	1	2	3	4	5	6	7	8	9	10	11	12	13	14
U	.000	.034	.073	.118	.171	.229	.290	.351	.408	.458	.497	.546	.614	.685	.754
Z	.035	.035	.035	.036	.037	.038	.040	.042	.044	.047	.051	.054	.057	.059	.062

DIST. .9599
LOC. 15
U .809
Z .000

FULL-FLOWING PIPE SYSTEM

LOC.	(1,0)	(1,1)	(2,0)	(2,10)	(2,20)	(2,30)	(2,40)	(2,50)
V	.5953	.746	.9312	.9366	.9196	.9077	.8979	.8947
H	11.3000	11.3484	11.3484	21.4994	24.2330	25.7316	28.9461	31.1730

COMPUTATION HAS BEEN HALTED BY CUTOFF.

**** ALL INPUT DATA HAVE BEEN PROCESSED.
AT LOC 37716



THE UNIVERSITY OF MICHIGAN
ENGIN. - TRANS. LIBRARY
312 UNDERGRADUATE LIBRARY
754-7494
OVERDUE FINE = 25¢ PER DAY
DATE DUE

~~DEC 01 1982~~

JUL 02 1992